# GM-CSF licenses microglia to mediate tissue damage in the CNS


## Diana Arseni MSci Hons


**Thesis submitted in fulfilment of the requirements for the degree Doctor of Philosophy**



**College of Medical, Veterinary, and Life Sciences**

**Institute of Infection, Immunity, and Inflammation**

**University of Glasgow**


**September 2019**

# Abstract

**Granulocyte-macrophage colony stimulating factor (GM-CSF**) plays multiple roles in the development, maintenance and regulation of the immune system. In experimental autoimmune encephalomyelitis (EAE), an animal model of multiple sclerosis (MS), the absence of GM-CSF expression by CNS antigen-specific Th1/17 T cells abolishes their encephalitogenic potential; an effect attributed to the inability of GM-CSF$^{-/-}$ T cells to activate myeloid cells within the CNS. To address the mechanisms involved, we investigated the effects of GM-CSF in myelinated cultures derived from embryonic mouse spinal cord. Our data demonstrate GM-CSF "activates" microglia inducing marked changes in morphology and enhancing their phagocytic potential. However, in isolation, this is unable to damage myelin or axons.

These data suggest GM-CSF synergises with other effector mechanisms to mediate tissue damage in EAE. We therefore investigated its ability to potentiate the cytopathic effects of IFN-γ and TNF-α, two pro-inflammatory cytokines associated with EAE and MS pathogenesis.

We report a combination of all three cytokines is required to induce rapid and extensive cell death. Cell death was associated with induction of iNOS in microglia, elevated nitric oxide and was inhibited completely by an iNOS inhibitor, AMT hydrochloride. Additionally, cell supernatant analyses revealed that the synergy between GM-CSF, IFN-γ and TNF-α is also responsible for extensive pro-inflammatory cytokines release, including IL-6 and IL-1ß.

# Table of Contents

# List of Tables

# List of Figures

# Acknowledgement

I would like to begin by thanking my supervisor, Prof. Chris Linington. You have provided invaluable guidance, mentoring and pints throughout my PhD that helped me develop as a scientist and person. To my second supervisor, Dr. Julia Edgar, thank you for being there to guide me every time I needed help (including last minute!). Katja, thank you for all your advice and support (and listening to my rants). I want to thank everyone in the AstraZeneca neuroscience team for all their help and for making me feel like home during my placement. Pete, thank you very much for all your help, mentoring and enthusiasm. Furthermore, I would like to thank my assessors, Prof. Simon Milling and Prof. Sue Barnett for their advice.

To my fellow Liningtons, Daniel, Lorna, Tiia (in alphabetical order), I really much appreciate you being there for me when I needed help in the lab, help with pints, an emergency Paesano, or better said help with anything. I could not have imagined my PhD experience without each of you, including Liz, the honorary Linington. I will miss our recipe/food exchange conventions.

Times have changed and I cannot simply refer to everyone else in the office as The Barnetts (again alphabetically George, Mike 1, Mike 2, Sara and Susan), so from now, past and present inhabitants of B319 will collectively be referred as THE OFFICE. My intention is not strip anyone of their identity, but to make sure everyone is appreciated (list of name available in appendix Figure 7.4). Anyway, old OFFICE, thank you very much for being there for me when I started this great adventure, I could not have asked for more exceptional drinking companions. I would like to thank the fresher additions Colin and Claire (not so fresh anymore) and now Becky for being great laughing partners and shoulders to cry on. Thank you everyone on level 3 for your ever willingness to help and stop for her a chat.

To my housemates, Eve, Andreea and Marc, thank you for coping with my 2 am baking. I know you did not put up with it just for the sweet rewards. I am still extremely fortunate to have you as friends.
Finally, mum and dad, thank you for being there for every step I took, including these last four years. Sper ca v-am facut mandri!

# Author's Declaration

I declare that, except where referenced to others, this thesis is the product of my own work and has not been submitted for any other degree at the University of Glasgow or any other institution.

Signature:

Printed name: DIANA ARSENI

# Definitions/Abbreviations

| | |
|---|---|
| AD | Alzheimer's disease |
| AMT hydrochloride | 2-Amino-5,6-dihydro-6-methyl-4H-1,3-thiazine HCL |
| ANOVA | analysis of variance |
| AOI | area of interest |
| APP/PS1dE9 | human amyloid precursor protein/ presenilin 1 mutations |
| aprox. | aproximatively |
| BCA | bicinchoninic acid |
| BSA | bovine serum albumin |
| Ca | calcium |
| CD | cluster of differentiation |
| cDNA | complementary DNA |
| CIS | clinically isolated syndrome |
| CLR | C-type lectin |
| CNS | central nervous system |
| CSF | cerebrospinal fluid |
| DAMP | danger associated molecular pattern |
| DAPI | 4',6- Diamidino-2-Phenylindole, Dihydrochloride |
| DAVID | The Database for Annotation, Visualization and Integrated Discovery |
| DC | dendritic cell |
| DIV | day in vitro |
| DMD | disease modifying drugs |
| DMEM | Dulbecco's Modified Eagle Mediu |
| DMEM/F12 | Dulbecco's Modified Eagle Medium: Nutrient Mixture F-12 |
| DMSO | dimethyl sulfoxide |
| E | embryonic |
| *E. coli* | *Escherichia coli* |
| EAE | experimental autoimmune encephalomyelitis |
| EGF | epidermal growth factor |
| FACS | fluorescence-activated cell sorting |
| FBS | feotal bovine serum |
| FDR | false discovery rate |
| GM-CSF | granulocyte macrophage stimulating factor |
| GM-CSFR | granulocyte macrophage stimulating factor receptor |

| | |
|---|---|
| GWAS | Genome wide association study |
| HBSS | Hanks balanced salt solution |
| HDAC | histone deacetylase inhibitors |
| HEPES | (4-(2-hydroxyethyl)-1-piperazineethanesulfonic acid |
| HLA | human leuokocyte antigen |
| IC50 | half maximal inhibitory concentration |
| IFN-γ | interferon gamma |
| IgG | immunoglobulin |
| IL- | interleukin |
| iNOS | inducible nitric oxidase |
| KEGG | Kyoto Encyclopedia of Genes and Genomes |
| KO | knock out |
| LDH | lactate dehydrogenase |
| LPS | lipopolysaccharide |
| MBP | myelin basic protein |
| M-CSF | macrophage colony stimulating factor |
| Mg | magnesium |
| MHC | major histocompatibility complex |
| MOG | myelin oligodendrocyte glycoprotein |
| MRI | magnetic resonance imaging |
| MS | multiple sclerosis |
| MSD | meso scale discovey |
| NF-H | neurofilament heavy-chain |
| NF-κB | nuclear factor κB |
| NO | nitric oxide |
| NSM | neurosphere media |
| P | post-natal |
| PAMP | pattern associated molecular pattern |
| PBS-T | 0.5% Tween in PBS |
| PCR | polymerase chain reaction |
| PFA | paraformaldehyde |
| PLL | poly-l-lysine |
| PLP | proteolipid protein |
| PM | plating media |
| poly I:C | polyinosinic:polycytidylic acid |
| PPMS | primary progressive multiple sclerosis |

| | |
|---|---|
| PRR | pattern recognition receptor |
| qRT-PCR | quantitative reverse transcription PCR |
| RNAseq | RNA sequencing |
| RNS | reactive nitrogen species |
| ROS | reactive oxygen species |
| rpm | rotation per minute |
| RRMS | remitting relapsing multiple sclerosis |
| SD | Sprague Dawley |
| SD | standard deviation |
| SDS | Sodium dodecyl sulphate |
| SPMS | secondary progressive multiple sclerosis |
| Th | T helper cell |
| Tiron | disodium-1,2-dihydroxybenzene-3,5-disulfonate |
| TLR | Toll-like receptor |
| TNF-α | tumour necrosis factor alpha |
| TPCA-1 | [(aminocarbonyl)amino]-5 -(4-fluorophenyl)-3-thiophenecarboxamide |
| wd | withdrawal |
| WM | white matter |
| WT | wild type |

# Chapter 1

## Introduction

# 1 Introduction

## 1.1 Multiple sclerosis

Multiple sclerosis (MS) is a chronic inflammatory demyelinating disease of the central nervous system (CNS) and the most common cause of chronic disability among young adults in Europe and North America (Lebrun-Frenay, Kobelt, Berg, Capsa, & Gannedahl, 2017). Neurological deficits in MS are due to demyelination and axonal injury attributed to the detrimental effects of repeated episodes of autoimmune T cell mediated inflammation. A concept developed from studies on experimental autoimmune encephalomyelitis (EAE), an animal model that replicates many of the pathological and clinical features of the human disease. This resulted in a number of treatments that reduce disease activity by suppressing immune-mediated inflammation in the CNS. However their efficacy remains limited by factors including large numbers of non-responders, side effects and cost. There is therefore a continuing need to develop more effective treatments, and more importantly strategies to stop disease developing in the first place. Current preclinical strategies include immune modulation and modalities to promote neuroprotection, remyelination and repair (Gholamzad et al., 2019).

### 1.1.1 Epidemiology and aetiology

It is estimated that there are 110,000 people living with MS in the UK, the highest incidence being in Scotland where it is > 200 per 100,000 (MS Trust, 2018) and in Orkney results in about 1 in every 170 women having the disease (Visser, Wilde, Wilson, Yong, & Counsell, 2012). This reflects the situation observed in several other autoimmune diseases in which more women are affected than men, the ratio for MS being between 2.3 - 3.5 to 1 (Harbo, Gold, & Tintora, 2013).

The exact cause of MS remains to be elucidated. There are extensive studies on environmental, genetic and epigenetic risk factors that individually or combined are associated with an increased incidence of multiple sclerosis (Ciccarelli, 2019). Environmental factors thought to play a role in causing MS are vitamin D deficiency, diet, and smoking (Ciccarelli, 2019), as well as certain infections such as Epstein-Barr virus (Levin et al., 2005). The dominant genetic risk factors

are associated with the MHC class II locus, for example it is three times more likely HLA DRB1*15:01 carriers will develop MS (Patsopoulos et al., 2013). Additionally, genome wide association studies (GWAS) are continuing to identify an increasing number of common non-HLA genetic variants associated with increased susceptibility to MS, virtually all of which are associated with immune function including *IL2RA, IL7RA, CD58, TYK2, STAT3,* and *TNFRSF1A* (Ciccarelli, 2019; Hafler et al., 2007).

## 1.1.2 Pathology and disease course

The main pathological hallmarks of MS are chronic inflammation, demyelination, and axonal loss that result in patients developing persistently demyelinated plaques of astrocytic scar tissue traversed by varying numbers of surviving axons (Brück, 2005; Lassmann, 2014; Prineas et al., 2001). There are three main disease courses in MS: relapsing remitting multiple sclerosis (RRMS), primary progressive multiple sclerosis (PPMS) and secondary progressive multiple sclerosis (SPMS).

### 1.1.2.1 Remitting relapsing multiple sclerosis

RRMS is the initial presentation in approximately 85 % of MS cases the majority of whom are in young adults, although about 5% of cases occur in children (Özakbaş, 2015). It is often is preceded by a clinically isolated syndrome (CIS) characterised by acute onset of neurological symptoms such as optic neuritis or numbness in the extremities which in many cases resolves spontaneously. The overall risk of CIS patients going on to develop MS is approximately 20%, but this increases to 60 to 80% if white matter (WM) lesions are detected by MRI (Fisniku et al., 2008). Typically, patients with RRMS will relapse on average every 1.5 years, although there is enormous variation in relapse frequency between patients.

These spontaneous and unpredictable episodes of neurological symptoms are associated with inflammatory activity in the corresponding regions of brain or spinal cord region. Symptoms often resolve completely during remission but over time complete recovery becomes less likely as patents accumulate an increasing

burden of chronic neurological deficits due to irreversible axonal injury and loss (Ciccarelli, 2019).

Histological evidence demonstrates 90% of immune cells in these inflammatory lesions are of myeloid origin (monocytes, monocyte-derived macrophages and microglia) and the remaining 5-10 % are compromising various lymphocyte subsets inflammation and large numbers of T cells (CD8+ T cells > CD4+ T cells) infiltrate the CNS parenchyma (Meinl, Krumbholz, & Hohlfeld, 2006). It is generally believed this inflammatory response is initiated in the CNS by autoantigen-specific CD4+ T cells. Reactivation of these T cells by professional antigen presenting cells within CNS triggers production of cytokines that orchestrate recruitment of peripheral immune cells across blood-brain and blood-CSF barriers (BBB) (Lucchinetti *et al.*, 2011; Lassmann, 2014; Perriard *et al.*, 2015; Setiadi *et al.*, 2019). These inflammatory lesions are associated with demyelination characterised by the presence of complement activation products, immunoglobulins and phagocytes laden with myelin debris (Breij *et al.*, 2008; Geurts and Barkhof, 2008), as well as widespread axonal injury and loss (Trapp et al., 1998). This axonal pathology is the underlying cause of clinical deficits in MS, but nonetheless MS is still considered a primary demyelinating disease. Loss of myelin not only disrupts axonal function per se, but also increases axonal susceptibility to inflammatory mediators whilst at the same time disrupting metabolic/trophic support normally provided by oligodendrocytes via the myelin sheath. A combination of effects believed to induce profound energy deficits that compromise the function and survival of affected axons (Brück, 2005; Fünfschilling et al., 2012; Lee et al., 2012).

Multiple effector mechanisms can contribute to demyelination and axonal injury in EAE, but their relative importance in driving lesion development in MS remains controversial (Constantinescu, Farooqi, O'Brien, & Gran, 2011; Gold, Linington, & Lassmann, 2006; Schuh et al., 2014). Nonetheless a consensus exists that tissue damage is initially dependent on recruitment and activation of immune cells in the CNS. Although it remains to be determined precisely how this inflammatory response leads to demyelination and axonal loss (Krementsov, Thornton, Teuscher, & Rincon, 2013; Lassmann, 2014). At early stages of lesion development axons are relatively preserved but over time sustained or repeated

inflammatory activity leads to irreversible axonal damage, the underlying cause of chronic disability in MS (Trapp *et al.*, 1998; Brück, 2005). Unravelling the mechanistic basis of tissue damage in these lesions is complicated by their immunopathological heterogeneity. Four distinct patterns of demyelination were defined on the basis of immunopathological criteria and attributed to different effect mechanisms (Lucchinetti *et al.*, 2000; Lassmann, Brück and Lucchinetti, 2007). Demyelination in Pattern I lesions is attributed to a T cell-mediated inflammatory response. Pattern II is similar to pattern I but accompanied by immunopathological evidence for antibody-mediated, complement-dependent demyelination and is the most prevalent being present in approximately 50% of cases (C. Lucchinetti et al., 2000). Pattern III lesions are characterised by selective loss of immune reactivity for myelin associated glycoprotein (MAG) and oligodendrocyte death at the active edge of lesions, whilst Pattern IV lesions are associated with oligodendrocyte death within periplaque white matter. The fine details of this classification scheme and its relationship to disease activity and lesion repair remain controversial (Chandran et al., 2008; Frischer et al., 2015; Lassmann et al., 2007). Although it appears remyelination is more frequent in cases associated with Patterns I and II (Chandran et al., 2008), whilst Pattern IV is far more frequent in patients diagnosed with PPMS (Popescu, Pirko, & Lucchinetti, 2013).

#### 1.1.2.2 Progressive multiple sclerosis

A majority of patients with RRMS will progress to develop secondary progressive MS (SPMS) within 20 years of disease onset. This is characterised by a continuous and often insidious increase in neurological disability in the absence of acute inflammatory episodes in the CNS as defined by MRI and neuropathological criteria. In view of this lack of evidence for acute inflammatory flares in SPMS it is perhaps not surprising the majority of patients do not benefit from current immunomodulatory, “anti-inflammatory” DMT’s (Ciotti & Cross, 2018; Faissner, Plemel, Gold, & Yong, 2019). In addition to SPMS, approximately 10% of patients present with a progressive disease course from the onset which is classified as primary progressive MS (PPMS) (Tutuncu et al., 2013).

In progressive MS lesions slowly expand leading to an increasing burden of neurological deficits due to irreversible axonal injury (Sáenz-Cuesta, Osorio-

Querejeta, & Otaegui, 2014). Immunohistological studies demonstrate this is associated with low grade inflammation in the absence of pronounced perivascular infiltrates of inflammatory cells recruited from the periphery, a pathological hallmark of RRMS (Confavreux, Vukusic, Moreau, & Adeleine, 2000; Gold et al., 2006). Demyelination and axonal loss in these lesions is associated with a pronounced microglial response (Trapp *et al.*, 1998; Confavreux *et al.*, 2000; Magliozzi *et al.*, 2007) and in white matter, infiltrating B and T lymphocytes (Frischer et al., 2009; Kutzelnigg et al., 2005). However, the extent of lymphocyte recruitment from the periphery is far lower than in RRMS. Phagocytes containing myelin debris are relatively scarce suggesting a slow rate of demyelination (Kutzelnigg et al., 2005), but when these studies were published there were no markers available to distinguish between resident microglia and invading myeloid cells. It therefore remains to be clarified whether these cells are microglia or monocyte-derived macrophages recruited from the periphery.

Grey matter lesions in particular cortical demyelination is a common and extensive feature of progressive multiple sclerosis (Kutzelnigg et al., 2005). These are also characterised by a pronounced microglial response at sites of ongoing demyelination and axonal damage that occur in the absence of large numbers of infiltrating lymphocytes. The role of microglia and their relationship to tissue injury in these lesions remains uncertain. Specifically the question remains do microglia actively contribute to tissue damage, or does microgliosis reflect their response damage mediated by some other mechanism? Cortical demyelination is often extensive in SPMS and in many cases is associated with inflammation and B cell follicle-like structures in the adjacent meninges suggesting this drive cortical pathology (S. R. Choi et al., 2012; Serafini, Rosicarelli, Magliozzi, Stigliano, & Aloisi, 2004). This may well be the case, but in view of the pathological heterogeneity of MS this probably represents just one facet of the mechanisms contributing to disease pathogenesis. Moreover, PPMS is also associated with cortical and other grey matter tracts but in this case B cell follicles are rare or possibly absent (Choi *et al.*, 2012).

### 1.1.3 Treatments

All current treatments for MS are immunomodulatory in nature and act primarily by reducing inflammatory activity in the CNS. As a consequence they have little or no impact on accumulation of disability in patients with progressive forms of the disease (Gholamzad et al., 2019). The only exception is ocrelizumab (Ocrevus®) that the US Food and Drug Administration approved as a treatment for PPMS and SPMS in 2017 (S. L. Hauser et al., 2017; Montalban et al., 2017). Approval was subsequently granted by the European Commission for ocrelizumab for treatment of RRMS and early active PPMS a year later. The efficacy of B cell depletion in MS was first reported in 2008 (Stephen L. Hauser et al., 2008) and provided unexpected new insights into the critical role played by B cells in disease pathogenesis (Lehmann-Horn, Kinzel, & Weber, 2017). Unfortunately whilst highly effective treatments are now available for RRMS, and to a limited extent progressive forms of the disease (Table 1.1), their efficacy is limited by factors including cost, adverse effects and large populations of non-responders. This identifies a large unmet clinical need that can only be met by increasing our understanding of the aetiology and pathogenesis of MS.

| **Treatment**<br>**Year approved** | **Efficacy** | **Mechanism of action** |
|---|---|---|
| Ocrelizumab<br>(RRMS,PPMS)<br>2017 | 46% reduction in relapses (RRMS), 40% reduction in progression of disability (RRMS), 30-36 % reduction in disability over 6 months (PPMS) | Anti-CD20 mediated B cell depletion |
| Daclizumab<br>(RRMS) 2016<br>DISCONTINUED | 41% reduction in relapses | Anti-IL-2rα mediated T cell depletion |
| Dimethyl fumarate<br>(RRMS) 2013 | 50% reduction in relapses, reduces progression of disability | Unclear, immunomodulatory and immunoprotective, |
| Alemtuzumab<br>(RRMS) 2013 | 78% reduction in relapses, 71% reduction in disability progression | Anti-CD52 mediated lymphocyte depletion |
| Teriflunomide<br>(RRMS) 2012 | 30% reduction in relapses and disability progression | inhibition of T and B cell proliferation |
| Fingolimod<br>(RRMS) 2010 | 50% reduction in relapses, 70% reduction in new lesions, brain atrophy slowed by 30% | Sequestration of lymphocytes in lymph nodes by sphingosine-1 phosphate inhibition |
| Natalizumab<br>(RRMS) 2004 | 68% reduction in relapses, 42% reduction in disability progression | Prevents lymphocyte recruitment across the BBB by α4β1-integin blockade |
| Mitoxantrone<br>(RRMS, SPMS) 2000 | Reduces probability of relapses, new lesion formation, and progression of disability | Reduced immune cell proliferation by Inhibits DNA synthesis reduces immune cell proliferation |
| Glatiramer acetate<br>(RRMS) 1997 | Reduces relapses, no effect on progression of disability | MBP mimetic, promotes Treg expansion |
| β interferons<br>(RRMS) 1993 | 30% reduction in relapses, effective in 70% of patients | Reduced expression of pro-inflammatory cytokines, increases expression of anti-inflammatory cytokines and nerve growth factor, reduces CNS inflammation |
| Plasma exchange<br>(RRMS) 1980 | Improves recovery from acute steroid resistant relapses | Reduced levels of circulating lymphocytes and immunoglobulins |
| Corticosteroids<br>(RRMS) 1950s | Shortens relapse duration | General anti-inflammatory and immunosuppressive |

**Table 1.1. Table showing the current approved therapies in MS**. Adapted from MS trust and Weiner *et al.*, 1983; Gholamzad *et al.*, 2019.

## 1.2 Experimental autoimmune encephalomyelitis

Our current understanding of the mechanistic basis of inflammatory demyelination in MS derives almost completely from studies on experimental autoimmune encephalomyelitis (EAE), an animal model that can reproduce many of the clinical and pathological features of MS. In its simplest form EAE is a $CD4^+$ T cell mediated autoimmune disease of the CNS in which inflammation is accompanied by varying degrees of demyelination and axonal injury (Gold et al., 2006). However, its pathophysiology and clinical manifestations are critically dependent on variables including genetic factors i.e. the species and strain in which disease is induced; the nature of the immunogen used to induce disease (e.g. whole CNS tissue homogenates versus CNS proteins or peptides and the composition of the adjuvant in which these are emulsified, or adoptive transfer of activated T cells); and route of immunization (Gold et al., 2006). Faced with this variability it is important to employ the EAE model most appropriate to investigate a specific question such as the effect of different therapeutic strategies on disease onset and severity (Gold et al., 2006). However, this is a very simplistic view as there are crucial differences between EAE and MS. The most evident one is being EAE is an induced autoimmune disease, whilst MS is spontaneous and what triggers disease development in susceptible individuals remains unknown. Several spontaneous models of EAE do now exist but these all require transgenic manipulations to counteract intrinsic regulatory mechanisms that normally suppress autoaggression (Waldner et al., 2000; Zehntner et al., 2003). In addition, most protocols used to induce EAE require a strong adjutant, an intense “immunological boost” which biases the T cell response to favour an encephalitogenic Th1/Th17 phenotype (Gold et al., 2006; Kerschensteiner et al., 2004). It is rather improbable this occurs under physiological conditions in man, even during infections. Finally to improve reproducibility EAE is mainly induced in inbred laboratory rodents, although MS patients are genetically heterogeneous (Gold et al., 2006). For these reasons one must interpret EAE data cautiously when extrapolating them to the situation in MS. Despite these constraints EAE has provided many insights into the pathogenesis of T cell mediated neuroinflammation and was used widely to develop new therapies.

Historically the first species reported to develop encephalomyelitis following sensitisation with nervous system antigens was the man. This occurred as a

complication of using dried spinal cord tissue from of rabies-infected rabbits to generate a rabies vaccine (Mackay & Anderson, 2010; Sabin & Wright, 1934). This resulted in some patients developing a demyelinating encephalomyelitis triggered by an autoimmune response to spinal cord contaminants in the vaccine. To gain a better understanding of the pathogenesis of this form of encephalomyelitis Rivers and colleagues injected primates and rabbits repeatedly with CNS tissue homogenates (Rivers & Schwentke, 1935). In some case this resulted in inflammatory demyelinating lesions similar to those seen in patients with MS. However, induction of reproducible models of EAE only became available following the introduction of complete Freund's adjuvant (CFA) to generate encephalitogenic emulsions (Mackay & Anderson, 2010).
Active EAE is induced in susceptible species/strains by immunization with CNS tissue homogenates, CNS myelin proteins or peptides (e.g. MBP, PLP, MOG) emulsified in complete Freund's adjuvant (CFA) (Stromnes & Goverman, 2006). Disease incidence is generally high and the first clinical signs of disease generally develop 9 to 14 days post immunization. The subsequent course of disease, its severity and pathology are then determined by the genetic background of the animal and the encephalitogen used to induce disease (Gran, O'Brien, Fitzgerald, & Rostami, 2008). A classical example is the response of strain 13 guinea pigs to immunization with MBP or CNS homogenate in CFA; the former results in acute monophasic and predominantly inflammatory disease whilst the latter initiates a chronic relapsing–remitting variant of EAE associated with development of macroscopic plaques of persistently demyelinated scar tissue (Alvord, Driscoll, & Kies, 1982). Relapsing-remitting disease can also be induced by immunizing SJL/J mice with PLP139-151, a disease course characterised by an expanding TCR repertoire to new myelin componenets following relapses , phenomenon known as epitope spreading (McRae, Vanderlugt, Dal Canto, & Miller, 1995).
EAE can also be induced by passive or adoptive transfer of encephalitogenic $CD4^+$ T cells harvested from actively immunised donors into syngeneic recipients (Stromnes & Goverman, 2006). Adoptive-transfer EAE models were of tremendous help in dissecting how myelin-reactive encephalitogenic T cells drive disease pathogenesis (Pettinelli & McFarlin, 1981). These models have the advantage they bypass the induction phase of EAE allowing elucidation of events contributing to the effector phase of disease. As previously described for MS,

EAE lesion pathology varies based on what animal strain was used (Gran et al., 2008). Table1.2 describes commonly used EAE models and their applicability to MS.

Spontaneous models of EAE have been developed using transgenic approaches that overcome regulatory events that normally subdue tissue-specific autoimmunity (Gold et al., 2006). Lafaille et al. generated a spontaneous EAE model by backcrossing TCR transgenic mice specific for myelin basic protein with *Rag-1*$^{-/-}$ mice, creating a strain where only T cells and no other lymphocytes express the transgenic TCR. These transgenic animals developed spontaneous EAE with varying disease course, but no remission (Lafaille, Nagashima, Katsuki, & Tonegawa, 1994). More recently other groups have created models of spontaneous EAE by generating transgenic TCRs targeting other CNS antigens using similar approaches as Lafaille et al. (Bettelli et al., 2003; Waldner et al., 2000).

In addition to EAE, viral models of inflammatory demyelination that mirror MS-like features are also employed (Lassmann & Bradl, 2017). The most common viral chronic encephalomyelitis models are induced by Theiler's virus (TMEV) or mouse hepatitits corona virus (MHV). These models allowed identifying the roles of different lymphocyte types in the inflammatory-demyelination process and axonal injury (Lassmann & Bradl, 2017). To study demyelination, remyelination and axonal degeneration in the absence of inflammation serveral toxic models were developed. The cuprizone, lysolecithin and ethidium bromide models were of tremendous use due to their reliable demyelination and remyelination timeline and well-defined pathomechanisms of demyelination (Lassmann & Bradl, 2017; Praet et al., 2014).

| Model | Analogy to human disease | Differences from human disease | Additional comments |
|---|---|---|---|
| Lewis rat Active EAE (CNS myelin, MBP, MOG, PLP | T cell inflammation and weak antibody response | Monophasic, little demyelination | Reliable model, commonly used for therapy studies. Whit guinea-pig MBP little demyelination |
| Adoptive transfer EAE (MBP, S100, MOG, GFAP) | Marked T cell inflammation. Topography of lesions | Monophasic, little demyelination | Homogenous course, rapid onset. Differential recruitment of T cells/ macrophages depending on autoantigen |
| Active EAE or Adoptive transfer EAE + co-transfer of anti MOG antibodies | T cell inflammation and demyelination | Only transient demyelination | Basic evidence for role of antibodies in demyelination |
| Congenic Lewis, DA, BN strains Active EAE (recombinant MOG aa 1–125) | Relapsing–remitting disorders, may completely mimic histopathology of multiple sclerosis and subtypes | No spontaneous disease | Chronic disease course, affection of the optic nerve, also axonal damage similar to multiple sclerosis |
| Murine EAE (SJL, C57BL/6, PL/J, Biozzi ABH) Active EAE (MBP, MOG, PLP and peptides) | Relapsing–remitting (SJL, Biozzi) and chronic-progressive (C57BL/6) disease courses with demyelination and axonal damage | No spontaneous disease | Pertussis (toxin) required for many strains, whilst it is often not needed for SJL and some Biozzi EAE models. Higher variability of disease incidence and course, often cytotoxic demyelination in C57BL/6. With rat MBP inflammatory vasculitis with little demyelination |
| Murine EAE in transgenic mice or knockout mice (mostly C57BL/6 background) | Specifically addresses role of defined immune molecules/neurotrophic cytokines/ neuroanatomical tracts | Most results obtained with artificial permanent transgenic or knockouts | Extensive backcrossing (>10 times) on C57BL/6 background required. |

**Table 1.2. Commonly used rodent models of EAE.** Adapted from (Gold et al., 2006)

## 1.3 GM-CSF

GM-CSF is a pleotropic growth factor and immune modulator (Hamilton, 2002). It was discovered in conditioned medium from lung tissue isolated from mice treated with lipopolysaccharide and shown to stimulate formation of granulocytes and macrophages from mouse bone marrow (Burgess, Camakaris, & Metcalf, 1977). The GM-CSF gene (*CSF2*) is located on chromosome 5q22-31 in humans in close proximity *CSF1*, *IL-3*, *IL-4*, and *CSF1R* (Van Leeuwen, Martinson, Webb, & Young, 1989). The human gene has four exons (Wong et al., 1985) and its murine homologue (*Csf2*) is located on chromosome 11 (Gough, Metcalf, Gough, Grail, & Dunn, 1985).

GM-CSF is produced as a small monomeric protein that exists in different glycosylation states due to the presence of with six glycosylation sites; O-linked at amino acid residues 22, 24, 26, and 27, and N-linked at amino acid residues 44 and 54 (Forno et al., 2004). The functional significance of glycosylation remains unknown, but because of different degrees of glycosylation the molecular mass of GM-CSF ranges from 14 to 35 kDa (Burgess et al., 1977). Human and murine GM-CSF are derived from a larger pre-protein containing a classical hydrophobic signal peptide. The amino acid sequence is species specific, human and murine GM-CSF contain 127 and 124 amino acid residues respectively, but exhibit an amino acid sequence homology of only with 56%. GM-CSF is present in normal human serum both as free cytokine, but also bound to naturally occurring GM-CSF-specific antibodies (Uchida et al., 2009). It can also complex with heparan sulphate proteoglycans in the extracellular matrix or expressed at the cell surface (Coombe, 2008).

GM-CSF is a key regulator of steady state/ systemic myelopoiesis as well as acting as a pro-inflammatory cytokine. It is produced by a variety of cell types, including macrophages, monocytes, T-cells, mast cells, fibroblasts, natural killer (NK) cells, and endothelial cells (Aram et al., 2019). Its expression is modulated by other cytokines and pattern/damage associated molecular patterns. The major cytokines influencing GM-CSF expression by T cells can be found in table 1.3. Additionally, depending on the cellular source GM-CSF expression is also stimulated by LPS, ionomycin, epidermal growth factor (EGF) and IgE (Griffin et al., 1990) and in the case of microglia, IFN-γ (Olson & Miller, 2004).

| Cytokine | Effect on GM-CSF prodution | Reference |
|---|---|---|
| IL-2 | stimulation | Noster et al. 2014 |
| IL-12 | stimulation on Th1 cells<br>inhibition on Th17 cells | Codarri et al. 2011<br>Noster et al. 2014<br>Grifka-Walk et al. 2015 |
| IL-23 | stimulation on Th17 cells | Codarri et al. 2011<br>El-Behi et al. 2011 |
| IL-4 | inhibition | Jansen et al. 1989<br>Codarri et al. 2011 |
| IL-10 | inhibition | Sagawa et al. 1996 |
| TGF-ß | inhibition | Jacobsen et al. 1991 |
| IFN-γ | no effect on Th1 cells<br>inhibition on Th17 cells | Codarri et al. 2011<br>Noster et al. 2014<br>Grifka-Walk et al. 2015 |
| IL-27 | inhibition on Th1 cells | Young et al. 2011 |
| IL-1ß | stimulation | Lukens et al. 2012 |
| TNF-α | stimulation | reviewed by Hamilton, 2008 |
| IL-7 | stimulation | Sheng et al. 2014 |

**Table 1.3. GM-CSF production regulation by major cytokines**. Adapted from (Aram et al., 2019)

### 1.3.1 GM-CSF receptor and signal transduction

Signal transduction by GM-CSF is mediated by high-affinity binding to the GM-CSF receptor (GM-CSFR). GM-CSFR is a heterodimer composed of GM-CSF-specific, but low affinity α chain (CD116), and a high affinity ß chain (CD131) which is shared with receptors for IL-3 and Il-5 (Hayashida et al., 1990a) (Figure 1.1). Based on structural and functional evidence the current model of GM-CSF signalling proposes the GM-CSFRß induces affinity conversion and is the main signal transducer of the receptor complex (Gearing, King, Gough, & Nicola, 1989). Initially, GM-CSF binds to its specific α chain with low affinity to generate GM-CSF/GM-CSFRα binary complexes that are then transformed to a high-affinity state by recruitment of preformed ß chain dimers to generate a 2:2:2 hexameric complex (Hayashida et al., 1990b; Hercus et al., 2009). GM-CSFR lacks intrinsic kinase activity and signalling is conveyed by the initiation of

the receptor dodecamer complex. GM-CSFß transduces the signal by binding to JAK2, which autophosphorylates and mediates phosphorylation of specific tyrosine and serine residues within the GM-CSFRß cytoplasmic tail (Figure 1.1). The absence of JAK2 or alternatively GM-CSFß mutations that impede JAK2 binding, abolish GM-CSF signalling (Quelle et al., 1994). The major pathways downstream of GM-CSF receptor activation that are responsible for its biological effects are JAK2/STAT5 (Janus Kinase 2/ Signal Transducer and Activator of Transcription 5), MAPK (mitogen-activated protein kinase), and PI3K (phosphoinositide 3-kinase) pathways (Carr et al., 2001).

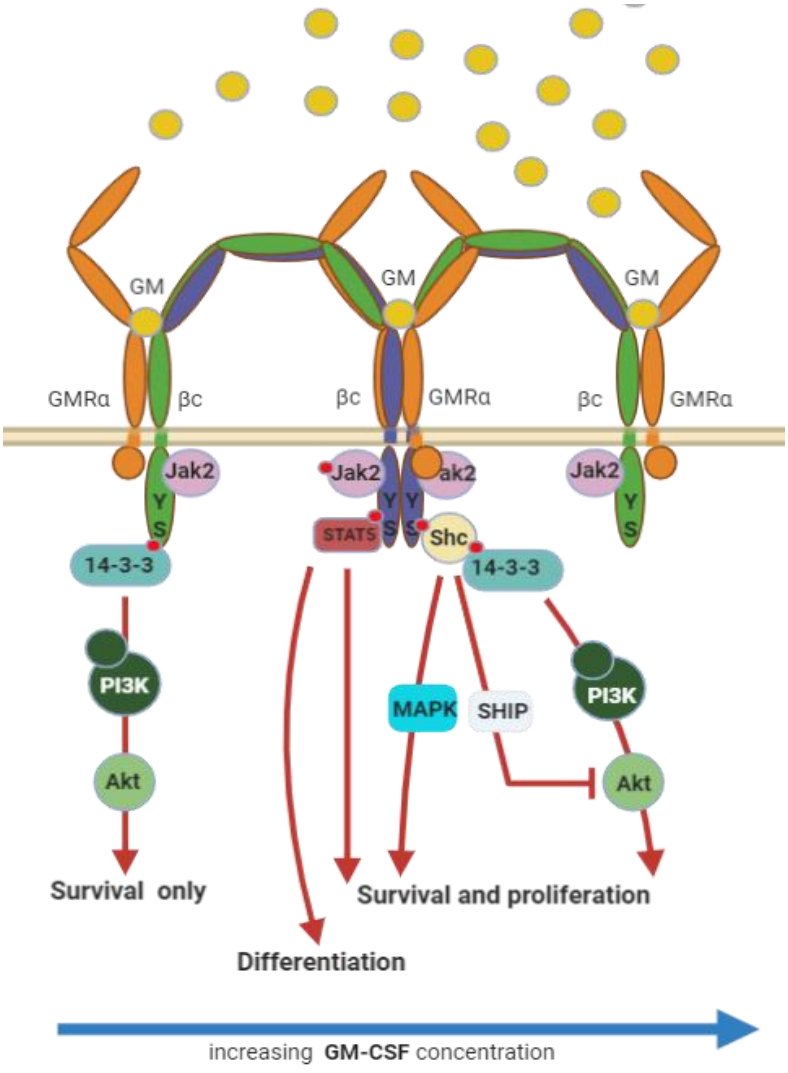


**Figure 1.1. Signal transduction through the GM-CSF receptor**. To initiate signal transduction GM-CSF binds to its high affinity receptor subunit GMRα. The GM-CSF/ GMRα complex binds to preformed homodimers of the common ß subunit (ßc) which have consitutively bound Jak2. Jak2 autophosphorylates and mediates signalling via the intracytoplasmic ßc tail which includes the mutual exclusive phosphorylation of residues tyrosine[577] (Y) and serine[585] (S). Phosphorylation of these two residues are necessary for

GM-CSF signal transduction. Low GM-CSF concentrations (0.01-10 pM) induce phosphorylation of serine$^{585}$ which recruits the adapter protein 14-3-3 leading to sigalling via PI3K and Akt promoting cell survival. Conversely, high GM-CSF concentration (above 10 pM) prompts phosphorylation tyrosine$^{577}$ which conveys the signal through STAT5 and Shc leading to cell survival, differentition and proliferation. Adapted from (Hercus et al., 2009; Trapnell et al., 2009). Diagram created in Biorender.

GM-CSFR is expressed on myeloid cells and some cells of non-haematopoietic origin such as endothelial cells, but is absent on lymphocytes (Prevost et al., 2002). There is a lack of consensus regarding expression of GM-CSFR outside of the immune system during steady state. In the healthy human CNS it was reported GM-CSFR is present on a small subset of activated microglia and astrocytes (Vogel et al., 2015), although others suggest GM-CSFRα is also present in astrocytes, ependymal choroid plexus cells and ubiquitously in grey matter neurons (Ridwan, Bauer, Frauenknecht, Von Pein, & Sommer, 2012). However, Vogel *et al*. (2015) were unable to identify GM-CSFR in normal grey matter (Vogel et al., 2015). A functional GM-CSFR was also reported on cultured rat oligodendrocytes (Baldwin, Benveniste, Chung, Gasson, & Golde, 1993), although transcriptional studies indicate only microglia can express functional GM-CSFR in postnatal murine brain (Y. Zhang et al., 2014).

### 1.3.2 GM-CSF expression and function

GM-CSF is expressed at a low basal level in healthy rodents, but it is rapidly up regulated in response to infection, inflammation and autoaggression (Becher, Tugues, & Greter, 2016; Yifan Zhan, Lieschke, Grail, Dunn, & Cheers, 1998). The main sources of GM-CSF are: macrophages, monocytes, T-cells, mast cells, fibroblasts, natural killer (NK) cells, and endothelial cells (Aram et al., 2019). These sources were identified primarily in *in vitro* experiments in which cells were stimulated with cytokines or pathogen associated molecular patterns (PAMPs).*In vitro,* GM-CSF promotes survival, differentiation and proliferation of monocytes/macrophages and granulocytes (Figure 1.1) (Gasson, 1991) . Because of overlapping functions with other cytokines, the homeostatic functions and sources of GM-CSF in healthy mammals are still under debate (Becher et al., 2016), although it is clear that in the lung GM-CSF is produced primarily by epithelial cells.

The most obvious characteristic of mice in which GM-CSF signalling is disabled (GM-CSF or GM-CSFR KO mice) is pulmonary alveolar proteinosis (PAP), no haematological and extra-pulmonary immune abnormalities were observed. PAP is characterized by accumulation of lipid and protein surfactant within the alveolar spaces caused by a lack or dysfunction of alveolar macrophages (Dirksen et al., 1998; Robb et al., 1995). Alveolar macrophages originate from foetal monocytes in the foetal liver and GM-CSF is crucial for their differentiation and maturation (Guilliams et al., 2013). The same study demonstrated alveolar macrophages require GM-CSF signalling to catabolise pulmonary surfactant (Guilliams et al., 2013). Additionaly, GM-CSF KO or GM-CSFR KO mice are more susceptible to pulmonary infections due to impaired alveolar macrophage function. GM-CSF $^{-/-}$ and GM-CSFR $^{-/-}$ alveolar macrophages exhibit decreased clearing of bacteria, fungi and viruses. GM-CSF deficient pulmonary macrophages showed reduced phagocytosis, cells adhesion, internalization of viruses and production of superoxide (LeVine, Reed, Kurak, Cianciolo, & Whitsett, 1999; Paine et al., 2000). Altough GM-CSF$^{-/-}$ and GM-CSFR$^{-/-}$ animals presented an exgerated inflammatory response in the lung when chanllenged with pathogens, GM-CSF$^{-/-}$ and GM-CSFR$^{-/-}$ alveolar macrophages did not produce TNF-α when challenged with LPS. On the same note, GM-CSF$^{-/-}$/ GM-CSFR$^{-/-}$ alveolar macrophages presented decreased expression of pathogen-associated molecular patterns such as the Toll-like receptors TLR4 and TLR2, but also the mannose receptor (Shibata et al., 2001). The symptoms presented by mice lacking GM-CSF signalling are consistent with human pulmonary proteinosis, a primary immunodeficiency characterised by the production of GM-CSF autoantibodies or disruptions in GM-CSFR signalling (Trapnell et al., 2009). These observations highlight the role of GM-CSF in lung homestasis and innate immune defense.

More recently it has been shown that mice deficient in GM-CSF signalling also have reduced numbers of non-lymphoid-tissue cDCs (conventional dendritic cells) in the lung, as well as intestine and dermis indicating GM-CSF is also important the development and/or survival of these cells (Greter et al., 2012). Additionally, it was demonstrated that GM-CSFR signalling was required in lung DCs to mount a CD8 $^{+}$ T cell response following immunazation with particulate antigens (Greter et al., 2012). Altogether, GM-CSF is generally considered inessential for steady-state myelopoiesis (Becher et al., 2016).

GM-CSF is also involved in non-haematopoietic functionas such as the maintenance and growth of lung epithelial cells. Overexpression of GM-CSF in this subset of epithelial cells resulted in increased lung size and weight (Huffman Reed et al., 1997). Histological assessment of lung tissue in mice with the same genotype as mentioned above showed that GM-CSF overexpression prevented hyperoxic lung injury (Paine et al., 2003). Additionally, GM-CSF treatment in wild type mice during hyperoxic lung injury reduced apoptosis of pulmonary cells (Paine et al., 2003).

### 1.3.3 GM-CSF in disease

As stated above GM-CSF is present at very low levels in systemic circulation (Becher et al., 2016; Yifan Zhan et al., 1998). Conversely, GM-CSF is produced locally at inflammation sites. The current consensus suggests that GM-CSF is involved in emergency haematopoiesis during infection/inflammation by stimulating production and survival of monocytes and granulocytes and their functional activation and/or priming at the site of insult (Hercus et al., 2009). For example, skin biopsies from patients with late-phase cutaneous reactions present increased levels of GM-CSF (Kay et al., 1991). Elevated concentrations of GM-CSF have also been detected in tissues from patients with autoimmune diseases including synovial fluid from rheumatoid arthritis patients and in CSF from patients with multiple sclerosis (Carrieri et al., 1998; Williamson, Begley, Vadas, & Metcalf, 1988). Experimentally, the level of circulating GM-CSF in mice can be raised by injecting endotoxin (Sheridan & Metcalf, 1972). Clinical observation and experimental data from animal models emphasize the role of GM-CSF in promoting and supporting inflammation (Becher et al., 2016). The experiments performed for thesis aimed to explore the mechanism through which GM-CSF mediate tissue damage in the CNS with respect to MS and EAE, so from now we will explore the available evidence involving GM-CSF in the pathogenesis of MS and EAE.

#### 1.3.3.1 GM-CSF in MS and EAE

Preclinical and clinical data support involvement of GM-CSF in the pathogenesis of MS and its animal model, EAE. Initial studies identified GM-CSF a non-redundant cytokine required to induce EAE in mice, but more recent studies

indicate its relative importance is strain and/or model dependent. As a consequence its role was revised and it is now considered a key communicator between pathogenic lymphocytes and inflammatory myeloid cells (Komuczki et al., 2019).

Studies indicating GM-CSF plays a non-redundant role in induction of EAE were performed using the MOG peptide induced model in wild type and *Csf2*$^{-/-}$ C57BL/6 mice. During the prodromal stage of disease the number of infiltrating immune cells was similar wild type and *Csf2*$^{-/-}$ mice, but in the absence of GM-CSF this incipient inflammatory response was unable to support a full blown inflammatory response in the CNS and clinical disease activity was minimal. It was concluded from these studies that GM-CSF deficient mice are resistant to EAE (Codarri et al., 2011; McQualter et al., 2001; Ponomarev et al., 2007). This concept was supported by experiments demonstrating GM-CSF neutralizing antibodies abrogated disease activity (McQualter et al., 2001) whilst systemic administration of GM-CSF accelerated disease onset (Marusic et al., 2002; McQualter et al., 2001). Hesske *et al*. also found that treating mouse primary microglia cultures with GM-CSF induces their differentiation into inflammatory dendritic cells suggesting this was how it contributed to disease development (Hesske et al., 2010). To emphasize the crucial role of T cell derived GM-CSF in EAE, and potentially in MS, Ponomarev *et al*. (2007) demonstrated that myelin basic protein (MBP)-specific T cells from GM-CSF deficient mice were unable to adoptively transfer EAE to wild type mice (Ponomarev et al., 2007). Very recently a discrete GM-CSF expressing Th cell subset was identified in which GM-CSF expression is under the control of IL-23 and IL-1ß. In agreement with previous studies selective ablation of this Th cell subset reduced accumulation of phagocytes but not T cells in the CNS of mice with EAE. An observation indicating GM-CSF is not just a marker for encephalitogenic T cells, but plays an important role in mediating inflammatory demyelination (Komuczki et al., 2019). On a similar note, conditional induction of GM-CSF in mature peripheral $CD4^+$ T cells triggers a neuroinflammatory response characterised by myeloid cell recruitment, production of ROS and spontaneous neurological deficits (Spath et al., 2017).

In contrast, another study reported adoptive transfer of wild-type MOG–auto-reactive T cells in to *Csf2*$^{-/-}$ mice resulted in monophasic disease characterised by an attenuated disease course, reduced recruitment of immune cells and less tissue damage in the CNS (Duncker, Stoolman, Huber, & Segal, 2018). Observations that led the authors to conclude: "*GM-CSF drives chronic tissue damage and disability in EAE via pleiotropic pathways, but it is dispensable during early lesion formation and the onset of neurologic deficits...*". Further evidence of GM-CSF redundancy was obtained in an adoptive transfer model of EAE in C3HeB/FeJ mice (Pierson & Goverman, 2017). In this case, lack of GM-CSF signalling did not prevent EAE due to an IL-17 compensatory mechanism. In this model a critical step in disease development is GM-CSF mediated neutrophil recruitment into the brain, but disrupting GM-CSF signalling did not prevent EAE due to an IL-17 compensatory mechanism. This highlights the heterogeneity of EAE and how genetic background influences the relative importance of specific effector pathways in disease development inbred strains of mice (Pierson & Goverman, 2017). It is important to bear this in mind when attempting to extrapolate these observations to MS, for which EAE is at best an incomplete model.

Nonetheless there is an increasing body of evidence implicating T- and B-cell derived GM-CSF as a factor contributing to the immunopathogenesis of MS. $CD4^+$ Th cells are believed to play a key role in MS pathogenesis and their production of GM-CSF is stimulated by interleukin-2 (IL-2) expression of which is elevated in MS lesions. Moreover, *IL2RA* polymorphisms are important risk factors of MS (Hafler et al., 2007; Rose et al., 2007). Binding of IL-2 to its receptor stimulates STAT5 dependent production of GM-CSF by human Th cells *in vitro* and intriguingly, *IL2RA* MS-associated polymorphisms enhance the number of GM-CSF producing Th cells in healthy individuals (Hartmann et al., 2014). These observations led Hartmann and colleagues to speculate this represents a mechanistic connection between an immunologically relevant genetic risk factor and a pathologically important Th subset in MS (Hartmann et al., 2014).

The role of STAT5 in determining encephalitogenicity of autoreactive Th cells was reinforced by studies in EAE (Sheng et al., 2014). This group reported Il-7-activated STAT5 promotes GM-CSF secretion by Th cells and this was strikingly

diminished in STAT5 deficient $CD4^+$ T cells. Additionally, adoptive transfer of *in vitro* polarised MOG-reactive $CD4^+$ T cells into *Rag2*$^{-/-}$ mice identified GM-CSF-secreting Th cells as the most encephalitogenic when compared to traditional Th1 and the Th17 T cell subsets. These GM-CSF-producing cells potentially constitute a new Th cell subset with a unique differentiation and cytokine profile, defined in part by GM-CSF as a signature cytokine and co-expression of interleukin-3 (Sheng et al., 2014). The potential clinical significance of these observations is only now becoming apparent following reports that GM-CSF is present at considerably high levels in plasma and cerebrospinal fluid of patients with relapsing-remitting MS (Carrieri et al., 1998); GM-CSF immune reactive T cells are present in MS lesions (Vogel et al., 2015, 2013); the frequency GM-CSF producing T cells is increased in MS patients ( Rasouli *et al.*, 2015; Restorick *et al.*, 2017; Imitola *et al.*, 2018; Ghezzi *et al.*, 2019) ;and the recent identification of a disease associated subset of Th cells co-expressing GM-CSF and CXCR4 (Galli et al., 2019). The most obvious target for T cell derived GM-CSF within the CNS are microglia and macrophages, a view supported by the observation the phenotype of human macrophages exposed to GM-CSF *in vitro* is comparable in their expression of MHC II, CD40 and MR (mannose receptor) to macrophages present in MS lesions (Vogel et al., 2015).The same group also found the GM-CSF receptor on microglia in astrocytes and neurons in the rim of gray/white matter lesions  These *in vitro* and *in vivo* data support the conclusion that GM-CSF produced by T cells in the periphery has an important role in the hyperactivation of the immune system in MS (Carrieri et al., 1998; Rasouli et al., 2015; Vogel et al., 2013).

There are also strong links between GM-CSF and B cell biology, a subject of increasing interest following the demonstration B cell depletion abrogates inflammation and clinical disease activity in MS. Harris *et al.* found GM-CSF promotes the survival of normal and malignant B cells in an autocrine fashion (Harris et al., 2000) and also behaves as a differentiation factor for cultured murine B cells. When combined with dextran-conjugated anti-IgD antibodies (alpha delta-dex), GM-CSF increases the IgM secretion in resting murine B cells, compared to alpha delta-dex, IL-1, and IL-2 only stimulation (Snapper et al., 1995). There is a growing interest in clarifying the role of cytokine-defined B cell subsets in the pathogenesis of MS.  It has been shown that abnormal cytokine

production by B cells plays an important role in disease pathogenesis (Bar-Or et al., 2010). In MOG-induced EAE, Hesske *et al*. demonstrated that subcortical injection with GM-CSF-producing B16 cells (mouse melanoma cells) promoted the accumulation of dendritic cells and exacerbated the disease (Hesske et al., 2010). Recently, Li *et al.,* identified a subset of pro-inflammatory GM-CSF-producing B cells in patients with MS and found following B cell depletion pro-inflammatory myeloid responses also diminished, presumably due to the loss of B cell derived GM-CSF (R. Li et al., 2015). The same group also found reciprocal regulation of GM-CSF and IL-10 production by human B cells via STAT5/6 signalling. Individual or combined inhibition of STAT5/6 strikingly decreased the induction and production of GM-CSF, while simultaneously increasing IL-10 production. It was also elucidated that GM-CSF is capable of inducing pro-inflammatory myeloid cell responses (R. Li et al., 2015). Furthermore, these pro-inflammatory responses decreased after anti-CD20 therapy (a mechanism to deplete B cells) in MS patients and remained diminished during B cell reconstitution (R. Li et al., 2015).

### 1.3.1 GM-CSF as a therapeutic target in MS

The evidence outlined above provides a logical rationale for pursuing GM-CSF signalling as therapeutic target in MS and other T cell mediated autoimmune conditions and several biologics targeting GM-CSF signalling have already been developed for possible use in rheumatoid arthritis, psoriasis and MS (Shiomi, Usui, & Mimori, 2016).

GlaxoSmithKline (GSK) licensed MOR103 (otilimab), a high affinity recombinant human IgG1 antibody against GM-CSF. MOR103 binds to GM-CSF blocking its interaction with the receptor therefore abrogating signalling (Behrens et al., 2015; Steidl, Ratsch, Brocks, Dürr, & Thomassen-Wolf, 2008). MOR103 initially entered clinical trials for rheumatoid arthritis (RA), there were no safety or tolerability issues and patients showed significant clinical improvement compared to placebo (Behrens et al., 2015). Based on the positive tolerability, safety, and efficacy data in patients RA, a phase1b trial commenced in patients with MS (Constantinescu et al., 2015). The goal of the trial was to determine the safety, immunogenicity and pharmacokinetics of MOR103 in MS. Adverse effects were mild or moderate, the most frequent was nasopharyngitis and overall the

antibody was well tolerated (Constantinescu et al., 2015). These outcomes are important since immune therapies can present unexpected or different adverse effects depending on the autoimmune condition (Aram et al., 2019).

Mavrililumab is a human monoclonal IgG1 against GM-CSFRα initially licensed by Medimmune. Mavrililumab binds to GM-CSFRα preventing GM-CSF binding and abrogating signalling and like otilimab, was developed initially for rheumatoid arthritis. Mavrililumab showed a good safety and tolerability profile and significant efficacy compared to placebo (Burmester et al., 2013). Although of potential as an MS therapy, clinical trials of mavrilimumab are restricted to giant cell arteritis, an inflammatory disease affecting the large blood vessels of the scalp, neck and arm (Pupim et al., 2019).

## 1.4 Microglia

### 1.4.1 General introduction

Microglia are the resident tissue macrophages of the central nervous system and represent 5-10% of the total brain cell population (Q. Li & Barres, 2018). The current consensus is microglia are derived from erythromyeloid precursors which generate yolk sack macrophages. Yolk sack macrophages are the immediate migratory precursors that enter the embryonic brain (Ginhoux & Guilliams, 2016). Mouse studies demonstrate microglial population of the CNS coincides with the development of the cardiovascular system and precedes the appearance of astrocytes and oligodendrocytes and closure of the BBB (reviewed by Lannes *et al.*, 2017; Petrik *et al.*, 2013; Minocha *et al.*, 2017). Under normal steady-state conditions microglia are self-renewing in the adult CNS (Ajami, Bennett, Krieger, Tetzlaff, & Rossi, 2007; Ginhoux et al., 2010). Besides microglia, other three types of CNS macrophages exist: perivascular, meningeal and choroid plexus macrophages. These macrophages are found at the interface between the parenchyma and circulation but their function is not very well understood (Prinz, Erny, & Hagemeyer, 2017).

### 1.4.2 Microglia function

Microglia support a variety of functions in the developing and adult brain, such as support of CNS developments and synaptogenesis, homeostasis and sustaining

structure, adult neurogenesis and regeneration, and the most recognized role in response against pathogens (Ginhoux & Guilliams, 2016). Microglia are also involved in neurodegenerative diseases, stroke and trauma (Ginhoux & Guilliams, 2016). The involvement of microglia in disease will be discussed in the next section entitled “Microglia in disease”.

“Resting” microglia are dynamic cells, time-lapse imagining studies have shown that microglia survey the entire brain parenchyma every few hours (Nimmerjahn, Kirchhoff, & Helmchen, 2005; Wake, Moorhouse, Jinno, Kohsaka, & Nabekura, 2009). During this process microglia using their processes make contact with neurons, including synaptic clefts. Evidence from animal studies demonstrate that microglia are active players in synapse remodelling and maturation (Hoshiko, Arnoux, Avignone, Yamamoto, & Audinat, 2012; Paolicelli et al., 2011; Schafer et al., 2012). The interaction between CX3CL1 (fractalkine) expressed on neurons and its receptor CX3CR1 expressed on microglia appears to be important synapse architecture. Silencing CX3CR1 in mice was associated with increased density of dendritic spines on hippocampal CA1 neurons. This was accompanied with a decrease in microglial number and a build-up of immature synapses, resulting in loss of functional connectivity across brain regions and autism-like behaviour (Paolicelli et al., 2011; Yang Zhan et al., 2014). The mechanism through which CX3CR1 mediated microglial control of synapse function remains to be elucidated (Q. Li & Barres, 2018). Microglia are also involved in complement-mediated synapse pruning (Q. Li & Barres, 2018). Mice lacking the complement proteins C1q or C3 show impaired CNS synapse elimination in the visual system (Schafer et al., 2012; Stevens et al., 2007). C1q and C3 tag synapses for elimination, which are subsequently phagocytised by microglia. C1q-tagged synapses have been detected throughout the CNS during development, indicating that microglial synaptic pruning extends beyond the visual system. This hypothesis is supported by the observation that *C1q* KO mice present with spontaneous seizures and have an abnormal high number of excitatory synapses in the neocortex (Chu et al., 2010).

Microglia are the professional phagocytic cells of the CNS. Microglial phagocytosis contributes to embryonic and adult neurogenesis (Q. Li & Barres, 2018). For example, it was showed that during cerebellar development,

microglia produce ROS which induce Purkinje neurons death. Subsequently, the dead neurons are engulfed by microglia (Marín-Teva et al., 2004). Steady-state microglia also sculpt the adult brain by phagocytosing apoptotic cells (Sierra et al., 2010).

Microglial function is dependent upon microglial survival. CSF1R signalling is necessary for microglial development and maintenance (Chitu, Gokhan, Nandi, Mehler, & Stanley, 2016; Chitu & Stanley, 2017). Yolk sack macrophages require CSF1R signalling for proliferation, differentiation, and survival (Ginhoux et al., 2010). The deletion of *Csf1r* in mice leads to a lack of yolk sack macrophages and subsequent absence of tissue resident macrophages, including microglia. These mice rarely survive after birth, the few surviving mice exhibit abnormal brain development and olfactory deficits (Dror Michaelson et al., 1996; Erblich, Zhu, Etgen, Dobrenis, & Pollard, 2011). Tonic CSF1R signalling is also essential for maintaining microglia in adult mice (Elmore et al., 2014). Pharmacological inhibition for 7 days depleted more than 90% of the microglial population in adult mice (Barres, 76). The CSF1R ligands are M-CSF and IL-34. Not much is known about the expression patterns of these microglial mitogens, although it is thought that neuronal cells and later the astrocytes are the main contributors (Lannes et al., 2017).

The evidence presented above is compelling that a lack of microglia or dysregulation in microglial developments and function affect normal neuronal function. Moreover, rare point mutations in both copies of the human CSF1R cause acute loss of microglia visualised using Iba1 (Oosterhof et al., 2019). Iba1 is a calcium binding protein expressed on macrophages/microglia involved in membrane ruffling and phagocytosis (Kanazawa et al., 2002). Increased Iba1 expression was also detected on microglia in the facial nucleus after facial nerve axotomy (Ito et al., 1998). Oosterhof et al. found that acute loss of microglia caused severe cerebral and cerebellar abnormalities, such as the absence of the corpus callosum and failure to develop parts of the cerebellum (Oosterhof et al., 2019). But more recently, mice without microglia due to a deletion in the *Csf1r* enhancer showed no neurological or developmental abnormalities (Rojo et al., 2019). The perpetual technological advances will be crucial to elucidate the roles of microglia.

Microglia are the primary innate immune effector cells in the CNS. Microglia initiate innate immune responses and mediate adaptive immune responses by engaging various pattern recognition receptors (PRRs) (Lannes et al., 2017). PRRs can sense endogenous danger-associated molecular patterns (DAMPs), such as heatshock proteins (Holtman et al., 2017). PRR also detect exogenous pathogen-associated molecular patterns (PAMPs), which include microbial production such as proteins, lipids, saccharides and nucleic acids (Saijo, Crotti, & Glass, 2013). Signalling through PRRs, such as toll-like receptors (TLRs) activate microglia in the case of inflammation resulted from CNS infection or damage. Activated microglia exert their functions via phagocytosis of invading pathogens/tissue damage products and by secreting soluble factors such as cytokines and ROS/ RNS (Jiang, Jiang, & Zhang, 2014; Voet, Prinz, & van Loo, 2019). Activated microglia can have deleterious or beneficial effects, an aspect that will be focused on later.

Signals from the surrounding environment drive microglia/macrophage heterogeneity. When microglia sense infection or injury, they become activated and migrate to the injury site (Voet et al., 2019). Initially, microglia/macrophages were categorised in two classes: M1- pro-inflammatory and M2- anti-inflammatory. Macrophages/ microglia are polarised towards an M1 phenotype by TLR stimulation with microbial products such as LPS, alone or combined with IFN-γ. M1, or classically activated microglia/ macrophages produce pro-inflammatory cytokines, including TNF-α, IL-1ß, IL-6, IL-12, and IL-23, as well as chemokines, such as, CXCL2, CXCL4, CXCL9, CXCL10, CCL4, CCL5, and CCL8. Additionally, M1 microglia release other reactive nitrogen species, such NO, produced by inducible nitric oxide synthase. M1 microglia/ macrophages also show enhanced phagocytosis of pathogens and antigen presentation (Voet et al., 2019)

M2 microglia/ macrophages also known as alternatively activated were initially observed after stimulation with IL-4 and IL-13 (Ransohoff, 2016; Stein, Keshav, Harris, & Gordon, 1992). M2 microglia/ macrophages release anti-inflammatory cytokines, such as IL-10, IL-13, and TGF-ß. Additionally, M2 also produce neurotrophic factors, VEGF (vascular endothelial growth factor), EGF (epidermal growth factor) and IL-1RA (IL-1ß receptor antagonist. Classic M2 markers include

arginase-1 and MR (mannose receptor, CD206). M2 microglia/ macrophages have immunoregulatory roles, including inhibition of inflammation, tissue remodelling, and promotion of angiogenesis. Nowadays, this simplistic view of microglia is challenged (Ransohoff, 2016). Microglia expressing M1 and M2 markers simultaneously were detected in mice following traumatic brain injury and also at MS lesions (Kumar, Alvarez-Croda, Stoica, Faden, & Loane, 2016; Vogel et al., 2013).

Until recently, it was very difficult to distinguish between microglia and other monocytes using phenotypical markers. Most studies based their discoveries on the fact that microglia in steady-state are CD45low or do not express CD44, Ly6c or CCR2. However, it should be taken in consideration that the expression or these markers changes in pathological conditions, making it impossible to discriminate between resident microglia and infiltrating myeloid cells (Korin et al., 2017; Masliah et al., 1991; Ponomarev, Shriver, & Dittel, 2006; Puli et al., 2012). New technologies combining single cell RNAseq and mass cytometry have emerged to allow discrimination between microglia and other myeloid cells in steady-state and disease (Voet et al., 2019). In addition, a new microglia marker, Tmem119, compatible with immunocytochemistry and FACS technique was discovered (Bennett et al., 2016).

### 1.4.3 Microglia in MS and EAE

There is still a lot to be uncovered about the role of microglia in disease, but it is now recognised that microglia can be both protective and detrimental in pathological conditions. Regardless of the vast unknowns, it is well established that microglia are the primary responders in the CNS to danger signals generated in response to infection, neurodegeneration, ageing and trauma (Jiang et al., 2014).

Although MS is pathologically heterogeneous microglial activation is common to virtually all active lesions irrespective of their anatomical localisation and extends out into normal appearing white matter (Zrzavy et al., 2017a). Clusters of activated microglia or microglial nodules can also be found in apparently unaffected white matter, where they are associated with degenerating axons and oligodendrocytes and complement activation products in the absence of

infiltrating leuokocytes. It has been suggested these microglial clusters represent “pre-active lesions” that have the potential to develop into “full-blown” demyelinating lesions (Ramaglia et al., 2012; S. Singh et al., 2013). Using Tmem119 as a microglia specific marker revealed large numbers of microglia are present at the advancing edge of active lesions. These cells express phagocytic markers implying they play an early role in lesion formation and tissue destruction (Zrzavy et al., 2017b) and express a pro-inflammatory profile characterised by proteins associated with phagocytosis (CD68), oxidative damage (p22hox, iNOS), antigen presentation and T cell stimulation (HLA-D, CD86), and increased iron loading (ferritin) (Zrzavy et al., 2017a). Chronic and slowly expanding lesions also feature a rim of activated microglia displaying a similar phenotype (Frischer et al., 2009). Van Loo and colleagues suggested that microglia are educated by soluble immune factors in MS to mediate pro-inflammatory functions, but are not themselves primary inducers of disease (Voet et al., 2019).

#### 1.4.3.1 Mechanistical insights into how microglia contribution to lesion development in MS.

The role of microglia in MS remains unclear, as it is impossible to study directly their contribution to disease development in the living patient. We are therefore dependent on data obtained using animal models to define how they contribute to the pathogenesis of T cell mediated neuroinflammation. Presentation of auto-antigens to T cells by APC within the CNS is essential to reactivate encephalitogenic T cells and trigger an inflammatory response. The current dogma is that CNS antigen-reactive T cells are primed in the peripheral lymph nodes and then migrate into the CNS to be restimulated by any of a number of potential APCs (Dendrou, Fugger, & Friese, 2015). These include microglia which can present antigens and reactivate effector memory T cells, and up regulate MHC expression in EAE and MS (S. K. Singh et al., 2011; Sosa, Murphey, Ji, Cardona, & Forsthuber, 2013; Zrzavy et al., 2017a). Time course studies indicate microglia are the cells to engulf myelin debris post disease induction (Sosa et al., 2013) and express co-stimulatory markers such as CD40, CD80, and CD86 necessary to support efficient T cell stimulation (S. Singh et al., 2013; Wolf et al., 2018). However, whilst it would appear logical that microglia might therefore play a key role in disease induction recent studies indicate this is not

the case, as lack of microglial MHC class II expression is not required to initiate EAE (Wolf et al., 2018). This does not disqualify a role for microglia in antigen spreading during disease (Voet et al., 2019). On the contrary, using MHC I mismatch bone-marrow chimers to distinguish between resident microglia and invading monocytes revealed that microglia priming/activation by GM-CSF was essential for EAE onset (Ponomarev et al., 2007). Together these observations imply initiation of EAE may require an initial T cell reactivation event mediated by APC's at the blood/CSF – brain interface. This provides a local, T cell derived source of GM-CSF that can then prime microglia to amplify the local inflammatory response and/or tissue damage. In GM-CSF deficient mice this can be circumvented by using LPS or CpG (oligodeoxynucleotide) to activate microglia to promote induction of clinical disease (Ponomarev et al., 2007)

Once lesion formation is initiated microglial phagocytosis plays an important role in determining whether there is effective remyelination once the inflammatory insult resolves, as myelin debris must be cleared from the site of injury to allow for effective remyelination (Kotter *et al.*, 2006; Voet, Prinz and van Loo, 2019). It was demonstrated that in EAE invading monocytes are damaging and initiate demyelination (Yamasaki et al., 2014). Same study also illustrates that microglia phagocyte myelin debris and promote remyelination (Yamasaki et al., 2014). Blockade of Trem2 in EAE, a receptor involved in phagocytosis and lipid metabolism, lead to an aggravated disease course and increased demyelination (Piccio et al., 2007). Taken together this data suggest that microglia play multiple and contrasting roles in EAE, a concept supported by studies investigating the effects of microglial depletion on disease development and pathogenesis.

Using a transgenic mouse model in which microglia depletion is triggered by treatment with ganciclovir it was shown that depletion of microglia abolished microglial production of TNF-α, NO and CCL4 in organotypic cultures and repressed development of EAE (Heppner et al., 2005). These data are consistent with the concept microglial activation in EAE contributes to recruitment of inflammatory cells and tissue damage. Similar results were obtained following pharmacological depletion of microglia reinforcing that they are necessary to drive disease progression (Nissen, Thompson, West, & Tsirka, 2018). However

this study should be interpreted with care as pharmacological inhibition of CSF1R *in vivo* not only depletes microglia in the CNS, but also monocyte-derived macrophages that would normally infiltrate the inflamed CNS. In contrast to this evidence that microglial activation is detrimental in EAE, Wlodarczyk and colleagues found intrathecal stimulation of CSF1R signalling with M-CSF and IL-34 at EAE onset ameliorated neurological deficits and demyelination in the CNS. This effect was attributed to microglia identified by FACS on the basis of their low level of CD45 expression (Wlodarczyk et al., 2019). However one has to be careful when interpreting these data as microglia can up regulate expression of CD45 to become $CD45^{high}$ in EAE and other pathological conditions (Masliah et al., 1991; Ponomarev et al., 2006; Puli et al., 2012).

The introduction of new transcriptomic and mass cytometry tools is providing new insights into the heterogeneity of myeloid cells in the CNS and how they respond during ageing and neurological disease models (Mrdjen et al., 2018). This strategy revealed microglia were highly reactive in EAE and had a very different phenotype to “steady state” microglia in healthy age matched control mice. This included down regulation of CX3CR1, MerTK, CD14 and Siglec-H, whilst expression of CD44, CD86, PDL1 and CD11c was increased in EAE. This disease-associated change in microglial phenotype was global, affecting the entire microglial population in mice with EAE. This was in contrast to the situation in aged mice and neurodegenerative disease models that were characterised small populations of activated microglia that co-exist with cells in “steady state“. This is of great interest as it demonstrates that although lesion formation is focal it nonetheless impacts on microglial function throughout the CNS in animals with EAE. This may reflect a response to leuokocyte-derived cytokines and other factors diffusing from developing lesions to activate microglia at remote sites throughout the CNS (Becher, Spath, & Goverman, 2017; Becher et al., 2016; Mrdjen et al., 2018). Similar effects mediated by diffusion of soluble factors may well explain the widespread microgliosis seen in MS and augment disease chronicity and neurodegeneration (Mrdjen et al., 2018).

In response to inflammation activated microglia can mediate a range of effector functions via activation of NF-κB, Jak/STAT, JNK, ERK1/2, and p38 dependent signalling pathways which under steady state conditions are regulated tightly

(Kaminska, Mota, & Pizzi, 2016). This results in generation of archetypical pro-inflammatory cytokines (TNF-α, IL-1ß, IL-6, IL-12, IL-23), chemokines (CCL2, CCL3, CCL4, CCL5, CCL7, CCL12, CCL22), and neurotoxic factors (ROS, RNS, glutamate) but the massive pool of invading leuokocytes that also produce these factors makes it difficult to assess the contribution to lesion formation made by microglia (Jiang et al., 2014; Voet et al., 2019). To add another layer of complexity many of these factors are pleiotropic. A classical example is TNF-α which can mediate pro-inflammatory or cell survival functions depending on receptor usage (Pegoretti, Baron, Laman, & Eisel, 2018; Probert, 2015). In globally TNF-α produced by microglia is dispensable for EAE, but ablation of the protective TNFR2 in microglia resulted in earlier disease onset associated with increased inflammation and demyelination (Gao et al., 2017; Wolf et al., 2017). Inhibition of the IL-1ß cascade at disease onset also ameliorates EAE, as demonstrated by pharmacological inhibition of caspase 1 to block microglial NLRP3 inflamasome activation and pyroptosis (Sutterwala et al., 2006; Voet et al., 2018). However factors produced by activated microglia also orchestrate the behaviour of other cells and *vice versa*. For example activated microglia can induce astrocyte-mediated neuronal and oligodendrocyte cell death (Liddelow et al., 2017), whilst IL-23 produced by microglia modulates T cell encephalitogenicity during the effector phase of EAE (Becher, Durell, & Noelle, 2003).

A major executor of microglial/myeloid mediated tissue damage in these models is oxidative injury due to increased production of ROS, RNS and glutamate (Jiang et al., 2014). Pharmacological inhibition of NADPH oxidase to suppress production of ROS reduced white matter damage and attenuated the clinical course EAE (B. Y. Choi et al., 2015). Furthermore, microglial NADPH oxidase is responsible for continuing synaptic dysfunction in the hippocampus and cognitive impairment during the remission stage in EAE (Di Filippo et al., 2016). However once again it should also be appreciated that in addition to causing tissue damage and enhancing inflammation, microglia also express anti-inflammatory and neuroprotective factors in a context dependent manner. Mice lacking expression of the anti-inflammatory protein A20 on microglia exhibit NLRP3 inflammasome hyperactivation and develop more severe EAE (Voet et al., 2018). Microglia also secrete factors that can promote remyelination; microglial IL-4

can promote oligodendrogenesis during EAE (Butovsky et al., 2006), whilst activin A secreted by M2-like microglia enhances remyelination (Miron et al., 2013).

There have been tremendous advances in elucidating microglial ontogeny and function but their roles in disease pathogenesis remain elusive and many questions remain unanswered (Voet et al., 2019). Addressing this question is complicated as many microglial markers are lost when they are cultured in isolation and it is difficult to replicate pathological environments *in vitro* (Jiang et al., 2014; Ponomarev et al., 2007; Voet et al., 2019). Moreover, the development of complex human microglial co-cultures that replicate the CNS environment is in its infancy. Fortunately, human and murine microglia they share a considerable number of disease relevant genes, including 76 associated with increased susceptibility to MS, meaning it is still relevant to used murine models to study microglial responses (Galatro et al., 2017; Gosselin et al., 2017; Voet et al., 2019).

## 1.5 Aims

The goal of this project was to investigate how GM-CSF influences microglia phenotype and function. As outlined above, GM-CSF plays a crucial role in the development of EAE but the underlying mechanisms remain unknown. I therefore set out to address the following questions in myelinated cultures that replicate the cellular complexity of the CNS:

1. Does GM-CSF mediated activation of microglia induce demyelination and/or axonal injury?

2. Does GM-CSF prime microglia to mediate demyelination and/or axonal injury?

3. Define the effector mechanisms by which GM-CSF mediates effects identified in points 1 and 2.

These investigations demonstrated that GM-CSF sensitises for IFN-γ and TNF-α to induce microglial, iNOS dependent cytotoxicity in the CNS, whilst simultaneously enhancing microglial phagocytosis. These effects were long lasting and are predicted to exacerbate lesion development and disease chronicity in EAE, and by extrapolation in MS. Future studies defining the mechanistic basis of these effects may identify new treatment strategies to slow if not halt accumulation of disability in MS.

# Chapter 2

## Materials and methods

# 2 Materials and methods

## 2.1 Animals

Mice C57BL/6 wild type (WT) and *Csf2rb*tm KO on a C57BL/B6 background were obtained from Jackson Laboratories. Sprague Dawley (SD) rats were purchased from Harlan Laboratories (Blackthorn, UK). Animals' age ranged between 8 weeks and 1 year old. Animals were maintained and culled at the University of Glasgow Central Research Facility in accordance with the UK Home Office standards.

## 2.2 Cell culture

Cell culture preparation and maintenance was carried out aseptically. Instruments and dissection tools were sterilised before use with 70% methylated spirit or by autoclave. Tissue harvesting and dissection was performed at the bench. Cell harvesting and all *in vitro* work were carried out using laminar flow cabinets to prevent contamination. Cell culture media contained the antibiotics penicillin and streptomycin and were sterilized using a 0.22 µm vacuum filter (Millipore).

### 2.2.1 Mouse myelinating cultures

Myelinating cultures were prepared as described previously by (C. E. Thomson et al., 2008; Christine E. Thomson, Hunter, Griffiths, Edgar, & McCulloch, 2006). Mouse embryos (WT or KO) for myelinating cultures were collected on embryonic day (E) 13.5 with the day of the plugging considered E 0.5. Pregnant females were sacrificed by cervical dislocation and death was ensured by decapitation. The abdomen and dissection tools were sterilised with 70% methylated spirit. An incision was made in the inguinal area of the animal and the skin and abdominal wall were cut in a V close to expose the embryos. The gravid uterus was removed and placed in a petri dish on ice. Once the embryos were removed from the embryonic sacs, they were place in a 35 mm petri dish containing HBSS with $Ca^{+2}$ and $Mg^{+2}$ (on ice). The embryos were dissected under the microscope using forceps and pointed-tweezers. Initially, embryos were decapitated with a cut rostral to the cervical flexure to preserve the medulla. The skin covering the

spinal cord was gently removed longitudinally and the cord was carefully lifted out. Spinal cords were stripped off meninges along with the dorsal root ganglia and placed in a bijou with 2 ml HBSS (Hank's balanced salt solution, Invitrogen) without $Ca^{+2}$ and $Mg^{+2}$ and enzymatically dissociated with 2.5% trypsin (Sigma) for 15 min at 37°C and 7% $CO_2$. The enzymatic reaction was stopped with 2 ml of a solution containing 0.52 mg/ml soybean trypsin inhibitor, 3.0 mg/ml bovine serum albumin, and 0.04 mg/ml DNase (all from Sigma). The digested tissue and all the media present in the bijou were transferred to a 15 ml tube and triturated to obtain a single cell suspension using a sterile glass Pasteur pipette. Five ml of plating media (PM) (50% DMEM, 25% horse serum, 25% HBSS with $Ca^{+2}$ and $Mg^{+2}$) were added to the cell suspension. The cell suspension was centrifuged at 141 g for 5 min at room temperature. After centrifugation the supernatant was removed, and the pellet was resuspended in 3 ml of PM. Viable cells were counted using trypan blue viability dye (Sigma) (1: 1 cell suspension to dye) on a haemocytometer. The cell suspension was further diluted to 1.5 million viable cells/ml. The cells were plated at a density of 150,000 cells/coverslip on poly-L- lysine coated coverslips into 35 mm Petri dishes (3 coverslips/ dish) and left to adhere for 3 hours at 37°C and 7% $CO_2$. After the appropriate time has passed 300 µl PM and 600 µl differentiation media (DM+) (DMEM 4500 mg/ml glucose, 10 ng/ml biotin,0.5X N1 supplement, 50 nM hydrocortisone, and 0.1 µg/ml insulin (all reagents from Sigma) were mixed and gently added to each petri dish. Cultures were fed 2-3 times/week with DM+ for the first 12 days and with DM without insulin (DM-) afterwards. During each feed 500 µl of old media was withdrawn and replaced with fresh media. Cultures were kept in a humidified incubator at 37°C and 7% $CO_2$ (C. E. Thomson et al., 2008; Christine E. Thomson et al., 2006).

Glass coverslips were prepared in advance and stored at 4°C . Boric acid buffer concentration at pH 7.4 was made by dissolving sodium tetraborate and boric acid in distilled water. PLL was dissolved in boric acid buffer to give a final concentration of 13 mg/ml. Glass coverslips (13 mm diameter; VWR International) were coated in the PLL mixture for at least 2 hours at 37°C. Next, coverslips were rinsed three times with sterile water and plated into 35 mm petri dishes. Coverslips were allowed to dry in a sterile environment. Prepared plates were sealed and stored at 4°C until ready to be used.

## 2.2.2 Rat myelinating cultures

### 2.2.2.1 Neurospheres

Neurospheres were generated using the methods described by Sorensen *et al.*, 2008 utilising the corpus striatum of post-natal day one (P1) rats (Sorensen et al., 2008). P1 rats were culled by intraperitoneal injection of Euthanal and decapitated. Brains were excised and transferred to a petri dish containing cold Leibovitz's L-15 media (Invitrogen). With the help of a scalpel, the brain was separated in the two cerebral hemispheres. The part of the cortex where the striatum is located was isolated by cutting coronal segments through the cortex at the corpus callosum and just prior to the olfactory bulb. The striatum was then excised out of the cortex and transferred into a bijou containing 1 mL of Leibovitz's L15 media, on ice. One flask of neurospheres requires 5-6 striata. The striata were mechanically dissociated into a single cell suspension by triturating repeatedly using a glass Pasteur pipette. The cell suspension was transferred into a 15 ml centrifuge tube and centrifuged at room temperature for 5 min at 136 g. The supernatant was discarded and the pellet was resuspended in 2 ml of neurosphere media (NSM). The NSM is composed of DMEM/F12 (Dulbecco's Modified Eagle Medium: Nutrient Mixture F-12) (1:1, DMEM containing 4500 mg/l glucose), supplemented with 7.5% NaHCO3, 2 mM glutamine, 5000 U/ml penicillin, 5 µg/ml streptomycin, 5.0 mM HEPES, 0.0001% bovine serum albumin (BSA) (all from Invitrogen), 25 g/ml insulin, 100 g/mL apotransferrin, 60 M putrescine, 20 nM progesterone, and 30 nM sodium selenite (all from Sigma). Next, the cell suspension in NSM was enriched with 4 µL of EGF (20 ng/mL mouse submaxillary gland epidermal growth factor from R&D Systems). The cell suspension was added into a 75 $cm^3$ uncoated tissue culture flask (Greiner), already containing 18 ml of NSM, preheated at 37°C. The neurosphere cultures were maintained in a humified incubator at 37°C and 7% $CO_2$ and fed twice a week with 5 ml NSM and 4 µL EGF. By visual inspection, after 7- 10 days the neurospheres grew sufficiently large to be plated down and grow astrocytes.

### 2.2.2.2 Neurosphere-derived astrocyte monolayer

Astrocytes were differentiated from neurospheres as described by Thomson *et al.*, 2008 (C. E. Thomson et al., 2008). Glass coverslips were prepared similarly

as described before for mouse myelinating cultures with some exceptions. Distilled water instead of boric acid buffer was used to dissolve PLL and the coverslips were plated in 24 well plates. When the neurospheres were ready to be harvested, the flasks were scraped using a cell scraper (Greiner). One flask of neurospheres would typically yield 5- 6 24 well plates of astrocyte monolayers. The cell suspension was placed into a 50 ml centrifuge tube and centrifuged at 136 g for 5 minutes at room temperature. The pellet was dislodged using a glass Pasteur pipette resulting in a single cell suspension. The suspension was diluted to yield 12 ml per 24 well plate with low-glucose DMEM supplemented containing 10% foetal bovine serum and 2 mM L-glutamine (DMEM-FBS) (Sigma Aldrich). Each well was filled with 0.5 ml of cells suspended in DMEM-FBS followed by 0.5 ml of DMEM-FBS. The plates were placed in a humified atmosphere at 37°C and 7% $CO_2$. The monolayer was fed twice a week by replacing half of the media with fresh DMEM-FBS until it reached confluence. Typically, confluency was reached after 7- 10 days. As the astrocyte monolayer did not undergo cell-specific selection, other CNS cells can be present in small numbers. According to data previously produced in our lab by Daniel McElroy, the major contaminants at 7 DIV are oligodendrocyte lineage cells.

#### 2.2.2.3 Seeding of embryonic spinal cord cells on astrocyte monolayer

Time-mated female SD rats were sacrificed by $CO_2$ asphyxiation at E15.5. Embryos were removed and cells were prepared following the same procedure as described above for mouse myelinating cell cultures with a difference in the enzymatic digestion. Collagenase I (1.33%, 100 µl, Invitrogen) and trypsin were necessary for enzymatic digestion.

Coverslips covered with a neurosphere-derived astrocyte monolayer prepared as described in section 2.2.2.2 were removed from the 24 well plates with sterilised tweezers and transferred into 35 mm petri dishes (3 per dish). Fifty µl (150,000 cells) of the spinal cord suspension was added onto each coverslip. The coverslips were incubated for 2 hours at 37°C to allow adherence to the monolayer. The next steps comprising of the maintenance of the cultures were identical to the ones described above for mouse myelinating cultures.

### 2.2.3 Mouse primary microglia cultures

Primary mouse mixed glial cultures were prepared as described by Nicol *et al.*, 2018 (Nicol et al., 2018). P2 C57BL/6were culled using an intraperitoneal injection of Euthanal and decapitated. Brains were extracted with caution to avoid damaging the cortices and placed a petri dish and were transferred to a laminar flow cabinet. Five-six brains were sufficient to yield a flask of mixed glial cultures. Brains were rolled on sterile filter paper to remove the meninges and vasculature, before placing into a 50 ml centrifuge tube already containing warm DMEM containing 10% FBS and 1% penicillin/ streptomycin (total volume brains and media 20 ml). To mechanically dissociate, brain tissue was triturated vigorously using a 10 ml pipette for 2 mins and subsequently passed through a 40 µm cell strainer (aiming for a single cell suspension). The single cell suspension was centrifuged at 300 g for ~7 min, and cells were re-suspended in a total volume of 40 ml per 175 $cm^2$ flask (Corning). Cells were left for 1 week for the astrocyte layer to become confluent with microglia sitting mainly on the top. To increase the number of microglia in the mixed glial prep, 7 days later the media of each 175 $cm^2$ flask was refreshed by adding 5 ng/ml of murine GM-CSF (Immunotools). The cells were left in the GM-CSF-enriched media for one more week, to increase the yield by 5-6-fold. Microglia were removed by "shaking" overnight in an orbital shaker incubator (37℃, 100 rev per min, but no $CO_2$). To compensate for the difference in $CO_2$ HEPES was added to the media (50 mM final) just prior to shaking the cells overnight. Following overnight shaking, the supernatant was collected from the flasks (containing the dissociated microglia). Microglia were centrifuged and cells were re-suspended in media (10% FBS) without GM-CSF and counted using the haemocytometer and Trypan blue stain. Cells in media containing FBS were plated in 96 well plates (Greiner, for microscopy) at a density of 50,000 cells per well and left to adhere for 2 hours. After the cells adhered, media containing FBS was washed off and replaced with 100 µl of DMEM containing only 1% penicillin/ streptomycin. Cells were maintained at 37℃ and 7% $CO_2$. As verified by Nicol *et al.*, 2018 using flow cytometry, microglia cultures consistently exceeded a purity of at least 95%.

## 2.3 Cell culture treatments

### 2.3.1 Mouse myelinating cultures

#### 2.3.1.1 Developmental setting treatments

Mouse myelinating cultures (one petri dish per experimental condition) were treated with mouse recombinant GM-CSF (Immunotools) at a final concentration of 100 ng/ml. Treatment started at DIV 6 when myelination had not begun, and axonal density was not maximal until 24 DIV.

#### 2.3.1.2 Mature setting treatments

Mouse myelinating cultures (one petri dish per experiment condition) were treated with 100 ng/ml GM-CSF (Immunotools) at 24 DIV when myelination was established, and axonal density reached its peak. The duration of the treatment varied depending on the experimental design. Detailed descriptions of each experiment can be found in the results section. Briefly, the cells were either treated with GM-CSF alone or in the case of the GM-CSF priming experiments in combination with mouse recombinant interferon-γ (IFN-γ, R&D Systems) 100 ng/ml, mouse recombinant tumour necrosis factor α (TNF-α, R&D Systems) 25 ng/ml, 1 µg/ml LPS (lipopolysaccharide, Sigma), or 10 µg/ml poly I:C (polyinosinic:polycytidylic acid, Sigma).

### 2.3.2 Rat myelinating cultures

Rat myelinating cultures (one petri dish per experiment condition) were primed/unprimed with rat recombinant 100 ng/ml GM-CSF (Immunotools) from 24 DIV until 30 DIV. At 30 DIV the cultures were treated with various combinations of rat recombinant interferon-γ (IFN-γ, R&D Systems) 100 ng/ml and rat recombinant tumour necrosis factor α (TNF-α, R&D Systems) 25 ng/ml for 72h.

### 2.3.3 Mouse primary microglia

Mouse primary microglia (one well per experimental condition) were primed/unprimed with mouse recombinant 100 ng/ml GM-CSF (Immunotools) from 0 DIV (plating) until 3 DIV. At the end of the priming period the cells were

treated with various combinations of with mouse recombinant interferon-γ (IFN-γ, R&D Systems) 100 ng/ml and mouse recombinant tumour necrosis factor α (TNF-α, R&D Systems) 25 ng/ml for 72h.

## 2.4 Cell culture assays

### 2.4.1 Phagocytosis assay

Mouse myelinating cultures (one petri dish per experiment condition) were primed with 100 ng/ml GM-CSF from DIV 24 until DIV 30. At 30 DIV various phagocytic material were added for 2 hours as described below. At the end of the assay coverslips were fixed with 4% paraformaldehyde (PFA) and processed for immunocytochemistry. Coverslips were imaged as described in the section 2.5.1.2 and manually quantified. All reagents used for immunocytochemistry were maintained at 7.4 pH to avoid pHRodo activation and subsequent fluorescence when outside the cell.

#### 2.4.1.1 Fluorescently-labelled latex beads

Latex beads (Polysciences) with a diameter of 1 µm were added to GM-CSF primed and unprimed cultures (3 x $10^6$ beads per petri dish). The stock beads solution was dissolved directly in media before use.

#### 2.4.1.2 pHRodo labelled *E. coli* particles

pHrodo labelled *E. coli* particles (Thermofisher) were reconstituted in PBS (pH 7.4) and used at a final concentration of 0.1 mg/ml. The tubes containing the *E. coli* particles were vigorously vortexed to disintegrate the large aggregates which could interfere with phagocytic process.

#### 2.4.1.3 pHRodo labelled myelin particles

Rat myelin extracted and labelled with pHRodo as detailed in section 2.6.1 was added to GM-CSF primed and unprimed cultures at a final concentration of 0.1 mg/ml. As described above, the tubes containing labelled myelin were vigorously vortexed before use, to disintegrate large aggregates.

### 2.4.2 Lactate dehydrogenase (LDH) cytotoxicity assay

Cell viability was assessed using a lactate dehydrogenase (LDH, Promega) kit following the manufacturer's instructions. Briefly, 25 µl of cell supernatants (three technical repeats) were pipetted in a flat bottom 96 well plate (Corning). Next, 25 µl of CytoTox 96® Reagent were added to each sample well. The plate was covered and incubated for 30 mins in the dark at room temperature. At the end of the incubation period, the reaction was stopped with 25 µl of Stop Solution. Any large bubbles were pierced using a syringe needle. The absorbance was recorded at 492 nm using a Tecan Sunrise microplate reader. Additionally, cells lysed with 10X lysing buffer 1 hour prior to the start of the assay served as the maximum LDH release control. Media was used as a negative control. To evaluate the results the percentage cytotoxicity was calculated. Initially, the average value of the culture media background was subtracted from all experimental values. To compute percentage cytotoxicity the following formula was used: Percentage cytotoxicity= $\frac{\text{Experimental LDH release}}{\text{Maximum LDH release}}$ x 100.

### 2.4.3 Griess assay

The levels of nitric oxide (NO) in culture supernatant were detected using nitrite ($NO_2^-$) as a surrogate readout. $NO_2^-$ was measured using the Griess Reagent System (Promega) according to the manufacturer's protocol. Prior to the start of the assay $NO_2^-$ standards were made by dissolving the nitrite standard stock. Twenty-five µl of fresh cell supernatants (three technical repeats) and standards were pipetted in a flat bottom 96 well plate (Corning). Next, 25 µl of sulphanilamide solution were added to each sample well. The plate was covered and incubated for 5-10 min in the dark at room temperature. At the end of the incubation period, 25 µl of NED solution were dispensed to each well. The absorbance was measured at 570 nm using a Tecan Sunrise microplate reader. A standard curve was generated to calculate the amount of NO in each sample.

## 2.5 Immunocytochemistry and Microscopy

### 2.5.1.1 Staining

At the end of the treatment, coverslips were fixed and stained with antibodies to perform immunofluorescence microscopy. All staining procedures were performed at the bench. Media was removed from culture dishes and depending on the antibody's specifications (Table 2.1), the cells were fixed for 10 min with 4% PFA at room temperature or acetone at -20℃. When PFA was used, the fixation step was followed by 3 washes with PBS and permeabilization with Triton X-100 0.5% (Sigma Aldrich) for 10 mins. Coverslips were then washed again (x3) with PBS and blocked for 1 hour in blocking buffer containing (1% BSA (bovine serum albumin), 10% horse serum, in PBS. If acetone was used as a fixation method, the permeabilization step was not required. Acetone was washed off with PBS and the coverslips were transferred into blocking buffer. Next, the coverslips were incubated overnight 4℃ at in 50 µl primary antibody (Table 2.1) dissolved in blocking buffer. The following day, coverslips were washed three times in PBS and incubated with fluorescently-tagged secondary antibodies (Table 2.2), diluted in blocking buffer, for 30 mins in the dark at room temperature. Secondary antibodies were washed off 3X with PBS and a final wash in distilled water and mounted on glass slides (Thermofisher) using Mowiol 4-88 + DAPI (4',6- Diamidino-2-Phenylindole, Dihydrochloride) (Sigma). When cells were grown in a 96 well plate the staining procedure was identical, except for the mounting step. Instead of using Mowiol + DAPI, the nuclei were identified with Hoechst stain (1: 10,000 in PBS, Thermofisher) for 10 min in the dark. the Hoechst solution was washed off and replaced with PBS.

### 2.5.1.2 Imagining and quantitative analysis

Olympus BX51 fluorescent microscope and Ocular software were used to image and capture all cells grown on glass coverslips. Quantitative analysis of each experiment was performed by taking 10-5 random images of each coverslip (depending on the number of experimental conditions) at x20 magnification. Therefore, the number of images between experiments varied between 15 to 30 (3 coverslips per condition).

Pipelines developed for CellProfiler software (http://www.cellprofiler.org/) were used to measure fluorescence intensity of each antibody staining. The pipelines quantified pixel intensity from individual colour channels; pipelines can be downloaded from https://github.com/muecs/cp. The percentages of myelination and axonal density were quantified using myelin.cp pipeline. The total cell number was determined using dapi.cp which counts DAPI positive nuclei. The number of cell positive for a marker of interest was determined by manual counting.

| Antigen | Host | Isotype | Dilution | Fixation | Source | Catalog number |
|---|---|---|---|---|---|---|
| CD45 | Rat | IgG2b | 1 in 300 | Acetone | Biorad | MCA1388 |
| Dectin2 | Rat | IgG2a | 1 in 100 | PFA | Miltenyi | 130-094-481 |
| Iba1 | Rabbit | IgG | 1 in 800 | PFA | Wako Chem | 019-19741 |
| iNOS | Rabbit | IgG | 1 in 100 | Acetone | Abcam | ab15323 |
| MOG | Mouse | IgG2a | 1 in 500 | PFA | Hybridoma | Z2 clone |
| NF-H | Mouse | IgG1 | 1 in 1000 | PFA | Biolegend | SMI 31P |

**Table 2.1. Primary antibody list**

| Antibody | AlexaFluor 488 | AlexaFluor 568 |
|---|---|---|
| Goat-anti-mouse IgG1 | | + |
| Goat-anti-mouse IgG2a | + | |
| Goat-anti-rabbit IgG | + | |
| Goat-anti-rat IgG | | + |

**Table 2.2. Secondary antibody list.** All secondary antibodies were purchased from Thermofisher and used at a dilution of 1:600.

# 2.6 Biochemical methods

## 2.6.1 Myelin fraction extraction and labelling

### 2.6.1.1 Myelin fraction extraction

Spinal cords were removed from SD female rats (after embryo collection), placed in an autoclaved tube and immediately frozen at -80℃. The spinal cord removal was performed on the bench with care to avoid any hair contamination. Utensils and animals were cleaned thoroughly with 70% methylated spirit. When sufficient cords were collected (5 spinal cords, aprox. 3g of tissue) they were thawed on ice. The tissue was weighted and place in 25 ml of pre-cooled 0.32 M sucrose solution containing 10 mM HEPES. The tissue was homogenised on ice using a polytron homogenizer at high speed. Prior to use, the homogeniser was soaked in Distel overnight, rinsed well, sprayed with ethanol and UVed. The tissue homogenate was divided in two equal parts and place in autoclaved centrifuge tubes. The tubes were spun in a fix angle centrifuge using a pre-cooled J25.5 rotor at 20,000 rpm (48831g) for 30 min at 4℃. The heavier/denser myelin fraction pelleted through the less dense 0.32 M sucrose solution. The supernatant was discarded and tubes containing the pellet were placed on ice. Each pellet was resuspended in 7 ml of 0.32 M sucrose. Gradient centrifuge tubes (compatible with Beckam SW41 rotor) were filled with 6 ml of 0.85 M sucrose 10 mM HEPES solution. The 0.32 M sucrose myelin homogenate was laid gently on top of the 0.85 M sucrose with a gun pipette set on gravity mode. The weight of the tubes was checked and in case of discrepancy more 0.32 M solution was added to balance the weights. The tubes were centrifuged in a swinging bucket rotor centrifuge (Beckam SW41 Ti) at 49,392 g for 45 min at 4℃. The less dense myelin/fat fraction floated on top of the denser 0.85M sucrose while the rest of the unwanted material (nuclei, mitochondria etc.) sank to the bottom of the tube. After centrifugation, the interphase was carefully removed with a glass Pasteur pipette from each tube without disturbing the upper or the lower phase. The interphase was transferred into centrifuge tubes (compatible with J25.5 fixed angle rotor) and resuspended in 20 ml of sterile PBS. The tubes were centrifuged rotor at 48,831 g for 30 min at 4℃. The supernatant was discarded after centrifugation and the pellet was resuspended in PBS as described above and centrifuged again. This process was repeated once more. The pellet was

resuspended in 10 ml of PBS, retaining a small aliquot to test the protein concentration. The protein concentration was evaluated using the BCA assay (described below). The entire myelin fraction obtained was diluted to 1 mg/ml in sterile PBS under a laminar flow hood. Finally, the myelin fraction sample was sterilised using an ARAD 225 X-ray generator and given a dose of 50,000 cGy. The myelin fraction was stored at -80℃.

#### 2.6.1.2 pHrodo labelling

The myelin fraction was conjugated with an amine-reactive pH-sensitive pHrodo® Green STP ester dye (Thermofisher). The STP ester reacts with primary amines on proteins, labelling them. The dye only fluoresces in acidic pH, an increase in fluorescence correlates with the acidification of the environment. The labelling reaction was performed according to the manufacturer's protocol in a laminar flow hood to avoid contamination. Before performing the labelling reaction, the myelin fraction was centrifuged and resuspend in sterile 0.1 M sodium bicarbonate buffer pH 8.3 at 1 mg/ml. Five hundred µg of amine-reactive pHrodo™ Green STP ester was reconstituted in 75 µL of DMSO to yield approximately 8.9 mM. The dye solution was added to the myelin fraction, mixed by pipetting up and down and left to incubate for 45 min at room temperature protected from light. To remove the unconjugated dye the myelin fraction was centrifuged for 5 min at 94 g. The supernatant was discarded, and the pellet was resuspended in PBS pH 7.4. This process was repeated three times. At the end myelin was diluted in PBS pH 7.4 at 1 mg/ml, aliquoted in autoclaved Eppendorf tubes and frozen immediately at -80℃.

### 2.6.2 BCA assay

The protein concentration in samples was determined using the Thermo Scientific™ Pierce™ BCA Protein Assay following the manufacturer's protocol with some alterations. For protein quantification in the myelin fraction, due to its high lipid content 0.1% SDS final concentration (same as RIPA lysing buffer) was added to the samples (including the blank). As lipids interfere with protein reading, breaking down by detergent was necessary to impede light scattering artefacts.

Briefly, the first step was making bovine serum albumin (BSA) standards as detailed in the manufacturer's instructions. The sample of interest was diluted 1 in 2 and 1 in 10 to take into account if the protein concentration of the original sample exceeds the working range of the assay. Next, 12.5 µl of standards and un/diluted samples were added to a flat bottom 96 well plate (Corning). One hundred µl of WR (working reagent) were dispensed onto the plate. The plate was covered and incubated at 37℃ for 30 min. At the end of the incubation time the plate was cooled at room temperature and the absorbance was measured at 570 nm using a Tecan Sunrise microplate reader. A standard curve was generated to calculate the protein concentration in each sample, accounting for the dilution factor.

## 2.6.3 Western blotting

### 2.6.3.1 Cell lysis

Cells were lysed using RIPA buffer (Sigma). To ensure that sufficient amount of protein will be obtained, three cell culture dishes were used for each condition. Before lysis, culture dished were placed on ice, the supernatant was removed, and the coverslips were washed with ice-cold PBS. PBS was removed and 20 µl of RIPA buffer was added to each coverslip. Cells were scraped off with the pipette tip, triturated and transferred to Eppendorf tubes to be further triturated. A BCA assay was performed to measure the protein concentration and the samples were frozen immediately.

### 2.6.3.2 Gel electrophoresis and protein detection

Twenty-six µl of sample were mixed with 10 µl 4X Laemmli sample buffer and 4 µl NUPAGE reducing agent (all from Thermofisher) and heated at 65℃ for 10 mins. Chameleon duo pre-stained protein ladder (Li-cor) and equal amounts of protein were loaded onto a NUPAGE NOVEX Tris-acetate gel and the gel was run (4–12%; Invitrogen) at 200 volts for 45 mins. The gel was then transferred using the iBlot Western Detection system (Thermofisher) to a PVDF membrane. Next, the membrane was incubated in Odyssey blocking buffer (Li-cor) for 1 hour at room temperature. At the end of the blocking step, the membrane was incubated in primary antibody (Table 2.3) diluted in Odyssey blocking buffer (Li-cor) overnight at 4ºC on a shaker. The membrane was quickly washed in PBS

followed by 5 washes (5 min) with PBST (0.5% Tween in PBS) on a shaker. Following the washes, the membrane was incubated in the appropriate NIR-tagged secondary antibodies (Li-cor, Table 2.4) diluted in Odyssey blocking buffer for 1 hour at room temperature on a shaker. The membrane was washed as described above and incubated in PBS. The membrane was imaged using the Odyssey CLx Near-Infrared Fluorescence Imaging System. The fluorescence intensity of the protein bands was evaluated using densitometer Gels tool on Image J software.

| Antigen | Host | Isotype | Dilution | Source | Catalog number |
|---|---|---|---|---|---|
| b-actin | Mouse | IgG1 | 1 in 100 | Abcam | ab8226 |
| iNOS | Rabbit | IgG | 1 in 100 | Abcam | ab15323 |

**Table 2.3 Primary antibody list for western blotting**

| Antigen | Host | IRDye Tag | Source | Catalog number |
|---|---|---|---|---|
| Mouse | Donkey | 680RD (red) | Li-Cor | 926-68072 |
| Rabbit IgG | Donkey | 800CW (green) | Li-Cor | 926-32213 |

**Table 2.4 Secondary antibody list.** All secondary antibodies were purchased from Li-cor and used at a dilution of 1:10,000.

## 2.7 Meso Scale Discovery assay

To study the production of proinflammatory cytokines culture supernatant was screened using the MSD (Meso Scale Discovery) U-PLEX® platform according to the manufacturer's instructions. Briefly, U-plex plates were coated with a cocktail of individual U-PLEX-coupled antibody solutions and incubated at 4ºC overnight. The plate was washed 3 times with PBST (PBS plus 0.05% Tween-20). Next, the plate was incubated with samples and standards for 1 hour on an orbital shaker at room temperature. Plate was washed as previously described and incubated with the detection antibody cocktail at room temperature while shaking for 1 hour. The detection antibody solution was washed with PBST followed by the addition of 1X MSD Wash Buffer. The plate was read and analysed on an MSD instrument.

## 2.8 Molecular biology

### 2.8.1 Total RNA extraction

RNA from myelinating cultures was extracted following the PureLink RNA Mini Kit (Ambion Life Technologies) protocol. Briefly, three petri dishes were used for RNA extraction for each experimental condition. Culture supernatant was removed and store for screening if necessary. Cells were lysed with 1 ml of TRIzol® Reagent Solution (Ambion™) for 10 min at room temperature. After complete lysis, 200 µl of chloroform were added for 5 min at room temperature to allow phase separation. The tubes were vigorously shacked for 15 seconds and centrifuged at 12,000 g and 4ºC for 15 min. Five hundred µl of the clear aqueous phase were transferred to a new RNAse-free Eppendorf tube containing an equal volume of 70% ethanol and vortexed. The content of the tube was pipetted into a spin cartridge containing RNA binding silica-based membrane and centrifuged at 12,000 g for 15 seconds at room temperature. The flow-through was discarded and the membrane was subjected to DNAse treatment for 20 min. Next, 700 µl of Wash Buffer I was added onto the column and centrifuged at 12,000 g for 30 seconds. The column was inserted into a new tube and 500 µl of Wash Buffer II was added followed by centrifugation at 12,000 g for 30 seconds. The flow-through was discarded and the wash step was performed one more time. The lids were removed, and tubes were centrifuged at 12,000 g for 2 mins to dry the membranes. The columns were inserted into collection tubes and 30 µl of RNAse-free water was added onto the membranes and incubated for 3 mins at room temperature. The purified RNA was eluted by centrifugation at maximum speed or 2 mins. The RNA was quantified using NanoDrop 1000 Spectrophotometer, diluted according to downstream requirements and stored at -80°C.

### 2.8.2 Gene expression by RNAseq

#### 2.8.2.1 RNAseq

RNA from myelinating cultures treated with 100 ng/ml GM-CSF at 24 DIV for 24 hours was extracted as described above. RNA quality and integrity were evaluated using Agilent Bioanalyser 6000 Nano LabChip platform system by Edinburgh Genomics at The University of Edinburgh. The sequencing was performed on Illumina HiSeq 4000 sequencing platform. Reads were adapter

trimmed using cutadapt version 1.3 with the parameters -q 30 -m 50 -a AGATCGGAAGAGC. Trimmed reads were aligned to the *Mus musculus* genome (Ensembl version 84) with star (version 2.5) using default parameters. Read counts were produced using htseq-count version 0.6.0, with parameters " -m union -s reverse -i gene_id -t exon -r pos " using the Ensembl gene annotation corresponding to Ensembl version 84 of the *Mus musculus* genome.

#### 2.8.2.2 RNAseq analysis

Differential expression analysis was generated by Edinburgh Genomics using Bioconductor package EdgeR (version 3.10.5) with R version 3.2.1. The "glmFit" function was used to compare the treated to the control samples, and the cell culture ID of was taken into account. Genes with less than 20 reads mapping to them across all samples were excluded from the analysis. False discovery rate (FDR) was set at FDR < 0.05.

The gene list produced by Edinburgh Genomics was used to perform pathway analysis using DAVID (The Database for Annotation, Visualization and Integrated Discovery; https://david.ncifcrf.gov/). Maintaining default settings, DAVID interpreted the differentially expressed gene list into biological pathways by utilising the KEGG *Mus musculus* database.

### 2.8.3 qRT-PCR validation

#### 2.8.3.1 cDNA synthesis

The Qiagen QuantiTect Reverse Transcription Kit and instructions were used to synthesise cDNA from 500 ng of purified RNA diluted in 12 µl with RNase free water. Two µL of genomic DNA wipe-out buffer were added to the sample and incubated 42°C for 2 minutes using a thermocycler. Samples were immediately cooled on ice. Next, 4 µl reaction buffer, 1 µl reverse transcriptase and 1 µl random primer mix were added to the reaction and incubated 42°C for 20 mins, then 3 mins for 95°C. cDNA was diluted 1 : 5 with RNAse-free water and stored at -20°C.

### 2.8.3.2 Primer design

Mouse specific primers were designed using Primer3: WWW primer tool (http://biotools.umassmed.edu/bioapps/primer3_www.cgi) from FASTA sequences in the NCBI nucleotide database. The primer specifications can be found in table 2.5. BLAST tool was used to test primer specificity (BLAST; ttp://blast.ncbi.nlm.nih.gov/Blast.cgi). Primers were purchased from Integrated DNA Technologies. Prior to use, primers were dissolved in RNAse-free water at 100μM concentration and made into a master mix containing f 1:1 forward and reverse primers. Primers were stored at -20°C. Primer sequences can be found in table 2.6.

| | |
|---|---|
| **Primer size** | 18 to 23 base pairs (bp) (20 bp optimal) |
| **Melting temperature (Tm)** | 59.0°C to 61.0°C (60.0°C optimal) |
| **GC content** | 40 % to 65 % (50 % optimal) |
| **Max self-complementarity** | 2. 00 |
| **Max 3' complementarity** | 1. 00 |

**Table 2.5. Primer design parameters.**

| Target | Inner Primer (5' - 3') | | Outer Primer (5' - 3') | |
|---|---|---|---|---|
| | **Forward** | **Reverse** | **Forward** | **Reverse** |
| ***18 S*** | GACTCAACACGGGAAACCTC | TAACCAGACAAATCGCTCCAC | CGTAGTTCCGACCATAAACGA | ACATCTAAGGGCATCACAGACC |
| ***Tbt*** | GACTCAACACGGGAAACCTC | TAACCAGACAAATCGCTCCAC | CGTAGTTCCGACCATAAACGA | ACATCTAAGGGCATCACAGACC |
| ***Mgl2*** | TTGGAGCGGGAAGAGAAAA | AGGGAGAACAGGAGGAGGTG | TCGCCTCTGGTCATTGCT | TCACCTTCTGGCTCAAGTCTC |
| ***Ccr2*** | GTGGGACAGAGGAAGTGGTG | TGAGGAGGCAGAAAATAGCAG | CTTCATCAGGCACAGAGAGC | CCACAGACCACAAACCACAA |
| ***Clec4n*** | CAGAAGAGCGGTGTGTTTCA | ACATCATTCCAGCCCCATT | GGATGCTGCCCAAATCAC | CAAGAAAATGCCCCCAGAC |
| ***Tnfsf8*** | CTGGTGGGGTTCCTGTTATG | TGGATAGGGATTGGTGTTCC | ACAATGACCAGAAGGCAAGG | AATGGCAGGGGTACACAAAG |
| ***Csf2rb*** | GAGCAAGTGGAGCGAAGAGT | GGAGCAAGGTGAGGATGAGA | GAGCCAGACACCTCATACTGC | GGTCCCTCTACTTGAACATTGG |

**Table 2.6. Primer sequences.**

#### 2.8.3.3 Primer testing by end-point PCR

Primer specificity was tested using end-point PCR using cDNA containing the gene of interest. Specificity was considered accurate if only one amplicon was produced of the correct size. The PCR reaction was performed using REDTaq® ReadyMix™ PCR Reaction Mix (Sigma) following the manufacturer's protocol. Briefly, 2 µl cDNA, 2 µl primer mix, 5 µl master mix and 1 µl nuclease-free water were mixed and placed in thermocycler. Cycling parameters were as follows: 5 min at 50˚C, 10 min at 95˚C, followed by 15 seconds at 95˚C, 1 min 60˚C, 30 sec 95˚C, 15 seconds at 60˚C repeated 40 times. The PCR products were run on an 1.5% agarose gel using ethidium bromide labelling.

#### 2.8.3.4 qRT-PCR

A panel of genes (table 2.6) differentially modulated in the RNAseq study were selected to be validated by qRT-PCR. Quantitative PCR was performed on an Applied Biosystems Fast Real-Time PCR System (ABI 7500) following the same cycling setting described in section 2.8.3.3. The reaction mix consisted of 7.5 µl 1X SYBR Green master mix (Applied Biosystems), 10 ng cDNA template (2 µl), 50 pmol/µL (0.3 µl) primer mix and 5.2 µl RNase-free water per sample. The difference in gene expression was assessed using quantitative analysis based on standard copy number method where the gene of interest was normalized to the housekeeping gene (*18S* or *Tbt*).

## 2.9 Statistical analysis

Statistical analysis was performed using GraphPad Prism version 5.0 software. Depending on the experimental set up, statistical significance was calculated using Paired Student's T test, or one-way ANOVA followed by a Tukey post-hoc test. Significance was set at $p < 0.05$*. Data were expressed as means ± standard deviation (SD) except for MSD proinflammatory cytokine profiles. MSD data were represented as means ± standard error of the mean (SEM).

# Chapter 3

## GM-CSF alone is incapable of inducing pathology in an *in vitro* model of the CNS, but it exerts a pronounced effect on microglia

# 3 GM-CSF alone is incapable of inducing pathology in an *in vitro* model of the CNS, but it exerts a pronounced effect on microglia

## 3.3 Introduction

Recent studies identified GM-CSF as a key T cell-derived effector cytokine required to initiate tissue damage and neurological deficits in EAE (Ponomarev et al., 2007), but precisely how it contributes to disease development remains unclear. This influential publication emphasised effects of GM-CSF in the periphery where it was described as “licensing” myeloid cells to mediate tissue damage in the CNS (Ponomarev et al., 2007). In view of this report we addressed the question whether GM-CSF itself can mediate demyelination and/or axonal injury in the CNS. Microglia are the only cells in the CNS that express both GM-CSF receptor subunits (Y. Zhang et al., 2014) leading us to predict microglia will be the only cells that respond directly to GM-CSF in myelinating cultures derived from embryonic mouse spinal cord (C. E. Thomson et al., 2008). We therefore used this culture system to determine if GM-CSF mediated activation of microglia had any impact on myelination and/or neuronal function/survival.

## 3.4 Results

### 3.4.1 GM-CSF alone is insufficient to induce axonal or myelin loss

To study the effects of GM-CSF on neurite outgrowth and myelination mouse myelinating cultures were treated with GM-CSF. In this *in vitro* model, neurite outgrowth is essentially complete by day in vitro (DIV) 15-17 and oligodendrocytes start myelinating axons from 15 DIV onwards (C. E. Thomson et al., 2008). Therefore, cultures were treated with 100 ng/ml GM-CSF from (i) 6 to 24 DIV to determine if it affects neurite outgrowth or myelin formation in a developmental setting and (ii) DIV 24 until DIV 30 to determine if it affects established myelinated axons. Following treatment cultures were fixed and stained with antibodies specific to MOG (clone Z2) and phosphorylated heavy and medium chain neurofilament (clone SMI31) and axonal density and myelination were quantified from fluorescence micrographs as described in the materials and methods section 2.5. Cultures with axonal density below 50% and percentage myelination less than 1% were discarded.

#### 3.4.1.1 GM-CSF has no effect on myelin formation or axonal growth *in vitro*

GM-CSF was found to have no effect on neurite outgrowth and myelination. There was no visible difference in staining for neurofilaments (SMI31) or myelin (MOG) between untreated control or GM-CSF treated cultures in a developmental setting (6 to 24 DIV) (Figure 3.1 a, b). This was confirmed when random fields of view were quantified for neurite density (untreated = 62.14 ± 4.590 %; GM-CSF = 55.77 ± 9.345 %; $p = 0.182$) and myelination (untreated = 3.926 ± 2.170 %; GM-CSF = 4.427 ± 2.202 %; $p = 0.755$) (Figure 3.1 c, d).

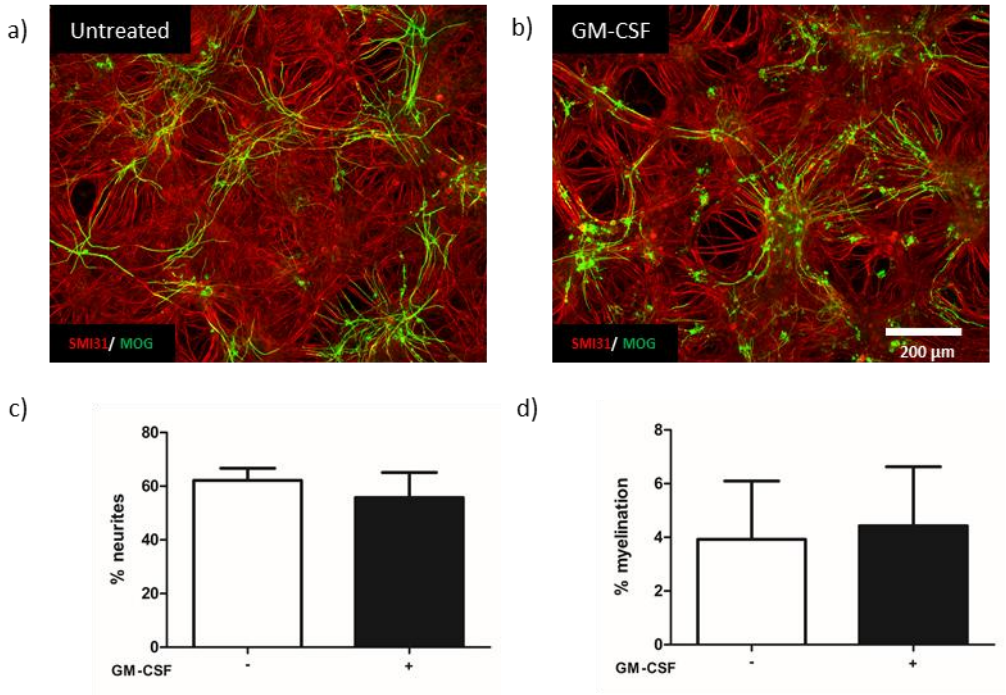


**Figure 3.1. GM-CSF has no effect on myelin formation and axonal growth *in vitro*.** (a, b) Representative images of myelinating cultures grown in the presence or absence of 100 ng/ml GM-CSF from 6 to 24 DIV. Images were aquired at 24 DIV. Myelin and axons were visualized with anti-MOG (clone Z2, green) and anti-neurofilament (SMI31, red) antibodies, respectively. GM-CSF had no effect on either (c) neurite out growth (p = 0.182) or (d) myelination (p= 0.755). Data presented as mean ± SD from four independent experiments, p values were calculated using a paired Student's t test.

### 3.4.1.2 GM-CSF does not induce demyelination or axonal loss *in vitro*

Adding GM-CSF to myelinating cultures in which myelin was already established had no effect on myelination or neurite density. There was no reduction in either SMI31 or MOG staining in response to GM-CSF, demonstrating that GM-CSF did not mediate demyelination and/or axonal damage in the CNS (Figure 3.2 a, b). This was reflected by lack of change in neurite density (SMI31 staining; untreated = 69.28 ± 2.720 %; GM-CSF = 75.09 ± 3.789 %; p= 0.131) or myelination (MOG staining; untreated = 3.954 ± 2.418 %; GM-CSF = 5.426 ± 1.706 %; p= 0.096) (Figure 3.3 c, d).

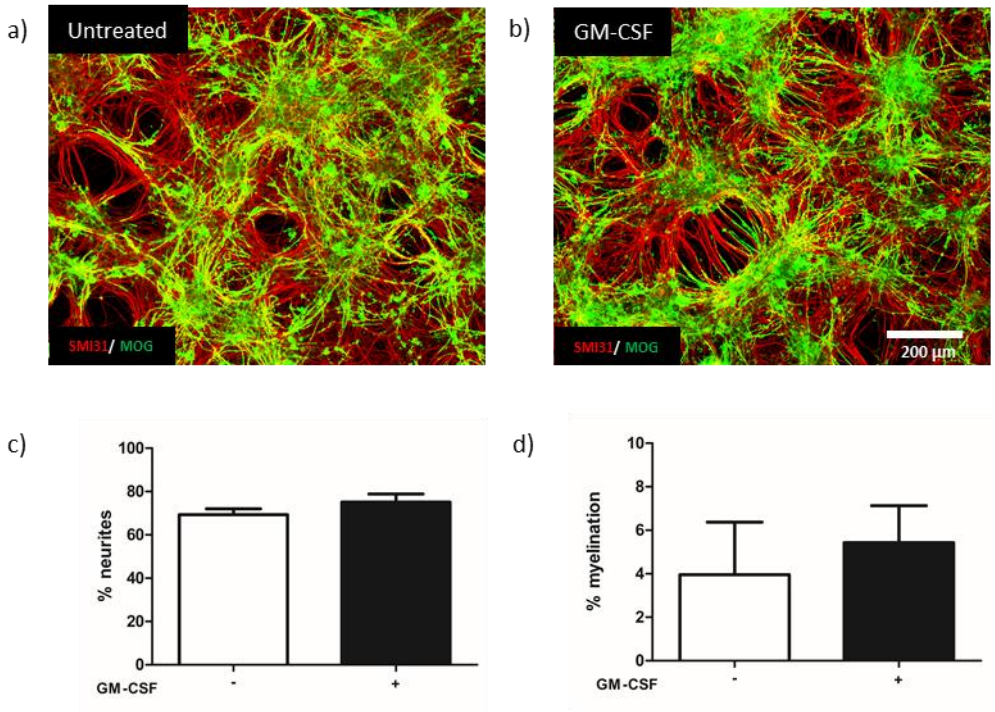


**Figure 3.2. GM-CSF does not induce demyelination or axonal loss *in vitro*.** (a, b) Representative images of myelinating cultures grown in the presence or absence of 100 ng/ml GM-CSF from 24 to 30 DIV. Images were aquired at 30 DIV. GM-CSF had no effect on either (c) neurite density (p= 0.131) or (d) myelination (p= 0.096). Data presented as mean ± SD from three independent experiments, p values were calculated using a paired Student's t test.

## 3.4.2 GM-CSF increases microglia number and induces morphological changes in these cells

To investigate the effect of GM-CSF on microglia, microglia were visualised using antibodies specific for Iba1 and/or CD45.

### 3.4.2.1 Extended exposure to GM-CSF augments microglial numbers and modifies their morphology

Long term treatment with GM-CSF (6 to 24 DIV) was associated with a massive increase in microglial numbers (Figure 3.3). The number of $CD45^+$ cells per area of interest increased >20-fold from 14.25 ± 7.386 in untreated cultures to 312.4 ± 30.61 in cultures treated with GM-CSF (Figure 3.3 a - c), an increase that resulted in a doubling of total (DAPI +ve) cell number per field of view (Figure 3.3e). However only a relatively small percentage these $CD45^+$ cells expressed detectable levels of Iba1, a classical microglial marker; the percentage of $CD45^+$

cells co-expressing Iba1 increased from 2.237 ± 0.905 % in untreated cultures to 30.22 ± 0.567 % in the presence of GM-CSF (Figure 3.3 a - d). This increase in $CD45^+$ microglia was associated with a pronounced change in morphology (Figure 3.4). This change in microglia morphology was assessed on the basis of dividing them into three categories: amoeboid, ramified and rounded (Thored et al., 2009). The majority of microglia in untreated cultures were ramified (85.59 ± 5.253%), whilst in GM-CSF treated cultures most adopted a rounded morphology (95.87± 2.891%) (Figures 3.4 a – c). This was associated with a phenotypic change with respect to Iba1 expression. Virtually all $Iba1^+$ microglia in untreated controls were also $CD45^+$ (96.77± 2.636 %), but in GM-CSF treated cultures this was reduced to 25.78 ± 2.058 % (Figure 3.4 d). GM-CSF therefore induces the appearance/expansion of a population of $CD45^+$, $Iba1^-$ cells.

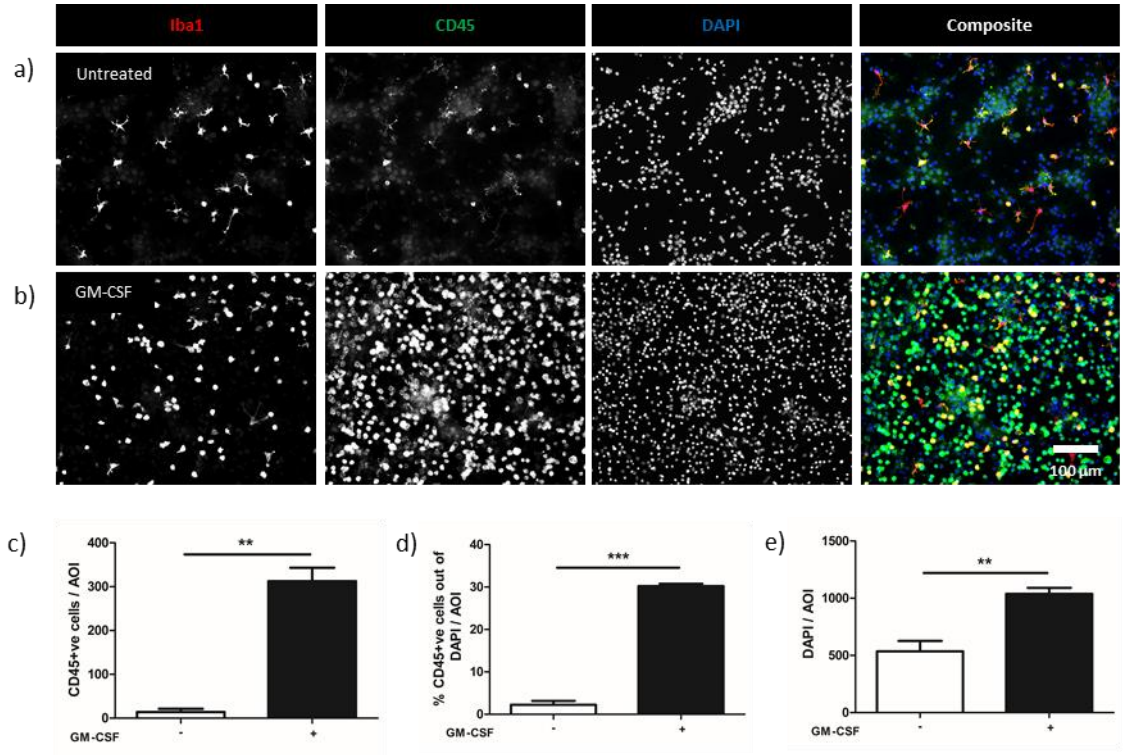


**Figure 3.3. Extended GM-CSF treatment in a developmental setting increases the density of microglia *in vitro*.** (a, b) Representative images of myelinating cultures grown in the presence or absence of 100 ng/ml GM-CSF from 6 to 24 DIV. Images were aquired at 24 DIV. Microglia were visualized with anti-Iba1 (red) and anti-CD45 (green), respectively. All nuclei were stained with DAPI (blue). GM-CSF treatment increased the (c) absolute density of microglia ($p< 0.01$), (d) the percentage of microglia as a proportion of all cells ($p< 0.001$) and (e) total cell density ($p< 0.001$). Data presented as mean ± SD from three independent experiments, p values were calculated using a paired Student's t test. AOI= area of interest.

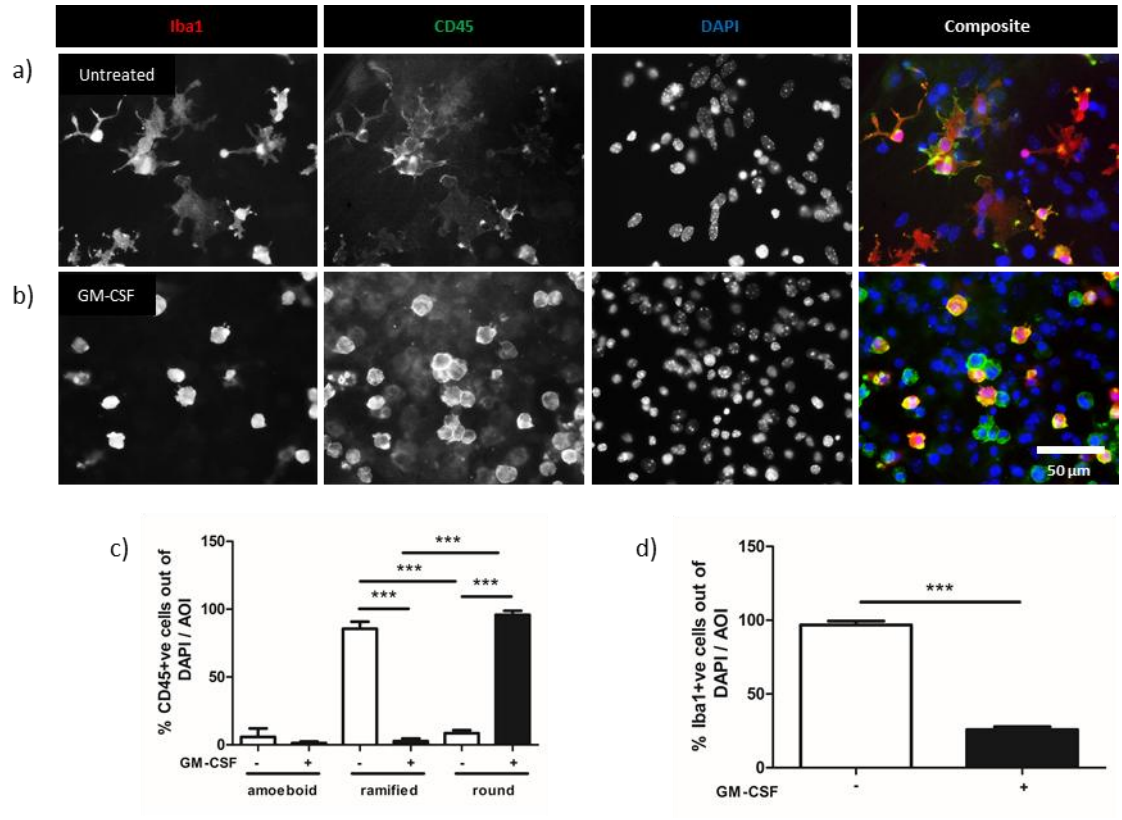


**Figure 3.4. GM-CSF induces a change in microglial morphology.** (a, b) Representative images of myelinating cultures grown in the presence or absence of 100 ng/ml GM-CSF from 6 to 24 DIV. Images were aquired at 24 DIV. Microglia were visualized with Iba1 (red) and -CD45 (green) specific antibodies. Nuclei were stained with DAPI (blue). (c) Microglial morphology was quantified using criteria adapted from (Thored et al., 2009). GM-CSF induces preferential expansion of microglia with a rounded morphology. (d) GM-CSF induces the expansion of Iba1$^-$ cells. Data presented as mean ± SD from three independent experiments. p values calculated using a (c) one-way ANOVA followed by a Tukey post-hoc test and (d) a paired Student's t test. AOI= area of interest.

### 3.4.2.2 GM-CSF treatment in a mature context increases the number of microglia which are all Iba1 and CD45 positive

To determine if GM-CSF has a similar effect on microglia in cultures that were already myelinated, cultures were treated with 100 ng/ml GM-CSF from 24 to 30 DIV. In this treatment paradigm GM-CSF induced a smaller but still significant increase in CD45$^+$ cell numbers (Figure 3.5 a – d). However, unlike the "developmental" setting, these CD45$^+$ cells also expressed the classical microglial marker Iba1 (Figure 3.5 a, b). Higher expression of CD45, reflected in increased intensity of staining and increased numbers of CD45$^+$ cells, in the developmental setting could be connected to the role of CD45 expression in

early myeloid progenitor cell differentiation (Broxmeyer, 1991; Shivtiel *et al.*, 2008). As all following experiments were performed using cultures at or beyond 24 DIV these two markers will be used interchangeably to identify microglia in order to accommodate co-staining for other targets using antibodies with different isotypes and/or from other species.

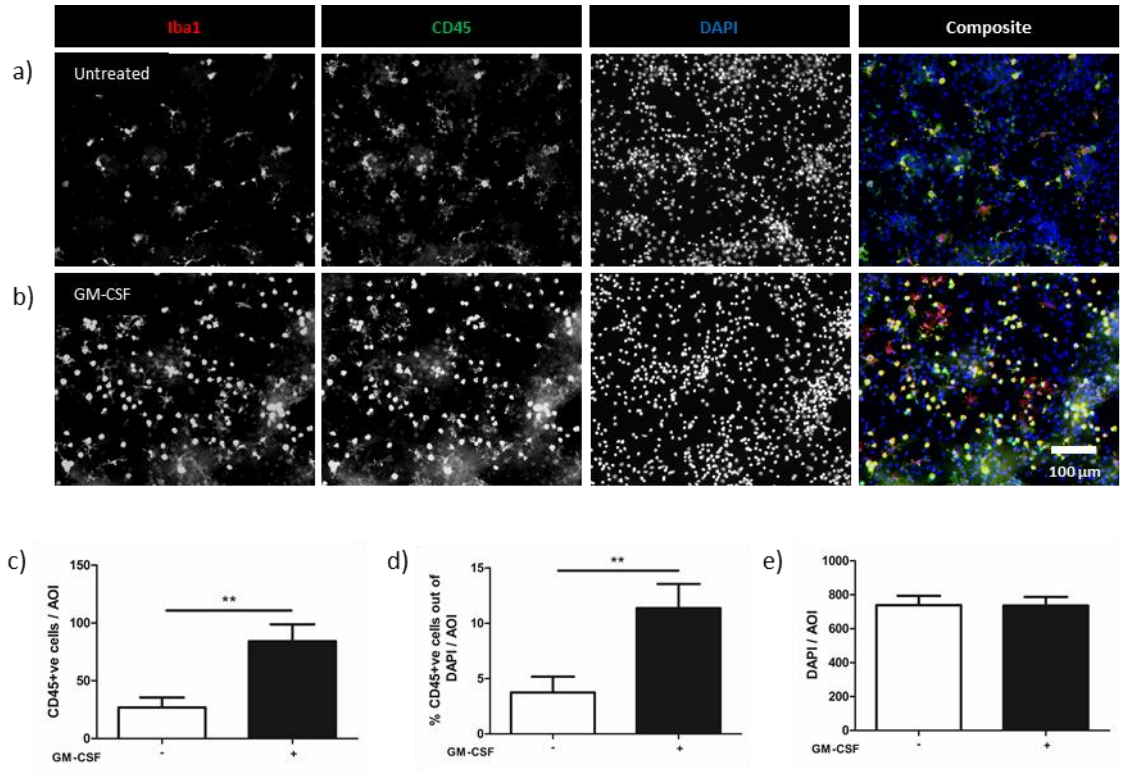


**Figure 3.5. GM-CSF treatment in a mature context increases the number of microglia which are both Iba1 and CD45 positive**. (a, b) Representative images of myelinating cultures grown in the presence or absence of 100 ng/ml GM-CSF from 24 to 30 DIV. Images were aquired at 30 DIV. Microglia were visualized with anti-Iba1 (red) and anti-CD45 (green) antibodies, respectively. All nuclei were stained with DAPI (blue). As evident from the photomicrographs all microglia were Iba1 and CD45 double positive in both conditions. (c, d) GM-CSF increased the absolute number of microglia and percentage of microglia as a proportion of all cells ($p < 0.01$), (e) but had no effect on the total number of cells ($p > 0.05$). Data presented as mean ± SD from three independent experiments, p values were calculated using a paired Student's t test. AOI= area of interest.

### 3.4.3 Lack of GM-CSF signalling has no effect on microglia number and morphology

To confirm the effects described above were dependent on signal transduction by GM-CSFR we used myelinating cultures derived from *Csf2rb* KO mouse embryos. These cultures lack a functional GM-CSF receptor and are hence incapable of responding to GM-CSF stimulation. Microglia in *Csf2rb* KO-derived cultures appear morphologically normal when stained with Iba1 and as anticipated, treatment with GM-CSF no longer induced changes in microglial numbers or morphology. The dominant microglial morphology remained ramified and Iba1$^{+}$ microglial numbers remained unchanged; 16.61 ± 2.216 per area of interest in untreated cultures and 14.69 ± 3.994 in GM-CSF treated cultures (Figure 3.6).

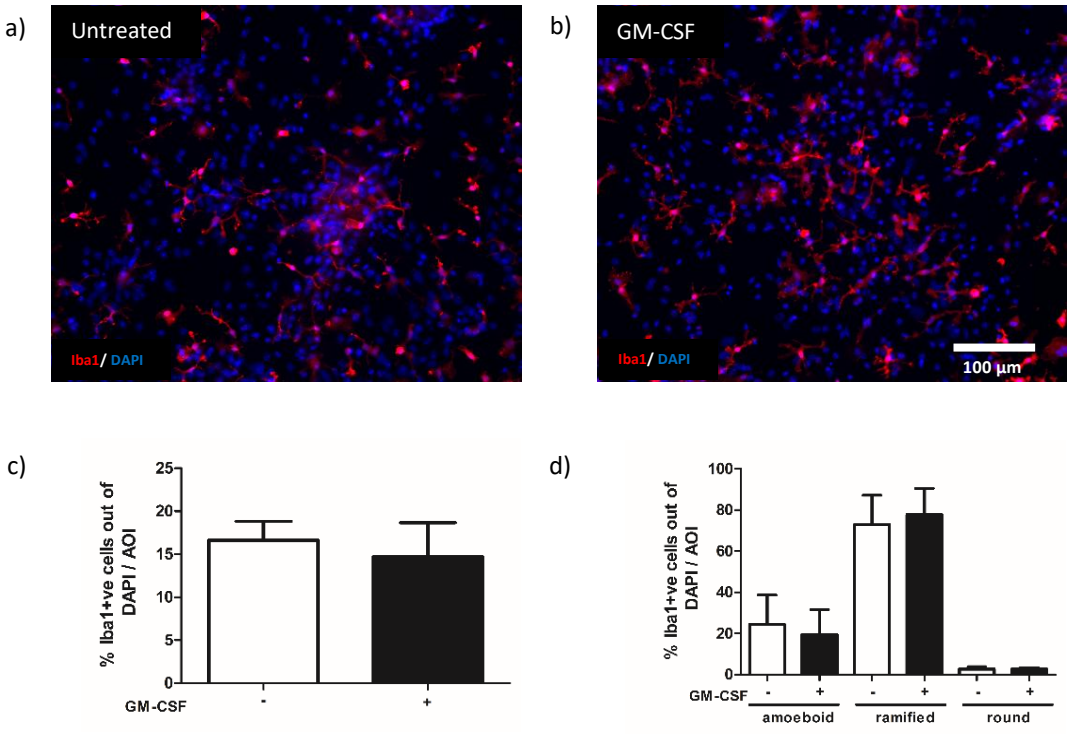


**Figure 3.6. Abolition of GM-CSF signalling eliminates the impact of GM-CSF on microglial numbers and morphology** (a, b) Representative images of *Csf2rb* KO myelinating cultures grown in the presence or absence of 100 ng/ml GM-CSF from 6 to 24 DIV. Images were aquired at 30 DIV. Microglia were visualized with anti-Iba1 and the nuclei with DAPI (blue). (c) Microglia density is unaltered by GM-CSF in *Csf2rb* KO cultures ($p > 0.05$). (d) GM-CSF had no effect on microglial morphology in *Csf2rb* KO cultures ($p > 0.05$). Data presented as mean ± SD from three independent experiments. p values were calculated using (c) paired Student's t test and (d) a one-way ANOVA followed by a Tukey post-hoc test. AOI= area of interest.

## 3.5 Discussion

To study the effects of GM-CSF in the CNS in the absence of a peripheral immune compartment we used myelinating cultures generated from embryonic mouse spinal cord and investigated its effects in two treatment paradigms; a developmental setting (DIV 6 to 24) and an 'adult' setting (DIV 24 -30). In summary GM-CSF had no detrimental effects on quantities of anti-MOG positive myelin or phosphorylated neurofilament positive neurites (largely axons), and no obvious effect on the morphology of either, under either treatment paradigms. However, in both treatment paradigms, GM-CSF increased microglia numbers and induced a marked change in microglial morphology.

These microglial responses are in agreement with published studies documenting GM-CSF as a microglial mitogen (Esen & Kielian, 2007) and the distribution of mRNA transcripts for GM-CSF receptor subunits which predicts only microglia express a functional, high affinity receptor (Zhang *et al* 2014). Attempts to validate microglial expression of GM-CSF receptor by immunofluorescence were unsuccessful as available antibodies were found to lack specificity. This may also explain why there is no immunohistological consensus as to expression of GM-CSF receptor in human brain. On one hand expression was reported to be restricted to a small subset of activated microglia and astrocytes in white matter, and undetectable in grey matter (Vogel et al., 2015), whilst according to Ridwan *et al*. GM-CSFRα is not only present in astrocytes, ependymal, choroid plexus cells but also uniformly in grey matter neurons (Ridwan et al., 2012). The presence of a functional GM-CSFR was also reported on cultured rat oligodendrocytes (Baldwin et al., 1993), but again this observation may be attributed to lack of reagent specificity and/or contamination by microglia.

GM-CSF treatment also induced a profound change in microglial morphology from a ramified to round phenotype indicative of a change in their activation status (Davis, Foster and Thomas, 1994; Kettenmann *et al.*, 2011). Rounded "activated" microglia are associated with lesion formation in MS as well as other neurodegenerative disorders. In the context of MS, Tmem119$^{+}$, rounded/oval microglia containing myelin debris were identified in early active lesions, an observation suggesting a significant number of phagocytes at this point in lesion development are derived from resident microglia (Zrzavy et al., 2017a).

Rounded $CD45^+$ microglia with negligent Iba1 expression were also reported to be increased in the brain parenchyma of APP/PS1dE9 mice, a transgenic mouse model of Alzheimer's disease (Puli et al., 2012). A corresponding increase in CD45 immune reactivity is also observed in AD brain (Masliah et al., 1991) ,whilst rounded $Iba1^+$ $CD68^+$ cells have been observed in the corticospinal tract of amyotrophic lateral sclerosis patients (Brettschneider et al., 2012). However not only does the functional relevance of these morphological changes in microglia remains controversial, but it is difficult to assess whether these $CD45^+/Iba1^+$cells are indeed microglia or invading peripheral phagocytes. My study demonstrates there are not invading peripheral cells. In the wider context, treatment of microglia with other pro-inflammatory stimuli also results in a transition toward a rounded "activated" morphology, as demonstrated following treatment of primary rat microglia with LPS or mixed neuronal-glial cultures infected with Borna disease virus, where a transition towards a round morphology of microglia was observed (Ovanesov et al., 2006).

In this experimental setting lack of GM-CSF signalling had no effect on microglial development, no differences in microglial morphology or numbers were observed in *Csf2rb* KO myelinating cultures. Lack of GM-CSF signalling did not result in major difference in haematopoietic compartment, but induced lung pathology (Stanley et al., 2006). Microglia survival in the CNS is dependent on tonic signalling via the Csf1r receptor by M-CSF or IL-34 (Erblich *et al.*, 2011; Elmore *et al.*, 2014).

However, although GM-CSF changes the morphology of microglia in myelinated cultures, it is clear that whatever pathways this response is associated with, in isolation this is unable to mediate tissue damage in this culture system, at least under the conditions investigated. This observation led us to explore in more detail how GM-CSF might contribute to the immunopathogenesis of demyelination and axonal injury in EAE.

# Chapter 4

## GM-CSF induces an immune signature and increases the phagocytic capacity of microglia

# 4 GM-CSF induces an immune signature and increases the phagocytic capacity of microglia

## 4.1 Introduction

The previous chapter demonstrated GM-CSF had no detrimental effect on neurites or myelin *in vitro* but increased microglial numbers and affected their morphology. The observation that GM-CSF targets microglia selectively is in accordance with data demonstrating microglia are the only CNS cell type expressing its high affinity receptor (Zhang *et al* 2014). However, in the absence of any obvious impact of GM-CSF signalling on cell survival, neurite outgrowth or myelin, it was important to determine the functional significance of this microglia response. Previous studies using isolated neonatal microglia led us to anticipate GM-CSF would up-regulate expression of genes encoding products associated with immune cell activation, migration, antigen presentation and phagocytosis. However, it was unknown if selective activation of quiescent microglia by GM-CSF in the CNS would trigger off-target transcriptional effects in other cell types. To investigate this and define the CNS transcriptome induced by GM-CSF, myelinated cultures (24 DIV) were treated with GM-CSF for 24h and then processed for RNAseq analysis.

## 4.2 Results

### 4.2.1 RNAseq based analysis of the effects of GM-CSF in myelinated cultures

To define the transcriptional response induced by GM-CSF an RNAseq study was performed on mouse myelinating cultures treated with100 ng/ml GM-CSF for 24 hours (DIV 24 to 25) (Figure 4.1). Fluorescence microscopy using Iba1 as a microglial marker revealed short-term treatment with GM-CSF had no effect on either microglial morphology or density in these cultures (Untreated = 45.91 ± 12.98 $Iba1^+$ cells/AOI; GM-CSF = 54.34 ± 9.003 $Iba1^+$ cells/AOI; p= 0.0839). The quality of the cell cultures was verified by quantifying neurite density, defined as neurofilament positive staining as a percentage of the total area of the AOI (Untreated = 75.61 ± 2.243 %; GM-CSF = 71.55 ± 4.758 %) and myelination, defined as MOG positive staining as a percentage of neurofilament positive staining (Untreated = 8.062 ± 1.780 %; GM-CSF = 7.495 ± 0.494 %) (Appendix 7.1).

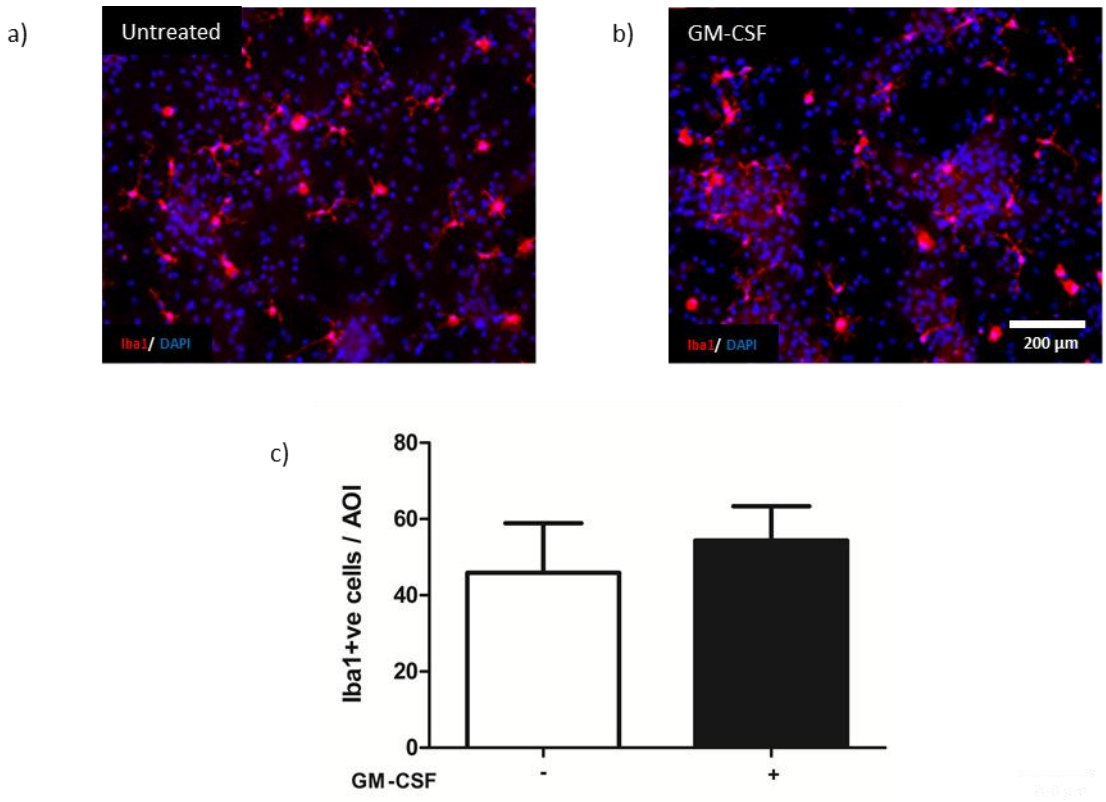


**Figure 4.1. 24h GM-CSF treatment does not affect microglial number**. (a, b) Representative images of mouse myelinating cultures grown in the presence or absence of 100 ng/ml GM-CSF for 24h from 24 DIV. Images were aquired at 24 DIV. Microglia were visualized with anti-Iba1 and the nuclei with DAPI (blue). (c) There was no difference in microglia number when GM-CSF was added for 24h compared to control

(p> 0.0839). Data presented as mean ± SD from three independent experiments, p values were calculated using a paired Student's t test. AOI= area of interest.

Input messenger RNA (mRNA) was quality controlled by Edinburgh Genomics who provided multi-dimensional scale (MDS) and volcano plots shown in Figures 4.2 and 4.3, respectively. The MDS plot demonstrates GM-CSF treatment induced a consistent change in the transcriptional profile of myelinating cultures with untreated control samples clustering at the bottom of the plot, whilst GM-CSF treated were located towards the top. This plot also indicates there was intra group variance. There was no correlation between the number of microglia in each biological replicate and the MDS plot distribution.

After eliminating genes with less than 20 reads across all samples, 137 differentially regulated genes were identified (108 up-, 29 down-regulated; ± >2 fold change, FDR < 0.05) (Figure 4.3). A complete gene list can be found in Figure 4.4 but it was apparent from visual inspection this was enriched in immune related genes. These could be divided into three main categories: surface receptors, chemokines/cytokines and chemokine/cytokine receptors (Figure 4.5). The latter included *Csf2rb* (log2FC= 1.992) that encodes the common beta chain of the high affinity receptor for IL-3, IL-5 and GM-CSF (Figure 4.5). We also compared our transcript list with the Zhang *et al*. CNS RNAseq data base. This comparison revealed that 74.4 % of the genes are differentially most expressed by microglia. There was also a much weaker endothelial cell signature (18.9 % of the GM-CSF differentially modulated genes most expressed in endothelial cells). Only 7.7 % of all differentially expressed genes are expressed by neurons, astrocytes, oligodendrocyte progenitor cells and/or myelinating oligodendrocytes.

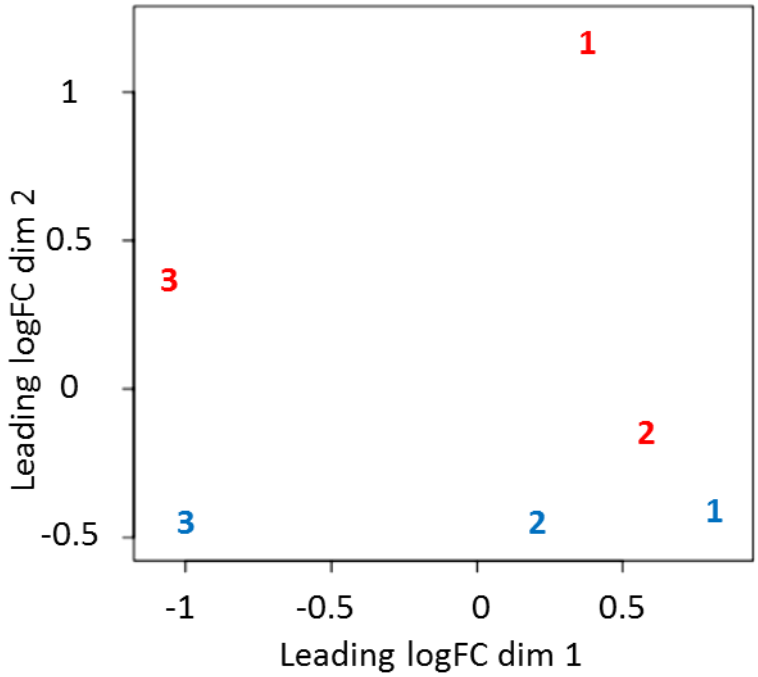


**Figure 4.2. Multi-dimensional scale plot (MDS) showing the similarities in gene expression between untreated and GM-CSF treated samples used for RNAseq.** Myelinating cultures (n = 3; numbered 1, 2 and 3) were untreated (blue) or treated with 100 ng/ml GM-CSF (red) at 24 DIV for 24h. RNA was extracted at 24 DIV. Closer grouping indicates closer similarity of the transcriptional profiles. Plot produced in edgeR by Edinburgh Genomics.

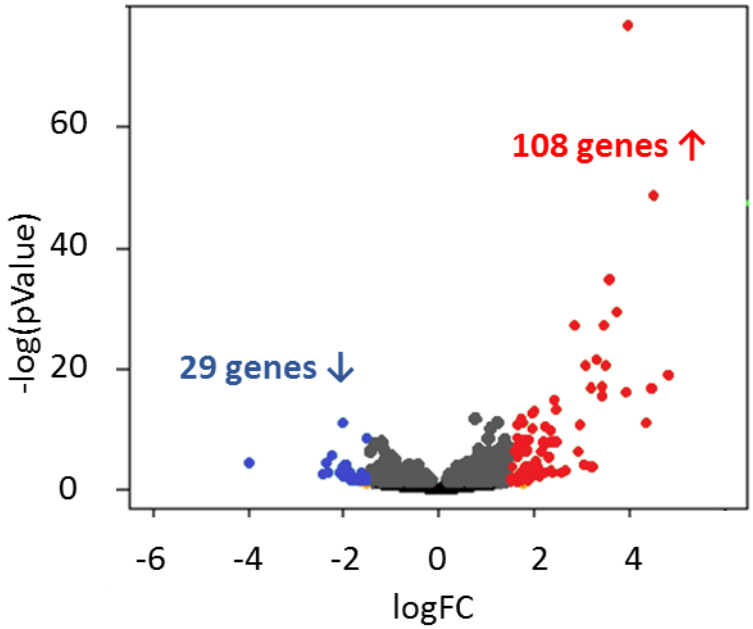


**Figure 4.3. Volcano plot showing the distribution of differentially expressed genes in untreated and GM-CSF treated myelinating cultures.** There were 137 differentially modulated genes (FDR< 0.05) in the RNAseq study; 29 genes down regulated (blue) and 108 upregulated genes (red). The points in grey represent genes with a fold change less than 2 (log2 FC= 1). Plot produced in edgeR by Edinburgh Genomics.

| Gene symbol | logFC | PValue | FDR | Zhang *et al* |
|---|---|---|---|---|
| *Mgl2* | 6.545283 | 4.51E-48 | 2.98E-44 | microglia > 2 FPKM |
| *Ccr2* | 4.80661 | 1.53E-19 | 2.76E-16 | microglia < 2 FPKM |
| *Ccr1* | 4.488449 | 2.03E-49 | 2.01E-45 | microglia > 2 FPKM |
| *Mmp8* | 4.48116 | 2.42E-17 | 3.43E-14 | microglia < 2 FPKM |
| *Gm16194* | 4.365004 | 1.05E-11 | 7.98E-09 | not found |
| *Spint1* | 3.981624 | 1.11E-77 | 2.19E-73 | same level |
| *Bcl2a1a* | 3.941623 | 5.54E-17 | 7.32E-14 | microglia > 2 FPKM |
| *Trem1* | 3.747021 | 4.07E-30 | 1.61E-26 | microglia < 2 FPKM |
| *Cd300lf* | 3.583926 | 1.85E-35 | 9.18E-32 | microglia > 2 FPKM |
| *Gm1966* | 3.504852 | 3.55E-21 | 7.03E-18 | not found |
| *Clec4n* | 3.448354 | 4.52E-28 | 1.49E-24 | microglia > 2 FPKM |
| *Ccl12* | 3.40799 | 4.69E-16 | 5.81E-13 | microglia > 2 FPKM |
| *Ccl6* | 3.406591 | 6.37E-18 | 1.05E-14 | microglia > 2 FPKM |
| *Rab44* | 3.323056 | 2.37E-22 | 5.87E-19 | same level |
| *Tnfsf8* | 3.222937 | 0.000151 | 0.026008 | same level |
| *Tfec* | 3.199487 | 2.05E-17 | 3.13E-14 | microglia > 2 FPKM |
| *4921529L05Rik* | 3.179897 | 0.000215 | 0.033788 | microglia > 2 FPKM |
| *Cdh1* | 3.088047 | 3.18E-21 | 7.02E-18 | same level |
| *Pilrb2* | 3.050372 | 5.94E-05 | 0.012135 | microglia < 2 FPKM |
| *Serpina3f* | 3.028043 | 7.87E-05 | 0.015613 | endothelial cells |
| *Scimp* | 2.973231 | 2.24E-11 | 1.58E-08 | not found |
| *Clec10a* | 2.923192 | 4.70E-07 | 0.000161 | microglia > 2 FPKM |
| *Cd74* | 2.852683 | 7.97E-28 | 2.26E-24 | microglia > 2 FPKM |
| *Mmp13* | 2.470581 | 6.67E-14 | 7.34E-11 | same level |
| *Amica1* | 2.444389 | 1.77E-08 | 8.35E-06 | microglia < 2 FPKM |
| *H2-DMb2* | 2.412916 | 1.61E-15 | 1.88E-12 | microglia > 2 FPKM |
| *Kynu* | 2.352608 | 1.39E-10 | 8.58E-08 | same level |
| *Siglecf* | 2.333867 | 1.65E-08 | 8.13E-06 | microglia > 2 FPKM |
| *Itgax* | 2.294974 | 3.40E-06 | 0.000964 | microglia > 2 FPKM |
| *Adora3* | 2.24725 | 1.95E-08 | 9.00E-06 | microglia > 2 FPKM |
| *Bcl2a1d* | 2.223198 | 3.31E-11 | 2.26E-08 | microglia > 2 FPKM |
| *Fam167b* | 2.199645 | 1.68E-08 | 8.13E-06 | microglia > 2 FPKM |
| *Gbp4* | 2.162368 | 4.49E-07 | 0.000156 | endothelial cells > 2 FPKM |
| *Trim30c* | 2.090533 | 0.000127 | 0.023067 | not found |

**Figure 4.4a. Complete list of GM-SF differentially expressed genes.** Transcripts are arranged in descending order based on their Log2FC. List is showing p-value and FDR (false discovery rate) for each gene. The last column represents the cellular expression of each gene in the resting CNS based on the Zhang *et al*. CNS transcriptomics data base (Y. Zhang et al., 2014). A transcript was considered most enriched in a particular cell type if its FPKM (Fragments per Kilobase of transcript per Million mapped reads) was higher than 2 and at least twice bigger than the second highest FPKM value. Out of 137 genes, 121 were found in the Zhang *et al*. data base, 31 (34.4 %) had the same expression level in all cell types, 67 (74.4 %) were most enriched in microglia, 17 (18.9 %) in endothelial cells, 3 (3.3 %) in oligodendrocyte progenitor cells (OPC), 2 (2.2 %) in neurons, 1 (1.1 %) in astrocytes, 1 (1.1 %) in MOC (myelinating oligodendrocytes).

Transcripts most enriched in microglia are highlighted in grey. The list continues on next 3 pages.

| Gene symbol | logFC | PValue | FDR | Zhang *et al* |
|---|---|---|---|---|
| *Ccl7* | 2.051569 | 1.69E-05 | 0.004041 | microglia > 2 FPKM |
| *Csf2rb* | 1.992225 | 1.21E-13 | 1.26E-10 | microglia > 2 FPKM |
| *F13a1* | 1.961582 | 6.54E-11 | 4.32E-08 | microglia > 2 FPKM |
| *Tifab* | 1.957255 | 1.95E-13 | 1.94E-10 | microglia > 2 FPKM |
| *Slfn3* | 1.919753 | 0.000178 | 0.029974 | same level |
| *Ccl2* | 1.869522 | 7.51E-09 | 4.02E-06 | microglia > 2 FPKM |
| *Il1rl2* | 1.831374 | 3.63E-07 | 0.000128 | microglia > 2 FPKM |
| *Rasgrp4* | 1.828526 | 3.03E-07 | 0.000109 | microglia/ endothelial cells > 2 FPKM |
| *Pilra* | 1.806432 | 0.000212 | 0.033659 | microglia > 2 FPKM |
| *Gapt* | 1.79363 | 0.000183 | 0.03046 | microglia < 2 FPKM |
| *Mrc1* | 1.778686 | 8.00E-09 | 4.18E-06 | microglia > 2 FPKM |
| *Batf* | 1.775251 | 5.39E-07 | 0.000178 | microglia > 2 FPKM |
| *Sla* | 1.749324 | 7.11E-12 | 5.88E-09 | microglia > 2 FPKM |
| *Il18rap* | 1.734669 | 1.94E-12 | 1.75E-09 | same level |
| *Ccl9* | 1.696582 | 7.97E-08 | 3.16E-05 | microglia > 2 FPKM |
| *Mmp12* | 1.664113 | 6.36E-06 | 0.001704 | microglia < 2 FPKM |
| *Scel* | 1.655481 | 1.90E-11 | 1.39E-08 | same level |
| *I830077J02Rik* | 1.654689 | 2.15E-09 | 1.29E-06 | not found |
| *Ccr5* | 1.653725 | 5.42E-08 | 2.29E-05 | microglia > 2 FPKM |
| *Wfdc17* | 1.577435 | 5.05E-07 | 0.00017 | not found |
| *Gm14005* | 1.548786 | 0.000202 | 0.032857 | endothelial cells > 2 FPKM |
| *Prr15* | 1.458989 | 2.53E-05 | 0.005776 | same level |
| *Cd274* | 1.45667 | 6.64E-08 | 2.69E-05 | neurons > 2 FPKM |
| *P2ry14* | 1.451709 | 4.45E-05 | 0.009591 | same level |
| *Msr1* | 1.41989 | 6.11E-08 | 2.52E-05 | microglia > 2 FPKM |
| *Egr2* | 1.380003 | 4.47E-09 | 2.46E-06 | microglia > 2 FPKM |
| *Ccl8* | 1.378187 | 8.32E-05 | 0.016167 | microglia > 2 FPKM |
| *Rhoh* | 1.373598 | 3.53E-06 | 0.000986 | microglia > 2 FPKM |
| *Fcgr2b* | 1.341499 | 4.59E-06 | 0.001263 | microglia > 2 FPKM |
| *Clec7a* | 1.329271 | 1.60E-05 | 0.003864 | microglia < 2 FPKM |
| *Pik3r6* | 1.328437 | 0.000263 | 0.040791 | endothelial cells > 2 FPKM |
| *Cd33* | 1.3143 | 2.81E-07 | 0.000103 | microglia > 2 FPKM |
| *Clec5a* | 1.306924 | 1.39E-07 | 5.40E-05 | microglia > 2 FPKM |
| *Pstpip2* | 1.284738 | 1.18E-05 | 0.00296 | OPC > 2 FPKM |

**Figure 4.4b. Complete list of GM-SF differentially expressed genes.** (Continues on the next page)

| Gene symbol | logFC | PValue | FDR | Zhang *et al* |
|---|---|---|---|---|
| *Ms4a4a* | 1.278668 | 0.000111 | 0.020393 | microglia > 2 FPKM |
| *Pyhin1* | 1.265976 | 9.41E-05 | 0.01761 | same level |
| *Ptgs1* | 1.220168 | 7.10E-12 | 5.88E-09 | microglia > 2 FPKM |
| *Slfn2* | 1.21445 | 1.41E-05 | 0.003491 | microglia > 2 FPKM |
| *Il4ra* | 1.204609 | 7.26E-07 | 0.000229 | microglia > 2 FPKM |
| *Gm8995* | 1.193093 | 1.86E-06 | 0.000559 | same level |
| *Runx1* | 1.141074 | 5.57E-06 | 0.001513 | microglia > 2 FPKM |
| *Ch25h* | 1.087988 | 3.62E-05 | 0.008161 | microglia > 2 FPKM |
| *Plaur* | 1.087022 | 0.000301 | 0.044866 | microglia > 2 FPKM |
| *H2-DMa* | 1.083368 | 8.20E-11 | 5.25E-08 | microglia > 2 FPKM |
| *Lsr* | 1.079997 | 1.77E-05 | 0.004166 | endothelial cells |
| *Ctsc* | 1.068894 | 8.43E-07 | 0.000261 | microglia > 2 FPKM |
| *Gbp9* | 1.06642 | 1.04E-05 | 0.002633 | endothelial cells |
| *Cysltr1* | 1.054882 | 4.74E-05 | 0.010098 | microglia > 2 FPKM |
| *Gbp7* | 1.049414 | 4.37E-09 | 2.46E-06 | endothelial cells |
| *Gpr160* | 1.040466 | 0.000288 | 0.043576 | endothelial cells |
| *P2ry13* | 1.02401 | 6.14E-07 | 0.000199 | microglia > 2 FPKM |
| *St14* | 1.011414 | 0.000146 | 0.025567 | microglia > 2 FPKM |
| *Fcgr3* | 1.007673 | 2.18E-05 | 0.005086 | microglia > 2 FPKM |
| *Itgal* | 0.974566 | 5.73E-05 | 0.011961 | microglia < 2 FPKM |
| *B3gnt7* | 0.914678 | 8.14E-05 | 0.01597 | same level |
| *Slco4a1* | 0.900685 | 0.000212 | 0.033659 | same level |
| *Cish* | 0.887356 | 4.13E-05 | 0.009001 | endothelial cells > 2 FPKM |
| *Pnp* | 0.867774 | 2.79E-06 | 0.000803 | microglia > 2 FPKM |
| *Slc1a5* | 0.863831 | 5.92E-05 | 0.012135 | microglia / endothelial cells > 2 FPKM |
| *Emilin2* | 0.854265 | 0.000139 | 0.024538 | microglia / MOC > 2 FPKM |
| *Nabp1* | 0.844596 | 1.09E-06 | 0.000333 | not found |
| *Ier3* | 0.828143 | 0.000132 | 0.023736 | not found |
| *Cebpb* | 0.825605 | 0.000323 | 0.046732 | microglia > 2 FPKM |
| *Coro2a* | 0.821955 | 2.74E-07 | 0.000102 | microglia > 2 FPKM |
| *Rgs14* | 0.819442 | 0.000316 | 0.046408 | microglia > 2 FPKM |
| *Pim1* | 0.780399 | 0.000294 | 0.044221 | microglia > 2 FPKM |
| *Gbp3* | 0.762526 | 0.000272 | 0.041645 | endothelial cells > 2 FPKM |
| *Egr1* | 0.753026 | 1.91E-12 | 1.75E-09 | same level |

**Figure 4.4c. Complete list of GM-SF differentially expressed genes.** (Continues on the next page)

| Gene symbol | logFC | PValue | FDR | Zhang *et al* |
|---|---|---|---|---|
| *Dna2* | 0.727032 | 2.39E-05 | 0.005517726 | same level |
| *Fos* | 0.557385 | 3.91E-05 | 0.008607457 | neurons > 2 FPKM |
| *Coro1a* | 0.493128 | 0.000227 | 0.035427644 | microglia > 2 FPKM |
| *1600014C10Rik* | 0.425288 | 0.000137 | 0.024429769 | not found |
| *Arc* | 0.423204 | 0.000314 | 0.046408271 | neurons > 2 FPKM |
| *Snx2* | 0.390796 | 0.000148 | 0.025727715 | endothelial cells > 2 FPKM |
| *Bcl6* | -0.444 | 7.40E-05 | 0.014824312 | OPC > 2 FPKM |
| *Kcnj2* | -0.61031 | 0.0001 | 0.018621618 | endothelial cells > 2 FPKM |
| *Mpeg1* | -0.80078 | 0.000321 | 0.046732346 | microglia > 2 FPKM |
| *Cd36* | -0.8646 | 0.000192 | 0.031719307 | microglia < 2 FPKM |
| *Adap2* | -0.92037 | 0.000159 | 0.027243092 | microglia > 2 FPKM |
| *Pik3ap1* | -0.92564 | 1.01E-05 | 0.002592218 | microglia > 2 FPKM |
| *Ighm* | -0.94904 | 7.09E-06 | 0.001874517 | not found |
| *Gpr34* | -1.01872 | 2.30E-06 | 0.000681333 | microglia > 2 FPKM |
| *Fyb* | -1.06447 | 8.41E-05 | 0.016179923 | microglia > 2 FPKM |
| *Ms4a7* | -1.07221 | 0.000273 | 0.0416452 | microglia > 2 FPKM |
| *Slc16a10* | -1.08009 | 1.43E-05 | 0.003492744 | microglia > 2 FPKM |
| *Slamf9* | -1.10723 | 7.62E-06 | 0.001986836 | microglia > 2 FPKM |
| *Pkd2l1* | -1.1122 | 6.32E-05 | 0.012788404 | same level |
| *Fcgr4* | -1.12435 | 0.000177 | 0.02991399 | microglia > 2 FPKM |
| *Cd72* | -1.17024 | 2.39E-07 | 9.11E-05 | microglia > 2 FPKM |
| *Cd180* | -1.2116 | 1.35E-08 | 6.87E-06 | microglia > 2 FPKM |
| *Cd5l* | -1.24509 | 2.25E-08 | 1.01E-05 | microglia < 2 FPKM |
| *Gm26714* | -1.2697 | 0.00021 | 0.033658595 | not found |
| *Serpinb6b* | -1.34647 | 3.68E-08 | 1.58E-05 | endothelial cells |
| *G530011O06Rik* | -1.35035 | 2.55E-08 | 1.12E-05 | not found |
| *Hmga2* | -1.426 | 6.41E-07 | 0.000205044 | astrocytes/ endothelial cells > 2 FPKM |
| *Ctla2b* | -1.52402 | 3.19E-09 | 1.86E-06 | endothelial cells |
| *Gm6377* | -1.94698 | 9.39E-05 | 0.017609898 | microglia < 2 FPKM |
| *Cxcr3* | -1.96462 | 9.14E-05 | 0.017423451 | microglia > 2 FPKM |
| *Fcrl1* | -2.01817 | 8.04E-12 | 6.38E-09 | microglia > 2 FPKM |
| *Gm29291* | -2.02608 | 0.000195 | 0.031891264 | not found |
| *Cmah* | -2.23445 | 2.46E-06 | 0.00071756 | same level |
| *Plxna4os1* | -2.35042 | 3.79E-05 | 0.008434008 | not found |
| *Rmrp* | -3.99982 | 5.66E-05 | 0.011936182 | astrocytes/ OPC > 2 FPKM |

**Figure 4.4d. Complete list of GM-SF differentially expressed genes.**

| Surface Receptors | Gene name | Rank | Log2 FC |
|---|---|---|---|
| *Mgl2* | Macrophage galactose N-acetyl-galactosamine specific lectin 2 (CD301b) | 1 | 6.555 |
| *Clec4n* | C-type lectin domain family 4, member n (Clec6a, Dectin-2) | 11 | 3.458 |
| *Clec10a* | C-Type lectin domain family 10 member A (CD301a, Macrophage galactose N-acetyl-galactosamine specific lectin 1) | 22 | 2.923 |
| *Siglecf* | Cluster of Differentiation 170 (Sialic acid binding Ig like lectin 5 ) | 28 | 2.334 |
| *Mrc1* | Mannose receptor C-type 1 (C-Type lectin domain family 13 member D) | 45 | 1.789 |
| *Clec7a* | C-Type lectin domain family 7 member A (Beta-glucan receptor, Dectin-1) | 64 | 1.329 |
| *Clec5a* | C-type lectin domain family 5 member A | 67 | 1.307 |
| **Cytokine** | **Gene name** | **Rank** | **Log2 FC** |
| *Ccl12* | Chemokine (C-C motif) ligand 12 (Monocyte chemotactic protein-5) | 12 | 3.408 |
| *Tnfsf8* | Tumor necrosis factor superfamily member 8 (CD153 Antigen, CD3 Ligand) | 15 | 3.223 |
| *Ccl6* | Chemokine (C-C motif) ligand 6 | 13 | 3.407 |
| *Ccl7* | Chemokine (C-C motif) ligand 7 (Monocyte chemoattractant protein 3 ) | 35 | 2.052 |
| *Ccl2* | Chemokine (C-C motif) ligand 2 (Monocyte chemoattractant protein 1) | 40 | 1.87 |
| *Ccl9* | Chemokine (C-C motif) ligand 9 | 49 | 1.697 |
| *Ccl8* | Chemokine (C-C motif) ligand 8 (Monocyte chemotactic protein 2) | 61 | 1.378 |
| **Cytokine Receptor** | **Gene name** | **Rank** | **Log2 FC** |
| *Ccr2* | C-C chemokine receptor type 2 | 2 | 4.806 |
| *Ccr1* | C-C chemokine receptor type 1 (Macrophage inflammatory protein 1-alpha receptor) | 3 | 4.489 |
| *Csf2rb* | Colony stimulating factor 2 receptor Beta common subunit (GM-CSF/IL-3/IL-5 Receptor common Beta subunit) | 36 | 1.992 |
| *Il1rl2* | Interleukin 1 receptor like 2 | 41 | 1.831 |
| *Ccr5* | C-C chemokine receptor type 5 (HIV-1 fusion coreceptor) | 53 | 1.654 |
| *Il4ra* | Interleukin 4 Receptor | 73 | 1.205 |
| *Cxcr3* | C-X-C motif chemokine receptor 3 (Interferon-Inducible Protein 10 Receptor) | 132 | -1.965 |

**Figure 4.5. List showing the three main categories of immune related genes: surface receptors from the lectin family, cytokines and cytokine receptors modulated by GM-CSF in myelinating cultures.** The three main categories of immune associated transcripts were manually selected from the gene list and arranged in descending order of log2 FC.

#### 4.2.1.1 Pathway analysis

Pathway analysis was performed using the Database for Annotation, Visualization and Integrated Discovery (DAVID) which allows unbiased biological interpretation of the differentially expressed genes and groups them into influential pathways utilising the KEGG database (Huang, Sherman, & Lempicki, 2009). This revealed

the GM-CSF associated transcriptome was enriched in multiple immune related pathways shown in descending order based on the p-value in Figure 4.6, alongside the contributing genes differentially regulated by GM-CSF. With the exception of "Transcriptional misregulation in cancer pathway" all these pathways are related to immune function in health and disease.

| pathway name | Enrichment p-value | % genes in the pathway | name of genes enriched |
|---|---|---|---|
| **Cytokine-cytokine receptor interaction** | 1.70E-07 | 10.9 | *Ccl12↑, Ccl2↑, Ccl6↑, Ccl7↑, Ccl8↑, Ccl9↑, Ccr1↑, Ccr5↑, Cxcr3↓, Csf2rb↑, Il18rap↑, Il4ra↑, Tnfsf8↑* |
| **Tuberculosis** | 3.20E-06 | 8.5 | *Clec7a↑, Cebpb↑, Cd74↑, Fcgr3↑, Fcgr2b↑, Fcgr4↓, Coro1a↑, H2-Dma↑, H2-DMb2↑, Itgax↑, Mrc1↑* |
| **Phagosome** | 1.90E-05 | 7.8 | *Clec7a↑, Fcgr3↑, Fcgr2b↑, Fcgr4↓, Coro1a↑, H2-Dma↑, H2-DMb2↑, Itgax↑, Mrc1↑* |
| **Chemokine signalling pathway** | 5.70E-05 | 7.8 | *Ccl12↑, Ccl2↑, Ccl6↑, Ccl7↑, Ccl8↑, Ccl9↑, Ccr1↑, Ccr2↑, Ccr5↑, Cxcr3↑* |
| **Transcriptional misregulation in cancer** | 3.50E-03 | 5.4 | *Bcl2a1a↑, Bcl2a1d↑, Bcl6↓, Cebpb↑, Hmga2↓, Runx1↑, Spint1↑* |
| **Herpes simplex infection** | 1.10E-02 | 5.4 | *Cd74↑, Fos↑, Ccl2↑, H2-Dma↑, H2-DMb2↑, Pilra↑* |
| **Staphylococcus aureus infection** | 7.80E-05 | 4.7 | *Fcgr3↑, Fcgr2b↑, Fcgr4↓, H2-Dma↑, H2-DMb2↑, Itgal↑* |
| **Rheumatoid arthritis** | 8.00E-04 | 4.7 | *Fos↑, Ccl2↑, H2-Dma↑, H2-DMb2↑, Itgal↑* |
| **Leishmaniasis** | 2.50E-03 | 3.9 | *Fos↑, Fcgr3↑, Fcgr4↓, H2-Dma↑, H2-DMb2↑* |
| **Cell adhesion molecules (CAMs)** | 5.70E-02 | 3.9 | *Cd274↑, Cdh1↑, H2-Dma↑, H2-DMb2↑, Itgal↑* |
| **Malaria** | 9.00E-03 | 3.1 | *Cd36↓, Ccl12↑, Itgal↑* |
| **Inflammatory bowel disease (IBD)** | 1.60E-02 | 3.1 | *H2-Dma↑, H2-DMb2↑, Il18rap↑, Il4ra↑* |
| **B cell receptor signalling pathway** | 2.50E-02 | 3.1 | *Cd72↑, Fos↑, Fcgr2b↑, Pik3ap1↑* |
| **TNF signalling pathway** | 2.50E-02 | 3.1 | *Cebpb↑, Fos↑, Ccl12↑, Ccl2↑* |

**Figure 4.6. Table showing the enriched pathways significantly modulated by GM-CSF in myelinating cultures.** Pathway analysis of genes with FDR> 0.05 using DAVID (default settings) by utilizing the KEGG data base. Table also shows the percentage and identity of genes involved in each pathway.

#### 4.2.1.2 qRT-PCR validation

Five genes were selected to validate RNAseq data by qRT-PCR (*Mgl2, Clec4n, Tnfsf8, Ccr2, Csf2rb*) using wild type and *Csf2rb*$^{-/-}$ myelinated cultures, untreated or treated with GM-CSF (Figure 4.5). Significance was calculated using log10 relative copy numbers of gene of interest per $10^7$ copies of *18S* ribosomal RNA or *Tbt* housekeeping genes, depending which of them was stable with treatment.

To facilitate direct comparison between RNAseq and qRT-PCR data the copy number for each gene after GM-CSF treatment was normalised to the untreated control and presented as log2 fold change. Log2 fold change and p-value for each gene tested by qRT-PCR and its corresponding RNAseq values can be found in Figure 4.5. GM-CSF increased expression of all five target genes in this validation study and in all cases this effect was abolished in *Csf2rb*$^{-/-}$ cultures confirming its dependence on GM-CSF signalling. The fold change induced by GM-CSF as assessed by qRT-PCR was similar to that in the RNAseq study for *Mgl2, Ccr2* and *Clec4*, but was less pronounced for *Tnfsf8* and higher for *Csf2rb*, but was significant in all cases ($p < 0.05$ paired Student's t test) (Figure 4.7).

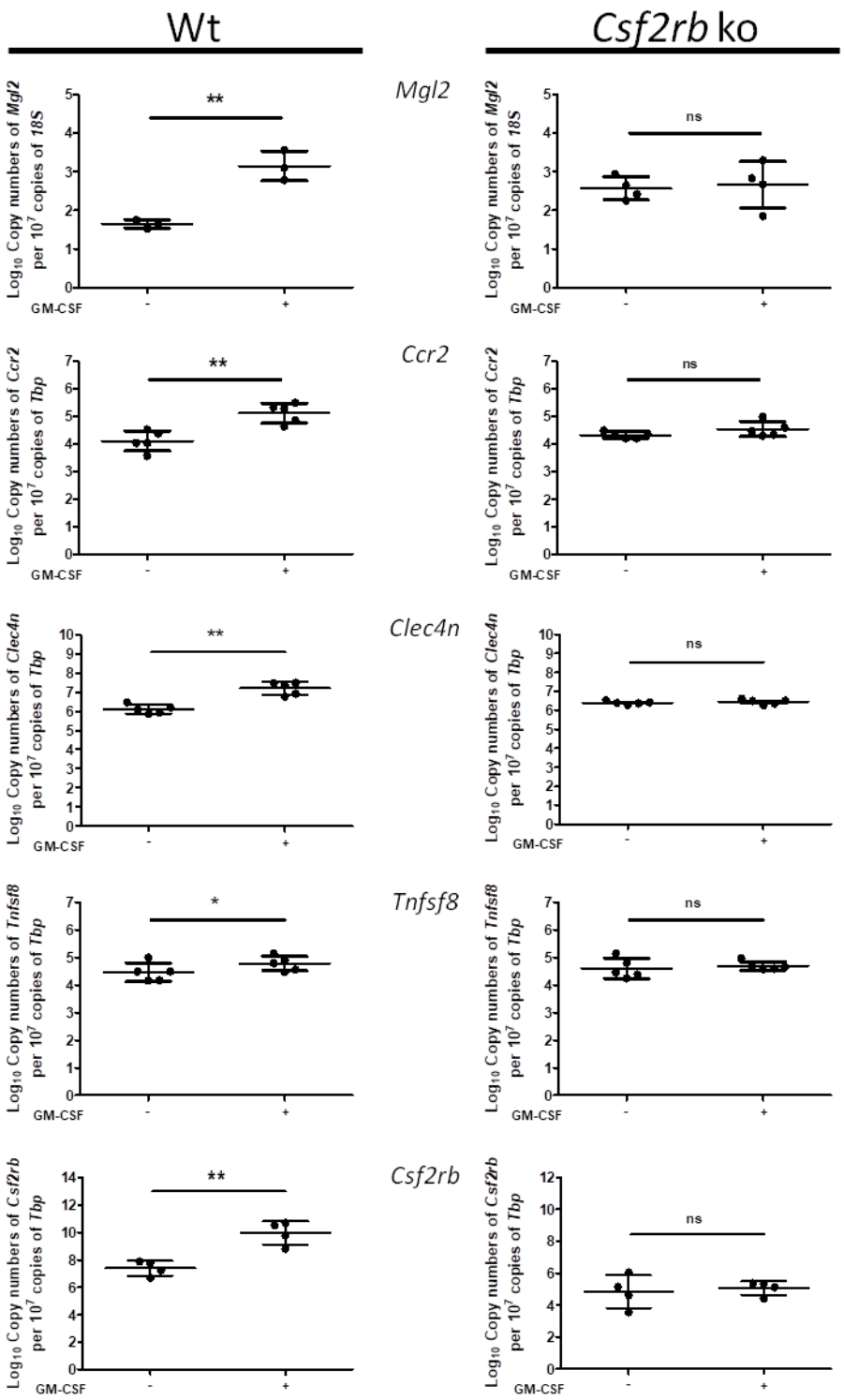


| Gene | RNAseq | qRT-PCR p-value | |
|---|---|---|---|
| | log2FC | Wt | *Csf2rb* ko |
| *Mgl2* | 6.545 | 0.0029 | 0.7786 |
| *Ccr2* | 4.806 | 0.0019 | 0.0642 |
| *Clec4n* | 4.448 | 0.0239 | 0.1031 |
| *Tnfsf8* | 3.222 | 0.0358 | 0.6982 |
| *Csf2rb* | 1.992 | 0.0043 | 0.738 |

**Figure 4.7. Validation of the RNAseq study using qRT-PCR of selected genes belonging to the three main immune associated categories presented in fig4.3.** qRT-PCR was performed using cDNA synthesised from wt and *Csf2rb KO* cultures treated with

GM-CSF for 24h at 24 DIV (n=5). RNA was extracted at 25 DIV. *18S* was used as a house keeping gene for the *Mgl2*. The rest of the experiments were performed using *Tbp* (*TATA box binding protein*) as a house keeping gene. Data presented as mean ± SD from four independent experiments, p values were calculated using a paired Student's t test. The p-value for each qRT-PCR and the corresponding log2 FC for each gene can be found in the table above

### 4.2.2 The effect of GM-CSF priming is retained after GM-CSF withdrawal

The data presented so far demonstrate priming with GM-CSF preferentially up regulates expression of genes associated with immune function, in particular immunity to infectious agents. This led to a number of inter-related questions, in particular (1) was this effect focused on microglia as indicated by the cellular distribution of GM-CSF receptor, and (2) did the effect persist after withdrawal of GM-CSF?

To address these questions, Dectin2 (encoded by *Clec4n*) was chosen to validate the effects of GM-CSF at the protein level in wild type and *Csf2rb*$^{-/-}$ myelinated cultures. This choice was determined by availability of antibodies specific for gene products upregulated by GM-CSF. This provided a limited list of candidates of which Dectin2 was a leading contender because *Clec4n* expression was increased 3 to 4 fold within 24 hours of GM-CSF exposure and encodes a cell surface pattern recognition receptor (PRR) that binds high mannose-containing glycans (Feinberg et al., 2017). Functionally this stimulates phagocytosis and leads to activation of the NLRP3 inflammasome in myeloid cells during fungal infections (Chiffoleau, 2018), but whether or not it mediates other responses in the CNS is unknown.

### 4.2.2.1 GM-CSF induces microglial expression of Dectin2 (*Clec4n*)

Mouse wild type cultures were treated with 100 ng/ml GM-CSF from 24 to 30 DIV and stained for Iba1 and Dectin2. In untreated cultures Dectin2 immunoreactivity was restricted to a small population of Iba1$^+$ microglia (5.671 ± 2.039 % of Iba1$^+$ cells) (Figure 4.8 a-c). GM-CSF treatment resulted in a marked increase in Dectin2 immunoreactivity which again was restricted to Iba1$^+$ microglia (93.63 ± 3.428 % of Iba1$^+$ cells; Figure 4.7 a, b, d). Consistent with previous experiments, 6 days of treatment with GM-CSF induced a significant increase in Iba1$^+$ microglia (Figure 4.7 d) almost all which were now Dectin2 positive. This was not observed in *Csf2rb*$^{-/-}$ cultures confirming induction of Dectin2 is dependent on GM-CSF signalling (Figure 4.9).

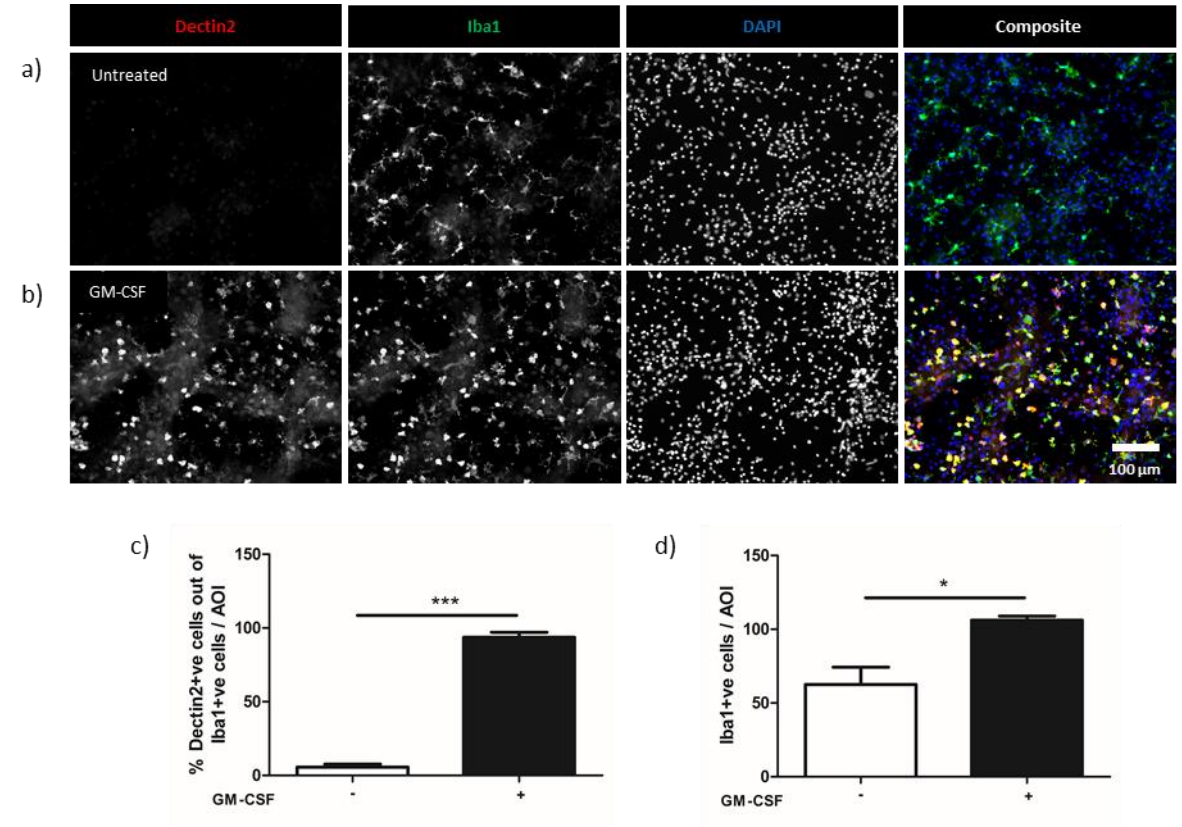


**Figure 4.8. GM-CSF up-regulates Dectin2 expression exclusively on microglia**. (a, b) Representative images of myelinating cultures grown in the presence or absence of 100 ng/ml GM-CSF from 24 to 30 DIV. Images were aquired at 30 DIV. Microglia were visualized with anti-Iba1 (green) and Dectin2 (red). All nuclei were labelled with DAPI (blue). (c) GM-CSF increased numbers of Dectin2 positive microglia (p= 0.0005). (d) GM-CSF increased the number of Iba1$^+$ microglia (p= 0.03). Data presented are mean ± SD from three independent experiments, p values were calculated using a paired Student's t test. AOI= area of interest.

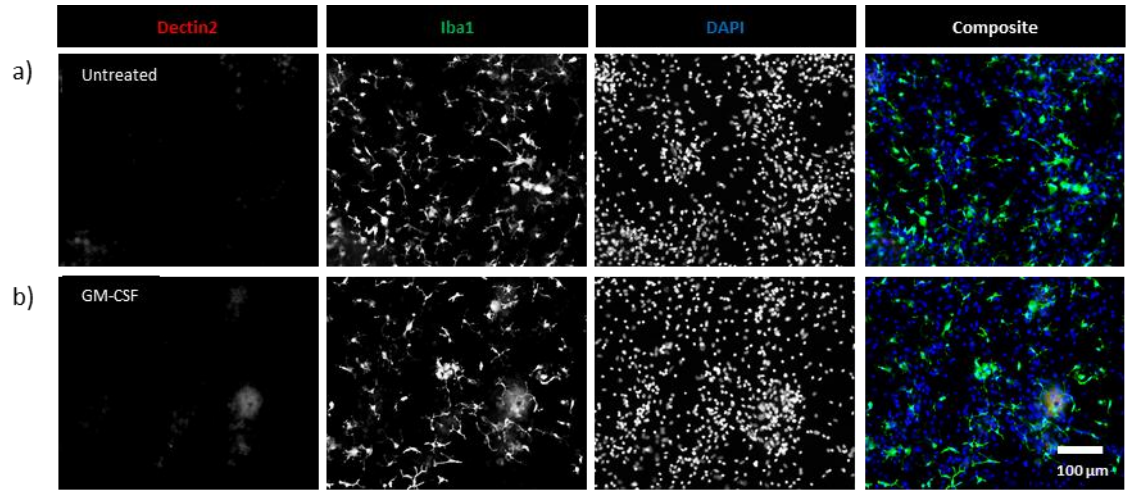


**Figure 4.9. Microglia from *Csf2rb* KO cultures do not express Dectin2.** (a, b) Representative images of *Csf2rb*$^{-/-}$ myelinating cultures grown in the presence or absence of 100 ng/ml GM-CSF from 24 to 30 DIV. Images were aquired at 30 DIV. Iba1$^{+}$ microglia (green), Dectin2 (red). Nuclei were labelled with DAPI (blue). No Dectin2 immunoreactivity was detected. The experiment was performed twice.

#### 4.2.2.2 Dectin2 expression by microglia is maintained after GM-CSF withdrawal

To address whether Dectin2 was down regulated after withdrawal of GM-CSF, this was investigated in myelinating cultures grown in the presence or absence of 100 ng/ml GM-CSF from 24 to 30 DIV after which GM-CSF withdrawn. Dectin2 and Iba1 immunoreactivity was then investigated six days later (36 DIV). Cultures grown in the presence or absence of 100 ng/ml GM-CSF from 24 to 36 DIV (12 days) were used as controls.

A majority of Iba1+ microglia (70.91 ± 5.59 %) still co-expressed Dectin2 six days after withdrawal of GM-CSF. However, this was significantly lower than in cultures treated continuously for twelve days (DIV 24 to 36; 90.23 ± 11.72%; $p < 0.05$), and was associated with a marked decrease in intensity of Dectin2 staining (Figure 4.10). Withdrawal of GM-CSF was also associated with a reduction in Iba1$^{+}$ microglia which decreased to levels similar to that in untreated cultures (Figure 4.9 e; Untreated: 59.67 ± 9.391 Iba1$^{+}$ cells/AOI; GM-CSF for 12 days: 154.5 ± 41.22 Iba1$^{+}$ cells/AOI; After GM-CSF withdrawal: 89.65 ± 9.232 Iba1$^{+}$ cells/AOI). Further, there was a partial reversal of the GM-CSF induced change in microglial morphology from a ramified to rounded phenotype

(Percent microglia with a “rounded” phenotype (DIV 36): continuous GM-CSF, 64.84 ± 10.13%; withdrawal of GM-CSF, 41.9 ± 11.54 %). The dominant microglial morphologies in each experimental condition were as follows: untreated-ramified (75.38 ± 20.62 %); continuous GM-CSF treatment - rounded (64.84 ± 10.13 %); after withdrawal - ramified (54.89 ± 14.47 %). Six days after withdrawal of GM-CSF, there is a decrease in Iba1+ microglial, and a partial reversal of its effects on Dectin2 expression and cell morphology.

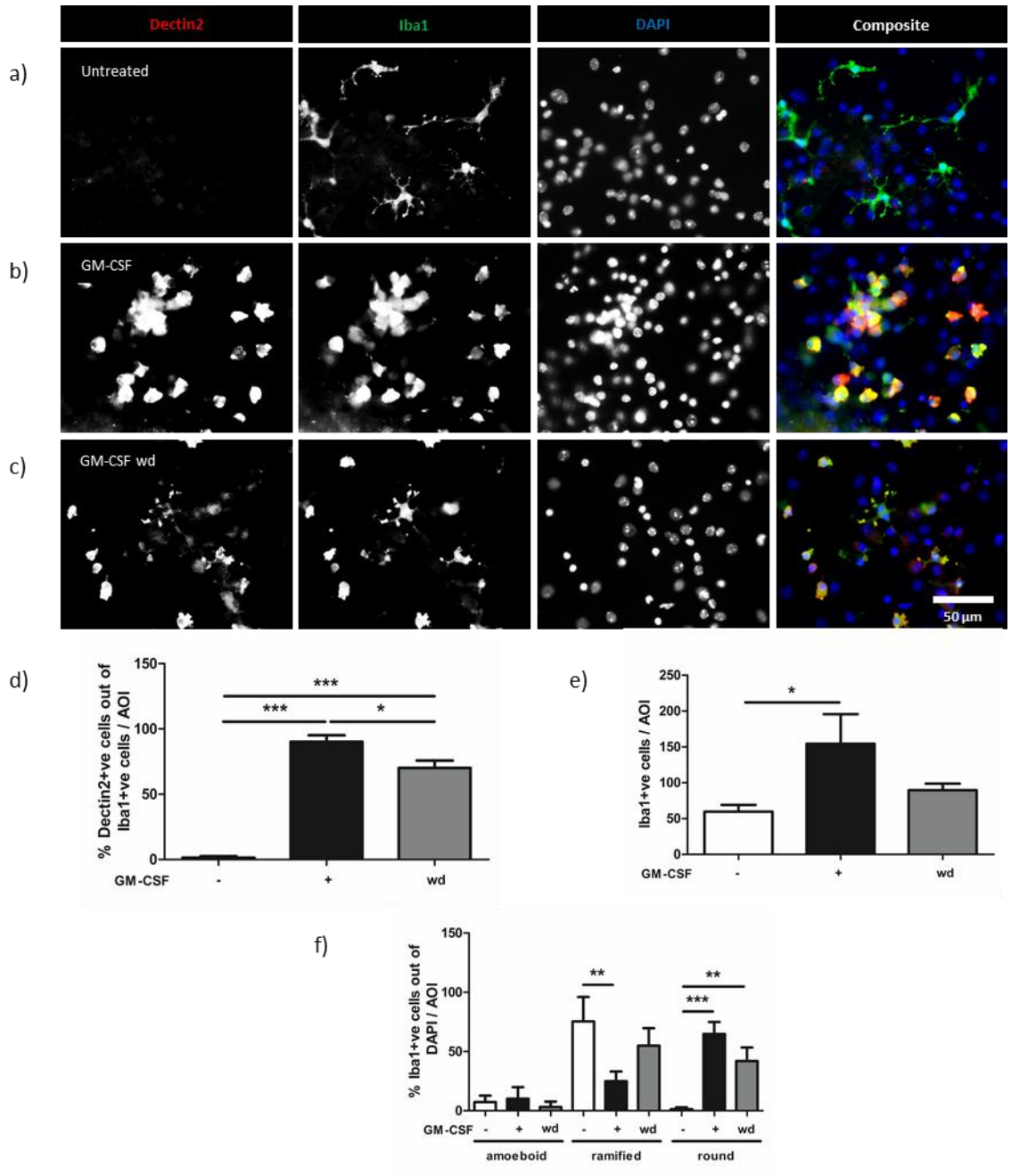


**Figure 4.10. Dectin2 expression is retained after GM-CSF withdrawal**. Representative images of myelinating cultures grown in the presence or absence of 100 ng/ml GM-CSF from 24 to 36 DIV and (c) and treated with GM-CSF from 24-30 DIV followed by GM-CSF

removal from 30 DIV until 36 DIV. Images were acquired at 36 DIV. Microglia were visualized with anti-Iba1 (green) and Dectin2 (red). Nuclei were labelled with DAPI (blue). (d) Removing GM-CSF for 6 days post GM-CSF treatment decreased the percentage of microglia expressing Dectin2 ($p < 0.05$), but the remaining Dectin2 level was still significantly different from control? ($p < 0.001$). (e) GM-CSF treatment increased the number of microglia and withdrawing GM-CSF had no statistically significant effect compared to untreated control or GM-CSF treatment ($p > 0.05$). (f) GM-CSF withdrawal had no significant effect on microglial morphology compared to continuous GM-CSF treatment. Data presented are mean ± SD from three independent experiments, p values were calculated using a one-way ANOVA followed by a Tukey post-hoc test. wd: withdrawal. AOI= area of interest.

### 4.2.3 GM-CSF increases the phagocytic capacity of microglia

Dectin2 is only one of several cell surface receptors upregulated by GM-CSF that are involved in pathogen recognition and phagocytosis; the "phagosome" being one of the pathways significantly enriched after GM-CSF treatment. This suggests GM-CSF may enhance the phagocytic potential of microglia. To test this hypothesis, myelinating cultures were primed with 100ng/ml GM-CSF for 6 days (24 to 30 DIV) and the percentage of microglia with phagocytic activity assessed using three targets: (1) latex beads; (2) pHRodo labelled *E. coli* particles; and (3) pHRodo labelled myelin (subsequently referred to as myelin debris) for 2 hours. pHRodo is a pH sensitive dye that only fluoresces once internalized within the lysosome at pH < 4 (Thermofisher.com) to ensure only internalised material was detected. Incubations were carried out for 2 hours after which microglia were detected by immunofluorescence microscopy using a CD45-specific antibody.

Priming with GM-CSF increased significantly the proportion of $CD45^+$ microglia phagocytosing all 3 targets (Figure 4.11, 4.12, 4.13). Basal phagocytosis in untreated cultures was similar for latex beads (51.55 ± 7.89 % of $CD45^+$ microglia) and *E. coli* (41.68 ± 9.92 of $CD45^+$ microglia), but markedly lower for myelin debris (14.62 ± 3.1 % of $CD45^+$ microglia). After GM-CSF priming these values increased by 1.45-fold for latex beads (74.68 ± 5.009 % of $CD45^+$ microglia), 1.80 fold for *E. coli* (74.68 ± 6.339 of $CD45^+$ microglia) and 2.64 fold for myelin debris (37.53 % of $CD45^+$ microglia). GM-CSF therefore enhances phagocytosis by microglia in these cultures, an effect predicted to enhance remyelination *in vivo* by accelerating phagocytosis of myelin debris in a demyelinating environment (Voß et al., 2012).

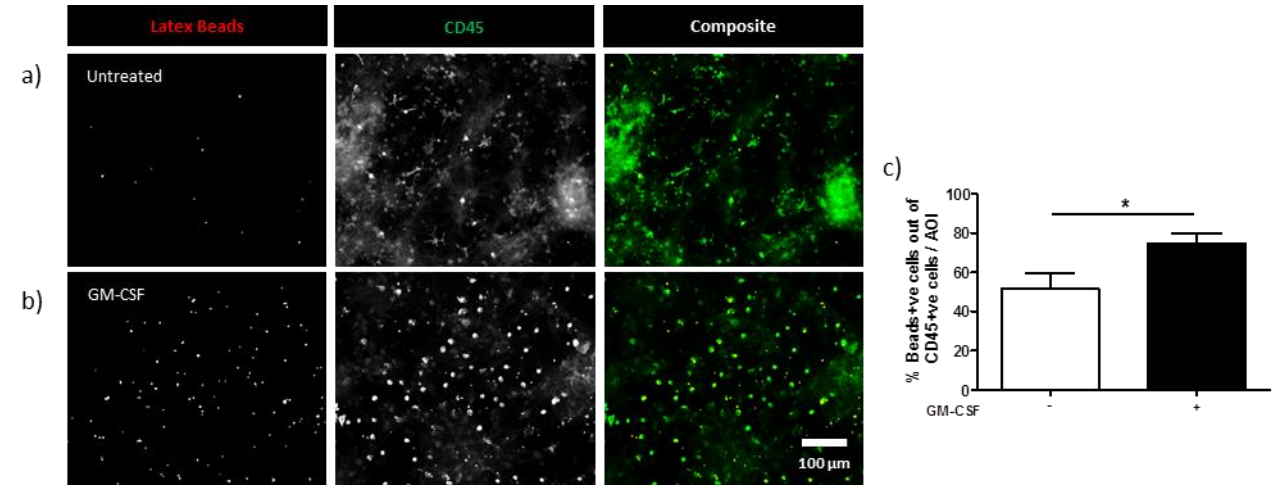


**Figure 4.11. GM-CSF enhances phagocytosis of latex beads by microglia.** (a, b) Representative images of myelinating cultures grown in the presence or absence of 100 ng/ml GM-CSF from 24 to 30 DIV and incubated with 3 x $10^6$ latex beads /ml for 2h. Images were acquired at 30 DIV. Microglia were visualized with anti-CD45 (green) and the rhodamine-labelled latex beads are shown in red. GM-CSF treatment increased the percentage of microglia phagocyting latex beads ($p < 0.05$). Data presented are mean ± SD from three independent experiments, p values were calculated using a paired Student's t test. AOI= area of interest.

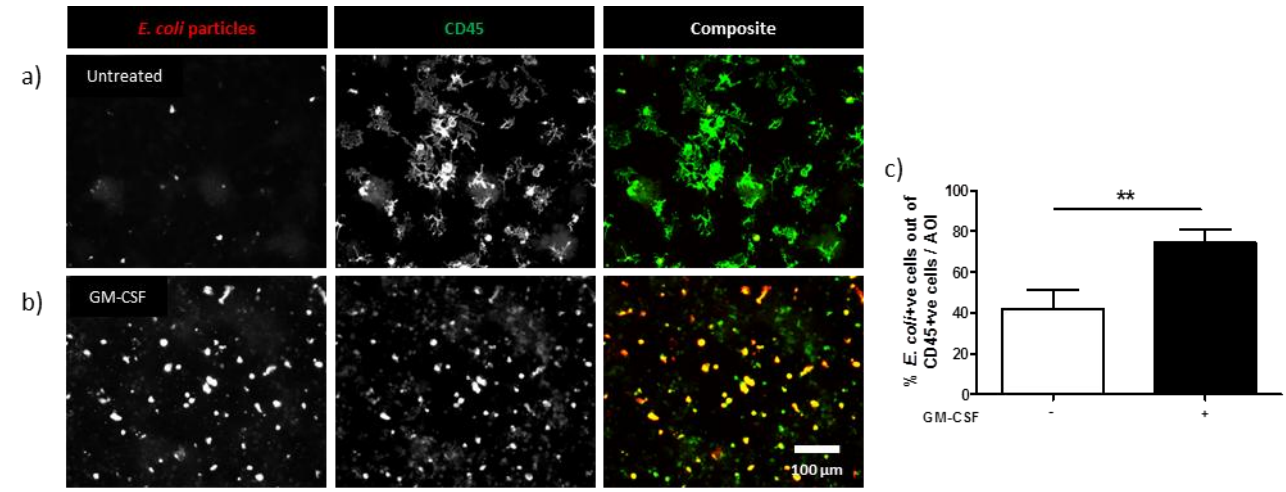


**Figure 4.12. GM-CSF enhances phagocytosis of *E. coli* by microglia.** (a, b) Representative images of myelinating cultures grown in the presence or absence of 100 ng/ml GM-CSF from 24 to 30 DIV and incubated with 0.1 mg/ml *E. coli* particles for 2h. Images were acquired at 30 DIV. Microglia were visualized with anti-CD45 (green) and the *E. coli* particles are shown in red. GM-CSF treatment increased the percentage of microglia phagocyting *E. coli* particles ($p < 0.01$). Data presented as mean ± SD from three independent experiments, p values were calculated using a paired Student's t test. AOI= area of interest.

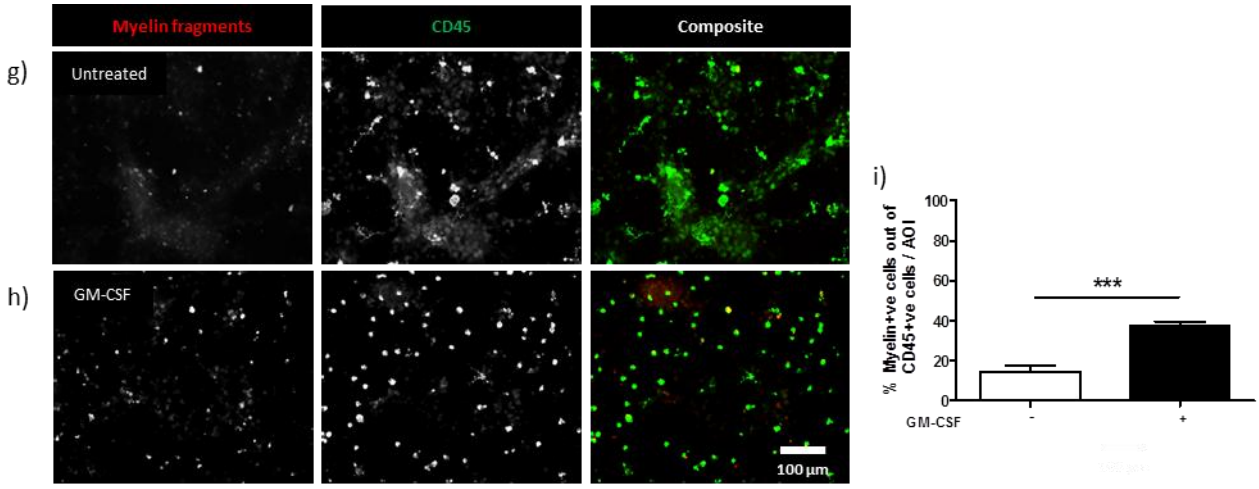


**Figure 4.13. GM-CSF enhances phagocytosis of myelin fragments by microglia**. (a, b) Representative images of myelinating cultures grown in the presence or absence of 100 ng/ml GM-CSF from 24 to 30 DIV and incubated with 0.1 mg/ml myelin particles for 2h. Images were acquired at 30 DIV. Microglia were visualized with anti-CD45 (green) and the labelled-myelin fragments are shown in red. GM-CSF treatment increased the percentage of microglia phagocyting myelin fragments ($p< 0.001$). Data presented are mean ± SD from three independent experiments, p values were calculated using a paired Student's t test. AOI=area of interest.

## 4.3 Discussion

To determine if GM-CSF induced functional responses in myelinated cultures, the transcriptional response to GM-CSF after 24 hours was investigated by RNAseq. GM-CSF differentially regulated expression (> 2-fold) of a small set of 137 transcripts, which, in agreement with the cellular distribution of the high affinity GM-CSF receptor, was enriched in microglial associated genes. Seventy four percent of these transcripts encoded gene enriched at least 2-fold in microglia compared to astrocytes, neurons, oligodendrocytes or endothelial cells in young postnatal mice in vivo (Zhang *et al.*, 2014). Furthermore, > 80% were expressed by microglia isolated from mice with EAE (Appendix Figure 7.2) (Lewis, Hill, Juchem, Stefanopoulos, & Modis, 2014). There was little or no evidence this microglial response triggered off-target responses in other cell types *in vitro* as GM-CSF had no effect on expression of any myelin/oligodendroglial-, astrocyte- or neuron-specific genes. The only exception was *Cd274,* which encodes programmed death-ligand 1 (PD-L1). *Cd274* is expressed preferentially by neurons in naïve mice in which it is also

expressed at lowers level by microglia (Zhang *et al.*, 2014), but is up regulated significantly in dorsal root ganglion (DRG) neurons by GM-CSF (Bali *et al.*, 2013). This is of interest as PD-L1 is best known as an immunoregulatory molecule that down regulates effector T cell function through its interaction with the inhibitory checkpoint molecule PD-1 (Hui *et al.*, 2017). However, in the CNS it can also inhibit pain by suppressing nociceptive neuronal activity (Chen et al., 2017). This suggests GM-CSF may not only act to suppress T cell dependent effector functions in the CNS, but also ameliorate pathophysiological sequela associated with tissue damage (Bryant-Hudson & Carr, 2012; Kiyota et al., 2018; Kosloski, Kosmacek, Olson, Mosley, & Gendelman, 2013). This concept is supported further by the observation GM-CSF up-regulated expression of *Lsr*, an endothelial-enriched gene that encodes lipolysis-stimulated lipoprotein receptor, a protein required to maintain blood brain-barrier function (Sohet et al., 2015). This raises the interesting possibility that activation of GM-CSF signalling in microglia is potentially beneficial rather than detrimental in the CNS. Certainly our data demonstrate GM-CSF in our experimental setting does not up-regulate expression of key genes associated with inflammatory damage in the CNS such as *Il1*, *Tnf-a* and *Nos2* (Conti et al., 2007), or mediate tissue CNS damage *in vitro* by some other pathway. Nonetheless the balance of data from EAE models demonstrates GM-CSF is an essential effector cytokine that primes myeloid cells to target myelin and exacerbate tissue damage in the inflamed CNS (Codarri et al., 2011; Ousman & David, 2001; Ponomarev et al., 2007). The transcriptional data generated in this study helps to explain this apparent dichotomy as they suggest GM-CSF, whilst not cytopathic in its own right, primes microglia to respond to infection and/or interact with infiltrating T cells.

This was first suggested by pathway enrichment analysis that demonstrated the GM-CSF associated transcriptome was enriched in pathways related to immune function in health and disease (Figure 4.6). Visual inspection of genes differentially modulated by GM-CSF associated this “immune genotype” with three functional clusters (Figure 4.5). The most obvious were increased expression of genes encoding (1) cell surface receptor associated with innate immunity; (2) chemokines associated with immune cell migration and (3) chemokine/cytokine receptors, all of which are expressed by microglia in EAE (Lewis et al., 2014).

Cell surface receptors differentially upregulated by GM-CSF included C-type lectins (CLR) [*Mgl2* and *Clec10a* which encode CD301b and CD301a, respectively; *Clec7a* encoding Dectin1; *Clec4n* encoding Dectin2; and Mrc1 encoding Mannose Receptor C type 1 (MRC1)], *Siglecf* which encodes CD170, a sialic acid–binding Ig-like lectin and two IgG receptors (*Fcgr2b* and *Fcgr3*). CLRs are expressed by a variety of cells including many innate immune cells such as monocytes, macrophages, dendritic cells and microglia (Brown, Willment, & Whitehead, 2018; Gensel et al., 2015). CLRs bind a variety of glycans present on pathogens, facilitating phagocytic uptake and modulation of inflammation as well direct killing of invading microorganisms (Brown et al., 2018). For example Dectin2 binds to α-mannans and is implicated in innate anti-fungal immunity (Drummond, Saijo, Iwakura, & Brown, 2011); Dectin1 recognises fungal ß-glucans (Brown et al., 2003; Steele et al., 2003); CD301a (*Clec10a*) and CD301b (*Mgl2*) (homologues of CLEC10A in humans) recognise terminal *N*-acetylgalactosamine residues and are implicated in antigen presentation and antitumor immunity (Denda-Nagai et al., 2010; S. K. Singh et al., 2011). These proteins together with Siglecf, Fcgr2b and Fcgr3 play multiple roles in orchestrating recognition of pathogens and immune complexes to trigger innate and adaptive immune responses. Phagocytosis plays a central role in this complex response leading us to speculate GM-CSF would enhance phagocytosis by microglia in myelinated cultures. This concept is supported by enrichment of the phagosome (Figure 4.4) and studies demonstrating GM-CSF enhances phagocytosis of microspheres by enriched neonatal mouse microglia (H. Li et al., 2011), sheep erythrocytes by peritoneal mouse macrophages (Coleman, Chodakewitz, Bartiss, & Mellors, 1988) and *Staphylococcus aureus* by human neutrophils (Fleischmann, Golde, Weisbart, & Gasson, 1986).

It was found that treating myelinating cultures for six days with GM-CSF had only a modest effect on enhancing phagocytosis by microglia. GM-CSF increased the number of microglia phagocytosing latex beads, pHrodo labelled *E. coli* particles, and pHrodo labelled myelin debris by no more than a factor of two. There was no obvious specificity for any particular ligand, although the absolute number of phagocytic microglia was consistently lowest in cultures challenged with pHrodo labelled myelin debris. However, this may simply reflect differences in particle size and/or number as we were unable to accurately

assess either the number of myelin particles added, or restrict their size distribution to approximate to that of *E. coli* or latex beads. The functional significance of increasing phagocytosis of myelin by microglia is unclear. Historically, this was thought to promote disease progression and loss of neuronal function by destroying the myelin sheath in MS and EAE but new evidence indicates clearance of myelin debris by microglia enhances lesion repair (Bijland et al., 2019; Grajchen, Hendriks, & Bogie, 2018; Kotter et al., 2006; Lampron et al., 2015; Miron et al., 2013). This is yet another mechanism in addition to those mentioned earlier by which GM-CSF may mediate a potentially beneficial response in the CNS.

However, it must be noted phagocytoses of myelin debris in the context of a neuroinflammatory disease such as MS or EAE has the potential to enhance presentation of myelin-derived epitopes to infiltrating autoreactive T cells. This is supported in particular, by our observation that GM-CSF upregulated expression of *H2-dma* (histocompatibility 2, class II, locus DMa), *H2-DMb2* (histocompatibility 2, class II, locus Mb2) and *Cd74,* which are involved in antigen processing and presentation (Ong, Goldenberg, Hansen, & Mattes, 1999; Russell, York, Rock, & Monaco, 1999). This is in line with previous reports that GM-CSF primes neonatal microglia for antigen presentation and increases their expression of MHC class II proteins and the invariant chain (H. Li et al., 2011; Re et al., 2002). The *in vivo* significance of antigen presentation by microglia is as yet unknown, although most studies concur that although this is unlikely to prime naïve T cells it may contribute to reactivation of antigen-experienced effector and regulatory cells invading the CNS parenchyma (Waisman & Johann, 2018).

Two other important gene clusters differentially modulated by GM-CSF in our sequencing study were cytokines and their cognate receptors involved in chemotaxis and cell mobility. Their presence was also reflected in the enriched pathway list: cytokine-cytokine receptor interaction and chemokine signalling pathways. Chemokines prompt movement of inflammatory cells to the site of inflammation/injury by inducing a chemotactic gradient (Adams & Lloyd, 1997).

In terms of functional significance, chemokines play a major role in orchestrating recruitment of immune cells across the blood brain-barrier into the CNS parenchyma (Gyoneva & Ransohoff, 2015). This is facilitated by matrix metalloproteinases such as *Mmp8*, *Mmp12* and *Mmp13* which up are also regulated by GM-CSF and which mediate tissue breakdown to facilitate cell migration to sites of inflammation MMPs (Lo, Wang, & Louise Cuzner, 2002). MMPs also regulate inflammatory mediators, such as cytokines, which can result in loss or gain of function (Chopra, Overall, & Dufour, 2019; Manicone & McGuire, 2008). However, in addition to their roles in neuroinflammation these molecules all contribute to CNS homeostasis and repair (Trettel, Di Castro, & Limatola, 2019; Trivedi et al., 2019). It is therefore difficult to define any single function to GM-CSF mediated expression of chemokines and MMP's in the CNS. However, they would certainly promote a dynamic environment in which microglia and immune cells recruited from the periphery are attracted via chemokine gradients to where GM-CSF is being expressed in the CNS. Intriguingly GM-CSF also up-regulated the expression of its common β-subunit (*Csf2rβ*) suggesting it could induce a positive feedback loop as well as enhancing signal transduction by IL-3 and IL-5 whose receptors share this signal transducing subunit.

Induction of two CLR's, *Mgl2* and *Clec4n* by GM-CSF was validated by qRT-PCR. Expression of both was increased in WT cultures but remained unchanged in GM-CSF signalling deficient mice (Figure 4.5). It was also possible to validate induction of Dectin2 at protein level by immunofluorescence microscopy. In unstimulated wild type cultures immune reactivity for Dectin2 was weak and restricted to a small population (5.671 ± 2.039 %) of $Iba1^{+}$ microglia. In contrast GM-CSF induced Dectin2 expression on $Iba1^{+}$ cells. Again, GM-CSF failed to induce this response in cultures established from *Csf2rb*$^{-/-}$ *donors*. Monitoring Dectin2 immunoreactivity provided a simple tool to monitor the longevity of the response induced by GM-CSF after its withdrawal. This revealed there was no rapid reversion to the Dectin2 negative phenotype. However, there was a trend for microglia to adopt the ramified morphology characteristic of microglia before they were exposed to GM-CSF. Unexpectedly, the absolute number of microglia declined after withdrawing GM-CSF. Why this was the case is unknown,

but suggests that in addition to promoting proliferation, GM-CSF also induces factors required to supports microglia survival.

Taken as a whole these data demonstrate that whilst GM-CSF does not induce microglial expression of cytopathic/demyelinating effector mechanisms in myelinating cell cultures it does prime microglia to up-regulate pathways that would enable them to respond more rapidly to infectious or autoimmune insults to the CNS. Functionally this was demonstrated with respect to phagocytosis, but the question remains what are the additional triggers required to push these cells into cytopathic effectors able to mediate tissue damage in the CNS.

# Chapter 5

## GM-CSF sensitises for IFN-γ and TNF-α to induce tissue damage

# 5 GM-CSF sensitises for IFN-γ and TNF-α to induce tissue damage

## 5.1 Introduction

The previous chapters demonstrated GM-CSF does not induce axonal and myelin pathology in myelinated cultures, but nonetheless up regulates expression of genes encoding cell surface receptors associated with phagocytosis and innate immunity. Bioinformatics and validation studies using Clec4n confirmed microglia are the primary target of GM-CSF, but provided no further insight as to how GM-CSF might 'license' these cells to mediate tissue damage in the CNS. We reasoned this may be dependent on synergy with other cytokines and considered IFN-γ and TNF-α as potential candidates. These pro-inflammatory cytokines are themselves cytotoxic under certain conditions, are involved in the pathogenesis of EAE and have been implicated as key factors contributing to lesion development in MS (Beck et al., 1988; Montgomery & Bowers, 2012; Patel & Balabanov, 2012). IFN-γ in MS lesions may derive in part from infiltrating encephalitogenic Th1 cells (Merrill et al., 1992; Nylander & Hafler, 2012). In contrast, although TNF-α is produced predominantly by myeloid cells, it is also expressed by T cell subsets infiltrating the CNS in MS. Its ability to kill human oligodendrocytes *in vitro* leads to speculation this mechanism contributes to lesion development in patients (Jurewicz, Matysiak, Tybor, & Selmaj, 2003; Renno, Krakowski, Piccirillo, Lin, & Owens, 1995). We therefore investigated whether GM-CSF can enhance the cytolytic activity of IFN-γ and TNF-α in myelinated cultures.

## 5.2 Results

### 5.2.1 GM-CSF synergizes with IFN-γ and TNF-α to induce axonal loss and myelin damage

Myelinating cultures were primed by treating them with GM-CSF for six days (100 ng/ml; 24 to 30 DIV) then treated with IFN-γ (25 ng/ml) and TNF-α (100 ng/ml), individually or in combination for 72 hours, after which cell death was assessed using a commercial LDH release assay. Under these conditions, release of LDH was only observed in GM-CSF primed cultures treated with both IFN-γ and TNF-α (74.49 ± 15.92 % max LDH release, $p < 0.001$ relative to untreated control cultures). No significant release of LDH was observed with any other treatment combination (Figure 5.1a). The high level of LDH release caused by IFN-γ and TNF-α was associated with extensive and often complete destruction of GM-CSF primed cultures. Immunofluorescence microscopy revealed the dense network of neurofilament$^+$ neurites and associated myelin sheaths was often disrupted completely; only occasionally did residual neurites and MOG$^+$ myelin debris and oligodendrocytes remain. (Figure 5.1 c, d). The number of DAPI labelled nuclei remaining after 72 hours was less than 50 % of controls (Untreated, 792.2 +/- 216.8; GM-CSF primed and 72 hours IFN-γ and TNF-α, 387.9 +/- 143.9I) (Figure 5.1 b, e, f). These results not only demonstrate priming with GM-CSF massively enhances IFN-γ/ TNF-α mediated cytotoxicity in this culture system, but this effect requires all three cytokines.

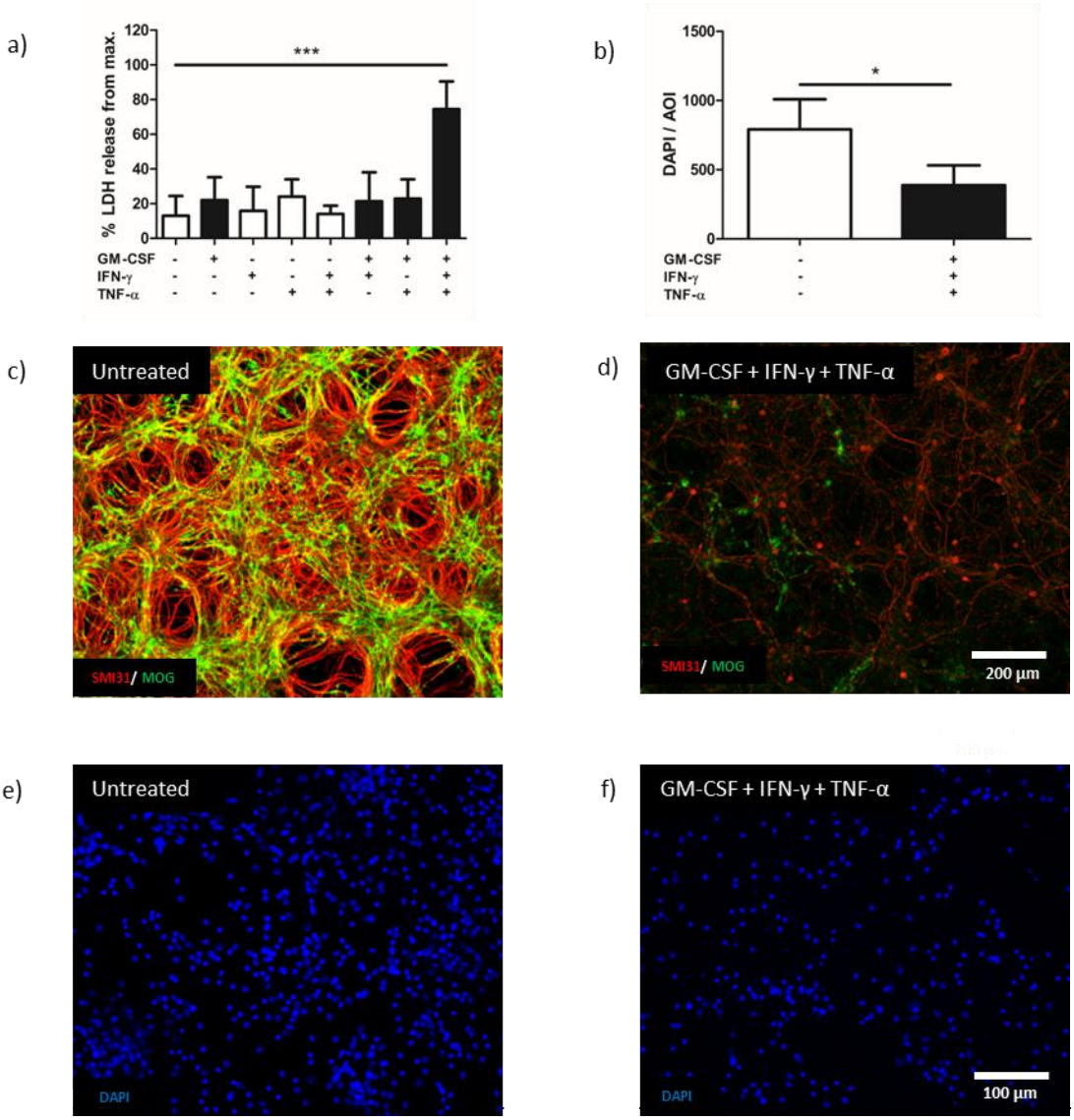


**Figure 5.1. GM-CSF synergises with IFN-γ and TNF-α to induce tissue damage.** Mouse myelinating cultures were primed or unprimed with 100 ng/ml GM-CSF from 24 to 30 DIV, followed by 100 ng/ml IFN-γ and 25 ng/ml TNF-α for 72h. GM-CSF priming followed by IFN-γ and TNF-α treatment induced extensive cytotoxicity shown as (a) LDH release (n= 6, p< 0.001) and (b) decreased total cell numbers ($DAPI^{+}$nuclei) (n=4, p= 0.032 < 0.05). Representative images of (c, e) untreated myelinating cultures and (d, f) cultures primed with 100 ng/ml GM-CSF from 24 to 30 DIV, followed by 100 ng/ml IFN-γ and 25 ng/ml TNF-α for 72h. Images were acquired at 33 DIV. Myelin and axons were visualized with anti-MOG (clone Z2, green) and anti-neurofilament (SMI31, red) antibodies, respectively and nuclei were stained with DAPI. (d, f) GM-CSF priming followed by IFN-γ and TNF-α induced extensive loss of MOG and SMI31 immunoreactivity and DAPI positive nuclei. Data presented as mean ± SD, p values were calculated using a one-way ANOVA followed by a Tukey post-hoc test or using a paired Student's t test. AOI= area of interest.

## 5.2.2 GM-CSF induced tissue damage is mediated by iNOS induction, selectively in microglia, and nitric oxide production

Previous studies suggest tissue damage caused by IFN-γ and TNF-α is at least in part dependent on induction of iNOS (Gibbons & Dragunow, 2006; Mir, Tolosa, Asensio, Lladó, & Olmos, 2008). We therefore investigated if GM-CSF priming sensitised for IFN-γ and TNF-α to induce microglia to express iNOS and generate nitric oxide. In view of the almost complete destruction observed at 72 hours these experiments were performed on cultures treated with IFN-γ and/or TNF-α for 24 hours.

### 5.2.2.1 GM-CSF priming synergises with IFN-γ and TNF-α to induce rapid expression of iNOS in microglia and nitric oxide synthesis

Myelinating cultures were primed with GM-CSF for six days before being treated with 100 ng/ml IFN-γ and/or 25 ng/ml TNF-α for 24 hours. Cultures were then fixed and stained for microglia (CD45) and inducible nitric oxide synthase (iNOS). Induction of iNOS was observed only under three conditions (Figure 5.2). iNOS immunoreactivity was most prominent in GM-CSF primed cultures treated with the combination of IFN-γ and TNF-α which induced expression of iNOS in 78.05 ± 4.93 % of microglia (Figures 5.2 h and 5.3 a). Far fainter iNOS immunoreactivity was also detected in a small number of microglia in cultures primed with GM-CSF and treated with IFN-γ only (Figures 5.2 f; Figure 5.3 a: 9.27 ± 10.29 % of microglia) and in unprimed cultures treated with IFN-γ plus TNF-α (Figures 5.2 e; Figure 5.3 a: 9.27 ± 5.88 % of microglia). No iNOS immunoreactivity was detected in untreated cultures, or in response to any other experimental condition investigated in these experiments.

This pattern of iNOS induction by GM-CSF, IFN-γ and TNF-α was confirmed by western blotting of protein lysates from treated and untreated myelinating cultures (Figure 5.3b). A band corresponding to iNOS was only observed under the three conditions described above. Semi-quantitative analysis confirmed expression was highest in GM-CSF primed cultures treated with IFN-γ and TNF-α (0.689 ± 0.321 arbitrary units), an order of magnitude lower in GM-CSF primed treated with IFN-γ alone (0.059 ± 0.056 arbitrary units) and lower again in unprimed cultures treated IFN-γ and TNF-α (0.040 ± 0.038 arbitrary units)(Figure

5.3 b). Once again iNOS was not detected under any other experimental condition.

To determine if induction of iNOS in microglia was associated with a significant increase in nitric oxide synthesis, culture supernatants were harvested and analysed using a modified Griess assay. Relative to nitrite concentrations in supernatants from untreated cultures, a significant increase in nitrite concentrations was only observed following GM-CSF priming and treatment with IFN-γ and TNF-α (5.787 ± 1.572 μM, $p < .001$; Figure 5.3 c). The low levels of iNOS detected by immunofluorescence microscopy and western blotting in (i) unprimed cultures treated with IFN-γ and TNF-α, and (ii) primed cultures treated with IFN-γ did not support a statistically significant increase in nitric oxide synthesis (in both cases $p > 0.05$).

As anticipated from data presented in Chapter 3, priming with GM-CSF for six days increased microglial numbers significantly, but this was not influenced further by treatment with INF-$\gamma$ and/or TNF-$\alpha$ (GM-CSF = 163.7 ± 20.22; GM-CSF + IFN-γ = 137 ± 7.172; GM-CSF + TNF-α =176.9 ± 23.42; GM-CSF + IFN-γ + TNF-α = 144.1 ± 11.32) (Figure 5.3 d).

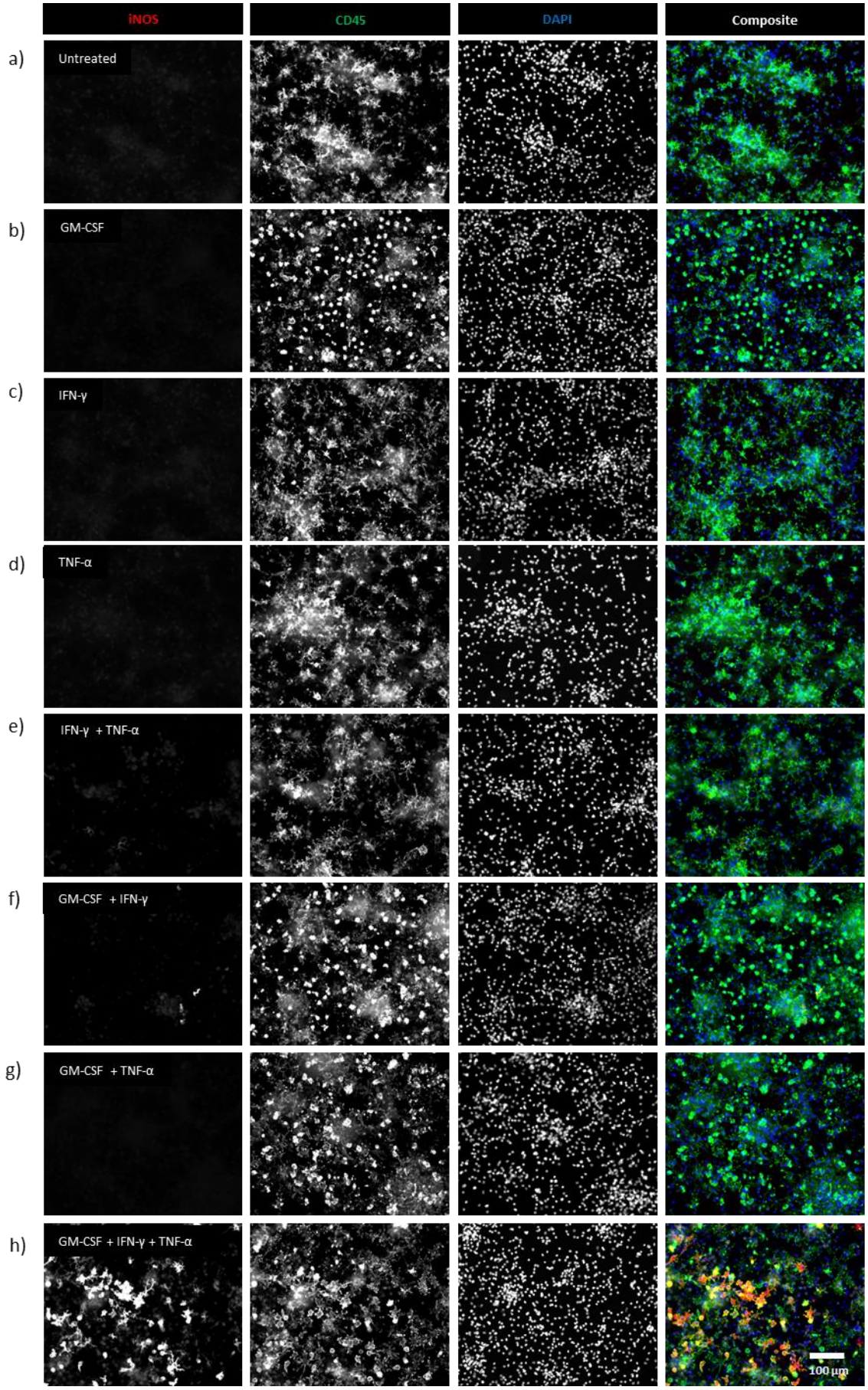


**Figure 5.2. GM-CSF priming synergises with IFN-γ and TNF-α to induce rapid expression of iNOS in microglia.** Representative images of mouse myelinating cultures

(a) untreated 31 DIV; (b) primed with 100 ng/ml GM-CSF from 24 to 31 DIV; (c) 100 ng/ml IFN-γ for 24 hours, DIV 30 – 31; (d) 25 ng/ml TNF-α for 24 hours DIV 30 – 31; (e) 100 ng/ml IFN-γ and 25 ng/ml TNF-α for 24 hours, DIV 30 – 31; (f) GM-CSF primed plus 100 ng/ml IFN-γ for 24 hours, DIV 30 – 31; (g) GM-CSF primed plus 25 ng/ml TNF-α for 24 hours, DIV 30 – 31; (h) GM-CSF primed plus 100 ng/ml IFN-γ and 25 ng/ml TNF-α for 24 hours. Images were acquired at 31 DIV. iNOS immunoreactivity (red) is shown in the first column. Microglia were visualized using an anti-CD45 antibody (green), second column and nuclei visualised with DAPI (blue) in the third column. The composite of the three channels is shown in the last column. Note intense iNOS immune reactivity was only observed if cultures were first primed with GM-CSF and the treated with IFN-γ and TNF-α. iNOS expression was restricted to $CD45^{+}$ microglia.

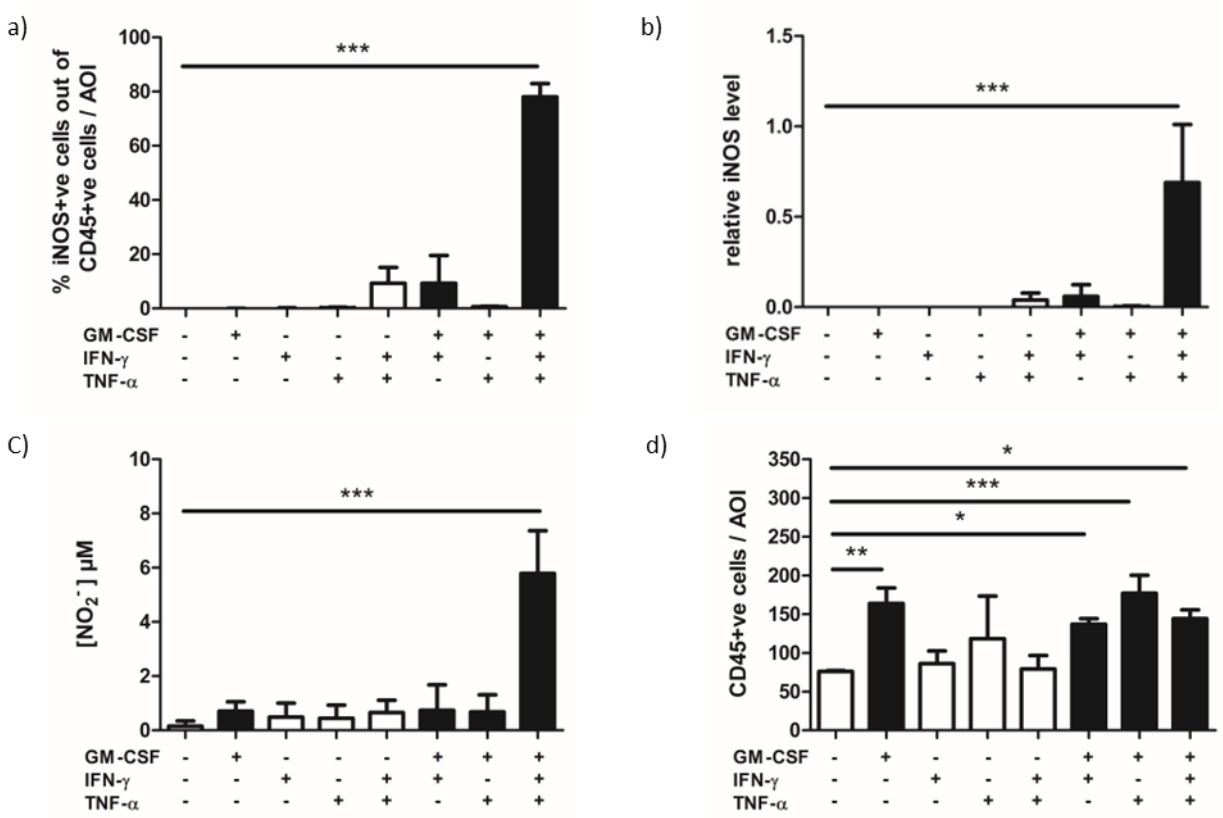


**Figure 5.3. iNOS expression in microglia translates into nitric oxide production**. Mouse myelinating cultures were primed or unprimed with 100 ng/ml GM-CSF from 24 to 30 DIV, followed by treatment with 100 ng/ml IFN-γ and 25 ng/ml TNF-α for 24h. Images were acquired and supernatants were assessed at 31 DIV. (a) GM-CSF priming followed by IFN-γ and TNF-α increased the percentage of microglia expressing iNOS ($p< 0.001$, n=3), also confirmed by (b) western blotting ($p< 0.001$, n=4). (c) The iNOS expression in GM-CSF primed cultures treated with IFN-γ and TNF-α translated into (c) nitric oxide production ($p< 0.001$, n=3). (d) GM-CSF priming increased the number of microglia in every treatment ($p< 0.05$- 0.001, n=3). Raw western blot data can be found in the appendix (Figure 7.3). Data is presented as mean ± SD, p values were calculated using a one-way ANOVA followed by a Tukey post-hoc test. AOI= area of interest.

#### 5.2.2.2 GM-CSF priming synergises with IFN-γ and TNF-α to induce iNOS expression and NO production in mouse primary microglia

To determine if these effects of GM-CSF, IFN-γ and TNF-α on iNOS expression and nitic oxide synthesis were influenced by other cell types in myelinated cultures we used primary mouse microglia isolated from mixed glial cultures using the "shake off" method and primed with GM-CSF. Following priming with 100 ng/ml GM-CSF in serum-free media for 3 days, they were treated with IFN-γ and/or TNF-α as described previously. After 72 hours expression of CD45 and iNOS was determined by immunofluorescence microscopy.

Cytokine mediated induction of iNOS in primary microglia mirrored what was seen in myelinated cultures (Figure 5.4). In GM-CSF primed cultures treated with IFN-γ and TNF-α, the majority of microglial were $iNOS^+$, as were some microglia primed with GM-CSF and treated with IFN-γ alone,  ortreated only with IFN-γ and TNF-α (Figure 5.4 e and f).

Induction of iNOS also stimulated nitric oxide production (Figure 5.5). Nitrite levels were highest in supernatants from primed microglia treated with IFN-γ and TNF-α (89.33 ± 1.443 μM), but nitrite was also present in supernatants from GM-CSF primed cells treated with IFN-γ (23.85 ± 8.05 μM) and unprimed cells treated with IFN-γ and TNF-α (18.73 ± 1.148 μM) (Figure 5.5).

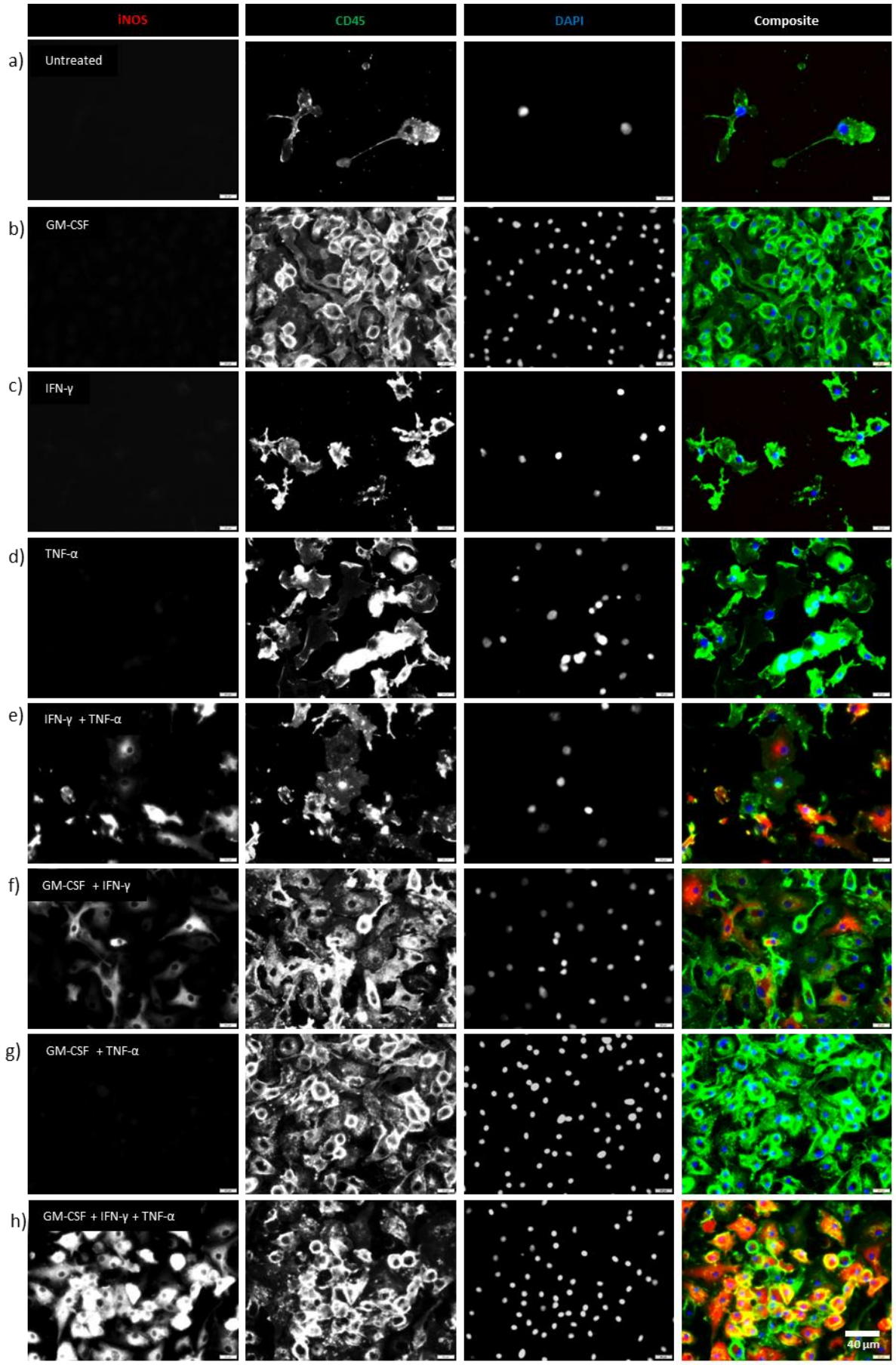


**Figure 5.4. GM-CSF priming synergises with IFN-γ and TNF-α to induce rapid expression of iNOS in mouse primary microglia.** Representative images of mouse

primary microglia cultures after different cytokine treatments. (a) untreated 6 DIV; (b) primed with 100 ng/ml GM-CSF from 0 to 3 DIV, continued GM-CSF until DIV 6; (c) 100 ng/ml IFN-γ for 72h hours, DIV 3 – 6; (d) 25 ng/ml TNF-α for 72 hours DIV 3 – 6; (e) 100 ng/ml IFN-γ and 25 ng/ml TNF-α for 72 hours, DIV 3 – 6; (f) GM-CSF primed plus 100 ng/ml IFN-γ for 72h hours, DIV 3 – 6; (g) GM-CSF primed plus 25 ng/ml TNF-α for 72 hours, DIV 3 – 6; (h) GM-CSF primed plus 100 ng/ml IFN-γ and 25 ng/ml TNF-α for 72 hours. Images were acquired at 6 DIV. iNOS immunoreactivity (red) is shown in the first column. Microglia were visualized using an anti-CD45 (green), second column and nuclei visualised with DAPI (blue) in the third column. The composite of the three channels is shown in the last column. iNOS immunoreactivity was observed with IFN-γ and TNF-α, GM-CSF priming and IFN-γ, and more intense staining if cultures were first primed with GM-CSF and the treated with IFN-γ and TNF-α.

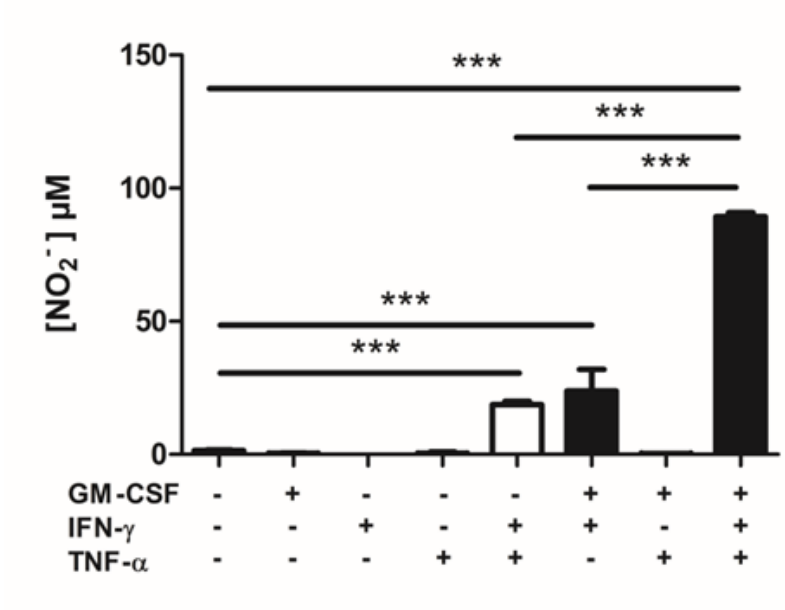


**Figure 5.5. GM-CSF priming synergises with IFN-γ and TNF-α to induce NO production in mouse primary microglia.** Mouse primary microglia cultures were primed or unprimed with 100 ng/ml GM-CSF from 0 to 3 DIV, followed by treatment with 100 ng/ml IFN-γ and 25 ng/ml TNF-α for 72h. Supernatants were assessed at 6 DIV. GM-CSF priming followed by IFN-γ and TNF-α induced a greater NO production than the combinations of IFN-γ with TNF-α and GM-CSF with IFN-γ ($p < 0.001$). Data is presented as mean from three independent wells from cells collected and pooled from two litters ± SD, p values were calculated using a one-way ANOVA followed by a Tukey post-hoc test.

#### 5.2.2.3 Inhibition of iNOS abrogates cytokine-induced NO production and cytotoxicity

The contribution of iNOS-dependent mechanisms to cytokine-induced cytotoxicity was investigated in myelinating rat rather than mouse cultures as they exhibit less variability in myelination. Comparison of myelination across 4 independent cultures from each species at 33 DIV demonstrated an average percentage of 4.279 ± 3.917 % or 17.26 ± 2.482 % for mouse and rat respectively. Cultures were primed with GM-CSF and treated with IFN-γ and TNF-α as described above, in the presence or absence of 100 μM AMT hydrochloride (2-Amino-5,6-dihydro-6-methyl-4H-1,3-thiazine HCL), a relatively selective, reversible inhibitor of iNOS which only inhibits other NOS isoforms at far higher concentrations: iNOS, $IC_{50}$ = 3.6 nM; nNOS, $IC_{50}$ = 34 nM; eNOS, $IC_{50}$ = 150 nM (Nakane et al., 1995).

The response of myelinated rat cultures to these cytokine treatments was essentially identical to described for mouse cultures. Specifically, nitric oxide production and LDH release were only increased significantly in culture primed with GM-CSF and then treated with IFN-γ and TNF-α (Figure 5.6 a, b). Immunofluorescence microscopy revealed this was also associated with extensive loss of neurites and myelin (Figure 5.6 d). Neurite density and myelination were reduced by at least 20 and 65 %, respectively, suggesting myelinating oligodendrocytes were more susceptible than axons (Figure 5.6 e, f).

Inhibition of iNOS abrogated these cytokine-dependent effects completely demonstrating they are NOS-dependent (Figure 5.7). AMT reduced NO synthesis (Figure 5.7 a) and LDH release (Figure 5.7 b) to levels indistinguishable from those in untreated control cultures. Perhaps not surprisingly this was associated with complete preservation of neurites and myelin (Figure 5.7 c, d). Quantitative analysis of neurite density and myelination revealed no significant differences between cultures treated with AMT alone (Neurite density, 68.51 ± 5.767 %; myelination, 9.007 ± 3.176 %) or AMT plus GM-CSF and IFN-γ and TNF-α (Neurite density, 68.2 ± 2.084 %; myelination, 9.133 ± 4.64 %) (Figure 5.7 e, f).

To confirm this was not a species-specific effect this experiment was repeated in mouse cultures in which AMT also completely abolished cytokine-mediated NO production and its associated cytotoxicity (Figure 5.8).

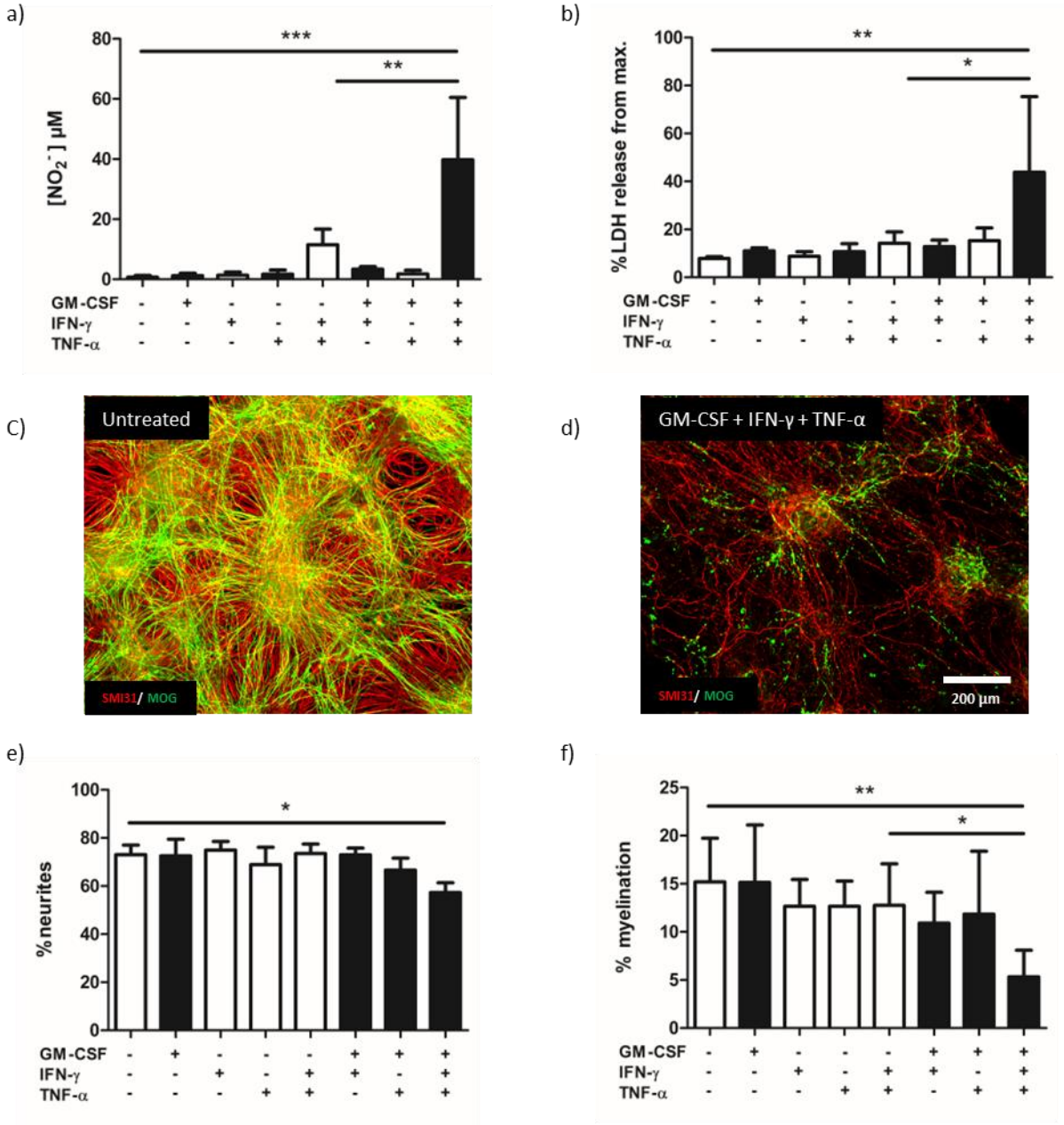


**Figure 5.6. GM-CSF synergises with IFN-γ and TNF-α to induce tissue damage in rat myelinating cultures.** Rat myelinating cultures were primed or unprimed with 100 ng/ml GM-CSF from 24 to 30 DIV, followed by treatment with 100 ng/ml IFN-γ and 25 ng/ml TNF-α for 72h. Images were acquired and supernatants were assessed at 33 DIV. (a) GM-CSF priming followed by IFN-γ and TNF-α treatment induced NO production ($p< 0.001$), which translates in (b) significantly elevated LDH level ($p< 0.01$). Representative images of (c) untreated rat myelinating cultures and (d) cultures primed with 100 ng/ml GM-CSF from 24 to 30 DIV, followed by 100 ng/ml IFN-γ and 25 ng/ml TNF-α for 72h. Myelin and axons were visualized with anti-MOG (clone Z2, green) and anti-neurofilament (SMI31, red) antibodies, respectively. GM-CSF priming followed by IFN-γ

and TNF-α induced extensive loss of MOG and SMI31 immunoreactivity. (e and f) graphs of percentage neurites and myelination ($p < 0.05, 0.001$). Data is presented as mean from three different experiments ± SD, p values were calculated using a one-way ANOVA followed by a Tukey post-hoc test.

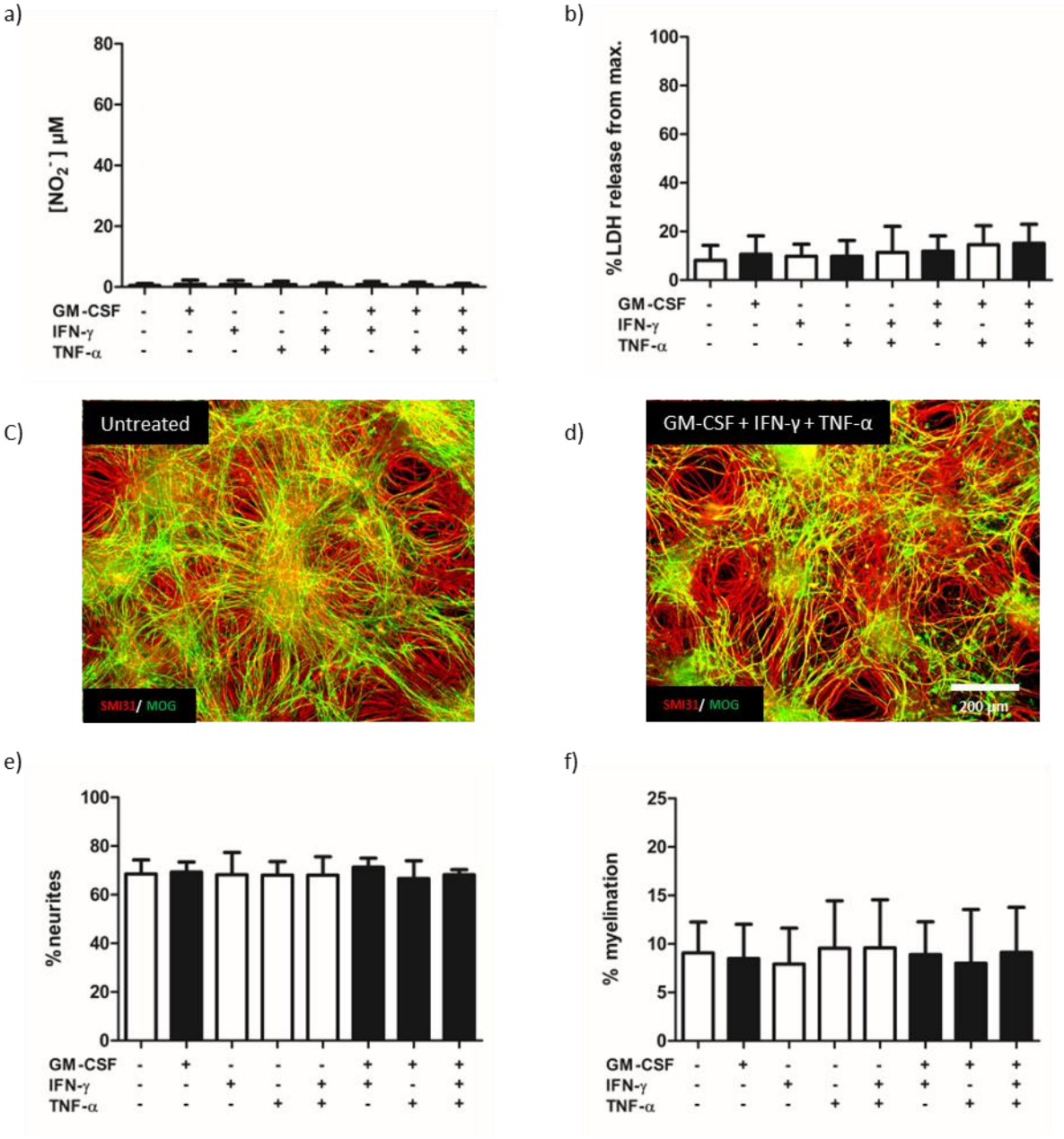


**Figure 5.7. Inhibiting iNOS stops NO production and prevents cytotoxicity.** Rat myelinating cultures were primed or unprimed with 100 ng/ml GM-CSF from 24 to 30 DIV, followed by treatment with 100 ng/ml IFN-γ and 25 ng/ml TNF-α for 72h in the presence of presence 100 µM AMT hydrochloride (iNOS inhibitor). Images were acquired and supernatants were assessed at 33 DIV. (a) Priming rat myelinating cultures with GM-CSF followed by IFN-γ and TNF-α treatment in the presence 100 µM AMT hydrochloride (iNOS inhibitor) (a) blocked production of NO and ($p > 0.05$) (b) reduced LDH back to background level ($p > 0.05$). Representative images of (c) untreated rat myelinating cultures and (d) cultures primed with 100 ng/ml GM-CSF from 24 to 30 DIV, followed by 100 ng/ml IFN-γ and 25 ng/ml TNF-α in the presence of AMT hydrochloride for 72h. AMT

rescued neurite and myelin integrity, also observed in the graphs the percentage of neurites and myelination ($p > 0.05$ for both) (e, f). Myelin and axons were visualized with anti-MOG (clone Z2, green) and anti-neurofilament (SMI31, red) antibodies, respectively. Data is presented as mean from three different experiments ± SD, p values were calculated using a one-way ANOVA followed by a Tukey post-hoc test. Control cultures without AMT inhibitor are presented in Figure 5.6.

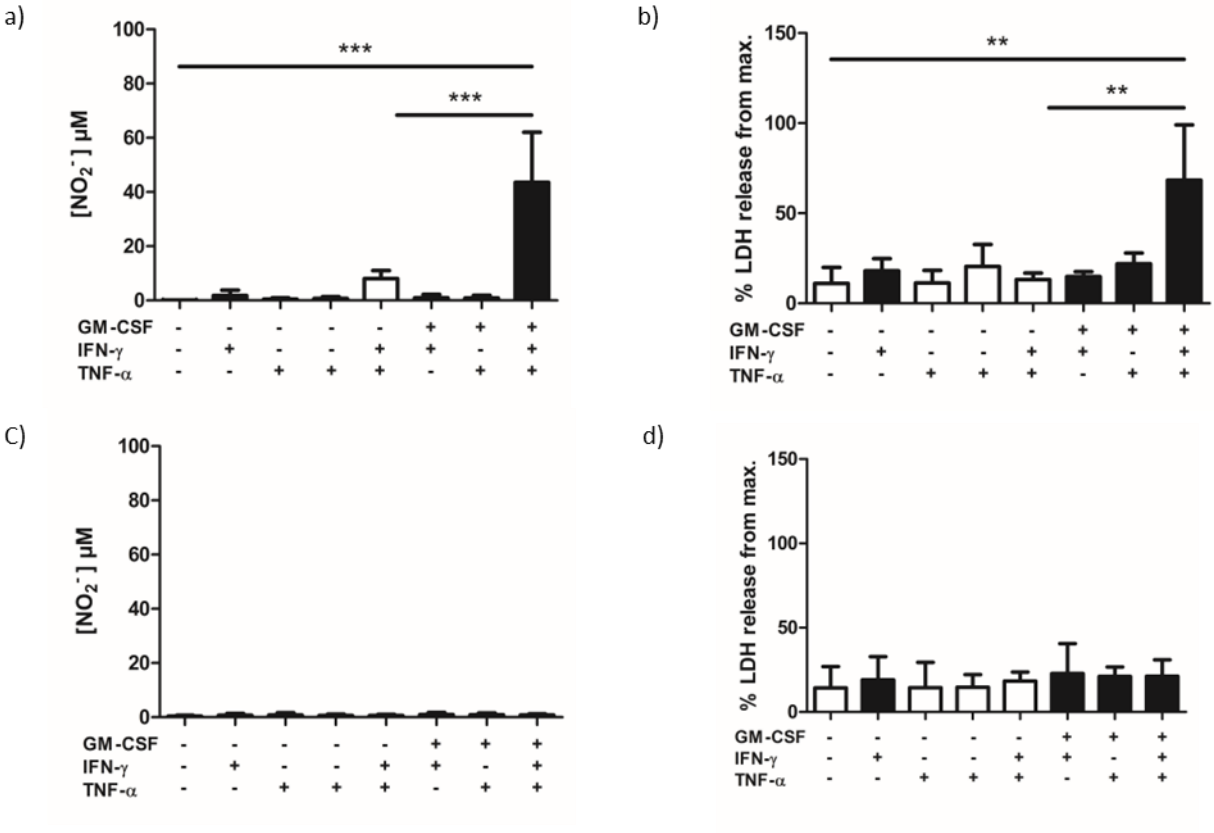


**Figure 5.8. Inhibiting iNOS ablates cytotoxicity in mouse cultures.** Mouse myelinating cultures were primed or unprimed with 100 ng/ml GM-CSF from 24 to 30 DIV, followed by treatment with 100 ng/ml IFN-γ and 25 ng/ml TNF-α in the presence of 100 µM AMT hydrochloride (iNOS inhibitor) for 72h. Supernatants were assessed at 33 DIV. (a) GM-CSF priming followed by IFN-γ and TNF-α treatment induced NO production ($p < 0.001$), which translated in (b) significantly elevated LDH level. AMT hydrochloride (c) inhibited NO production ($p > 0.05$) which (d) reduced the LDH back to the untreated level ($p > 0.05$). Data is presented as mean ± SD, p values were calculated using a one-way ANOVA followed by a Tukey post-hoc test.

### 5.2.2.4 Superoxide-dependent pathways do not contribute to cytokine-mediated cytotoxicity

Previous studies suggest peroxynitrite ($ONOO^-$) rather than nitric oxide is the major executor of tissue damage mediated by microglia (B. Y. Choi et al., 2015; J. Li, Baud, Vartanian, Volpe, & Rosenberg, 2005). As peroxynitrite formation is dependent on the reaction of nitric oxide with superoxide radicals (Ríos, Prolo, Álvarez, Piacenza, & Radi, 2017), its role in this model of cytokine-mediated cytotoxicity was investigated using Tiron (disodium-1,2-dihydroxybenzene-3,5-disulfonate), a cell permeable superoxide scavenger. We found Tiron had no effect on cytokine-induced cytotoxicity (Percent maximal LDH release: GM-CSF + IFN-γ + TNF-α = 61.73 ± 15.89 %; GM-CSF + IFN-γ + TNF-α + Tiron = 72.27 ± 13.78 %) (Figure 5.9). INOS dependent cytotoxicity is therefore independent of superoxide dependent effects that might generate peroxynitrite or hydroxyl radicals.

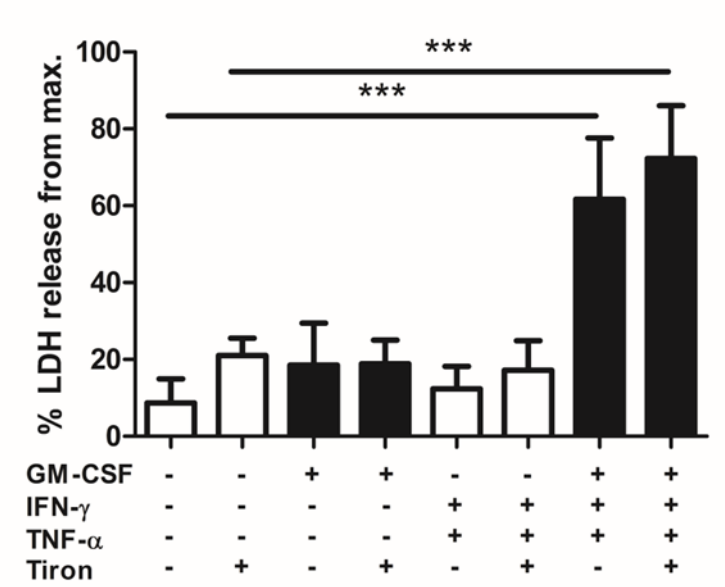


**Figure 5.9. Tiron, a superoxide scavenger, has no effect on cytokine-mediated tissue cytotoxicity**. Myelinating cultures were primed or unprimed with 100 ng/ml GM-CSF from 24 to 30 DIV, followed by 100 ng/ml IFN-γ and 25 ng/ml TNF-α in the presence or absence of 1 mM Tiron (superoxide scavenger) for 72h. Supernatants were assessed at 33 DIV. The addition of Tiron did not halt GM-CSF induced cell death ($p < 0.001$). Data presented as mean ± SD from six independent experiments, p values were calculated using a one-way ANOVA followed by a Tukey post-hoc test.

### 5.2.3 Microglia retain the ability to mediate tissue damage after long term GM-CSF withdrawal

In Chapter 4 it was shown microglia expression of Dectin2 is retained for at least six days following GM-CSF withdrawal suggesting the effect of GM-CSF priming on cytokine-mediated cytotoxicity may also be retained for an extended period. To test this hypothesis, mouse myelinating cultures were primed with GM-CSF for six days (24 to 30 DIV). GM-CSF was then withdrawn and cultures maintained for a further 12 days until DIV 42 when they were challenged with IFN-γ and TNF as described previously.

Although GM-CSF was withdrawn twelve days earlier (referred to as 'previously primed') there was still a demonstrable priming effect on microglia as demonstrated by (i) induction of iNOS in $CD45^+$ microglia; (ii) nitric oxide production and (iii) LDH release (Figure 5.10). The percentage of $iNOS^+$ microglia in cultures previously primed with GM-CSF and treated with IFN-γ and TNF (88.32 ± 5.564%) was significantly higher than in unprimed cultures treated with these cytokines (51.24 ± 11.54 %) (Figure 5.10 e). Similarly, previously primed cultures produced more nitric oxide (Primed: IFN-γ + TNF-α, 60.14 ± 6.087 μM; Unprimed: IFN-γ + TNF-α = 12.21 ± 4.03 μM) (Figure 5.10 f) and retained their cytotoxic potential compared to unprimed cultures (Primed: IFN-γ + TNF-α = 39.53 ± 9.058%; Unprimed: IFN-γ + TNF-α = 10.80 ± 2.65 %; Untreated = 7.627 ± 2.944 % maximal LDH release) (Figure 5.10 g).

The number of microglia after GM-CSF withdrawal was higher than in the untreated control (untreated = 85.71 ± 5.545; GM-CSF wd = 130.8 ± 7.616; $CD45^+$ cells/field of view), but decreased after 72 hours with IFN-γ and TNF (96.42 ± 26.91 $CD45^+$ cells/field of view) (Figure 5.10 h). An observation that may reflect autocrine killing of microglia by nitric oxide.

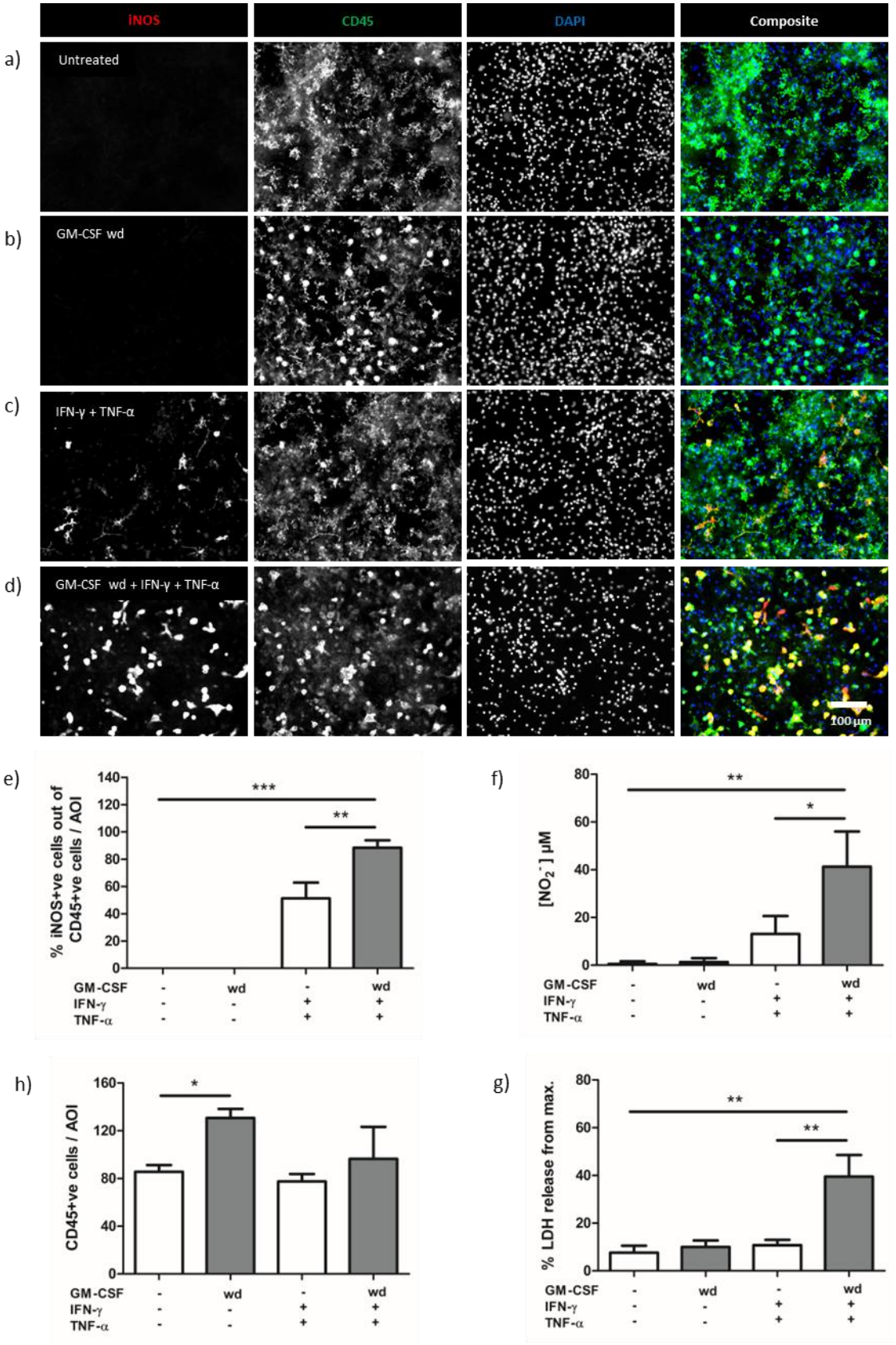


**Figure 5.10. Microglia retain the ability to mediate tissue damage after long term GM-CSF withdrawal.** (a-d) Representative images of myelinating cultures grown (a) in the absence of GM-CSF, (b) treated with 100 ng/ml GM-CSF from 24 to 30 DIV followed by 12 days GM-CSF withdrawal (wd), (c) treated with 100 ng/ml IFN-γ and 25 ng/ml TNF-α for 72h at 42h, and (d) treated with GM-CSF from 24-30 DIV followed by 12 days

GM-CSF withdrawal and treated with 100 ng/ml IFN-γ and 25 ng/ml TNF-α. Images were acquired and supernatants were assessed at 45 DIV. iNOS immune reactivity (red) is shown in the first column. Microglia were visualized using an anti-CD45 antibody (green), second column and nuclei visualised with DAPI (blue) in the third column. The composite of the three channels is shown in the last column. (e, f) There were significantly more microglia expressing iNOS and NO produced in cultures which were previously primed with GM-CSF and treated with IFN-γ and TNF-α than IFN-γ and TNF-α alone ($p< 0.01$, 0.05). (g) Previous GM-CSF priming also caused significantly more LDH release when challenged with IFN-γ and TNF-α ($p< 0.001$). (h) The number of microglia after 12 days GM-CSF withdrawal remained significantly higher than in the untreated control ($p< 0.05$). Data presented as mean ± SD from three independent experiments, p values were calculated using a one-way ANOVA followed by a Tukey post-hoc test. AOI= area of interest.

### 5.2.4 GM-CSF priming modulates IFN-γ and TNF-α mediated induction of pro-inflammatory cytokines

As demonstrated, GM-CSF priming has a dramatic effect on cytokine-mediated induction of iNOS dependent cytotoxicity. However, as it would be naïve to consider this was the only microglial response to GM-CSF priming the study was extended invest if this also modulated synthesis of pro-inflammatory cytokines. Supernatants were collected from cytokine treated myelinated cultures and screened using the MSD platform for the presence of a panel of pro-inflammatory cytokines (IL-1ß, IL-6, IL-15, IP-10, KC/GRO, MCP-1, MIP-2α, MIP-3α).

There was significant variation between individual cultures but focusing on the effects of GM-CSF priming on the response to IFN-γ and TNF-α some interesting trends emerged from these experiments. First, with the exception of IL-15 which was slightly elevated, simply priming cultures with GM-CSF had no effect on the concentrations of the cytokines studied. However, priming plus combined treatment with IFN-γ and TNF-α was associated with increased a significant increase in the concentrations of IL-6 and a tendency towards increase in IL-1b. Unexpectedly, examining the individual effects IFN-γ or TNF-α on IL-1β and IL-6 in primed cultures suggest this involves different mechanisms. TNF alone was sufficient to account for the increase in IL-1β, whereas the increase in IL-6 could not be attributed to either cytokine alone. With respect to the other cytokines examined, there was a general trend for priming to increase their concentrations, but variation between experiments prevented a clear conclusion being drawn. Why this was the case was unclear, but it could reflect differences

in microglial density between cultures, effects due to iNOS dependent injury and/or cytokine production by astrocytes or other cells present in these cultures (Rothhammer & Quintana, 2015) (Figure 5.11, 5.12).

To address this variability, the study was repeated using supernatants harvested from cultures of primary mouse microglia which had been untreated or primed with GM-CSF for 3 days and then treated with IFN-γ and TNF-α singly or in combination for 72h (Figure 5.13). This provided data sets with far less variability and confirmed the treatment enhanced secretion of IL-β, IL-6, IL-15, CXCL1, CXCL2 and CCL2 compared to untreated controls. However, it is apparent from the data presented in Figure 5.12 the response is complex. This is illustrated by the differential effects on CXCL10, CXCL1 and CXCL2, and CCL2. First, priming did not significantly alter CXCL10 production in response to IFN-γ and TNF-α, but completely abolished the ability of TNF-α to enhance CXCL10 production i.e. GM-CSF appears to antagonize or inhibits the effect of TNF-α on CXCL10 production. Secondly, priming with GM-CSF enhanced production of CXCL1 and CXCL2 in response to TNF-α, but this effect was markedly decreased by IFN-γ. Thirdly, priming with GM-CSF also enhanced production of CCL2 in response to IFN-γ, but in this case, TNF-α appeared to act as an antagonist.

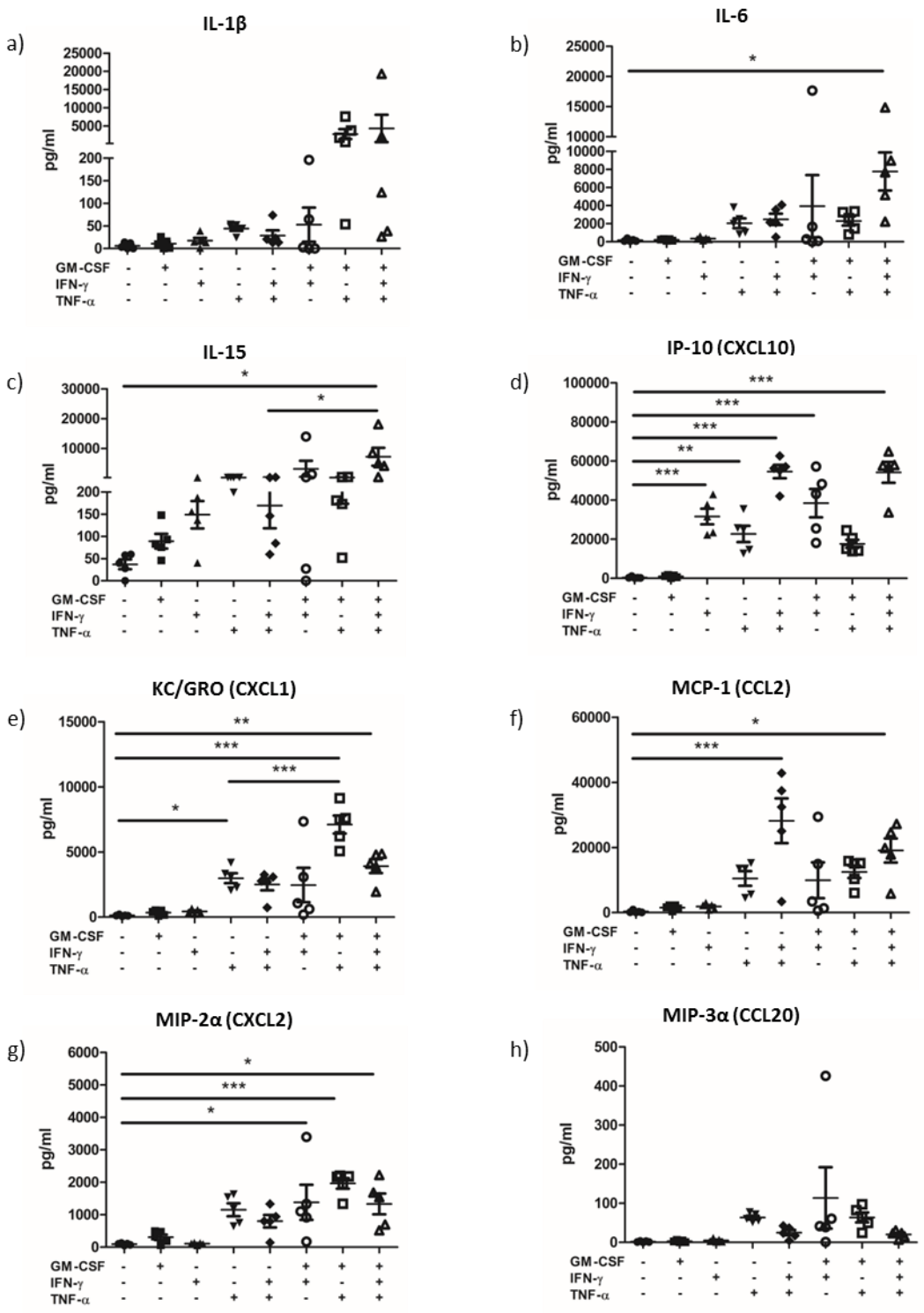


**Figure 5.11. GM-CSF synergised with IFN-γ and TNF-α to increase the production of some pro-inflammatory cytokines.** Mouse myelinating cultures were primed or unprimed with 100 ng/ml GM-CSF from 24 to 30 DIV, followed by treatment with 100 ng/ml IFN-γ and 25 ng/ml TNF-α, singly or in combination, for 24h. Supernatants were assessed at 31 DIV. (a-h) Cell supernatants were screened for pro-inflammatory cytokines, Il-1ß, IL-6, IL-15, IP-10, KC/GRO, MCP-1, MIP-2α, MIP-3α, using the MSD

platform. Data are presented as mean from five independent experiments ± SEM, p values were calculated using a one-way ANOVA followed by a Tukey post-hoc test.

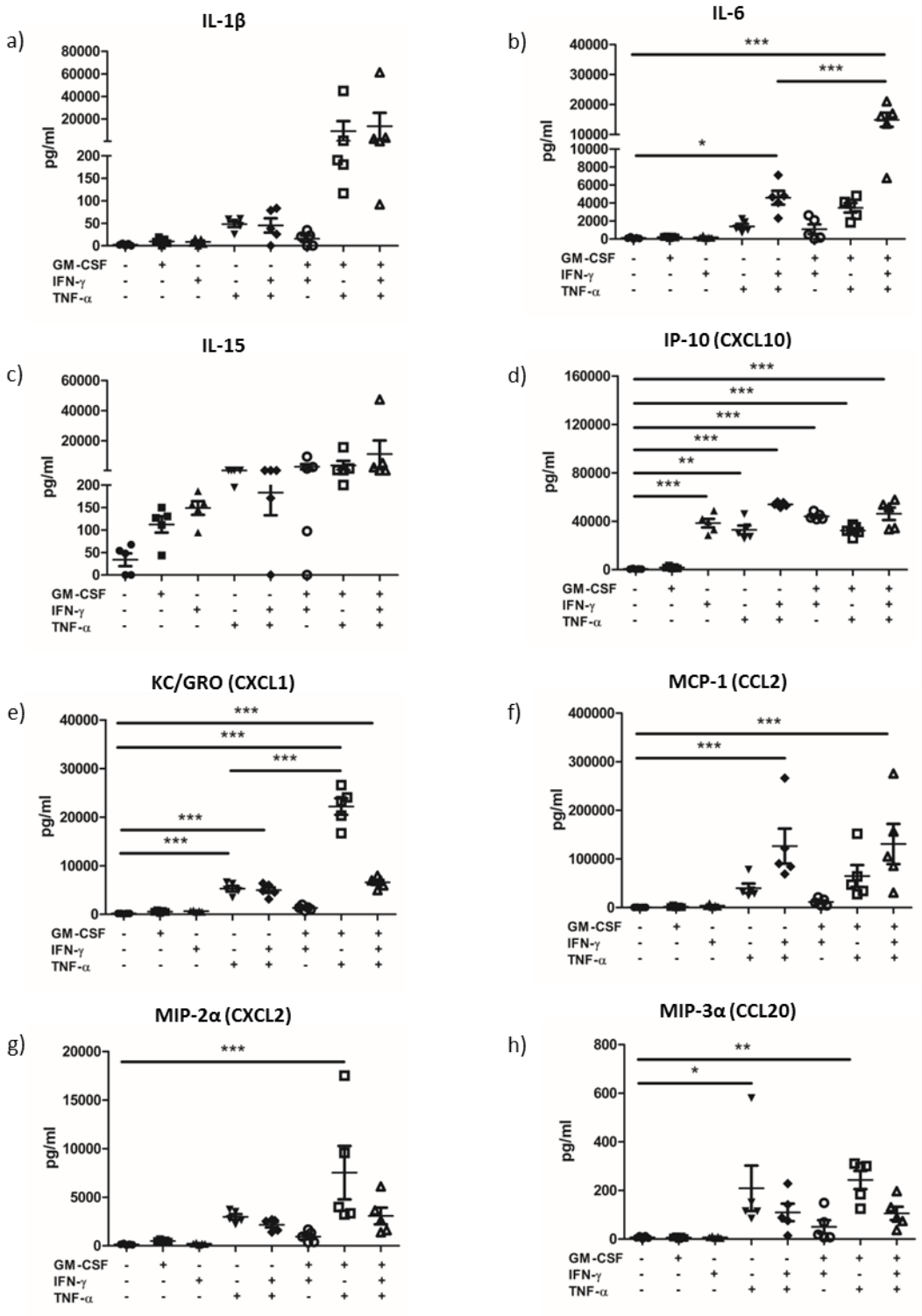


**Figure 5.12. GM-CSF synergised with IFN-γ and TNF-α to increase the production of some pro-inflammatory cytokines.** Mouse myelinating cultures were primed or unprimed with 100 ng/ml GM-CSF from 24 to 30 DIV, followed by treatment with 100 ng/ml IFN-γ and 25 ng/ml TNF-α, singly or in combination, for 72h. Supernatants were assessed at 33 DIV. (a-h) Cell supernatants were screened for pro-inflammatory cytokines, Il-1ß, IL-6, IL-15, IP-10, KC/GRO, MCP-1, MIP-2α, MIP-3α, using the MSD

platform. Data are presented as mean from five independent experiments ± SEM, p values were calculated using a one-way ANOVA followed by a Tukey post-hoc test.

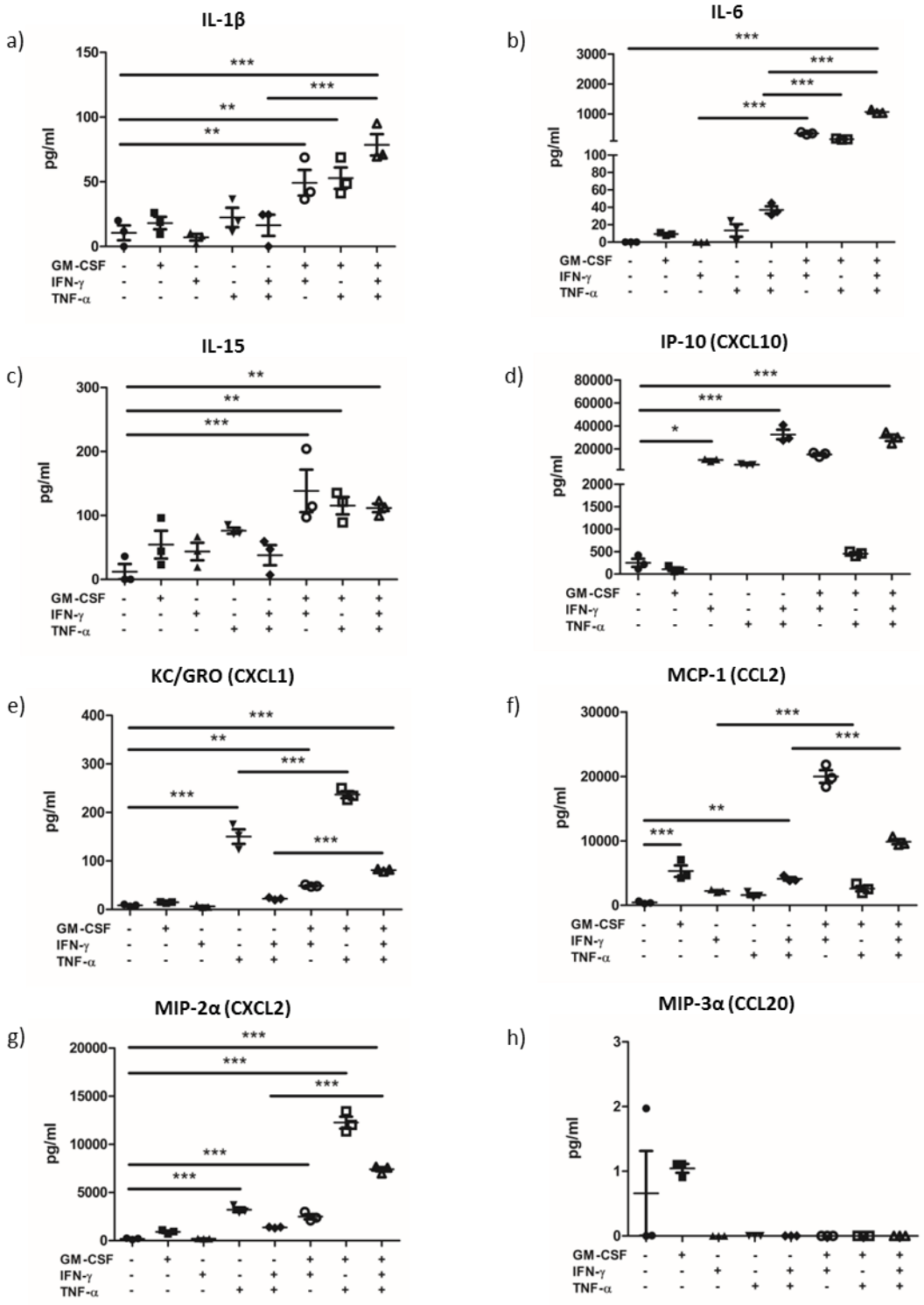


**Figure 5.13. GM-CSF synergised with IFN-γ and TNF-α to increase the production of some pro-inflammatory cytokines in primary microglia.** Mouse primary microglia cultures were primed or unprimed with 100 ng/ml GM-CSF from 0 to 3 DIV, followed by treatment with 100 ng/ml IFN-γ and 25 ng/ml TNF-α, singly or in combination, for 72h.

Supernatants were assessed at 6 DIV. (a-h) Cell supernatants were screened for pro-inflammatory cytokines, Il-1ß, IL-6, IL-15, IP-10, KC/GRO, MCP-1, MIP-2α, MIP-3α, using the MSD platform. Data are presented as mean from five independent experiments ± SEM, p values were calculated using a one-way ANOVA followed by a Tukey post-hoc test.

## 5.3 Discussion

GM-CSF synthesis by encephalitogenic $CD4^+$ Th cells (Th-GM cells) plays an important role in development of EAE due to effects that include microglial activation, activation and recruitment of monocyte-derived macrophages, and enhanced antigen presentation (Codarri et al., 2011; Komuczki et al., 2019; Ponomarev et al., 2007; Sheng et al., 2014). However, the pathophysiological consequences and underlying mechanisms by which GM-CSF mediates its effects on microglia to contribute to disease development remain obscure.

As GM-CSF had no direct effects on the physical integrity of myelin and axons in tissue culture (Chapters 2 and 3) we reasoned any contribution to lesion development involved synergy with other cytokines secreted by encephalitogenic Th-GM, Th1 and/or Th17 T cells (Ponomarev *et al.*, 2007). Prime candidates were IFN-γ and TNF-α which kill neurons and oligodendrocytes in tissue culture (Renno *et al.*, 1995; Agresti *et al.*, 1996; Baerwald and Popko, 1998; Andrews *et al.*, 1998; Bate *et al.*, 2006; Mount *et al.*, 2007; Neniskyte *et al*, 2014) and contribute to the pathogenesis of EAE (Akassoglou et al., 1998; Kerschensteiner et al., 2004; Probert, 2000) and MS (Panitch, Hirsch, Schindler, & Johnson, 1987; Pegoretti et al., 2018). It should however be stressed cytotoxicity is only one facet of the roles these cytokines might play in disease development, as they can also promote cell survival and differentiation (Wang et al., 2018). In the case of TNF-α, signal transduction via TNFR1 enhances oligodendrocyte apoptosis and demyelination , whilst activation of TNFR2 promotes cell survival and oligodendrocyte maturation (Pegoretti et al., 2018; Probert, 2015).

Concentrations of IFN-γ and TNF-α used in studies mentioned above varied considerably so a preliminary screen was carried out to identify concentrations that individually or in combination had no detrimental effect on myelin or axons following exposure for 3 days. These were then used to investigate whether GM-

CSF amplified their cytopathic potential in myelinated cultures. At the selected concentrations (100 ng/ml IFN-γ; 25 ng/ml TNF-α) neither cytokine was cytotoxic or induced myelin or axonal injury in naïve cultures. However, in cultures primed for six days with GM-CSF this combination of cytokines was cytopathic and induced extensive demyelination and axonal loss. Moreover, this priming effect was long lasting and continued to exacerbate tissue damage caused by IFN-γ and TNF-α for at least twelve days after GM-CSF withdrawal. An observation that suggests once triggered this priming effect will continue to influence microglial function for many days after GM-CSF secreting T cells are cleared from the CNS in animals with EAE.

To identify the mechanisms involved we focused on iNOS, as IFN-γ and TNF-α not only upregulate iNOS in microglia (Romero *et al.*, 1996; Delgado, 2003; Lively and Schlichter, 2018; Ding *et al.*, 2015; Ta *et al.*, 2019) but its product, nitric oxide, plays a significant role in the pathogenesis of EAE (Willenborg, Staykova, & Cowden, 1999) and MS (Liu *et al.*, 2001; Smith and Lassmann, 2002; Jack *et al.*, 2007). In myelinated cultures priming with GM-CSF for 6 days followed by 24 hours treatment with IFN-γ and TNF-α induced iNOS expression in approximately 80% of microglia (Figure 5.2, 5.3). Some weak iNOS immunoreactive was also observed in GM-CSF primed cultures treated with IFN-γ as well as unprimed cultures treated with IFN-γ and TNF-α. This pattern of iNOS expression in response to different cytokine treatments was confirmed by western blotting and translated into a significant increase in nitric oxide production in GM-CSF primed cultures treated with IFN-γ and TNF-α (Figure 5.3 c). To eliminate a role for effects secondary to IFN-γ and/or TNF-α signalling in other cell types the study was repeated using primary mouse microglia. This replicated the findings made in myelinated cultures confirming IFN-γ and TNF-α act directly on GM-CSF primed microglia to induce expression of iNOS.

The cytotoxic potential of this response was then investigated using AMT hydrochloride, a potent and selective iNOS inhibitor (Nakane et al., 1995). This revealed the cytopathic potential of IFN-γ and TNF-α was iNOS dependent in GM-CSF primed cultures. This protective effect was seen in rat and mouse cultures demonstrating cytokine-mediated, iNOS-dependent cytotoxicity is not a species-specific response. Previous studies led us to speculative this would not be

mediated by nitric oxide itself, but peroxynitrite generated by NO reacting with superoxide radicals (Beckman, Beckman, Chen, Marshall, & Freeman, 1990; Mander & Brown, 2005; Pacher, Beckman, & Liaudet, 2007). However, our data suggest this is not the case as the superoxide scavenger Tiron failed to inhibit iNOS-dependent injury. The concentration of Tiron used (1 mM) protects PC12 cells from superoxide induced cell death (Yamada *et al.*, 2003), but it would be prudent to test higher concentrations and/or alternative inhibitors before finally concluding cell death was mediated directly by nitric oxide. Nonetheless several mechanisms are available by which increased bioavailability of nitric oxide may compromise survival of myelinating oligodendrocytes and/or neurons. The most important is likely to be its inhibitory effects on oxidative phosphorylation which are predicted to result in profound energy deficits and ultimately demyelination and neurodegeneration (Desai & Smith, 2017; Sadeghian et al., 2016). In addition, nitic oxide may S-nitrosylate myelin proteins leading to destabilisation of the myelin sheath (Bizzozero, Dejesus, & Howard, 2004). Together, these data suggest iNOS is an attractive target for therapeutic strategies designed to reduce tissue damage in the CNS in EAE and MS but this is impractical (Willenborg et al., 1999), because, in addition to its pro-inflammatory and cytotoxic properties (Bogdan, Röllinghoff and Diefenbach, 2000), nitric oxide is involved in multiple homeostatic and immunoregulatory pathways. This was first observed in $iNOS^{-/-}$ mice which developed more severe EAE than wild type controls (Fenyk-Melody et al., 1998), Subsequent studies revealed this is in part due in part to immunoregulatory effects that modulate T cell apoptosis and development of autoreactive Th1/17 T cell responses (Dalton and Wittmer, 2005; Yang et al., 2013).

To investigate if GM-CSF priming affects other microglial effector mechanisms we screened myelinating cultures and microglial supernatants for pro-inflammatory cytokine production. There was significant variation between individual myelinating cultures, making it impossible to draw a clear conclusion. On the other hand, primary microglia primed with GM-CSF for 3 days before cytokine treatment revealed that priming significantly increased supernatant concentrations of IL-1ß, IL-6, IL-15, CXCL1, CXCL2 and CCL2, but had no effect on cytokine mediated induction of CXCL10. These observations are similar to those reported by Parajuli and colleagues who found GM-CSF increases

production of Il-1ß, IL-6 and TNF-α by primary microglia after TLR-4 stimulation (Parajuli et al., 2012). Functionally these effects are important as all these cytokines modulate neuroinflammation in EAE. Disease severity is attenuated in mice deficient in IL-1 and IL6 signalling (Eugster *et al.*, 1998;Sutton *et al.*, 2006) whilst IL-15 knockout mice develop more severe disease (Gomez-Nicola, Spagnolo, Guaza, & Nieto-Sampedro, 2010) and CXCL1 (Hasseldam, Rasmussen, & Johansen, 2016), CXCL2 (Tran, Prince, & Owens, 2000; Tsutsui et al., 2018) and CCL2 (Mahad & Ransohoff, 2003) chemokines contribute to immune cell recruitment across the blood brain-barrier. GM-CSF therefore primes microglia to amplify induction of multiple gene products predicted to exacerbate inflammatory activity in the CNS. But is this relevant to MS?

It is not possible to provide a definitive answer to this question, but in MS patients concentrations of GM-CSF, IL-6, CCL2, CXCL1 and other factors are elevated in plasma and/or cerebrospinal fluid, compared with healthy subjects, and this correlates with lesion burden and MS clinical severity (Carrieri *et al.*, 1998; Ishizu *et al.*, 2005; Campbell *et al.*, 2010; Matsushita *et al.*, 2013; Rumble *et al.*, 2015). Immunopathological studies have also identified several of these cytokines in MS lesions (Filipovic, Jakovcevski, & Zecevic, 2003; Lin & Edelson, 2017; McManus et al., 1998; Simpson, Newcombe, Cuzner, & Woodroofe, 1998). However, how these observations are related to reports that (a) GM-CSF producing T cells are enriched in cerebrospinal fluid from MS patients (Ghezzi et al., 2019) and (b) expression of GM-CSF defines a novel disease associated T cell subset (Galli et al., 2019) remain unclear. It is tempting to assume these associations are functionally related, but even if this is not the case, increasing evidence indicates GM-CSF is a relevant target in neuroinflammatory diseases (Aram et al., 2019; Becher et al., 2016; Hamilton, 2015).

Nonetheless more research is required to determine the functional significance and mechanisms by which GM-CSF modulated cytokine networks potentiate tissue damage in the CNS. One approach to these questions is to use myelinating cultures as described in this this thesis. A start has been made in this direction by mapping transcriptional profiles induced by treatments with IFN-γ and TNF-α, individually and in combination, with and without GM-CSF priming. Analysis of preliminary microarray study is currently ongoing and some preliminary data will

be discussed in Chapter 6. However, rodent models do not reproduce fully many aspects of lesion development in MS, in particular expression of molecules associated with oxidative tissue damage (Höftberger, Leisser, Bauer, & Lassmann, 2015; Schuh et al., 2014). A better strategy would therefore be to exploit recent developments in reprogramming iPSC to generate co-cultures containing as appropriate defined populations of iPSC derived microglia, astrocytes, neurons and/or oligodendrocytes.

# Chapter 6

## Elucidating the mechanism through which GM-CSF synergises with IFN-γ and TNF-α to induce cytotoxicity

# 6 Elucidating the mechanism through which GM-CSF synergises with IFN-γ and TNF-α to induce cytotoxicity

## 6.1 Introduction

The previous chapters demonstrate that priming myelinated cultures with GM-CSF sensitises for TNF-α and IFN-γ to mediate iNOS-dependent demyelination and axonal loss. In this chapter I focus on the mechanism through which GM-CSF priming synergises with IFN-γ and TNF-α to up-regulate iNOS and induce tissue damage. We first investigated whether NO production and cytotoxicity are dependent on the concentration of GM-CSF used during priming, but also on the length of priming. Secondly, as NF-κB has been identified as one of the main transcription factors regulators of *Nos2* expression (Farlik et al., 2010; Kleinert, Art, & Pautz, 2010) we explored if GM-CSF mediated cytotoxicity is also NF-κB dependent. Finally, to gain insight in the mechanistic relationship between GM-CSF priming and cytokine-mediated induction of iNOS and cytotoxicity during inflammation we also investigated whether GM-CSF priming synergises with TLR3 and TLR4 signalling.

## 6.2 Results

### 6.2.1 GM-CSF priming is dose-dependent

To investigate dose-dependent effects of GM-CSF priming on NO production and cytotoxicity, myelinating cultures were primed with various concentrations of GM-CSF for six days (0.001, 0.01, 0.1, 1, 10, and 100 ng/ml; 24 - 30 DIV). They were then treated with 100 ng/ml IFN-γ and 25 ng/ml TNF-α for 72h as described previously. Dose response effects were observed for both parameters (NO concentration and LDH release), but across different concentration ranges. NO production increased from back ground levels to >40 μM in cultures primed with between 0.1 to 100 ng whilst cytotoxicity only increased significantly between 1 and 100 GM-CSF/ml (Figure 6.1 b).

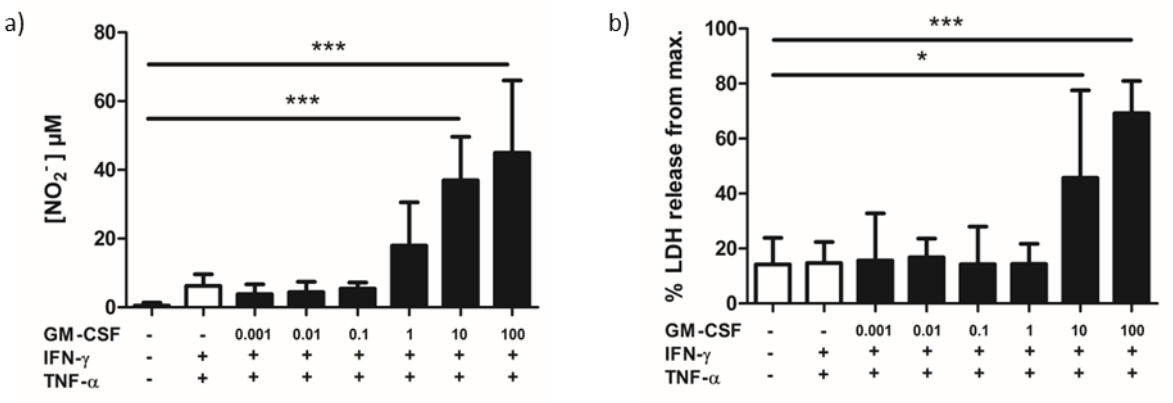


**Figure 6.1. GM-CSF priming is dose-dependent.** Mouse myelinating cultures were primed with increasing concentrations of GM-CSF and after six days (at 30 DIV) treated with 100 ng/ml IFN-γ and 25 ng/ml TNF-α 72h after which culture supernatants were harvested and assayed for (a) NO production and (b) LDH release. Supernatants were assessed at 33 DIV. Data are presented as mean of five independent experiments ± SD; p values were calculated using a one-way ANOVA followed by a Tukey post-hoc test.

### 6.2.2. GM-CSF priming requires time to enhance NO production and cytotoxicity

To determine if the effects of GM-CSF priming on NO production and cytotoxicity are time dependent, myelinating cultures were primed with 100 ng/ml GM-CSF for one, three or six days before treatment with 100 ng/ml IFN-γ and 25 ng/ml TNF-α treatment for 72h after which supernatants were harvested and assayed for NO and LDH (Figure 6.2). Three days priming was required to induce a significant increase in cytokine induced NO production (primed, 36.54 ± 20.07 μM; unprimed 6.746 ± 6.338 μM), but prolonging priming for six days had no further effect (primed, 41.30 ± 14 μM; unprimed 6.746 ± 6.338 μM) (Figure 6.2 a). However, only 24 hours priming was required to increase the proportion of microglia expressing iNOS to values similar to those in cultures primed for six days (Figures 6.3 a and 6.4). Nonetheless, no increase in cytokine-mediated cytotoxicity was observed unless cultures were primed for six days as demonstrated by LDH release (Figure 6.2 b) and decrease in total cell number (Figure 6.3 c).

These observations demonstrate that whilst short exposure to GM-CSF enhances cytokine-mediated expression of iNOS in microglia, considerably longer priming is necessary for this to translate into a cytopathic response. This is not a consequence of differences in NO production as there is no obvious correlation between $NO^{2-}$ concentration and LDH release in cultures primed for three or six days (Figure 6.2). Moreover, there was no significant difference in either the percentage or absolute number of $iNOS^{+}$ microglia in cultures primed with GM-CSF for three or six days (Figures 6.2 and 6.4).

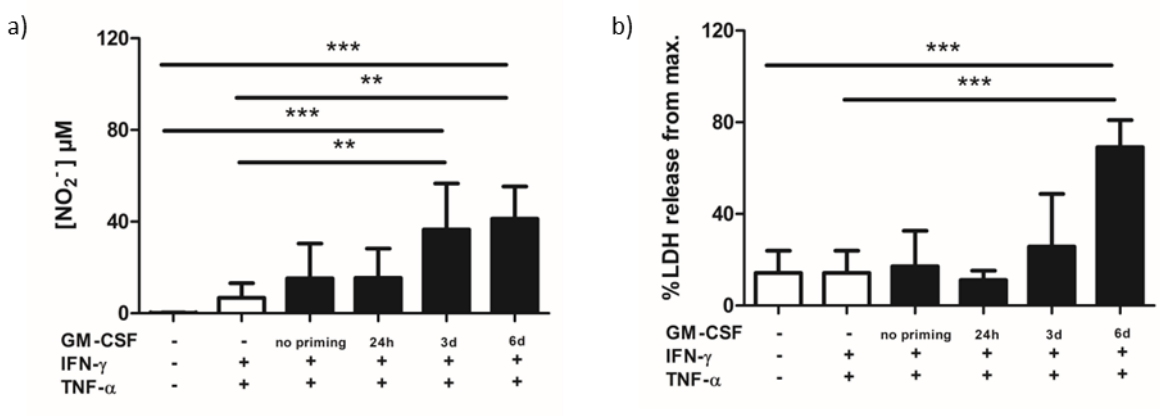


**Figure 6.2. GM-CSF associated NO production and cytotoxicity are priming time- dependent.** Mouse myelinating cultures were primed with 100 ng/ml GM-CSF for one, three or six days after which they were treated with 100 ng/ml IFN-γ and 25 ng/ml TNF-α for 72h after which supernatants were assayed for (a) NO production; (b) LDH release. Supernatants were assessed at 33 DIV. Data are presented as mean from three independent experiments ± SD, p values were calculated using a one-way ANOVA followed by a Tukey post-hoc test.

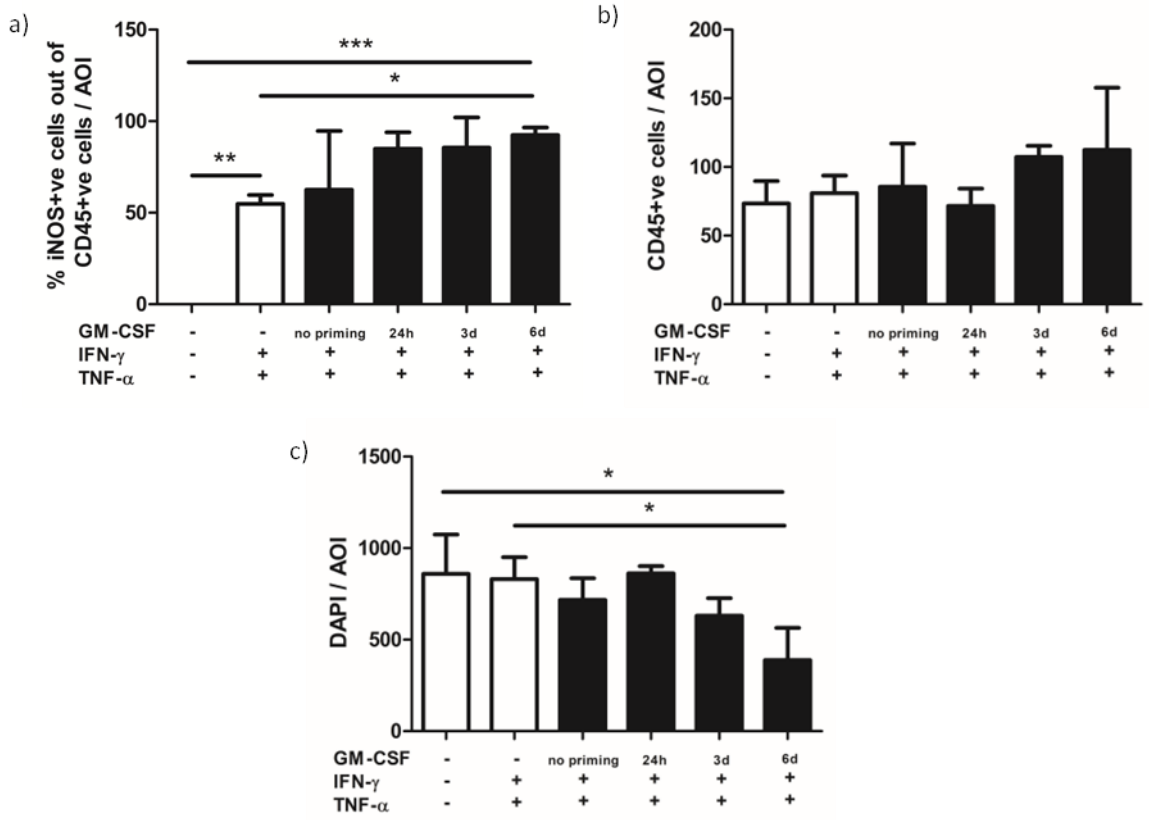


**Figure 6.3. Effect of GM-CSF priming duration on CD45$^+$ microglia.** Mouse myelinating cultures were primed with 100 ng/ml GM-CSF for one, three and six days after which they were treated with 100 ng/ml IFN-γ and 25 ng/ml TNF-α for 72h. Images were acquired at 33 DIV. (a) percentage CD45$^+$ microglia expressing iNOS; (b) number of

$CD45^+$ microglia/AOI. (c) total cell number/AOI, DAPI staining). Data are presented as mean from three independent experiments ± SD, p values were calculated using a one-way ANOVA followed by a Tukey post-hoc test. AOI= area of interest.

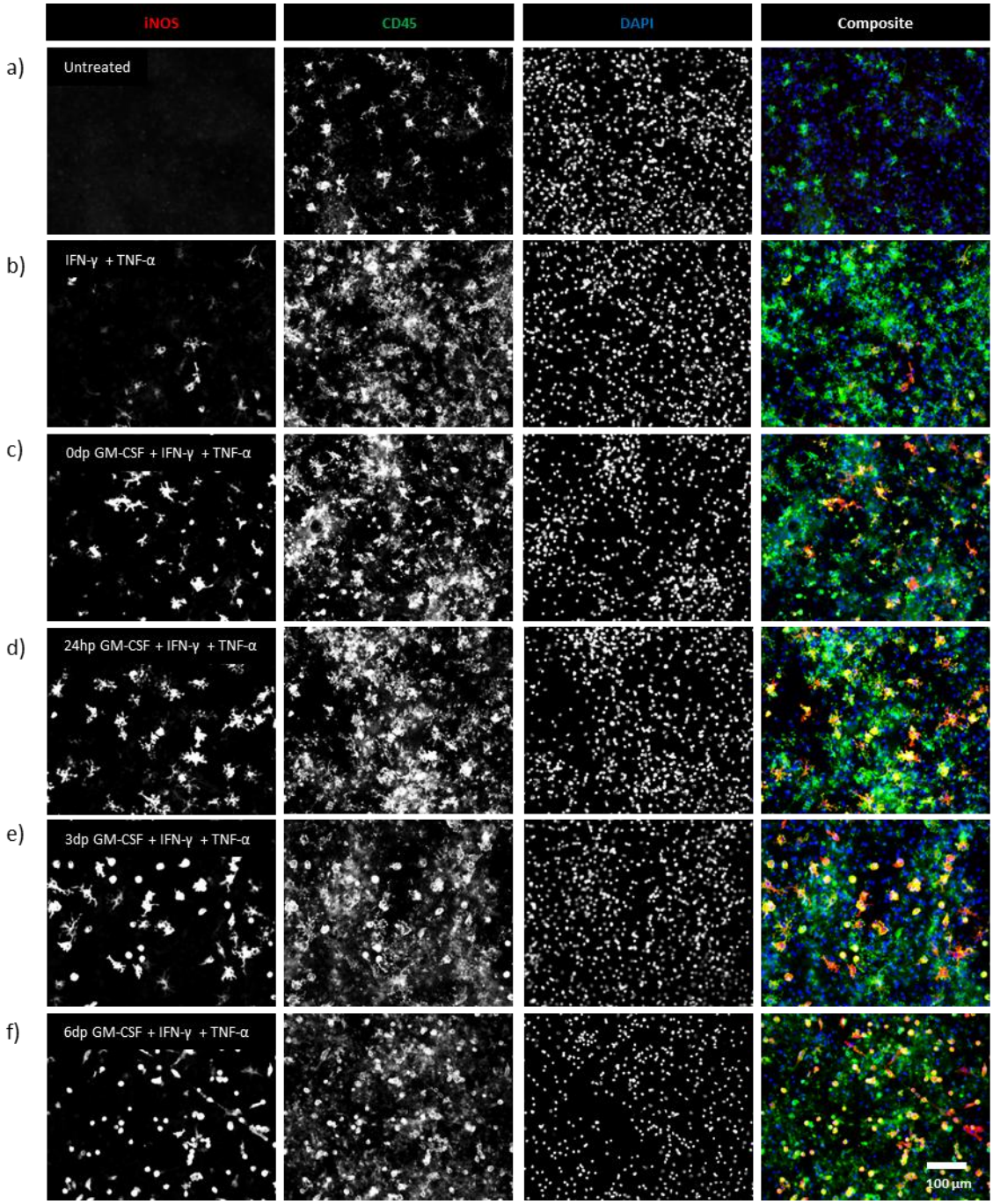


**Figure 6.4. Representative images of mouse myelinating primed with GM-CSF for different lengths of time and treated with IFN-γ and TNF-α for 72h.**
(a) Untreated; (b) IFN-γ + TNF-α (c) GM-CSF + IFN-γ + TNF-α; (d) GM-CSF primed for one day then IFN-γ + TNF-α; (e) GM-CSF primed for three days then IFN-γ + TNF-α; (f) GM-CSF primed for six days then IFN-γ + TNF-α. Images were acquired at 33 DIV. Microglia were visualized using an anti-CD45 antibody (green), iNOS (red) and nuclei visualised with DAPI (blue).

### 6.2.2 GM-CSF priming synergises with LPS and Poly I:C to induce rapid expression of iNOS in microglia and amplify NO production

To gain insight in the mechanistic relationship between GM-CSF priming and cytokine-mediated induction of iNOS and cytotoxicity, we tested if GM-CSF priming had similar effects on TLR signalling. Myelinating cultures were primed as described previously (100 ng/ml GM-CSF from 24 to 30 DIV) then treated with 1 µg/ml LPS (activates TLR4) or 10 µg/ml poly I:C (polyinosinic:polycytidylic acid, activates TLR 3).

LPS induced low levels of iNOS immunoreactivity and NO production in unprimed myelinated cultures (Figure 6.5 a, e), but these effects increased significantly following priming with GM-CSF (Figure 6.5 b, e). LPS induced iNOS expression in approximately 60% of microglia in primed cultures, an effect associated with a significant increase in NO production (Figure 6.5 e, f). GM-CSF priming had a similar but less pronounced effect on induction of iNOS and NO production by poly I:C (Figure 6.5 c, d, I, j). It should be noted iNOS immunoreactivity induced by these TLR ligands was not restricted to microglia as it was also observed in occasional $CD45^-$ cells (Figure 6.5 b, d). This is not surprising as TLR3 and TLR4 are expressed by many CNS cell types (Zhang *et al*., 2014). In neither case did GM-CSF priming enable these ligands to mediate a cytopathic effect (Figure 6.6). Although, poly I:C abolished the GM-CSF-mediated increase in $CD45^+$ microglia number this was not associated with a significant increase in LDH release raising the possibility activation of TLR3 by poly I:C may down regulate expression of CD45 rather than killing these cells.

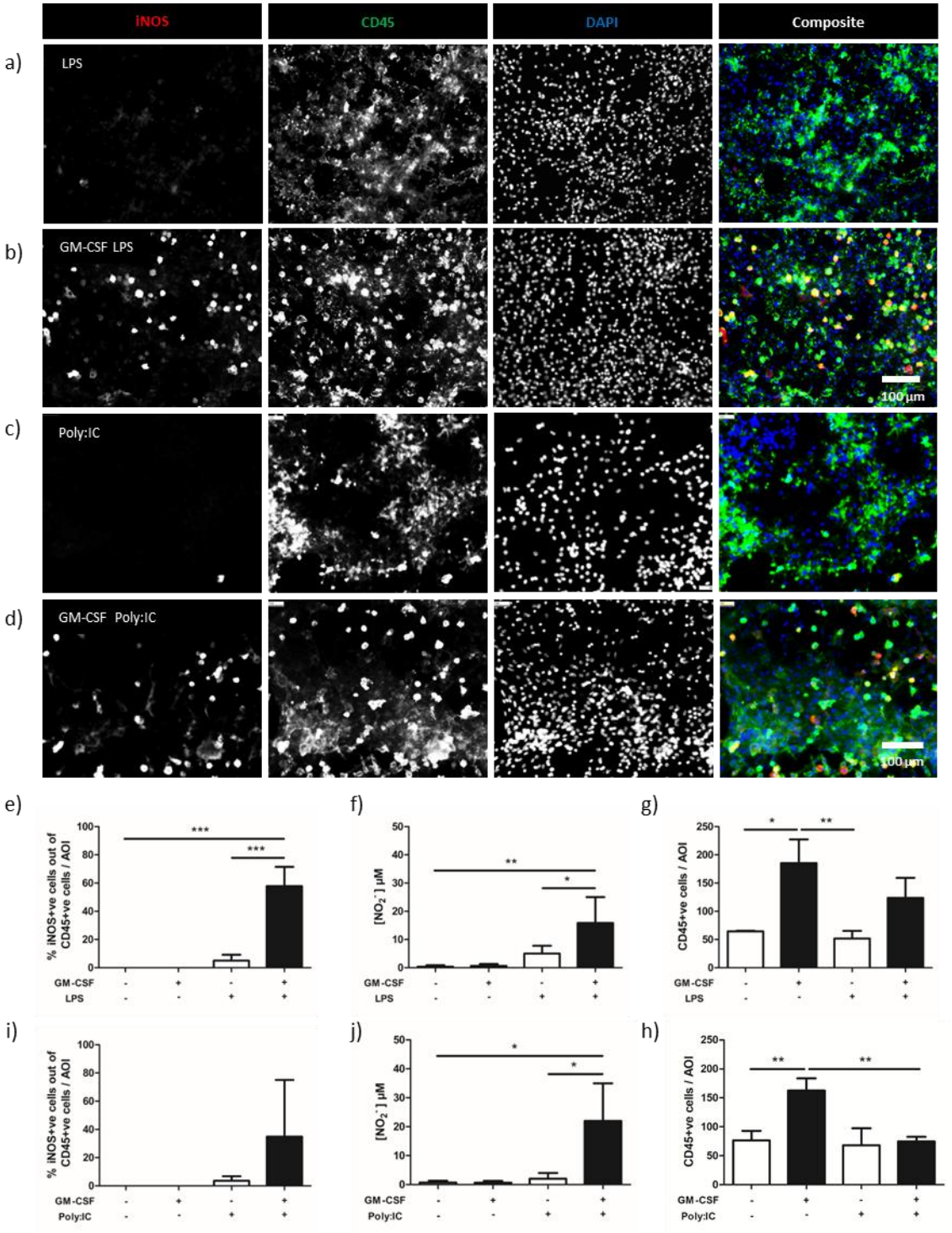


**Figure 6.5. GM-CSF priming enhances induction of iNOS and NO production by LPS and Poly I:C.** Representative images of mouse myelinating cultures after different cytokine treatments. (a) treated with 1 µg/ml LPS for 72h at 30 DIV; (b) primed with 100 ng/ml GM-CSF from 24 to 30 followed by 1 µg/ml LPS for 72h; (c) treated with 10 µg/ml Poly I:C for 72h at 30 DIV; (d) primed with 100 ng/ml GM-CSF from 24 to 30 followed by 10 µg/ml Poly:IC for 72h. Images were acquired and supernatants were assessed at 33 DIV. iNOS immune reactivity (red) is shown in the first column. Microglia were visualized using an anti-CD45 antibody (green), second column and nuclei visualised with DAPI (blue) in the third column. The composite of the three channels is shown in the last column. Note intense iNOS immune reactivity in multiple $CD45^{+}$ cells was only observed if cultures were first primed with GM-CSF and the treated with LPS

and Poly I:C. (e, f) There were significantly more microglia expressing iNOS and NO produced in cultures which were previously primed with GM-CSF and treated with LPS than LPS alone($p < 0.001$, 0.001). (g) GM-CSF priming increased microglia density ($p < 0.05$), while LPS treatment had no effect ($p > 0.05$). (h) The increase in microglia percentage expressing iNOS following GM-CSF priming at Poly I:C treatment did not reach statistical significance ($p > 0.05$). (i) GM-CSF priming followed by Poly I:C treatment induced NO production ($p < 0.05$). (j) GM-CSF priming increased microglia density ($p < 0.01$), while Poly I:C decreased $CD45^+$ microglial density in GM-CSF primed cultures ($p < 0.01$). Data presented as mean ± SD from three independent experiments, p values were calculated using a one-way ANOVA followed by a Tukey post-hoc test. AOI= area of interest.

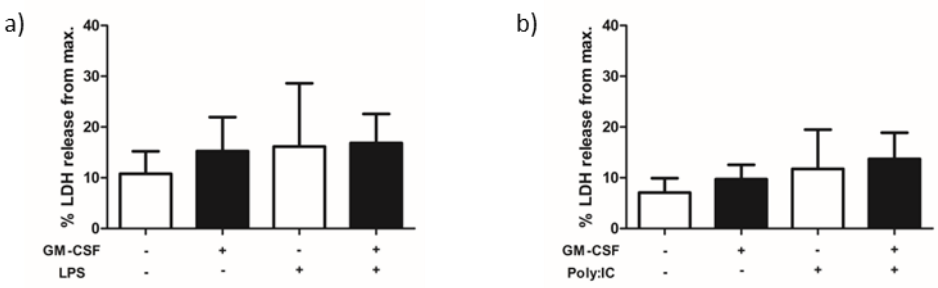


**Figure 6.6. GM-CSF priming does not potentiate LPS or Poly I:C cytotoxicity.** (a) Treating with 1 µg/ml LPS for 72h on unprimed cultures at 30 DIV or cultures primed with 100 ng/ml GM-CSF from 24 to 30 has no effect on LDH release ($p > 0.05$). (b) Treating with 10 µg/ml Poly I:C for 72h on unprimed cultures at 30 DIV or cultures primed with 100 ng/ml GM-CSF from 24 to 30 has no effect on LDH release ($p > 0.05$). Supernatants were assessed at 33 DIV. Data presented as mean ± SD from three independent experiments, p values were calculated using a one-way ANOVA followed by a Tukey post-hoc test

## 6.2.3 NF-κB signalling is involved in GM-CSF mediated cytotoxicity

### 6.2.3.1 Inhibiting NF-κB signalling globally inhibits iNOS expression and negates NO production, but has no effect on cytotoxicity

The data presented above suggest priming with GM-CSF has two distinct effects on the response of myelinating cultures to treatment IFN-γ + TNF-α. First a relatively rapid effect of GM-CSF priming which cooperates with IFN-γ and TNF-α to induce microglia to express iNOS. Second, a response dependent on extended priming (over six days) necessary for these cytokines to mediate iNOS dependent cytotoxicity. As induction of iNOS is dependent on cooperation between NF-κB and ISGF3 transcription factors (Farlik et al., 2010) we therefore reasoned that inhibiting NF-kB would abolish the priming effects of GM-CSF on cytokine-mediated induction of iNOS and cytotoxicity.

To test this hypothesis, myelinating cultures were primed with 100 ng/ml GM-CSF in the presence or absence of 10 μM 2-[(aminocarbonyl)amino]-5 -(4-fluorophenyl)-3-thiophenecarboxamide (TPCA-1), a well characterised IkB kinase (IKK) antagonist that inhibits activation of NF-κB and its translocation to the nucleus (Podolin et al., 2005). TPCA-1 completely abolished iNOS expression by microglia in primed and unprimed cultures treated with IFN-γ + TNF-α (Figure 6.7 a, 6.8 a), and led to a significant decrease in NO production (Figure 6.8 b). However, this was not associated with a significant decrease in LDH release (Figure 6.8 c), implying inhibition of NF-κB exposes an alternative cytokine-mediated cytopathic effect in GM-CSF primed cultures.

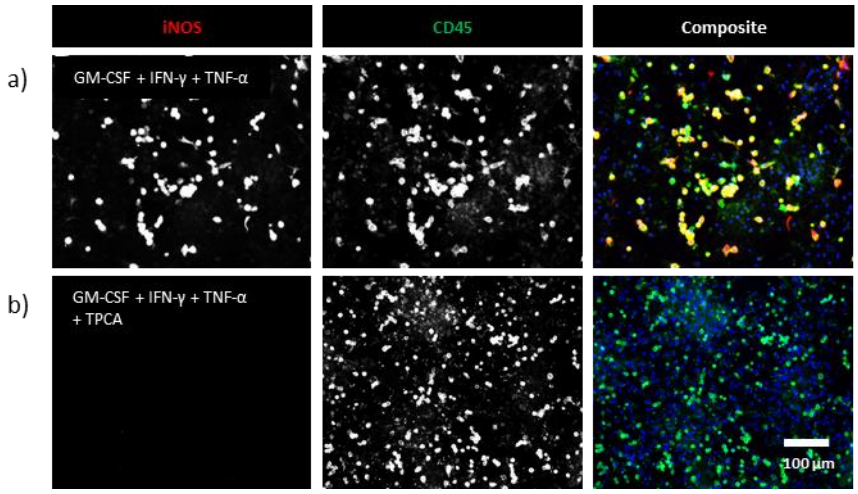


**Figure 6.7. Representative images of mouse myelinating primed with GM-CSF and treated with IFN-γ and TNF-α in the presence of TPCA-1.** Mouse myelinating cultures were primed or unprimed with 100 ng/ml GM-CSF from 24 to 30 DIV, followed by treatment with 100 ng/ml IFN-γ and 25 ng/ml TNF-α in the presence of 10 µM TPCA-1 or DMSO (vehicle control) for 72h. (b) TPCA-1 abolished iNOS immune reactivity in microglia after treatment with IFN-γ and TNF-α ($p < 0.001$). Images were acquired at 33 DIV.

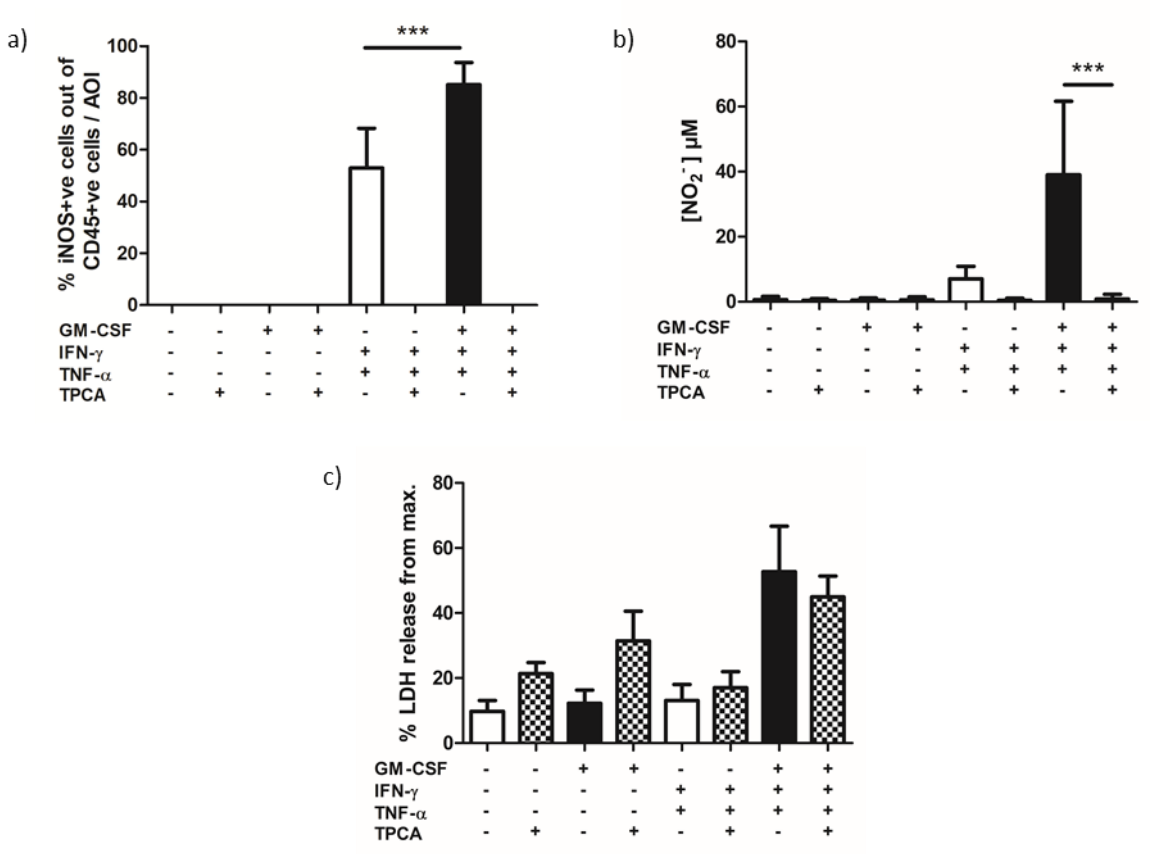


**Figure 6.8. TPCA-1, an IkκB kinases inhibitor, decreases GM-CSF mediated NO production, but has no effect on cytotoxicity.** Mouse myelinating cultures were primed or unprimed with 100 ng/ml GM-CSF from 24 to 30 DIV, followed by treatment

with 100 ng/ml IFN-γ and 25 ng/ml TNF-α in the presence of 10 μM TPCA-1 or DMSO (vehicle control) for 72h. Images were acquired and supernatants were assessed at 33 DIV. (a) TPCA-1 inhibited iNOS expression in microglia and (b) and suppressed NO production ($p < 0.001$). (b) The reduction in NO by TPCA-1 did not translate into reduced LDH levels ($p > 0.05$). Data are presented as mean from four independent experiments ± SD, p values were calculated using a one-way ANOVA followed by a Tukey post-hoc test. AOI= area of interest.

#### 6.2.3.2 Givinostat, a histone deacetylase inhibitor, decreases NO production and ablates cytotoxicity and rescues axons and myelin

To explore this further we used an alternative approach using Givinostat (a class I and II histone deacetylase (HDAC) inhibitor to modulate the transcriptional activity of NF-κB (Ghizzoni, Haisma, Maarsingh, & Dekker, 2011; Leoni et al., 2005). Myelinating cultures were primed with 100 ng/ml GM-CSF (24-30 DIV) and then treated with 100 ng/ml IFN-γ and 25 ng/ml TNF-α for 72h in the presence or absence of 1 μM Givinostat. Givinostat reduced NO production induced by IFN-γ + TNF-α in primed cultures by 75 % (GM-CSF + IFN-γ + TNF-α + DMSO = 48.07 ± 18.09 μM vs GM-CSF + IFN-γ + TNF-α + Givinostat = 15.82 ± 10.49 μM, $p < 0.001$), an effect accompanied by a >65 % decrease in cytotoxicity (Percentage maximal LDH: GM-CSF + IFN-γ + TNF-α + DMSO, 46.86 ± 16.79 %; GM-CSF + IFN-γ + TNF-α + Givinostat, 21.35 ± 5.794 %; untreated + DMSO, 8.921 ± 3.871% ) (Figure 6.10).

However, this protective effect was not paralleled by a corresponding decrease in the percentage of $CD45^+$ microglia expressing iNOS in GM-CSF primed cultures. Despite that, in unprimed cultures, Givinostat decreased the percentage of microglia expressing iNOS in cultures treated with IFN-γ and TNF-α by 75% (IFN-γ + TNF-α + DMSO, 67.30 ± 10.85 %; IFN-γ + TNF-α + Givinostat, 17.39 ± 4.211 %, $p < 0.001$) but there was no significant effect in GM-CSF primed cultures (Figure 6.9, 6.10). However, although there was also no significant change in the absolute number of $CD45^+$ cells expressing iNOS, it appeared the relative intensity of CD45 immunoreactivity was reduced as evidenced by the present of more $iNOS^{bright}CD45^{dim}$ cells (Figure 6.9). Givinostat itself exhibited no inherent toxicity (Figure 6.10 c).

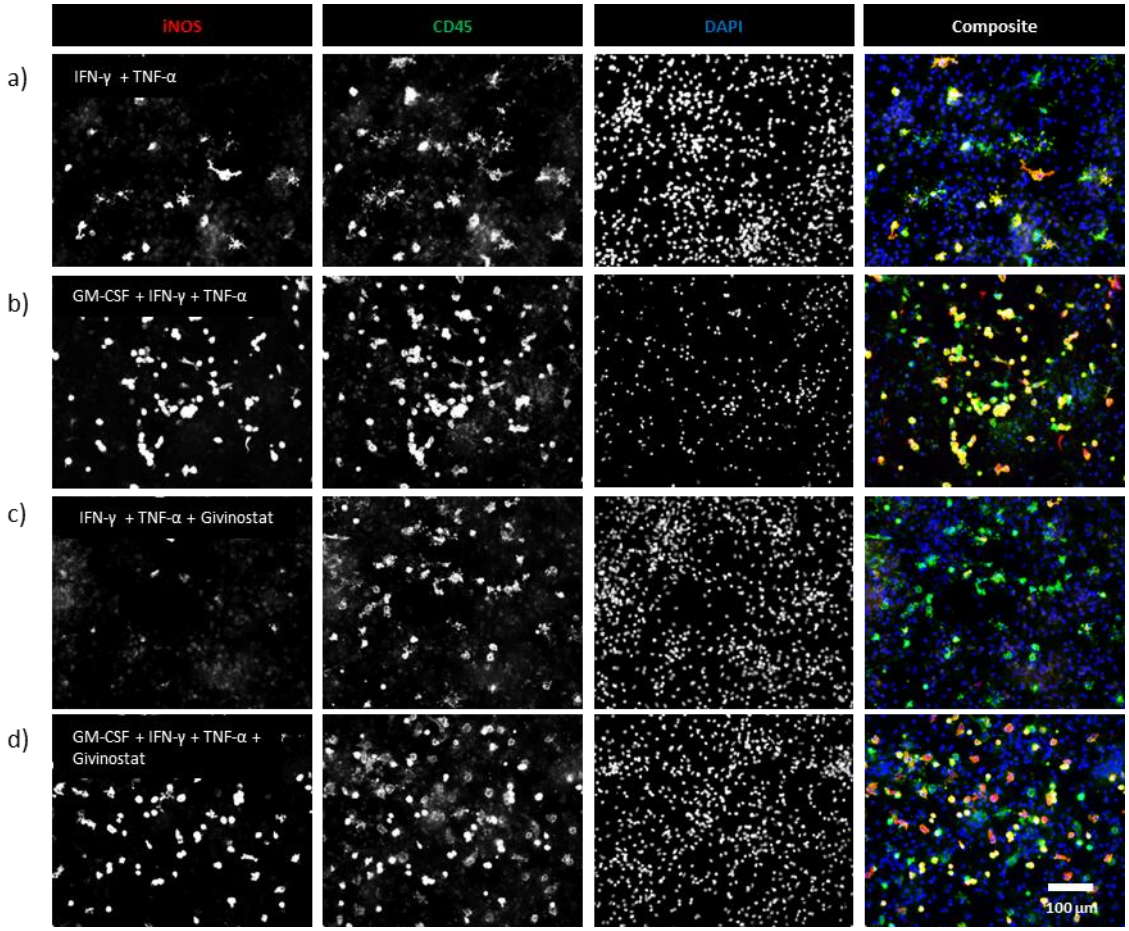


**Figure 6.9. Representative images of mouse myelinating cultures primed with GM-CSF and treated with IFN-γ and TNF-α in the presence of Givinostat.** Mouse myelinating cultures were primed or unprimed with 100 ng/ml GM-CSF from 24 to 30 DIV, followed by treatment with 100 ng/ml IFN-γ and 25 ng/ml TNF-α in the presence of 1 µM Givinostat (histone deacetylase inhibitor) or DMSO (vehicle control) for 72h. Images were acquired at 33 DIV. (a, c) Givinostat decreased the iNOS immune reactivity in microglia after treatment with IFN-γ and TNF-α ($p < 0.001$). (b, d) Givinostat had no obvious effect on iNOS staining in GM-CSF primed cultures treated with IFN-γ and TNF-α in, but appeared to decrease the intensity of CD45 staining.

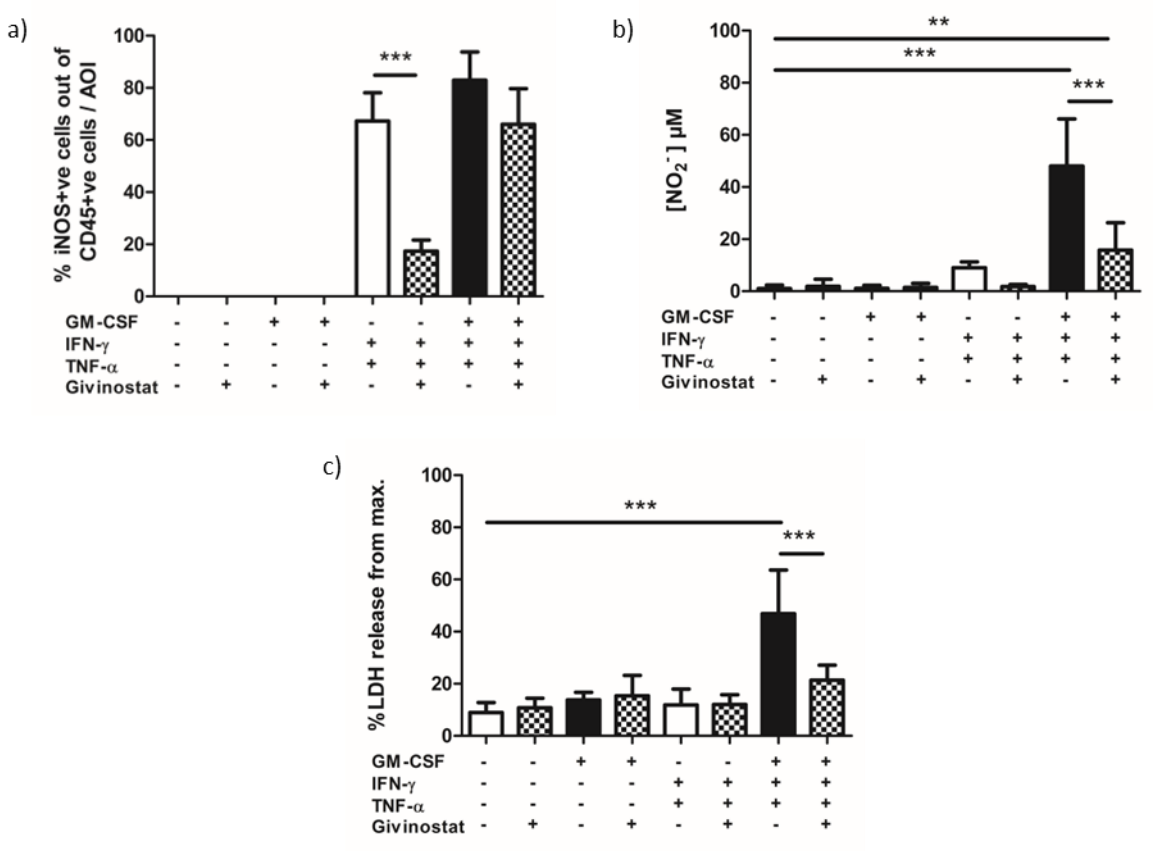


**Figure 6.10. Givinostat, a histone deacetylase inhibitor, decreases NO production and abrogates cytotoxicity.** Mouse myelinating cultures were primed or unprimed with 100 ng/ml GM-CSF from 24 to 30 DIV, followed by treatment with 100 ng/ml IFN-γ and 25 ng/ml TNF-α in the presence of 1 µM Givinostat (histone deacetylase inhibitor) or DMSO (vehicle control) for 72h. Images were acquired and supernatants were assessed at 33 DIV. (a) Givinostat decreased the percentage of microglia expressing iNOS after treatment with IFN-γ and TNF-α ($p < 0.001$); the decrease in the percentage of iNOS expressing microglia in cultures primed with GM-CSF followed by IFN-γ and TNF-α treatment did not reach statistical significance ($p< 0.05$). (b) NO production was greatly suppressed when primed with 100 ng/ml GM-CSF followed by 100 ng/ml IFN-γ and 25 ng/ml TNF-α in the presence of Givinostat ($p< 0.001$). (b) The reduction in NO by Givinostat was translated into a decrease of LDH release back to background levels ($p< 0.001$). Data is presented as mean from four independent experiments ± SD, p values were calculated using a one-way ANOVA followed by a Tukey post-hoc test. AOI= area of interest.

Adding Givinostat simultaneously with IFN-γ and TNF-α after GM-CSF priming rescued axons and myelin. Givinostat impeded the loss of neurites (GM-CSF + IFN-γ + TNF-α + Givinostat = 74.81 ± 2.872 % vs GM-CSF + IFN-γ + TNF-α + DMSO = 60.38 ± 5.302 %, p< 0.001; untreated DMSO = 74.1 ± 2.582 %, p> 0.05) and myelin (GM-CSF + IFN-γ + TNF-α + Givinostat = 5.517 ± 3.289 % vs GM-CSF + IFN-γ + TNF-α + DMSO = 1.67 ± 1.349 %, p< 0.05; untreated DMSO = 3.355 ± 1.982 %, p> 0.05) (Figure 6.11 a, b). GM-CSF priming combined with IFN-γ and TNF-α treatment induced extensive loss of SMI31 (axons) and MBP (myelin) immunoreactivity (Figure 6.11 c). This was negated by Givinostat as demonstrated by the intact neurofilament (SMI31) and MBP staining in Figure 6.11 d.

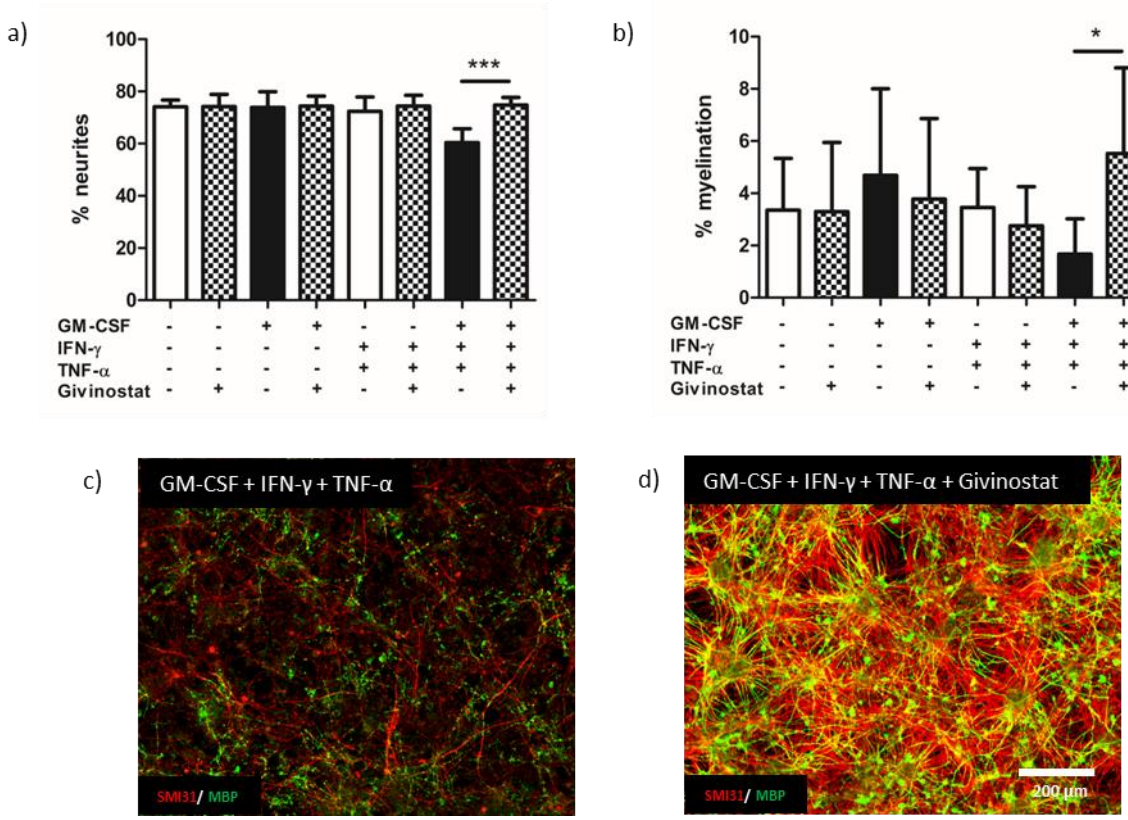


**Figure 6.11. Givinostat rescues axons and myelin from the combinatorial effect of GM-CSF priming and IFN-γ and TNF-α.** Mouse myelinating cultures were primed or unprimed with 100 ng/ml GM-CSF from 24 to 30 DIV, followed by treatment with 100 ng/ml IFN-γ and 25 ng/ml TNF-α in the presence of 1 µM Givinostat (histone deacetylase inhibitor) or DMSO (vehicle control) for 72h. Images were acquired at 33 DIV. (a, b) Givinostat maintained axonal density and myelin when added together with IFN-γ and TNF-α on GM-CSF primed cultures (p< 0.001, 0.05). Representative images of cultures primed with 100 ng/ml GM-CSF from 24 to 30 DIV, followed by 100 ng/ml IFN-γ and 25 ng/ml TNF-α in the (c) absence and (d) in the presence of Givinostat 1 µM for 72h.

Myelin and axons were visualized with anti-MBP (myelin basic protein, green) and anti-neurofilament (SMI31, red) antibodies, respectively. To be noted that the (c) loss of neurofilament and MBP immune reactivity mediated by GM-CSF priming followed by IFN-γ and TNF-α treatment was rescued by (d) Givinostat. Data are presented as mean from five independent experiments ± SD, p values were calculated using a one-way ANOVA followed by a Tukey post-hoc test

## 6.3 Discussion

Data presented in previous chapters demonstrated that priming myelinated cultures with GM-CSF sensitises for TNF-α and IFN-γ to mediate iNOS-dependent demyelination and axonal loss. It was assumed a linear relationship existed between these effects i.e. expression of iNOS results in production of NO which in turn causes cell death. However, data presented in this chapter demonstrate the situation is more complex as high levels of NO production do not necessarily result in cell death. This first became apparent from experiments investigating how duration of priming influenced iNOS expression by microglia, NO production and cytotoxicity. These revealed that priming with GM-CSF for 72 hours was sufficient to induce high levels of nitric oxide production, but this did not result in significant cell death as assessed by LDH release. This was not due to production of too little nitric oxide, as extending priming for a further three days resulted in extensive cell death in the absence of any additional effect on nitric oxide production. This was not simply due to insensitivity of the Griess assay to detect levels above those detected after 72 hours because the upper limit of the assay is 100 μM. This suggests GM-CSF priming mediates two distinct effects that act synergistically but differ in their kinetics. The first occurs within 72 hours and senisitises for the synergy of TNF-α and IFN-γ to induce iNOS in microglia. The second is far slower (> 3 days) but once established acts to increase the susceptibility of CNS cells to damage by nitric oxide.

The first phase, induction of iNOS, seems to require cooperative signalling between TNF-α and IFN-γ on microglia. This may be explained by the fact that the murine *Nos2* promoter contains both an IFN response region and binding sites for NF-κB (Kleinert et al., 2010). Optimal expression of *Nos2* is dependent on co-operative signalling involving the transcription complex ISGF3 (comprised of

STAT1, STAT2, and IRF9) and NF-kB (Farlik et al., 2010). We propose that in CNS myelinating cultures and the CNS in general, IFN-γ signals through the STAT/IRF3 pathway to generate the ISGF3 complex which, in combination with NF-κB, provides optimal transcription activation of *Nos2* in microglia. However the question remains as to how GM-CSF signalling sensitises for TNF-α and IFN-γ to induce this effect.

As cooperation between TNF/NF-κB and IFN/ISGF pathways is required for maximal transcriptional induction of *Nos2* it is logical to ask whether GM-CSF priming up-regulates expression of any key components of these pathways, or alternatively down-regulates expression of intrinsic inhibitors. To address this question a gene microarray study is underway to investigate the individual and combinatory effects of TNF-α and IFN-γ in GM-CSF primed versus unprimed myelinated cultures. This study is not yet complete but preliminary analysis indicates priming with GM-CSF increases TNF-α and IFN-γ receptor expression (*Tnfsfr1a,* +2.42 fold; *Infr1,* +1.34 fold; *Ifnr2,* +1.34 fold – after six days) However, in isolation, this does not up-regulate expression of *Nos2*. This hypothesis will require validation, ideally using human microglia to dissect the relative importance of different components of each pathway.

As NF-κB signalling plays a major role in regulating induction of iNOS we investigated its importance using NF-κB inhibitors with different modes of action. TCPA-1 is a potent IkB kinase inhibitor that prevents NF-κB activation and its translocation to the nucleus (Podolin et al., 2005). TPCA-1 completely abolished cytokine-mediated induction of nitric oxide confirming this is NF-κB dependent. However, abolition of iNOS activity had no significant effect on cytokine-mediated cytotoxicity in GM-CSF primed cultures. We propose this dichotomy reflects the functional pleiotropy of TNFR and NF-κB signalling pathways in the CNS. NF-kB is a multifaceted transcription factor that mediates pro-survival functions as well as activating pro-inflammatory signalling cascades (Mincheva et al., 2011), whilst TNF-α signalling via TNFR1 is pro-inflammatory and via TNFR2 induces cell death (Wajant & Siegmund, 2019). Global inhibition of NF-κB in GM-CSF primed cultures suppressed induction of iNOS but uncovered an alternative mechanism by which inhibtion of NF-κB renders primed cultures

more susceptible to the effects of cytokine mediated cytotoxicity; an observation underlining the pro-survival role of this transcription factor in the nervous system (Dresselhaus & Meffert, 2019; Stone et al., 2017).

Intriguingly, this was not observed when NF-κB activity was down-regulated (rather than being completely inhibited) when we used Givinostat, a class I and II histone deacetylase (HDAC) inhibitor, to modulate the transcriptional activity of NF-κB (Christensen et al., 2014; Ghizzoni et al., 2011; Leoni et al., 2005). Givinostat reduced cytokine induced nitric oxide production in primed cultures to a level at which it was unable to mediate cell death, axonal loss and demyelination. Indeed, reviewing data collected during this study indicates a threshold exists that NO production must exceed if it is to induce extensive cell death in myelinated cultures. Sensitivity to nitric oxide mediated cytotoxicity could be investigated in more detail using $NO^{\cdot}$ donors to define its dependence on concentration and time of exposure in GM-CSF primed v unprimed cultures. Together, our data suggest that less NO is necessary to induce damage in GM-CSF primed cultures. However, one cannot be sure Givinostat mediated effects were entirely NF-κB specific as in addition to non-histone effects such changing the acylation status of p65, HDAC inhibitors also mediate epigenetic effects may modulate *Nos2* transcription in microglia (Kaminska et al., 2016; Leus, Zwinderman, & Dekker, 2016).

Mining data obtained from the microarray study may provide further insight of temporal dependence and relationship between *Nos2* expression, accumulation of iNOS, NO production and sensitivity to cytokine-mediated cytotoxicity. Our current data show three days priming with GM-CSF is sufficient to induce a significant increase in NO production, although six days of priming is required to induce a significant increase in numbers of $iNOS^{+}$ microglia. This apparent discrepancy may be due to differences in the relative sensitivity of the methods used to assay these effects in myelinating cultures. One way forward would be to explore regulation of *Nos2* and iNOS expression in enriched primary microglial cultures as these respond in the same way as microglia in myelinating culture (see Chapter 5).

However, this approach is not appropriate to investigate why extended priming is required to increase susceptibility of cultures to cytokine-mediated tissue damage because mechanisms such as increased substrate availability and/or decreased expression of intrinsic antioxidants might be important, and these might be absent in enriched microglial cultures. To add another layer of complexity, there is also evidence NO can itself regulate NF-κB activity. Enhanced NO production increases the activities of the transcription factors p53 and nuclear factor κB (NF-κB) in several models of disease-associated inflammation suggesting that above a certain threshold, this may establish a positive feedback loop (Nakazawa et al., 2017; Shinozaki et al., 2014). Conversely, other groups have shown NO mediated s-nitrosylation will inhibit NF-κB signaling (Dela Torre, Schroeder, Punzalan, & Kuo, 1999; Marshall & Stamler, 2001).

The key question however is whether or not my observations are relevant to the pathogenesis of MS. This can only be answered by a more detailed analysis of GM-CSF availability in patients and possibly, by examining its effects in human iPSC derived and/or organoid culture models. A recent study reported the concentration of GM-CSF in the CSF of MS patients is 990.6 ± 517.9 pg/ml (Khaibullin et al., 2017). This is at the lower end of the concentration range required for GM-CSF priming to enhance NO production in myelinated cultures. Assuming local concentrations within the CNS will be significantly higher, we propose T and/or B cell derived GM-CSF will prime microglia in developing lesions to exacerbate NO dependent tissue damage (Imitola et al., 2018; Parajuli et al., 2012; Ponomarev et al., 2007; Rasouli et al., 2015). If this turns out indeed to be the case it will support the concept GM-CSF is an important therapeutic target in MS.

# Chapter 7

## General discussion

# 7 General discussion

GM-CSF is a key T cell derived cytokine necessary to induce tissue damage and neurological deficits in EAE (Codarri et al., 2011; McQualter et al., 2001; Ponomarev et al., 2007). The presence of increased GM-CSF levels and GM-CSF producing T cells in the CSF of MS patients suggest it plays a similar role in the immunopathogenesis of MS (Carrieri et al., 1998; Rasouli et al., 2015). Yet little is known about the mechanisms by which GM-CSF mediates tissue damage during these diseases. Microglia are the only cell expressing functional GM-CSFR in the CNS parenchyma and were therefore a logical starting point to investigate how GM-CSF contributes to lesion development in EAE (Y. Zhang et al., 2014).

Our current view is EAE is initiated by reactivation of CNS autoantigen-specific effector memory T cells in the CNS (Wekerle, Linington, Lassmann, & Meyermann, 1986), in particular a subset of T cell that produce GM-CSF. Reactivation may involve contributions from a number of different antigen presenting cells (Waisman & Johann, 2018), but it is probable microglia play an important early role in this reactivation event (Sosa et al., 2013). To investigate down stream effects of T cell derived GM-CSF within the CNS we used myelinating cultures, a model of the CNS that is devoid of immune input from the periphery. This provided insight into the role of GM-CSF in the pathogenesis of EAE and possibly more importantly, additional data confirming its significance as a potential therapeutic target in MS.

The first important observation was that GM-CSF had no detrimental effect on neurites, oligodendrocytes or myelin in this culture system, despite inducing a marked microglial response characterised by an increase in microglial density and “activation” as defined by a change from a ramified to rounded morphology. This led us to speculate GM-CSF primes microglia to contribute to lesion development, a concept supported by data from an RNAseq study of the effects of this cytokine on myelinated cultures and other studies (Davis et al., 1994; Kettenmann et al., 2011; Zrzavy et al., 2017a). GM-CSF induced a transcriptional fingerprint dominated by up-regulation of genes associated with microglia. Intriguingly these included genes with immunomodulatory and homeostatic functions raising the possibility GM–CSF may also support responses that limit inflammatory damage in the CNS. One of these was *Clec10a* which

encodes Mgl1 a C-type lectin that can induce apoptosis of $CD4^+$ T cells (Ilarregui et al., 2019). Intriguingly *Clec10a* is most highly expressed during recovery from EAE, and *Clec10a* "knock-out" mice show an exacerbated disease course (Ilarregui et al., 2019). The same research group also reported its human homologue (MGL) is expressed on "anti-inflammatory" M2-like microglia *in vitro* and by microglia in active and chronic active MS lesions. Observations that led the authors to conclude MGL is a microglial anti-inflammatory and immunomodulatory marker that may act in part by inducing apoptosis of encephalitogenic T cells (Ilarregui et al., 2019). However our RNAseq data demonstrated *Clec10a* is just one of a number of C-type lectins and other cell surface receptors up regulated by GM-CSF. Functionally, this translated into a generalised increase in phagocytosis by microglia. This too may be interpreted as a beneficial response as clearance of myelin debris enhances remyelination in the CNS (Adams & Lloyd, 1997; Bijland et al., 2019; Chung et al., 2014; Grajchen et al., 2018; Kotter et al., 2006; Lampron et al., 2015; Miron et al., 2013). However, this effect might be a doubled-edged sword as phagocytosis of myelin debris and the concomitant up-regulation of molecules involved in antigen presentation an processing could contribute to epitope spreading and reactivation of encephalitogenic T cells (H. Li et al., 2011; Ong et al., 1999; Re et al., 2002). Moreover, in some experimental models GM-CSF primes myeloid cells, including microglia, to target myelin and exacerbate tissue damage (Codarri et al., 2011; Ousman & David, 2001; Ponomarev et al., 2007). Whatever the final outcome of GM-CSF priming, its effects are long-lasting rather than transient, as demonstrated by the maintenance of Dectin2 expression by microglia after GM-CSF withdrawal. If we would extrapolate this to targeting GM-CSF as a treatment for MS, we would predict the effects of neutralizing GM-CSF would not be immediate but would ultimately suppress development of new lesions. This of course pre-supposes GM-CSF primes microglia to induce tissue damage.

We reasoned that any contribution of GM-CSF to lesion development would involve other cytokines derived initially from reactivated encephalitogenic T cells infiltrating the CNS. We considered IFN-γ and TNF-α as prime candidates as these pro-inflammatory cytokines are not only produced by encephalitogenic CD4+ T cells, but are also cytotoxic under certain conditions and implicated as

key contributors to lesion pathogenesis in MS (Beck et al., 1988; Montgomery & Bowers, 2012; Patel & Balabanov, 2012). We therefore investigated whether GM-CSF can enhance the cytopathic effect of IFN-γ and TNF-α in myelinated cultures. GM-CSF priming markedly sensitised for IFN-γ and TNF-α to induce cellular damage, an effect that was dependent on NO production by iNOS. This priming effect was mediated by physiologic concentrations of GM-CSF and was long lasting as it was still functional 12 days after GM-CSF was withdrawn. Such a dramatic and long-lasting effect was not anticipated, reinforcing our view priming by T cell derived GM-CSF mediates a long-lasting effect that exacerbates cytokine mediated cytotoxicity in EAE. Figure 7.1 summarizes how T cell derived GM-CSF and microglia cooperate to mediate tissue damage in EAE and potentially MS. We reasoned this effect might play a wider role in neuroinflammatory diseases other than EAE and MS, and preliminary data obtained using two TLR agonists suggest this is the case, as GM-CSF also enhance induction of iNOS by LPS (activates TLR4) or and poly I:C (activates TLR3). Observations suggesting GM-CSF might contribute to the immunopathogenesis of bacterial and viral infections of the nervous system.

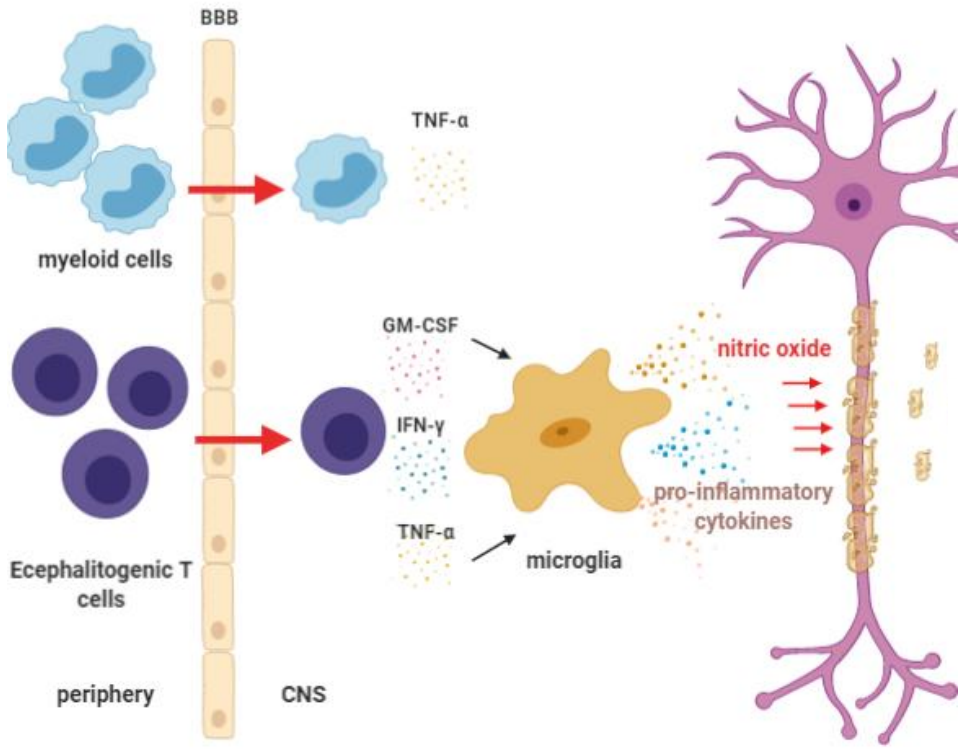


**Figure 7.1.Potential mechanism through which GM-CSF contributes to tissue damage during neuroflammation.** Encephalitogenic T cells of different phenotypes cross the blood-brain barrier and enter the CNS. Once in the CNS, they get reactivated and produce a plethora of cytokines including GM-CSF, IFN-γ and TNF-α. GM-CSF primes microglia which will synergise with IFN-γ and TNF-α to produce nitric oxide and other pro-inflammatory factors resulting in myelin and axonal destruction. Peripheral myeloid cells are also an important source of TNF-α. We do not exclude that invading myeloid cells mediate tissue damage via the same mechanism. Diagram created in www.Biorender.

A key question that remains unanswered is how does GM-CSF sensitise for cytokine mediated cytotoxicity? Mining of the transcriptional data generated by IFN-γ and TNF-α individually or combined on GM-CSF primed cultures is currently underway and we hope will address this point. We are looking to extract candidates involved in iNOS regulation, such as components of the NF-κb pathway or transcription factors and test them functionally. We already know from our experiments that NF-κb signalling contributes to NO production and should investigate the iNOS promoter for any additive transcription factor binding sites and epigenetic modifications. As demonstrated by our experiments using Givinostat, it is possible that an epigenetic component plays a role in GM-

CSF exacerbation of cytotoxicity. Additionally, we plan on investigating if any of the pathways involved in downstream GM-CSF signalling is hyperactivated in microglia and contributes to iNOS induction by IFN-γ and TNF-α. An elegant and efficient way to investigate pathway signalling in this context would be detection of phosphorylation status of key pathway components by HTRF (homogenous time resolved fluorescence).

In the context of EAE and by extrapolation MS, it is logical to anticipate GM-CSF will also affect infiltrating myeloid cells. On this note, we should investigate the behaviour of microglia versus peripheral phagocytes in the CNS. One possible approach would be to co-culture bone-marrow derived macrophages in myelinating cultures. Peripheral myeloid cells can be harvested from a fluorescent transgenic mouse strain to distinguish them from resident microglia expressing an alternative fluorophore, a strategy that would enable these cell populations to be analysed independently after recovery by FACSorting.

Our data all point towards GM-CSF signalling being a prime therapeutic target in MS, but this will require demonstrating human microglia respond in a similar manner to GM-CSF, ideally in a cellular context that replicates that of the CNS. A logical option would be to use iPSC-derived human organoids (Lancaster et al., 2013). It was recently demonstrated that microglia develop within cerebral organoids and mimic the transcriptome and inflammatory responses of adult human microglia isolated from post-mortem brain tissue (Ormel et al., 2018). It is important to note that despite extensive homology between mouse and human *NOS2*, there are known differences in their regulation and *NOS2* promoter is not as readily inducible as the rodent gene (X. Zhang et al., 1996). Multiple groups reporting mouse microglia are more robust at producing NO when stimulated with LPS, poly I:C, or IFN-γ than human microglia. This reduction in NO productions was attributed to post-transcriptional repression of human iNOS expression (Hoos et al., 2014; Schneemann & Schoeden, 2007; Taylor et al., 1998). It is crucial that we determine if our *in vitro* mouse model can be replicated using human cells to determine if GM-CSF priming exacerbates cytokine mediated tissue damage via NO or other effector pathways.

To summarise, we demonstrated that GM-CSF alone did not induce tissue damage in myelinating cultures, but prime microglia to up-regulate pathways

that enable them to respond more rapidly to infectious or autoimmune insults to the CNS. We demonstrated that GM-CSF priming sensitises for IFN-γ and TNF-α to induce tissue damage. Our data revealed that iNOS is central to the cytopathic mechanism underlying the synergism between GM-CSF, IFN-γ and TNF-α.

# Chapter 8

## Appendices

# 8 Appendices

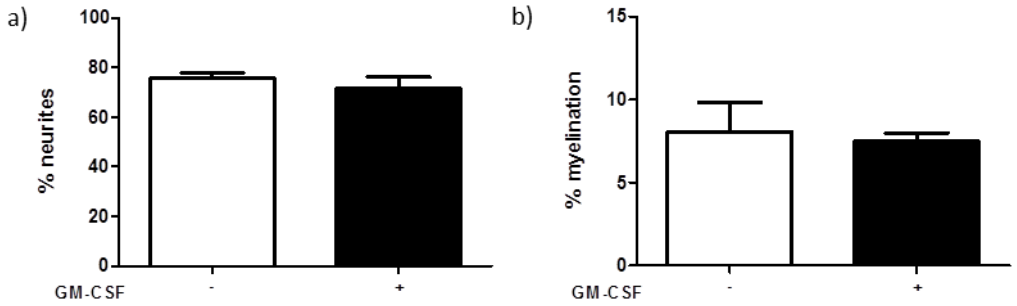


**Figure 8.1. Neurite density and myelination rates for cultures used for RNAseq**. (a, b) Representative images of myelinating cultures grown in the presence or absence of 100 ng/ml GM-CSF for 24 hours at 24 DIV. Myelin and axons were visualized with anti-MOG (clone Z2, green) and anti-neurofilament (SMI31, red) antibodies, respectively. GM-CSF had no effect on either (c) neurite out growth ($p = 0.119$) or (d) myelination ($p= 0.6340$). Data presented as mean ± SD from three independent experiments, p values were calculated using a paired Student's t test.

| Gene | logFC RNASeq | Naïve | Score 0 | Score 3 | FC N > 0 | FC N > 3 |
|---|---|---|---|---|---|---|
| *1600014C10Rik* | 0.425288487 | 0.583571 | 10.2629 | 4.91603 | 17.58638 | 8.424048 |
| *4921529L05Rik* | 3.179896731 | | | | | |
| *Adap2* | -0.920374697 | 27.2771 | 48.2882 | 55.3445 | 1.770283 | 2.028973 |
| *Adora3* | 2.247250035 | 28.0441 | 13.8053 | 17.3854 | -2.0314 | -1.61308 |
| *Amica1* | 2.444388821 | 0 | 0.029807 | 0.027211 | infinite | infinite |
| *Arc* | 0.423204343 | | | | | |
| *B3gnt7* | 0.914677926 | 3.9919 | 0.028059 | 5.12399 | -142.268 | 1.283597 |
| *Batf* | 1.775251132 | 0.099525 | 0.406073 | 5.5251 | 4.080127 | 55.51492 |
| *Bcl2a1a* | 3.941623235 | 16.6624 | 8.65976 | 73.5233 | -1.92412 | 4.412528 |
| *Bcl2a1d* | 2.223197837 | 80.1245 | 26.4127 | 167.545 | -3.03356 | 2.091058 |
| *Bcl6* | -0.443995992 | 3.12684 | 2.49123 | 4.928 | -1.25514 | 1.576032 |
| *Ccl12* | 3.407990043 | 25.9769 | 276.906 | 509.311 | 10.6597 | 19.6063 |
| *Ccl2* | 1.869521628 | 61.9474 | 298.591 | 744.025 | 4.820073 | 12.01059 |
| *Ccl6* | 3.406591217 | 13.2708 | 16.088 | 17.4417 | 1.212286 | 1.314292 |
| *Ccl7* | 2.051569371 | 2.96498 | 52.7327 | 162.455 | 17.78518 | 54.79126 |
| *Ccl8* | 1.378187256 | 0 | 8.2806 | 11.5751 | infinite | infinite |
| *Ccl9* | 1.696582232 | 10.4173 | 10.0864 | 10.6506 | -1.03281 | 1.022395 |
| *Ccr1* | 4.488449156 | 0.277042 | 1.73301 | 1.8853 | 6.255405 | 6.805105 |
| *Ccr2* | 4.806610325 | 1.83556 | 5.86154 | 0.668425 | 3.193325 | 0.364153 |
| *Ccr5* | 1.65372468 | 72.0889 | 91.7798 | 69.3395 | 1.273147 | 0.961861 |
| *Cd180* | -1.211599841 | 170.795 | 227.798 | 330.329 | 1.333751 | 1.934067 |
| *Cd274* | 1.456670427 | 2.8585 | 11.9118 | 52.5628 | 4.167151 | 18.38825 |
| *Cd300lf* | 3.583926492 | 0.095474 | 10.8326 | 26.9979 | 113.461 | 282.7769 |
| *Cd33* | 1.314299656 | 97.2793 | 61.1371 | 89.44 | -1.59117 | -1.08765 |
| *Cd36* | -0.864602996 | 27.9931 | 30.936 | 32.4598 | 1.105129 | 1.159564 |
| *Cd5l* | -1.245089011 | | | | | |
| *Cd72* | -1.170235475 | 0.205112 | 11.717 | 18.7842 | 57.12489 | 91.58021 |
| *Cd74* | 2.852683038 | 128.26 | 414.505 | 5588.54 | 3.231756 | 43.57196 |
| *Cdh1* | 3.088046576 | 0 | 0 | 0 | | |
| *Cebpb* | 0.825605176 | 4.77128 | 3.52617 | 4.41126 | -1.35311 | -1.08161 |
| *Ch25h* | 1.08798765 | 0.059023 | 1.61844 | 0.927778 | 27.42073 | 15.71906 |
| *Cish* | 0.88735608 | 0.136084 | 0.103376 | 8.08138 | -1.3164 | 59.38523 |
| *Clec10a* | 2.923191689 | 0 | 0.105738 | 1.39718 | infinite | infinite |
| *Clec4n* | 3.448354214 | 0.145703 | 0.074094 | 0.132967 | -1.96645 | -1.09578 |
| *Clec5a* | 1.306924312 | 9.37289 | 4.43799 | 4.38969 | -2.11197 | -2.13521 |
| *Clec7a* | 1.329270782 | 11.7387 | 7.89232 | 10.8496 | -1.48736 | -1.08195 |
| *Cmah* | -2.234445493 | | | | | |
| *Coro1a* | 0.49312775 | 48.3746 | 85.1655 | 85.5162 | 1.760542 | 1.767791 |
| *Coro2a* | 0.821955173 | 1.60836 | 2.80073 | 7.01817 | 1.741358 | 4.363557 |
| *Csf2rb* | 1.992224715 | 13.9275 | 27.0485 | 66.8757 | 1.942093 | 4.801702 |
| *Ctla2b* | -1.524023304 | 0.873828 | 2.13922 | 13.8873 | 2.448102 | 15.89249 |
| *Ctsc* | 1.068894164 | 31.1 | 103.811 | 152.206 | 3.337974 | 4.894084 |

**Figure 8.2 a. Figure showing a comparison between the genes differentially expressed by GM-CSF in our RNAseq ordered alphabetically and genes differentially expressed by microglia isolated from mice with EAE (compared to naive controls.** Microglia were isolated from animals with an EAE score of 0

and 3 and naive controls ) (Lewis et al., 2014). Additionally, we determined that fold changes (FC) between naive and diseased animals at both scores.

| Gene | logFC RNASeq | Naïve | Score 0 | Score 3 | FC N > 0 | FC N > 3 |
|---|---|---|---|---|---|---|
| *Cxcr3* | -1.964620856 | 0 | 0 | 0 | 0 | 0 |
| *Cysltr1* | 1.054881859 | 5.68534 | 9.22133 | 1.41551 | 1.621949 | 0.248975 |
| *Dna2* | 0.727031873 | 0 | 2.851 | 2.48169 | infinite | infinite |
| *Egr1* | 0.75302589 | 1320.49 | 616.344 | 1027.61 | -2.14246 | -1.28501 |
| *Egr2* | 1.380003145 | 31.2444 | 12.4268 | 13.74 | -2.51428 | -2.27397 |
| *Emilin2* | 0.854264619 | 3.48064 | 2.83696 | 1.57531 | -1.22689 | -2.2095 |
| *F13a1* | 1.961582213 | 4.77911 | 2.20644 | 0.249967 | -2.16598 | -19.119 |
| *Fam167b* | 2.199644785 | 4.31383 | 1.14718 | 6.07325 | -3.76038 | 1.407856 |
| *Fcgr2b* | 1.34149901 | 30.873 | 42.8612 | 92.8834 | 1.388307 | 3.008564 |
| *Fcgr3* | 1.007673273 | 50.8869 | 69.5479 | 150.609 | 1.366715 | 2.959681 |
| *Fcgr4* | -1.124353619 | 11.9041 | 18.3115 | 30.3176 | 1.538252 | 2.54682 |
| *Fcrl1* | -2.018170852 | 59.8317 | 2.46678 | 1.57479 | -24.255 | -37.9934 |
| *Fos* | 0.557385457 | 861.069 | 301.48 | 494.798 | -2.85614 | -1.74024 |
| *Fyb* | -1.064468102 | 40.3642 | 23.5297 | 92.6527 | 0.582935 | 2.295418 |
| *G530011O06Rik* | -1.350345515 | 122.329 | 125.061 | 72.6091 | 1.022333 | -1.68476 |
| *Gapt* | 1.793630473 | 0 | 0 | 0.033294 | 0 | infinite |
| *Gbp3* | 0.762525772 | 1.74148 | 7.18808 | 22.6078 | 4.12757 | 12.98195 |
| *Gbp4* | 2.162368155 | 0.062783 | 13.6178 | 21.2776 | 216.903 | 338.9076 |
| *Gbp7* | 1.049414412 | 0.983936 | 14.852 | 37.081 | 15.09448 | 37.68639 |
| *Gbp9* | 1.06642005 | 2.97637 | 11.7633 | 25.2309 | 3.95223 | 8.477071 |
| *Gm14005* | 1.548786203 | 0 | 7.7198 | 0.666055 | infinite | infinite |
| *Gm16194* | 4.365003604 | | | | | |
| *Gm1966* | 3.504852291 | | | | | |
| *Gm26714* | -1.26969578 | | | | | |
| *Gm29291* | -2.026077522 | | | | | |
| *Gm6377* | -1.946979896 | 0.203855 | 0 | 0.35324 | 0 | 1.7328 |
| *Gm8995* | 1.193092908 | | | | | |
| *Gpr160* | 1.040465754 | 4.33939 | 3.72916 | 10.641 | -1.16364 | 2.452188 |
| *Gpr34* | -1.018719048 | 62.1008 | 27.4296 | 28.483 | -2.26401 | -2.18028 |
| *Gpr34* | -1.018719048 | 62.1008 | 27.4296 | 28.483 | -2.26401 | -2.18028 |
| *H2-DMa* | 1.0833675 | 85.1039 | 220.198 | 385.116 | 2.587402 | 4.525245 |
| *H2-DMb2* | 2.412916112 | 0.608294 | 13.6496 | 4.76781 | 22.43915 | 7.838003 |
| *Hmga2* | -1.42599572 | | | | | |
| *I830077J02Rik* | 1.654689274 | 5.98037 | 11.4438 | 26.2566 | 1.913561 | 4.390464 |
| *Ier3* | 0.828143355 | 17.6602 | 26.6413 | 69.5641 | 1.50855 | 3.939032 |
| *Ighm* | -0.949042006 | | | | | |
| *Il18rap* | 1.734669014 | 0 | 0.117992 | 0.053861 | infinite | infinite |
| *Il1rl2* | 1.831374044 | 0.956162 | 1.62775 | 1.23735 | 1.702379 | 1.29408 |
| *Il4ra* | 1.204609441 | 13.8997 | 24.5017 | 24.2729 | 1.76275 | 1.746289 |
| *Itgal* | 0.974565867 | 0.143783 | 10.6171 | 20.3234 | 73.84114 | 141.3477 |
| *Itgax* | 2.294974078 | 0.034434 | 1.86258 | 7.1715 | 54.09068 | 208.2656 |
| *Kcnj2* | -0.610306507 | 7.1266 | 6.1277 | 6.97751 | -1.16301 | -1.02137 |

**Figure 7.8 b. Continued.**

| Gene | logFC RNASeq | Naïve | Score 0 | Score 3 | FC N > 0 | FC N > 3 |
|---|---|---|---|---|---|---|
| *Kynu* | 2.352608038 | 0 | 0 | 2.20173 | 0 | infinite |
| *Lsr* | 1.079997122 | 0.150942 | 0.420597 | 0.139521 | 2.786481 | 0.924335 |
| ***Mgl2*** | 6.545282515 | | | | | |
| *Mmp12* | 1.664112593 | | | | | |
| *Mmp13* | 2.47058141 | | | | | |
| *Mmp8* | 4.481159722 | 3.95425 | 6.00475 | 0.572733 | 1.518556 | 0.14484 |
| *Mpeg1* | -0.800784486 | 80.0409 | 144.034 | 208.649 | 1.799505 | 2.60678 |
| *Mrc1* | 1.778685815 | 4.03943 | 0.67387 | 0.983436 | -5.99438 | -4.10747 |
| *Ms4a4a* | 1.278668275 | | | | | |
| *Ms4a7* | -1.072208526 | 0 | 0.890233 | 0.096371 | infinite | infinite |
| *Msr1* | 1.419889846 | 1.13266 | 1.2859 | 1.96613 | 1.135292 | 1.735852 |
| *Nabp1* | 0.844596414 | | | | | |
| *P2ry13* | 1.024009565 | 184.627 | 92.2896 | 83.2047 | -2.00052 | -2.21895 |
| *P2ry14* | 1.45170909 | 0 | 0.085163 | 4.7139 | infinite | infinite |
| *Pik3ap1* | -0.925640822 | 8.96075 | 20.1702 | 27.41 | 2.25095 | 3.058896 |
| *Pik3r6* | 1.328436996 | 2.08906 | 2.44332 | 8.97576 | 1.169579 | 4.296554 |
| *Pilra* | 1.80643162 | 2.64851 | 3.4639 | 24.7802 | 1.307867 | 9.35628 |
| *Pilrb2* | 3.050372323 | 0.000336 | 0.330321 | 0.4665 | 982.2125 | 1387.142 |
| *Pim1* | 0.780398588 | 0.562423 | 2.58793 | 7.9187 | 4.601394 | 14.07962 |
| *Pkd2l1* | -1.112199988 | | | | | |
| *Plaur* | 1.087021952 | 3.68901 | 1.09487 | 3.0436 | -3.36936 | -1.21205 |
| *Plxna4os1* | -2.350420189 | | | | | |
| *Pnp* | 0.867773697 | 12.7765 | 36.691 | 24.3634 | 2.871757 | 1.906892 |
| *Prr15* | 1.458988871 | | | | | |
| *Pstpip2* | 1.284738382 | 0 | 1.5052 | 4.27067 | infinite | infinite |
| *Ptgs1* | 1.220168414 | 144.804 | 97.5304 | 122.651 | -1.48471 | -1.18062 |
| *Pyhin1* | 1.265975562 | 0.220197 | 3.40325 | 16.4294 | 15.45548 | 74.61228 |
| *Rab44* | 3.323055825 | 0 | 0.068181 | 1.49558 | Infinite | infinite |
| *Rasgrp4* | 1.828526493 | 2.48796 | 3.32488 | 0.42126 | 1.336388 | -5.906 |
| *Rgs14* | 0.819441689 | 0.833469 | 0.187534 | 0.998566 | 0.225004 | 1.198084 |
| *Rhoh* | 1.373597766 | 7.90655 | 5.63407 | 5.35485 | -1.40335 | -1.47652 |
| *Rmrp* | -3.999815987 | 12.771 | 29.9718 | 5.473 | 2.346864 | -2.33346 |
| *Runx1* | 1.141073608 | 24.2346 | 22.092 | 24.4064 | 0.911589 | 1.007089 |
| *Scel* | 1.655480637 | | | | | |
| *Scimp* | 2.973231189 | | | | | |
| *Serpina3f* | 3.028042799 | 0 | 1.9999 | 19.61 | | infinite |
| *Serpinb6b* | -1.346470985 | 0.040411 | 0 | 0.747102 | 0 | 18.48754 |
| *Siglecf* | 2.333866561 | | | | | |
| *Sla* | 1.749324245 | 30.1503 | 18.3596 | 53.0993 | -1.64221 | 1.761153 |
| *Slamf9* | -1.107234685 | 13.884 | 5.76675 | 26.488 | -2.4076 | 1.907808 |
| *Slc16a10* | -1.080087919 | 4.05554 | 2.63609 | 6.9574 | -1.53847 | 1.71553 |
| *Slc1a5* | 0.863831038 | 0.051838 | 1.75738 | 6.17998 | 33.90139 | 119.2172 |

**Figure 8.2 c. Continued.**

| Gene | logFC RNASeq | Naïve | Score 0 | Score 3 | FC N > 0 | FC N > 3 |
|---|---|---|---|---|---|---|
| *Slco4a1* | 0.900685007 | 1.39714 | 2.24758 | 2.85741 | 1.608701 | 2.045185 |
| *Slfn2* | 1.214450439 | 8.4619 | 11.139 | 22.9359 | 1.316371 | 2.710491 |
| *Slfn3* | 1.919752727 | 0 | 0.093576 | 0.115576 | infinite | infinite |
| *Snx2* | 0.390796274 | 11.6906 | 11.2468 | 19.1575 | -1.03946 | 1.63871 |
| *Spint1* | 3.981624006 | 12.527 | 50.7422 | 43.6408 | 4.050627 | 3.483739 |
| *St14* | 1.011414257 | 0.586628 | 0.941992 | 2.40741 | 1.605774 | 4.10381 |
| *Tfec* | 3.199487073 | 0.042527 | 0 | 0.039312 | 0 | -1.08177 |
| *Tifab* | 1.957254753 | 11.7869 | 7.40001 | 11.6317 | -1.59282 | -1.01334 |
| *Tnfsf8* | 3.222936517 | 0.098604 | 0.166433 | 3.97962 | 1.687895 | 40.35966 |
| *Trem1* | 3.747021001 | 0 | 0.30808 | 0 | infinite | 0 |
| *Trim30c* | 2.090532863 | | | | | |

**Figure 8.2 d. Continued.**

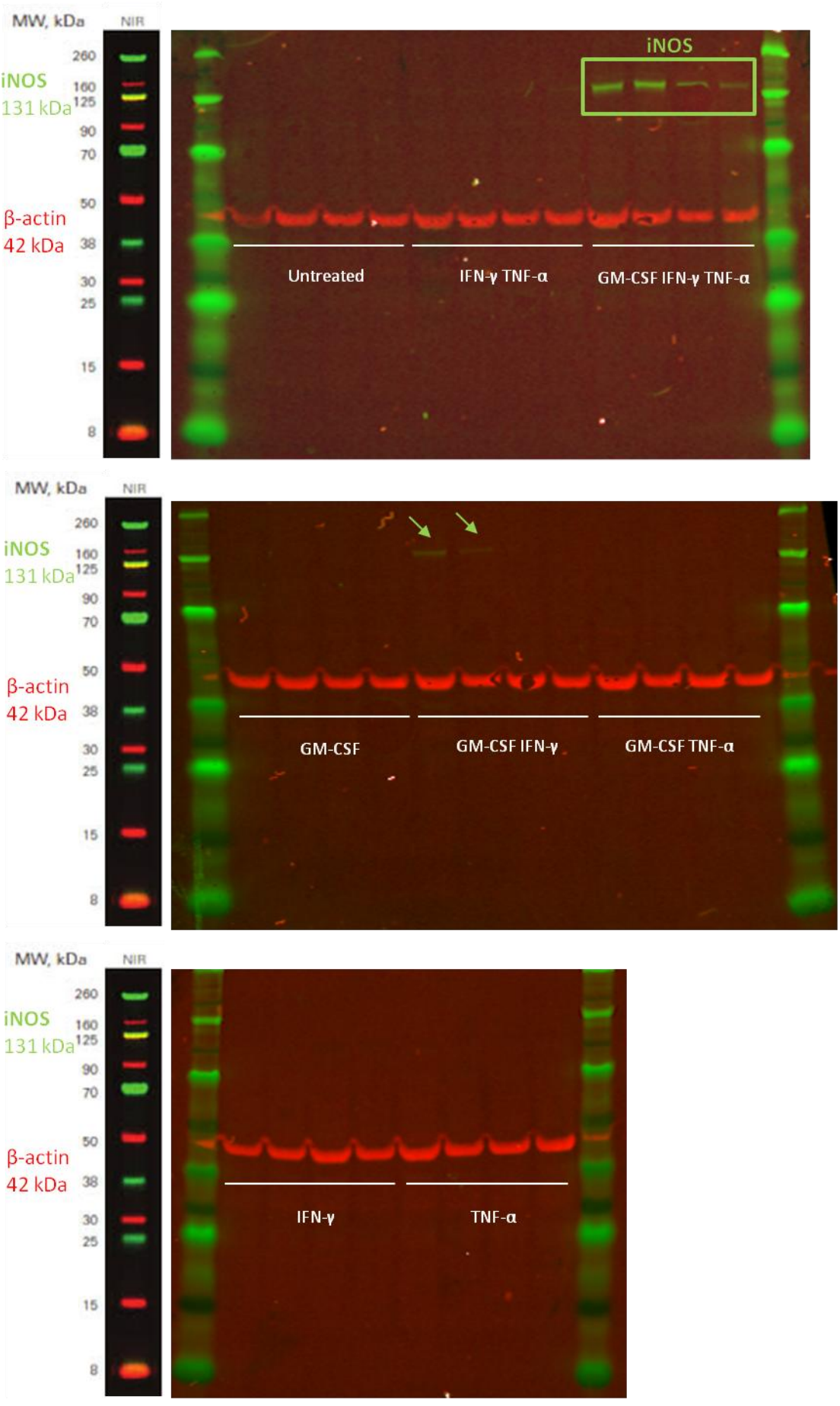


**Figure 8.3. Raw western blot data, relative intensity found in figure 5.3.**

Experiment performed four times. Equal amount of protein was loaded for each sample. Near Infrared detection system (Li-cor) was used to visualise the membranes (ß-actin in red- housekeeping protein; iNOS in green) standard exposure settings used to scan the membranes. No red marker on the protein ladder - The Odyssey blocking buffer blocked the protein marker in the red channel (common problem according to the Li-cor company representative).

# References

Adams, D. H., & Lloyd, A. R. (1997). Chemokines: Leucocyte recruitment and activation cytokines. *Lancet*. https://doi.org/10.1016/S0140-6736(96)07524-1

Ajami, B., Bennett, J. L., Krieger, C., Tetzlaff, W., & Rossi, F. M. V. (2007). Local self-renewal can sustain CNS microglia maintenance and function throughout adult life. *Nature Neuroscience*. https://doi.org/10.1038/nn2014

Akassoglou, K., Bauer, J., Kassiotis, G., Pasparakis, M., Lassmann, H., Kollias, G., & Probert, L. (1998). Oligodendrocyte apoptosis and primary demyelination induced by local TNF/p55TNF receptor signaling in the central nervous system of transgenic mice: Models for multiple sclerosis with primary oligodendrogliopathy. *American Journal of Pathology*. https://doi.org/10.1016/S0002-9440(10)65622-2

Alvord, E. C., Driscoll, B. F., & Kies, M. W. (1982). LARGE SUBPIAL PLAQUES OF DEMYELINATION IN EXPERIMENTAL ALLERGIC ENCEPHALOMYELITIS IN THE GUINEA PIG. *Journal of Neuropathology and Experimental Neurology*. https://doi.org/10.1097/00005072-198205000-00017

Aram, J., Francis, A., Tanasescu, R., & Constantinescu, C. S. (2019). Granulocyte-Macrophage Colony-Stimulating Factor as a Therapeutic Target in Multiple Sclerosis. *Neurology and Therapy*. https://doi.org/10.1007/s40120-018-0120-1

Baldwin, G. C., Benveniste, E. N., Chung, G. Y., Gasson, J. C., & Golde, D. W. (1993). Identification and characterization of a high-affinity granulocyte-macrophage colony-stimulating factor receptor on primary rat oligodendrocytes. *Blood*.

Bar-Or, A., Fawaz, L., Fan, B., Darlington, P. J., Rieger, A., Ghorayeb, C., … Smith, C. H. (2010). Abnormal B-cell cytokine responses a trigger of T-cell-mediated disease in MS? *Annals of Neurology*. https://doi.org/10.1002/ana.21939

Becher, B., Durell, B. G., & Noelle, R. J. (2003). IL-23 produced by CNS-resident cells controls T cell encephalitogenicity during the effector phase of experimental autoimmune encephalomyelitis. *Journal of Clinical Investigation*. https://doi.org/10.1172/JCI200319079

Becher, B., Spath, S., & Goverman, J. (2017). Cytokine networks in neuroinflammation. *Nature Reviews Immunology*. https://doi.org/10.1038/nri.2016.123

Becher, B., Tugues, S., & Greter, M. (2016). GM-CSF: From Growth Factor to Central Mediator of Tissue Inflammation. *Immunity*.

https://doi.org/10.1016/j.immuni.2016.10.026

Beck, J., Rondot, P., Catinot, L., Falcoff, E., Kirchner, H., & Wietzerbin, J. (1988). Increased production of interferon gamma and tumor necrosis factor precedes clinical manifestation in multiple sclerosis: Do cytokines trigger off exacerbations? *Acta Neurologica Scandinavica*. https://doi.org/10.1111/j.1600-0404.1988.tb03663.x

Beckman, J. S., Beckman, T. W., Chen, J., Marshall, P. A., & Freeman, B. A. (1990). Apparent hydroxyl radical production by peroxynitrite: Implications for endothelial injury from nitric oxide and superoxide. *Proceedings of the National Academy of Sciences of the United States of America*. https://doi.org/10.1073/pnas.87.4.1620

Behrens, F., Tak, P. P., Østergaard, M., Stoilov, R., Wiland, P., Huizinga, T. W., … Burkhardt, H. (2015). MOR103, a human monoclonal antibody to granulocyte - Macrophage colony-stimulating factor, in the treatment of patients with moderate rheumatoid arthritis: Results of a phase Ib/IIa randomised, double-blind, placebo-controlled, dose-escalation trial. *Annals of the Rheumatic Diseases*. https://doi.org/10.1136/annrheumdis-2013-204816

Bennett, M. L., Bennett, F. C., Liddelow, S. A., Ajami, B., Zamanian, J. L., Fernhoff, N. B., … Barres, B. A. (2016). New tools for studying microglia in the mouse and human CNS. *Proceedings of the National Academy of Sciences*. https://doi.org/10.1073/pnas.1525528113

Bettelli, E., Pagany, M., Weiner, H. L., Linington, C., Sobel, R. A., & Kuchroo, V. K. (2003). Myelin oligodendrocyte glycoprotein-specific T cell receptor transgenic mice develop spontaneous autoimmune optic neuritis. *Journal of Experimental Medicine*. https://doi.org/10.1084/jem.20021603

Bijland, S., Thomson, G., Euston, M., Michail, K., Thümmler, K., Mücklisch, S., … Edgar, J. M. (2019). An in vitro model for studying CNS white matter: Functional properties and experimental approaches. *F1000Research*. https://doi.org/10.12688/f1000research.16802.1

Bizzozero, O. A., Dejesus, G., & Howard, T. A. (2004). Exposure of rat optic nerves to nitric oxide causes protein S-nitrosation and myelin decompaction. *Neurochemical Research*. https://doi.org/10.1023/B:NERE.0000035802.27087.16

Breij, E. C. W., Brink, B. P., Veerhuis, R., Van Den Berg, C., Vloet, R., Yan, R., … Bö, L. (2008). Homogeneity of active demyelinating lesions in established multiple sclerosis. *Annals of Neurology*. https://doi.org/10.1002/ana.21311

Brettschneider, J., Toledo, J. B., van Deerlin, V. M., Elman, L., McCluskey, L., Lee, V. M. Y., & Trojanowski, J. Q. (2012). Microglial activation correlates with disease progression and upper motor neuron clinical symptoms in amyotrophic lateral sclerosis. *PLoS ONE*.

https://doi.org/10.1371/journal.pone.0039216

Brown, G. D., Herre, J., Williams, D. L., Willment, J. A., Marshall, A. S. J., & Gordon, S. (2003). Dectin-1 Mediates the Biological Effects of β-Glucans. *The Journal of Experimental Medicine*. https://doi.org/10.1084/jem.20021890

Brown, G. D., Willment, J. A., & Whitehead, L. (2018). C-type lectins in immunity and homeostasis. *Nature Reviews Immunology*. https://doi.org/10.1038/s41577-018-0004-8

Broxmeyer, H. E. (1991). CD45 cell surface antigens are linked to stimulation of early human myeloid progenitor cells by interleukin 3 (IL-3), granulocyte/macrophage colony-stimulating factor (GM-CSF), a GM-CSF/IL- 3 fusion protein, and mast cell growth factor (a c-kit ligand). *Journal of Experimental Medicine*. https://doi.org/10.1084/jem.174.2.447

Brück, W. (2005). The pathology of multiple sclerosis is the result of focal inflammatory demyelination with axonal damage. *Journal of Neurology*. https://doi.org/10.1007/s00415-005-5002-7

Bryant-Hudson, K. M., & Carr, D. J. J. (2012). PD-L1-expressing dendritic cells contribute to viral resistance during acute HSV-1 infection. *Clinical and Developmental Immunology*. https://doi.org/10.1155/2012/924619

Burgess, A. W., Camakaris, J., & Metcalf, D. (1977). Purification and properties of colony stimulating factor from mouse lung conditioned medium. *Journal of Biological Chemistry*.

Burmester, G. R., Weinblatt, M. E., McInnes, I. B., Porter, D., Barbarash, O., Vatutin, M., … Magrini, F. (2013). Efficacy and safety of mavrilimumab in subjects with rheumatoid arthritis. *Annals of the Rheumatic Diseases*. https://doi.org/10.1136/annrheumdis-2012-202450

Butovsky, O., Landa, G., Kunis, G., Ziv, Y., Avidan, H., Greenberg, N., … Schwartz, M. (2006). Induction and blockage of oligodendrogenesis by differently activated microglia in an animal model of multiple sclerosis. *Journal of Clinical Investigation*. https://doi.org/10.1172/JCI26836

Campbell, S. J., Meier, U., Mardiguian, S., Jiang, Y., Littleton, E. T., Bristow, A., … Anthony, D. C. (2010). Sickness behaviour is induced by a peripheral CXC-chemokine also expressed in Multiple Sclerosis and EAE. *Brain, Behavior, and Immunity*. https://doi.org/10.1016/j.bbi.2010.01.011

Carr, P. D., Gustin, S. E., Church, A. P., Murphy, J. M., Ford, S. C., Mann, D. A., … Young, I. G. (2001). Structure of the complete extracellular domain of the common β subunit of the human GM-CSF, IL-3, and IL-5 receptors reveals a novel dimer configuration. *Cell*. https://doi.org/10.1016/S0092-8674(01)00213-6

Carrieri, P. B., Provitera, V., De Rosa, T., Tartaglia, G., Gorga, F., & Perrella, O. (1998). Profile of cerebrospinal fluid and serum cytokines in patients with relapsing-remitting multiple sclerosis: A correlation with clinical activity. *Immunopharmacology and Immunotoxicology*. https://doi.org/10.3109/08923979809034820

Chandran, S., Hunt, D., Joannides, A., Zhao, C., Compston, A., & Franklin, R. J. M. (2008). Myelin repair: The role of stem and precursor cells in multiple sclerosis. *Philosophical Transactions of the Royal Society B: Biological Sciences*. https://doi.org/10.1098/rstb.2006.2019

Chen, G., Kim, Y. H., Li, H., Luo, H., Liu, D. L., Zhang, Z. J., … Ji, R. R. (2017). PD-L1 inhibits acute and chronic pain by suppressing nociceptive neuron activity via PD-1. *Nature Neuroscience*. https://doi.org/10.1038/nn.4571

Chiffoleau, E. (2018). C-type lectin-like receptors as emerging orchestrators of sterile inflammation represent potential therapeutic targets. *Frontiers in Immunology*. https://doi.org/10.3389/fimmu.2018.00227

Chitu, V., Gokhan, Ş., Nandi, S., Mehler, M. F., & Stanley, E. R. (2016). Emerging Roles for CSF-1 Receptor and its Ligands in the Nervous System. *Trends in Neurosciences*. https://doi.org/10.1016/j.tins.2016.03.005

Chitu, V., & Stanley, E. R. (2017). Regulation of Embryonic and Postnatal Development by the CSF-1 Receptor. In *Current Topics in Developmental Biology*. https://doi.org/10.1016/bs.ctdb.2016.10.004

Choi, B. Y., Kim, J. H., Kho, A. R., Kim, I. Y., Lee, S. H., Lee, B. E., … Suh, S. W. (2015). Inhibition of NADPH oxidase activation reduces EAE-induced white matter damage in mice. *Journal of Neuroinflammation*. https://doi.org/10.1186/s12974-015-0325-5

Choi, S. R., Howell, O. W., Carassiti, D., Magliozzi, R., Gveric, D., Muraro, P. A., … Reynolds, R. (2012). Meningeal inflammation plays a role in the pathology of primary progressive multiple sclerosis. *Brain*. https://doi.org/10.1093/brain/aws189

Chopra, S., Overall, C. M., & Dufour, A. (2019). Matrix metalloproteinases in the CNS: interferons get nervous. *Cellular and Molecular Life Sciences*. https://doi.org/10.1007/s00018-019-03171-9

Christensen, D. P., Gysemans, C., Lundh, M., Dahllöf, M. S., Noesgaard, D., Schmidt, S. F., … Mandrup-Poulsen, T. (2014). Lysine deacetylase inhibition prevents diabetes by chromatin-independent immunoregulation and β-cell protection. *Proceedings of the National Academy of Sciences of the United States of America*. https://doi.org/10.1073/pnas.1320850111

Chu, Y., Jin, X., Parada, I., Pesic, A., Stevens, B., Barres, B., & Prince, D. A. (2010). Enhanced synaptic connectivity and epilepsy in C1q knockout mice. *Proceedings of the National Academy of Sciences of the United States of*

*America*. https://doi.org/10.1073/pnas.0913449107

Chung, J., Kim, M. H., Yoon, Y. J., Kim, K. H., Park, S. R., & Choi, B. H. (2014). Effects of granulocyte colony-stimulating factor and granulocyte-macrophage colony-stimulating factor on glial scar formation after spinal cord injury in rats. *Journal of Neurosurgery: Spine*. https://doi.org/10.3171/2014.8.SPINE131090

Ciccarelli, O. (2019). Multiple sclerosis in 2018: new therapies and biomarkers. *The Lancet Neurology*. https://doi.org/10.1016/S1474-4422(18)30455-1

Ciotti, J. R., & Cross, A. H. (2018). Disease-Modifying Treatment in Progressive Multiple Sclerosis. *Current Treatment Options in Neurology*. https://doi.org/10.1007/s11940-018-0496-3

Codarri, L., Gyülvészii, G., Tosevski, V., Hesske, L., Fontana, A., Magnenat, L., … Becher, B. (2011). RORγ3t drives production of the cytokine GM-CSF in helper T cells, which is essential for the effector phase of autoimmune neuroinflammation. *Nature Immunology*. https://doi.org/10.1038/ni.2027

Coleman, D. L., Chodakewitz, J. A., Bartiss, A. H., & Mellors, J. W. (1988). Granulocyte-macrophage colony-stimulating factor enhances selective effector functions of tissue-derived macrophages. *Blood*.

Confavreux, C., Vukusic, S., Moreau, T., & Adeleine, P. (2000). Relapses and progression of disability in multiple sclerosis. *New England Journal of Medicine*. https://doi.org/10.1056/NEJM200011163432001

Constantinescu, C. S., Asher, A., Fryze, W., Kozubski, W., Wagner, F., Aram, J., … Radue, E. W. (2015). Randomized phase 1b trial of MOR103, a human antibody to GM-CSF, in multiple sclerosis. *Neurology: Neuroimmunology and NeuroInflammation*. https://doi.org/10.1212/NXI.0000000000000117

Constantinescu, C. S., Farooqi, N., O'Brien, K., & Gran, B. (2011). Experimental autoimmune encephalomyelitis (EAE) as a model for multiple sclerosis (MS). *British Journal of Pharmacology*. https://doi.org/10.1111/j.1476-5381.2011.01302.x

Conti, A., Miscusi, M., Cardali, S., Germanò, A., Suzuki, H., Cuzzocrea, S., & Tomasello, F. (2007). Nitric oxide in the injured spinal cord: Synthases cross-talk, oxidative stress and inflammation. *Brain Research Reviews*. https://doi.org/10.1016/j.brainresrev.2007.01.013

Coombe, D. R. (2008). Biological implications of glycosaminoglycan interactions with haemopoietic cytokines. *Immunology and Cell Biology*. https://doi.org/10.1038/icb.2008.49

Davis, E. J., Foster, T. D., & Thomas, W. E. (1994). Cellular forms and functions of brain microglia. *Brain Research Bulletin*. https://doi.org/10.1016/0361-

9230(94)90189-9

Dela Torre, A., Schroeder, R. A., Punzalan, C., & Kuo, P. C. (1999). Endotoxin-mediated S-nitrosylation of p50 alters NF-κB-dependent gene transcription in ANA-1 murine macrophages. *Journal of Immunology*.

Delgado, M. (2003). Inhibition of interferon (IFN) γ-induced Jak-STAT1 activation in microglia by vasoactive intestinal peptide. Inhibitory effect on CD40, IFN-induced protein-10, and inducible nitric-oxide synthase expression. *Journal of Biological Chemistry*. https://doi.org/10.1074/jbc.M303199200

Denda-Nagai, K., Aida, S., Saba, K., Suzuki, K., Moriyama, S., Oo-puthinan, S., … Irimura, T. (2010). Distribution and function of macrophage galactose-type C-type lectin 2 (MGL2/CD301b): Efficient uptake and presentation of glycosylated antigens by dendritic cells. *Journal of Biological Chemistry*. https://doi.org/10.1074/jbc.M110.113613

Dendrou, C. A., Fugger, L., & Friese, M. A. (2015). Immunopathology of MS. *Nature Reviews Immunology*. https://doi.org/10.1038/nri3871

Desai, R. A., & Smith, K. J. (2017). Experimental autoimmune encephalomyelitis from a tissue energy perspective. *F1000Research*. https://doi.org/10.12688/f1000research.11839.1

Di Filippo, M., De Iure, A., Giampà, C., Chiasserini, D., Tozzi, A., Orvietani, P. L., … Calabresi, P. (2016). Persistent activation of microglia and NADPH drive hippocampal dysfunction in experimental multiple sclerosis. *Scientific Reports*. https://doi.org/10.1038/srep20926

Dirksen, U., Hattenhorst, U., Schneider, P., Schroten, H., Göbel, U., Böcking, A., … Burdach, S. (1998). Defective expression of granulocyte-macrophage colony-stimulating factor/interleukin-3/interleukin-5 receptor common ß chain in children with acute myeloid leukemia associated with respiratory failure. *Blood*.

Dresselhaus, E. C., & Meffert, M. K. (2019). Cellular specificity of NF-κB function in the nervous system. *Frontiers in Immunology*. https://doi.org/10.3389/fimmu.2019.01043

Dror Michaelson, M., Bieri, P. L., Mehler, M. F., Xu, H., Arezzo, J. C., Pollard, J. W., & Kessler, J. A. (1996). CSF-1 deficiency in mice results in abnormal brain development. *Development*.

Drummond, R. A., Saijo, S., Iwakura, Y., & Brown, G. D. (2011). The role of Syk/CARD9 coupled C-type lectins in antifungal immunity. *European Journal of Immunology*. https://doi.org/10.1002/eji.201041252

Duncker, P. C., Stoolman, J. S., Huber, A. K., & Segal, B. M. (2018). GM-CSF Promotes Chronic Disability in Experimental Autoimmune Encephalomyelitis

by Altering the Composition of Central Nervous System–Infiltrating Cells, but Is Dispensable for Disease Induction. *The Journal of Immunology*. https://doi.org/10.4049/jimmunol.1701484

Elmore, M. R. P., Najafi, A. R., Koike, M. A., Dagher, N. N., Spangenberg, E. E., Rice, R. A., … Green, K. N. (2014). Colony-stimulating factor 1 receptor signaling is necessary for microglia viability, unmasking a microglia progenitor cell in the adult brain. *Neuron*. https://doi.org/10.1016/j.neuron.2014.02.040

Erblich, B., Zhu, L., Etgen, A. M., Dobrenis, K., & Pollard, J. W. (2011). Absence of colony stimulation factor-1 receptor results in loss of microglia, disrupted brain development and olfactory deficits. *PLoS ONE*. https://doi.org/10.1371/journal.pone.0026317

Esen, N., & Kielian, T. (2007). Effects of low dose GM-CSF on microglial inflammatory profiles to diverse pathogen-associated molecular patterns (PAMPs). *Journal of Neuroinflammation*. https://doi.org/10.1186/1742-2094-4-10

Faissner, S., Plemel, J. R., Gold, R., & Yong, V. W. (2019). Progressive multiple sclerosis: from pathophysiology to therapeutic strategies. *Nature Reviews Drug Discovery*. https://doi.org/10.1038/s41573-019-0035-2

Farlik, M., Reutterer, B., Schindler, C., Greten, F., Vogl, C., Müller, M., & Decker, T. (2010). Nonconventional initiation complex assembly by STAT and NF-κB transcription factors regulates nitric oxide synthase expression. *Immunity*. https://doi.org/10.1016/j.immuni.2010.07.001

Feinberg, H., Jégouzo, S. A. F., Rex, M. J., Drickamer, K., Weis, W. I., & Taylor, M. E. (2017). Mechanism of pathogen recognition by human dectin-2. *Journal of Biological Chemistry*. https://doi.org/10.1074/jbc.M117.799080

Filipovic, R., Jakovcevski, I., & Zecevic, N. (2003). GRO-α and CXCR2 in the human fetal brain and multiple sclerosis lesions. *Developmental Neuroscience*. https://doi.org/10.1159/000072275

Fisniku, L. K., Brex, P. A., Altmann, D. R., Miszkiel, K. A., Benton, C. E., Lanyon, R., … Miller, D. H. (2008). Disability and T2 MRI lesions: A 20-year follow-up of patients with relapse onset of multiple sclerosis. *Brain*. https://doi.org/10.1093/brain/awm329

Fleischmann, J., Golde, D. W., Weisbart, R. H., & Gasson, J. C. (1986). Granulocyte-macrophage colony-stimulating factor enhances phagocytosis of bacteria by human neutrophils. *Blood*.

Forno, G., Bollati Fogolin, M., Oggero, M., Kratje, R., Etcheverrigaray, M., Conradt, H. S., & Nimtz, M. (2004). N- and O-linked carbohydrates and glycosylation site occupancy in recombinant human granulocyte-macrophage colony-stimulating factor secreted by a Chinese hamster ovary cell line.

*European Journal of Biochemistry*. https://doi.org/10.1111/j.1432-1033.2004.03993.x

Frischer, J. M., Bramow, S., Dal-Bianco, A., Lucchinetti, C. F., Rauschka, H., Schmidbauer, M., … Lassmann, H. (2009). The relation between inflammation and neurodegeneration in multiple sclerosis brains. *Brain*. https://doi.org/10.1093/brain/awp070

Frischer, J. M., Weigand, S. D., Guo, Y., Kale, N., Parisi, J. E., Pirko, I., … Lucchinetti, C. F. (2015). Clinical and pathological insights into the dynamic nature of the white matter multiple sclerosis plaque. *Annals of Neurology*. https://doi.org/10.1002/ana.24497

Fünfschilling, U., Supplie, L. M., Mahad, D., Boretius, S., Saab, A. S., Edgar, J., … Nave, K. A. (2012). Glycolytic oligodendrocytes maintain myelin and long-term axonal integrity. *Nature*. https://doi.org/10.1038/nature11007

Galatro, T. F., Holtman, I. R., Lerario, A. M., Vainchtein, I. D., Brouwer, N., Sola, P. R., … Eggen, B. J. L. (2017). Transcriptomic analysis of purified human cortical microglia reveals age-associated changes. *Nature Neuroscience*. https://doi.org/10.1038/nn.4597

Galli, E., Hartmann, F. J., Schreiner, B., Ingelfinger, F., Arvaniti, E., Diebold, M., … Becher, B. (2019). GM-CSF and CXCR4 define a T helper cell signature in multiple sclerosis. *Nature Medicine*. https://doi.org/10.1038/s41591-019-0521-4

Gao, H., Danzi, M. C., Choi, C. S., Taherian, M., Dalby-Hansen, C., Ellman, D. G., … Brambilla, R. (2017). Opposing Functions of Microglial and Macrophagic TNFR2 in the Pathogenesis of Experimental Autoimmune Encephalomyelitis. *Cell Reports*. https://doi.org/10.1016/j.celrep.2016.11.083

Gasson, J. C. (1991). Molecular physiology of granulocyte-macrophage colony-stimulating factor. *Blood*. https://doi.org/10.1182/blood.v77.6.1131.bloodjournal7761131

Gearing, D. P., King, J. A., Gough, N. M., & Nicola, N. A. (1989). Expression cloning of a receptor for human granulocyte-macrophage colony-stimulating factor. *The EMBO Journal*. https://doi.org/10.1002/j.1460-2075.1989.tb08541.x

Gensel, J. C., Wang, Y., Guan, Z., Beckwith, K. A., Braun, K. J., Wei, P., … Popovich, P. G. (2015). Toll-Like Receptors and Dectin-1, a C-Type Lectin Receptor, Trigger Divergent Functions in CNS Macrophages. *Journal of Neuroscience*. https://doi.org/10.1523/jneurosci.0337-15.2015

Geurts, J. J., & Barkhof, F. (2008). Grey matter pathology in multiple sclerosis. *The Lancet Neurology*. https://doi.org/10.1016/S1474-4422(08)70191-1

Ghezzi, L., Cantoni, C., Cignarella, F., Bollman, B., Cross, A. H., Salter, A., … Piccio, L. (2019). T cells producing GM-CSF and IL-13 are enriched in the cerebrospinal fluid of relapsing MS patients. *Multiple Sclerosis Journal*. https://doi.org/10.1177/1352458519852092

Ghizzoni, M., Haisma, H. J., Maarsingh, H., & Dekker, F. J. (2011). Histone acetyltransferases are crucial regulators in NF-κB mediated inflammation. *Drug Discovery Today*. https://doi.org/10.1016/j.drudis.2011.03.009

Gholamzad, M., Ebtekar, M., Ardestani, M. S., Azimi, M., Mahmodi, Z., Mousavi, M. J., & Aslani, S. (2019). A comprehensive review on the treatment approaches of multiple sclerosis: currently and in the future. *Inflammation Research*. https://doi.org/10.1007/s00011-018-1185-0

Gibbons, H. M., & Dragunow, M. (2006). Microglia induce neural cell death via a proximity-dependent mechanism involving nitric oxide. *Brain Research*. https://doi.org/10.1016/j.brainres.2006.02.032

Ginhoux, F., Greter, M., Leboeuf, M., Nandi, S., See, P., Gokhan, S., … Merad, M. (2010). Fate mapping analysis reveals that adult microglia derive from primitive macrophages. *Science*. https://doi.org/10.1126/science.1194637

Ginhoux, F., & Guilliams, M. (2016). Tissue-Resident Macrophage Ontogeny and Homeostasis. *Immunity*. https://doi.org/10.1016/j.immuni.2016.02.024

Gold, R., Linington, C., & Lassmann, H. (2006). Understanding pathogenesis and therapy of multiple sclerosis via animal models: 70 Years of merits and culprits in experimental autoimmune encephalomyelitis research. *Brain*. https://doi.org/10.1093/brain/awl075

Gomez-Nicola, D., Spagnolo, A., Guaza, C., & Nieto-Sampedro, M. (2010). Aggravated experimental autoimmune encephalomyelitis in IL-15 knockout mice. *Experimental Neurology*. https://doi.org/10.1016/j.expneurol.2009.12.034

Gosselin, D., Skola, D., Coufal, N. G., Holtman, I. R., Schlachetzki, J. C. M., Sajti, E., … Glass, C. K. (2017). An environment-dependent transcriptional network specifies human microglia identity. *Science*. https://doi.org/10.1126/science.aal3222

Gough, N. M., Metcalf, D., Gough, J., Grail, D., & Dunn, A. R. (1985). Structure and expression of the mRNA for murine granulocyte-macrophage colony stimulating factor. *The EMBO Journal*. https://doi.org/10.1002/j.1460-2075.1985.tb03678.x

Grajchen, E., Hendriks, J. J. A., & Bogie, J. F. J. (2018). The physiology of foamy phagocytes in multiple sclerosis. *Acta Neuropathologica Communications*. https://doi.org/10.1186/s40478-018-0628-8

Gran, B., O'Brien, K., Fitzgerald, D., & Rostami, A. (2008). Experimental Autoimmune Encephalomyelitis BT - Handbook of Neurochemistry and Molecular Neurobiology: Neuroimmunology. In *Handbook of Neurochemistry and Molecular Neurobiology: Neuroimmunology*. https://doi.org/10.1007/978-0-387-30398-7_16

Greter, M., Helft, J., Chow, A., Hashimoto, D., Mortha, A., Agudo-Cantero, J., … Merad, M. (2012). GM-CSF Controls Nonlymphoid Tissue Dendritic Cell Homeostasis but Is Dispensable for the Differentiation of Inflammatory Dendritic Cells. *Immunity*. https://doi.org/10.1016/j.immuni.2012.03.027

Griffin, J. D., Cannistra, S. A., Demetri, G. D., Ernst, T. J., Kanakura, Y., & Sullivan, R. (1990). The biology of GM-CSF: Regulation of production and interaction with its receptor. *The International Journal of Cell Cloning*. https://doi.org/10.1002/stem.5530080705

Guilliams, M., De Kleer, I., Henri, S., Post, S., Vanhoutte, L., De Prijck, S., … Lambrecht, B. N. (2013). Alveolar macrophages develop from fetal monocytes that differentiate into long-lived cells in the first week of life via GM-CSF. *Journal of Experimental Medicine*. https://doi.org/10.1084/jem.20131199

Gyoneva, S., & Ransohoff, R. M. (2015). Inflammatory reaction after traumatic brain injury: Therapeutic potential of targeting cell-cell communication by chemokines. *Trends in Pharmacological Sciences*. https://doi.org/10.1016/j.tips.2015.04.003

Hafler, D. A., Compston, A., Sawcer, S., Lander, E. S., Daly, M. J., De Jager, P. L., … Hauser, S. L. (2007). Risk alleles for multiple sclerosis identified by a genomewide study. *New England Journal of Medicine*. https://doi.org/10.1056/NEJMoa073493

Hamilton, J. A. (2002). GM-CSF in inflammation and autoimmunity. *Trends in Immunology*. https://doi.org/10.1016/S1471-4906(02)02260-3

Hamilton, J. A. (2015). GM-CSF as a target in inflammatory/autoimmune disease: Current evidence and future therapeutic potential. *Expert Review of Clinical Immunology*. https://doi.org/10.1586/1744666X.2015.1024110

Harbo, H. F., Gold, R., & Tintora, M. (2013). Sex and gender issues in multiple sclerosis. *Therapeutic Advances in Neurological Disorders*. https://doi.org/10.1177/1756285613488434

Harris, R. J., Pettitt, A. R., Schmutz, C., Sherrington, P. D., Zuzel, M., Cawley, J. C., & Griffiths, S. D. (2000). Granuloctye-Macrophage Colony-Stimulating Factor as an Autocrine Survival Factor for Mature Normal and Malignant B Lymphocytes. *The Journal of Immunology*. https://doi.org/10.4049/jimmunol.164.7.3887

Hartmann, F. J., Khademi, M., Aram, J., Ammann, S., Kockum, I.,

Constantinescu, C., … Becher, B. (2014). Multiple sclerosis-associated IL2RA polymorphism controls GM-CSF production in human T H cells. *Nature Communications*. https://doi.org/10.1038/ncomms6056

Hasseldam, H., Rasmussen, R. S., & Johansen, F. F. (2016). Oxidative damage and chemokine production dominate days before immune cell infiltration and EAE disease debut. *Journal of Neuroinflammation*. https://doi.org/10.1186/s12974-016-0707-3

Hauser, S. L., Bar-Or, A., Comi, G., Giovannoni, G., Hartung, H. P., Hemmer, B., … Kappos, L. (2017). Ocrelizumab versus interferon beta-1a in relapsing multiple sclerosis. *New England Journal of Medicine*. https://doi.org/10.1056/NEJMoa1601277

Hauser, Stephen L., Waubant, E., Arnold, D. L., Vollmer, T., Antel, J., Fox, R. J., … Smith, C. H. (2008). B-cell depletion with rituximab in relapsing-remitting multiple sclerosis. *New England Journal of Medicine*. https://doi.org/10.1056/NEJMoa0706383

Hayashida, K., Kitamura, T., Gorman, D. M., Arai, K. I., Yokota, T., & Miyajima, A. (1990a). Molecular cloning of a second subunit of the receptor for human granulocyte-macrophage colony-stimulating factor (GM-CSF): Reconstitution of a high-affinity GM-CSF receptor. *Proceedings of the National Academy of Sciences of the United States of America*. https://doi.org/10.1073/pnas.87.24.9655

Hayashida, K., Kitamura, T., Gorman, D. M., Arai, K., Yokota, T., & Miyajima, A. (1990b). Molecular cloning of a second subunit of the receptor for human granulocyte-macrophage colony-stimulating factor (GM-CSF): reconstitution of a high-affinity GM-CSF receptor. *Proceedings of the National Academy of Sciences*. https://doi.org/10.1073/pnas.87.24.9655

Heppner, F. L., Greter, M., Marino, D., Falsig, J., Raivich, G., Hövelmeyer, N., … Aguzzi, A. (2005). Experimental autoimmune encephalomyelitis repressed by microglial paralysis. *Nature Medicine*. https://doi.org/10.1038/nm1177

Hercus, T. R., Thomas, D., Guthridge, M. A., Ekert, P. G., King-Scott, J., Parker, M. W., & Lopez, A. F. (2009). The granulocyte-macrophage colony-stimulating factor receptor: Linking its structure to cell signaling and its role in disease. *Blood*. https://doi.org/10.1182/blood-2008-12-164004

Hesske, L., Vincenzetti, C., Heikenwalder, M., Prinz, M., Reith, W., Fontana, A., & Suter, T. (2010). Induction of inhibitory central nervous system-derived and stimulatory blood-derived dendritic cells suggests a dual role for granulocyte-macrophage colony-stimulating factor in central nervous system inflammation. *Brain*. https://doi.org/10.1093/brain/awq081

Höftberger, R., Leisser, M., Bauer, J., & Lassmann, H. (2015). Autoimmune encephalitis in humans: how closely does it reflect multiple sclerosis ? *Acta Neuropathologica Communications*. https://doi.org/10.1186/s40478-015-

0260-9

Holtman, I. R., Bsibsi, M., Gerritsen, W. H., Boddeke, H. W. G. M., Eggen, B. J. L., van der Valk, P., … Amor, S. (2017). Identification of highly connected hub genes in the protective response program of human macrophages and microglia activated by alpha B-crystallin. *GLIA*. https://doi.org/10.1002/glia.23104

Hoos, M. D., Vitek, M. P., Ridnour, L. A., Wilson, J., Jansen, M., Everhart, A., … Colton, C. A. (2014). The impact of human and mouse differences in NOS2 gene expression on the brain's redox and immune environment. *Molecular Neurodegeneration*. https://doi.org/10.1186/1750-1326-9-50

Hoshiko, M., Arnoux, I., Avignone, E., Yamamoto, N., & Audinat, E. (2012). Deficiency of the microglial receptor CX3CR1 impairs postnatal functional development of thalamocortical synapses in the barrel cortex. *Journal of Neuroscience*. https://doi.org/10.1523/JNEUROSCI.1167-12.2012

Huang, D. W., Sherman, B. T., & Lempicki, R. A. (2009). Systematic and integrative analysis of large gene lists using DAVID bioinformatics resources. *Nature Protocols*. https://doi.org/10.1038/nprot.2008.211

Huffman Reed, J. A., Rice, W. R., Zsengellér, Z. K., Wert, S. E., Dranoff, G., & Whitsett, J. A. (1997). GM-CSF enhances lung growth and causes alveolar type II epithelial cell hyperplasia in transgenic mice. *American Journal of Physiology - Lung Cellular and Molecular Physiology*. https://doi.org/10.1152/ajplung.1997.273.4.l715

Ilarregui, J. M., Kooij, G., Rodríguez, E., Van Der Pol, S. M. A., Koning, N., Kalay, H., … Van Kooyk, Y. (2019). Macrophage galactose-type lectin (MGL) is induced on M2 microglia and participates in the resolution phase of autoimmune neuroinflammation. *Journal of Neuroinflammation*. https://doi.org/10.1186/s12974-019-1522-4

Imitola, J., Rasouli, J., Watanabe, F., Mahajan, K., Sharan, A. D., Ciric, B., … Rostami, A. (2018). Elevated expression of granulocyte-macrophage colony-stimulating factor receptor in multiple sclerosis lesions. *Journal of Neuroimmunology*. https://doi.org/10.1016/j.jneuroim.2017.12.017

Ito, D., Imai, Y., Ohsawa, K., Nakajima, K., Fukuuchi, Y., & Kohsaka, S. (1998). Microglia-specific localisation of a novel calcium binding protein, Iba1. *Molecular Brain Research*. https://doi.org/10.1016/S0169-328X(98)00040-0

Jiang, Z., Jiang, J. X., & Zhang, G. X. (2014). Macrophages: A double-edged sword in experimental autoimmune encephalomyelitis. *Immunology Letters*. https://doi.org/10.1016/j.imlet.2014.03.006

Jurewicz, A., Matysiak, M., Tybor, K., & Selmaj, K. (2003). TNF-induced death of adult human oligodendrocytes is mediated by c-jun NH2-terminal kinase-3. *Brain*. https://doi.org/10.1093/brain/awg146

Kaminska, B., Mota, M., & Pizzi, M. (2016). Signal transduction and epigenetic mechanisms in the control of microglia activation during neuroinflammation. *Biochimica et Biophysica Acta - Molecular Basis of Disease*. https://doi.org/10.1016/j.bbadis.2015.10.026

Kanazawa, H., Ohsawa, K., Sasaki, Y., Kohsaka, S., & Imai, Y. (2002). Macrophage/microglia-specific protein Iba1 enhances membrane ruffling and Rac activation via phospholipase C-γ-dependent pathway. *Journal of Biological Chemistry*. https://doi.org/10.1074/jbc.M109218200

Kay, A. B., Ying, S., Varney, V., Gaga, M., Durham, S. R., Moqbel, R., … Hamid, Q. (1991). Messenger RNA expression of the cytokine gene cluster, interleukin 3 (IL-3), IL-4, IL-5, and granulocyte/macrophage colony-stimulating factor, in allergen-induced late-phase cutaneous reactions in atopic subjects. *Journal of Experimental Medicine*. https://doi.org/10.1084/jem.173.3.775

Kerschensteiner, M., Stadelmann, C., Buddeberg, B. S., Merkler, D., Bareyre, F. M., Anthony, D. C., … Schwab, M. E. (2004). Targeting Experimental Autoimmune Encephalomyelitis Lesions to a Predetermined Axonal Tract System Allows for Refined Behavioral Testing in an Animal Model of Multiple Sclerosis. *American Journal of Pathology*. https://doi.org/10.1016/S0002-9440(10)63232-4

Kettenmann, H., Hanisch, U.-K., Noda, M., & Verkhratsky, A. (2011). Physiology of Microglia. *Physiological Reviews*. https://doi.org/10.1152/physrev.00011.2010

Khaibullin, T., Ivanova, V., Martynova, E., Cherepnev, G., Khabirov, F., Granatov, E., … Khaiboullina, S. (2017). Elevated levels of proinflammatory cytokines in cerebrospinal fluid of multiple sclerosis patients. *Frontiers in Immunology*. https://doi.org/10.3389/fimmu.2017.00531

Kiyota, T., Machhi, J., Lu, Y., Dyavarshetty, B., Nemati, M., Yokoyama, I., … Gendelman, H. E. (2018). Granulocyte-macrophage colony-stimulating factor neuroprotective activities in Alzheimer's disease mice. *Journal of Neuroimmunology*. https://doi.org/10.1016/j.jneuroim.2018.03.009

Kleinert, H., Art, J., & Pautz, A. (2010). Regulation of the Expression of Inducible Nitric Oxide Synthase. In *Nitric Oxide*. https://doi.org/10.1016/B978-0-12-373866-0.00007-1

Komuczki, J., Tuzlak, S., Friebel, E., Hartwig, T., Spath, S., Rosenstiel, P., … Becher, B. (2019). Fate-Mapping of GM-CSF Expression Identifies a Discrete Subset of Inflammation-Driving T Helper Cells Regulated by Cytokines IL-23 and IL-1β. *Immunity*. https://doi.org/10.1016/j.immuni.2019.04.006

Korin, B., Ben-Shaanan, T. L., Schiller, M., Dubovik, T., Azulay-Debby, H., Boshnak, N. T., … Rolls, A. (2017). High-dimensional, single-cell characterization of the brain's immune compartment. *Nature Neuroscience*.

https://doi.org/10.1038/nn.4610

Kosloski, L. M., Kosmacek, E. A., Olson, K. E., Mosley, R. L., & Gendelman, H. E. (2013). GM-CSF induces neuroprotective and anti-inflammatory responses in 1-methyl-4-phenyl-1,2,3,6-tetrahydropyridine intoxicated mice. *Journal of Neuroimmunology*. https://doi.org/10.1016/j.jneuroim.2013.10.009

Kotter, M. R., Li, W. W., Zhao, C., & Franklin, R. J. M. (2006). Myelin impairs CNS remyelination by inhibiting oligodendrocyte precursor cell differentiation. *Journal of Neuroscience*. https://doi.org/10.1523/JNEUROSCI.2615-05.2006

Krementsov, D. N., Thornton, T. M., Teuscher, C., & Rincon, M. (2013). The Emerging Role of p38 Mitogen-Activated Protein Kinase in Multiple Sclerosis and Its Models. *Molecular and Cellular Biology*. https://doi.org/10.1128/mcb.00688-13

Kumar, A., Alvarez-Croda, D. M., Stoica, B. A., Faden, A. I., & Loane, D. J. (2016). Microglial/Macrophage Polarization Dynamics following Traumatic Brain Injury. *Journal of Neurotrauma*. https://doi.org/10.1089/neu.2015.4268

Kutzelnigg, A., Lucchinetti, C. F., Stadelmann, C., Brück, W., Rauschka, H., Bergmann, M., … Lassmann, H. (2005). Cortical demyelination and diffuse white matter injury in multiple sclerosis. *Brain*. https://doi.org/10.1093/brain/awh641

Lafaille, J. J., Nagashima, K., Katsuki, M., & Tonegawa, S. (1994). High incidence of spontaneous autoimmune encephalomyelitis in immunodeficient anti-myelin basic protein T cell receptor transgenic mice. *Cell*. https://doi.org/10.1016/0092-8674(94)90419-7

Lampron, A., Larochelle, A., Laflamme, N., Préfontaine, P., Plante, M. M., Sánchez, M. G., … Rivest, S. (2015). Inefficient clearance of myelin debris by microglia impairs remyelinating processes. *Journal of Experimental Medicine*. https://doi.org/10.1084/jem.20141656

Lancaster, M. A., Renner, M., Martin, C. A., Wenzel, D., Bicknell, L. S., Hurles, M. E., … Knoblich, J. A. (2013). Cerebral organoids model human brain development and microcephaly. *Nature*. https://doi.org/10.1038/nature12517

Lannes, N., Eppler, E., Etemad, S., Yotovski, P., & Filgueira, L. (2017). Microglia at center stage: A comprehensive review about the versatile and unique residential macrophages of the central nervous system. *Oncotarget*. https://doi.org/10.18632/oncotarget.23106

Lassmann, H. (2014). Multiple sclerosis: Lessons from molecular neuropathology. *Experimental Neurology*. https://doi.org/10.1016/j.expneurol.2013.12.003

Lassmann, H., & Bradl, M. (2017). Multiple sclerosis: experimental models and reality. *Acta Neuropathologica*. https://doi.org/10.1007/s00401-016-1631-4

Lassmann, H., Brück, W., & Lucchinetti, C. F. (2007). The immunopathology of multiple sclerosis: An overview. *Brain Pathology*. https://doi.org/10.1111/j.1750-3639.2007.00064.x

Lebrun-Frenay, C., Kobelt, G., Berg, J., Capsa, D., & Gannedahl, M. (2017). New insights into the burden and costs of multiple sclerosis in Europe: Results for France. *Multiple Sclerosis Journal*. https://doi.org/10.1177/1352458517708125

Lee, Y., Morrison, B. M., Li, Y., Lengacher, S., Farah, M. H., Hoffman, P. N., … Rothstein, J. D. (2012). Oligodendroglia metabolically support axons and contribute to neurodegeneration. *Nature*. https://doi.org/10.1038/nature11314

Lehmann-Horn, K., Kinzel, S., & Weber, M. S. (2017). Deciphering the role of B cells in multiple sclerosis—towards specific targeting of pathogenic function. *International Journal of Molecular Sciences*. https://doi.org/10.3390/ijms18102048

Leoni, F., Fossati, G., Lewis, E. C., Lee, J. K., Porro, G., Pagani, P., … Mascagni, P. (2005). The histone deacetylase inhibitor ITF2357 reduces production of pro-inflammatory cytokines in vitro and systemic inflammation in vivo. *Molecular Medicine*. https://doi.org/10.2119/Molecular

Leus, N. G. J., Zwinderman, M. R. H., & Dekker, F. J. (2016). Histone deacetylase 3 (HDAC 3) as emerging drug target in NF-κB-mediated inflammation. *Current Opinion in Chemical Biology*. https://doi.org/10.1016/j.cbpa.2016.06.019

Levin, L. I., Munger, K. L., Rubertone, M. V., Peck, C. A., Lennette, E. T., Spiegelman, D., & Ascherio, A. (2005). Temporal relationship between elevation of Epstein-Barr virus antibody titers and initial onset of neurological symptoms in multiple sclerosis. *Journal of the American Medical Association*. https://doi.org/10.1001/jama.293.20.2496

LeVine, A. M., Reed, J. A., Kurak, K. E., Cianciolo, E., & Whitsett, J. A. (1999). GM-CSF-deficient mice are susceptible to pulmonary group B streptococcal infection. *Journal of Clinical Investigation*. https://doi.org/10.1172/JCI5212

Lewis, N. D., Hill, J. D., Juchem, K. W., Stefanopoulos, D. E., & Modis, L. K. (2014). RNA sequencing of microglia and monocyte-derived macrophages from mice with experimental autoimmune encephalomyelitis illustrates a changing phenotype with disease course. *Journal of Neuroimmunology*. https://doi.org/10.1016/j.jneuroim.2014.09.014

Li, H., Sonobe, Y., Tabata, H., Liang, J., Jin, S., Doi, Y., … Suzumura, A. (2011).

Tumor necrosis factor-α promotes granulocyte-macrophage colony-stimulating factor-stimulated microglia to differentiate into competent dendritic cell-like antigen-presenting cells. *Clinical and Experimental Neuroimmunology*. https://doi.org/10.1111/j.1759-1961.2010.00016.x

Li, J., Baud, O., Vartanian, T., Volpe, J. J., & Rosenberg, P. A. (2005). Peroxynitrite generated by inducible nitric oxide synthase and NADPH oxidase mediates microglial toxicity to oligodendrocytes. *Proceedings of the National Academy of Sciences of the United States of America*. https://doi.org/10.1073/pnas.0502552102

Li, Q., & Barres, B. A. (2018). Microglia and macrophages in brain homeostasis and disease. *Nature Reviews Immunology*. https://doi.org/10.1038/nri.2017.125

Li, R., Rezk, A., Miyazaki, Y., Hilgenberg, E., Touil, H., Shen, P., … Bar-Or, A. (2015). Proinflammatory GM-CSF-producing B cells in multiple sclerosis and B cell depletion therapy. *Science Translational Medicine*. https://doi.org/10.1126/scitranslmed.aab4176

Liddelow, S. A., Guttenplan, K. A., Clarke, L. E., Bennett, F. C., Bohlen, C. J., Schirmer, L., … Barres, B. A. (2017). Neurotoxic reactive astrocytes are induced by activated microglia. *Nature*. https://doi.org/10.1038/nature21029

Lin, C.-C., & Edelson, B. T. (2017). New Insights into the Role of IL-1β in Experimental Autoimmune Encephalomyelitis and Multiple Sclerosis. *The Journal of Immunology*. https://doi.org/10.4049/jimmunol.1700263

Lively, S., & Schlichter, L. C. (2018). Microglia responses to pro-inflammatory stimuli (LPS, IFNγ+TNFα) and reprogramming by resolving cytokines (IL-4, IL-10). *Frontiers in Cellular Neuroscience*. https://doi.org/10.3389/fncel.2018.00215

Lo, E. H., Wang, X., & Louise Cuzner, M. (2002). Extracellular proteolysis in brain injury and inflammation: Role for plasminogen activators and matrix metalloproteinases. *Journal of Neuroscience Research*. https://doi.org/10.1002/jnr.10270

Lucchinetti, C., Brück, W., Parisi, J., Scheithauer, B., Rodriguez, M., & Lassmann, H. (2000). Heterogeneity of multiple sclerosis lesions: Implications for the pathogenesis of demyelination. *Annals of Neurology*. https://doi.org/10.1002/1531-8249(200006)47:6<707::AID-ANA3>3.0.CO;2-Q

Lucchinetti, C. F., Popescu, B. F. G., Bunyan, R. F., Moll, N. M., Roemer, S. F., Lassmann, H., … Ransohoff, R. M. (2011). Inflammatory cortical demyelination in early multiple sclerosis. *New England Journal of Medicine*. https://doi.org/10.1056/NEJMoa1100648

Mackay, I. R., & Anderson, W. H. (2010). What's in a name? Experimental

encephalomyelitis: “Allergic” or “autoimmune.” *Journal of Neuroimmunology*. https://doi.org/10.1016/j.jneuroim.2010.03.017

Magliozzi, R., Howell, O., Vora, A., Serafini, B., Nicholas, R., Puopolo, M., … Aloisi, F. (2007). Meningeal B-cell follicles in secondary progressive multiple sclerosis associate with early onset of disease and severe cortical pathology. *Brain*. https://doi.org/10.1093/brain/awm038

Magliozzi, R., Howell, O. W., Reeves, C., Roncaroli, F., Nicholas, R., Serafini, B., … Reynolds, R. (2010). A Gradient of neuronal loss and meningeal inflammation in multiple sclerosis. *Annals of Neurology*. https://doi.org/10.1002/ana.22230

Mahad, D. J., & Ransohoff, R. M. (2003). The role of MCP-1 (CCL2) and CCR2 in multiple sclerosis and experimental autoimmune encephalomyelitis (EAE). *Seminars in Immunology*. https://doi.org/10.1016/S1044-5323(02)00125-2

Mander, P., & Brown, G. C. (2005). Activation of microglial NADPH oxidase is synergistic with glial iNOS expression in inducing neuronal death: A dual-key mechanism of inflammatory neurodegeneration. *Journal of Neuroinflammation*. https://doi.org/10.1186/1742-2094-2-20

Manicone, A. M., & McGuire, J. K. (2008). Matrix metalloproteinases as modulators of inflammation. *Seminars in Cell and Developmental Biology*. https://doi.org/10.1016/j.semcdb.2007.07.003

Marín-Teva, J. L., Dusart, I., Colin, C., Gervais, A., Van Rooijen, N., & Mallat, M. (2004). Microglia Promote the Death of Developing Purkinje Cells. *Neuron*. https://doi.org/10.1016/S0896-6273(04)00069-8

Marshall, H. E., & Stamler, J. S. (2001). Inhibition of NF-kappa B by S-nitrosylation. *Biochemistry*.

Marusic, S., Miyashiro, J. S., Douhan, J., Konz, R. F., Xuan, D. J., Pelker, J. W., … Jacobs, K. A. (2002). Local delivery of granulocyte macrophage colony-stimulating factor by retrovirally transduced antigen-specific T cells leads to severe, chronic experimental autoimmune encephalomyelitis in mice. *Neuroscience Letters*. https://doi.org/10.1016/S0304-3940(02)00947-3

Masliah, E., Mallory, M., Hansen, L., Alford, M., Albright, T., Terry, R., … Saitoh, T. (1991). Immunoreactivity of CD45, a protein phosphotyrosine phosphatase, in Alzheimer’s disease. *Acta Neuropathologica*. https://doi.org/10.1007/BF00294425

Matsushita, T., Tateishi, T., Isobe, N., Yonekawa, T., Yamasaki, R., Matsuse, D., … Kira, J. I. (2013). Characteristic Cerebrospinal Fluid Cytokine/Chemokine Profiles in Neuromyelitis Optica, Relapsing Remitting or Primary Progressive Multiple Sclerosis. *PLoS ONE*. https://doi.org/10.1371/journal.pone.0061835

McManus, C., Berman, J. W., Brett, F. M., Staunton, H., Farrell, M., & Brosnan, C. F. (1998). MCP-1, MCP-2 and MCP-3 expression in multiple sclerosis lesions: An immunohistochemical and in situ hybridization study. *Journal of Neuroimmunology*. https://doi.org/10.1016/S0165-5728(98)00002-2

McQualter, J. L., Darwiche, R., Ewing, C., Onuki, M., Kay, T. W., Hamilton, J. A., … Bernard, C. C. A. (2001). Granulocyte macrophage colony-stimulating factor: A new putative therapeutic target in multiple sclerosis. *Journal of Experimental Medicine*. https://doi.org/10.1084/jem.194.7.873

McRae, B. L., Vanderlugt, C. L., Dal Canto, M. C., & Miller, S. D. (1995). Functional evidence for epitope spreading in the relapsing pathology of experimental autoimmune encephalomyefitis. *Journal of Experimental Medicine*. https://doi.org/10.1084/jem.182.1.75

Meinl, E., Krumbholz, M., & Hohlfeld, R. (2006). B lineage cells in the inflammatory central nervous system environment: Migration, maintenance, local antibody production, and therapeutic modulation. *Annals of Neurology*. https://doi.org/10.1002/ana.20890

Merrill, J. E., Kono, D. H., Clayton, J., Ando, D. G., Hinton, D. R., & Hofman, F. M. (1992). Inflammatory leukocytes and cytokines in the peptide-induced disease of experimental allergic encephalomyelitis in SJL and B10.PL mice. *Proc Natl Acad Sci U S A*.

Mincheva, S., Garcera, A., Gou-Fabregas, M., Encinas, M., Dolcet, X., & Soler, R. M. (2011). The canonical nuclear factor-κB pathway regulates cell survival in a developmental model of spinal cord motoneurons. *Journal of Neuroscience*. https://doi.org/10.1523/JNEUROSCI.0206-11.2011

Minocha, S., Valloton, D., Arsenijevic, Y., Cardinaux, J. R., Guidi, R., Hornung, J. P., & Lebrand, C. (2017). Nkx2.1 regulates the generation of telencephalic astrocytes during embryonic development. *Scientific Reports*. https://doi.org/10.1038/srep43093

Mir, M., Tolosa, L., Asensio, V. J., Lladó, J., & Olmos, G. (2008). Complementary roles of tumor necrosis factor alpha and interferon gamma in inducible microglial nitric oxide generation. *Journal of Neuroimmunology*. https://doi.org/10.1016/j.jneuroim.2008.07.002

Miron, V. E., Boyd, A., Zhao, J. W., Yuen, T. J., Ruckh, J. M., Shadrach, J. L., … Ffrench-Constant, C. (2013). M2 microglia and macrophages drive oligodendrocyte differentiation during CNS remyelination. *Nature Neuroscience*. https://doi.org/10.1038/nn.3469

Montalban, X., Hauser, S. L., Kappos, L., Arnold, D. L., Bar-Or, A., Comi, G., … Wolinsky, J. S. (2017). Ocrelizumab versus placebo in primary progressive multiple sclerosis. *New England Journal of Medicine*. https://doi.org/10.1056/NEJMoa1606468

Montgomery, S. L., & Bowers, W. J. (2012). Tumor necrosis factor-alpha and the roles it plays in homeostatic and degenerative processes within the central nervous system. *Journal of Neuroimmune Pharmacology*. https://doi.org/10.1007/s11481-011-9287-2

Mount, M. P., Lira, A., Grimes, D., Smith, P. D., Faucher, S., Slack, R., … Park, D. S. (2007). Involvement of interferon-γ in microglial-mediated loss of dopaminergic neurons. *Journal of Neuroscience*. https://doi.org/10.1523/JNEUROSCI.5321-06.2007

Mrdjen, D., Pavlovic, A., Hartmann, F. J., Schreiner, B., Utz, S. G., Leung, B. P., … Becher, B. (2018). High-Dimensional Single-Cell Mapping of Central Nervous System Immune Cells Reveals Distinct Myeloid Subsets in Health, Aging, and Disease. *Immunity*. https://doi.org/10.1016/j.immuni.2018.01.011

Nakane, M., Klinghofer, V., Kuk, J. E., Donnelly, J. L., Budzik, G. P., Pollock, J. S., … Carter, G. W. (1995). Novel potent and selective inhibitors of inducible nitric oxide synthase. *Molecular Pharmacology*.

Nakazawa, H., Chang, K., Shinozaki, S., Yasukawa, T., Ishimaru, K., Yasuhara, S., … Kaneki, M. (2017). iNOS as a driver of inflammation and apoptosis in mouse skeletal muscle after burn injury: Possible involvement of sirt1 S-nitrosylation-mediated acetylation of p65 NFeKB and p53. *PLoS ONE*. https://doi.org/10.1371/journal.pone.0170391

Nicol, L. S. C., Thornton, P., Hatcher, J. P., Glover, C. P., Webster, C. I., Burrell, M., … Chessell, I. (2018). Central inhibition of granulocyte-macrophage colony-stimulating factor is analgesic in experimental neuropathic pain. *Pain*. https://doi.org/10.1097/j.pain.0000000000001130

Nimmerjahn, A., Kirchhoff, F., & Helmchen, F. (2005). Neuroscience: Resting microglial cells are highly dynamic surveillants of brain parenchyma in vivo. *Science*. https://doi.org/10.1126/science.1110647

Nissen, J. C., Thompson, K. K., West, B. L., & Tsirka, S. E. (2018). Csf1R inhibition attenuates experimental autoimmune encephalomyelitis and promotes recovery. *Experimental Neurology*. https://doi.org/10.1016/j.expneurol.2018.05.021

Nylander, A., & Hafler, D. A. (2012). Review series Multiple sclerosis. *Journal of Clinical Investigation*. https://doi.org/10.1172/JCI58649.1180

Olson, J. K., & Miller, S. D. (2004). Microglia Initiate Central Nervous System Innate and Adaptive Immune Responses through Multiple TLRs. *The Journal of Immunology*. https://doi.org/10.4049/jimmunol.173.6.3916

Ong, G. L., Goldenberg, D. M., Hansen, H. J., & Mattes, M. J. (1999). Cell surface expression and metabolism of major histocompatibility complex class II invariant chain (CD74) by diverse cell lines. *Immunology*.

https://doi.org/10.1046/j.1365-2567.1999.00868.x

Oosterhof, N., Chang, I. J., Karimiani, E. G., Kuil, L. E., Jensen, D. M., Daza, R., … Bennett, J. T. (2019). Homozygous Mutations in CSF1R Cause a Pediatric-Onset Leukoencephalopathy and Can Result in Congenital Absence of Microglia. *American Journal of Human Genetics*. https://doi.org/10.1016/j.ajhg.2019.03.010

Ormel, P. R., Vieira de Sá, R., van Bodegraven, E. J., Karst, H., Harschnitz, O., Sneeboer, M. A. M., … Pasterkamp, R. J. (2018). Microglia innately develop within cerebral organoids. *Nature Communications*. https://doi.org/10.1038/s41467-018-06684-2

Ousman, S. S., & David, S. (2001). MIP-1α, MCP-1, GM-CSF, and TNF-α control the immune cell response that mediates rapid phagocytosis of myelin from the adult mouse spinal cord. *Journal of Neuroscience*.

Ovanesov, M. V., Sauder, C., Rubin, S. A., Richt, J., Nath, A., Carbone, K. M., & Pletnikov, M. V. (2006). Activation of Microglia by Borna Disease Virus Infection: In Vitro Study. *Journal of Virology*. https://doi.org/10.1128/jvi.01648-06

Pacher, P., Beckman, J. S., & Liaudet, L. (2007). Nitric oxide and peroxynitrite in health and disease. *Physiological Reviews*. https://doi.org/10.1152/physrev.00029.2006

Paine, R., Preston, A. M., Wilcoxen, S., Jin, H., Siu, B. B., Morris, S. B., … Beck, J. M. (2000). Granulocyte-Macrophage Colony-Stimulating Factor in the Innate Immune Response to Pneumocystis carinii Pneumonia in Mice . *The Journal of Immunology*. https://doi.org/10.4049/jimmunol.164.5.2602

Paine, R., Wilcoxen, S. E., Morris, S. B., Sartori, C., Baleeiro, C. E. O., Matthay, M. A., & Christensen, P. J. (2003). Transgenic Overexpression of Granulocyte Macrophage-Colony Stimulating Factor in the Lung Prevents Hyperoxic Lung Injury. *American Journal of Pathology*. https://doi.org/10.1016/S0002-9440(10)63594-8

Panitch, H. S., Hirsch, R. L., Schindler, J., & Johnson, K. P. (1987). Treatment of multiple sclerosis with gamma interferon: Exacerbations associated with activation of the immune system. *Neurology*.

Paolicelli, R. C., Bolasco, G., Pagani, F., Maggi, L., Scianni, M., Panzanelli, P., … Gross, C. T. (2011). Synaptic pruning by microglia is necessary for normal brain development. *Science*. https://doi.org/10.1126/science.1202529

Parajuli, B., Sonobe, Y., Kawanokuchi, J., Doi, Y., Noda, M., Takeuchi, H., … Suzumura, A. (2012). GM-CSF increases LPS-induced production of proinflammatory mediators via upregulation of TLR4 and CD14 in murine microglia. *Journal of Neuroinflammation*. https://doi.org/10.1186/1742-2094-9-268

Patel, J., & Balabanov, R. (2012). Molecular mechanisms of oligodendrocyte injury in multiple sclerosis and experimental autoimmune encephalomyelitis. *International Journal of Molecular Sciences*. https://doi.org/10.3390/ijms130810647

Patsopoulos, N. A., Barcellos, L. F., Hintzen, R. Q., Schaefer, C., van Duijn, C. M., Noble, J. A., … Kermode, A. G. (2013). Fine-Mapping the Genetic Association of the Major Histocompatibility Complex in Multiple Sclerosis: HLA and Non-HLA Effects. *PLoS Genetics*. https://doi.org/10.1371/journal.pgen.1003926

Pegoretti, V., Baron, W., Laman, J. D., & Eisel, U. L. M. (2018). Selective modulation of TNF-TNFRs signaling: Insights for multiple sclerosis treatment. *Frontiers in Immunology*. https://doi.org/10.3389/fimmu.2018.00925

Perriard, G., Mathias, A., Enz, L., Canales, M., Schluep, M., Gentner, M., … Du Pasquier, R. A. (2015). Interleukin-22 is increased in multiple sclerosis patients and targets astrocytes. *Journal of Neuroinflammation*. https://doi.org/10.1186/s12974-015-0335-3

Petrik, D., Yun, S., Latchney, S. E., Kamrudin, S., LeBlanc, J. A., Bibb, J. A., & Eisch, A. J. (2013). Early Postnatal In Vivo Gliogenesis From Nestin-Lineage Progenitors Requires Cdk5. *PLoS ONE*. https://doi.org/10.1371/journal.pone.0072819

Pettinelli, C. B., & McFarlin, D. E. (1981). Adoptive transfer of experimental allergic encephalomyelitis in SJL/J mice after in vitro activation of lymph node cells by myelin basic protein: requirement for Lyt 1+ 2- T lymphocytes. *Journal of Immunology (Baltimore, Md. : 1950)*.

Piccio, L., Buonsanti, C., Mariani, M., Cella, M., Gilfillan, S., Cross, A. H., … Panina-Bordignon, P. (2007). Blockade of TREM-2 exacerbates experimental autoimmune encephalomyelitis. *European Journal of Immunology*. https://doi.org/10.1002/eji.200636837

Pierson, E. R., & Goverman, J. M. (2017). GM-CSF is not essential for experimental autoimmune encephalomyelitis but promotes brain-targeted disease. *JCI Insight*. https://doi.org/10.1172/jci.insight.92362

Podolin, P. L., Callahan, J. F., Bolognese, B. J., Li, Y. H., Carlson, K., Davis, T. G., … Roshak, A. K. (2005). Attenuation of murine collagen-induced arthritis by a novel, potent, selective small molecule inhibitor of IκB kinase 2, TPCA-1 (2-[(aminocarbonyl)amino]-5-(4-fluorophenyl)-3-thiophenecarboxamide), occurs via reduction of proinflammatory cytokines and ant. *Journal of Pharmacology and Experimental Therapeutics*. https://doi.org/10.1124/jpet.104.074484

Ponomarev, E. D., Shriver, L. P., & Dittel, B. N. (2006). CD40 Expression by Microglial Cells Is Required for Their Completion of a Two-Step Activation Process during Central Nervous System Autoimmune Inflammation. *The*

*Journal of Immunology*. https://doi.org/10.4049/jimmunol.176.3.1402

Ponomarev, E. D., Shriver, L. P., Maresz, K., Pedras-Vasconcelos, J., Verthelyi, D., & Dittel, B. N. (2007). GM-CSF Production by Autoreactive T Cells Is Required for the Activation of Microglial Cells and the Onset of Experimental Autoimmune Encephalomyelitis. *The Journal of Immunology*. https://doi.org/10.4049/jimmunol.178.1.39

Popescu, B. F. G., Pirko, I., & Lucchinetti, C. F. (2013). Pathology of multiple sclerosis: Where do we stand? *CONTINUUM Lifelong Learning in Neurology*. https://doi.org/10.1212/01.CON.0000433291.23091.65

Praet, J., Guglielmetti, C., Berneman, Z., Van der Linden, A., & Ponsaerts, P. (2014). Cellular and molecular neuropathology of the cuprizone mouse model: Clinical relevance for multiple sclerosis. *Neuroscience and Biobehavioral Reviews*. https://doi.org/10.1016/j.neubiorev.2014.10.004

Prevost, J. M., Pelley, J. L., Zhu, W., D'Egidio, G. E., Beaudry, P. P., Pihl, C., … Brown, C. B. (2002). Granulocyte-Macrophage Colony-Stimulating Factor (GM-CSF) and Inflammatory Stimuli Up-Regulate Secretion of the Soluble GM-CSF Receptor in Human Monocytes: Evidence for Ectodomain Shedding of the Cell Surface GM-CSF Receptor α Subunit. *The Journal of Immunology*. https://doi.org/10.4049/jimmunol.169.10.5679

Prineas, J. W., Kwon, E. E., Cho, E. S., Sharer, L. R., Barnett, M. H., Oleszak, E. L., … Morgan, B. P. (2001). Immunopathology of secondary-progressive multiple sclerosis. *Annals of Neurology*. https://doi.org/10.1002/ana.1255

Prinz, M., Erny, D., & Hagemeyer, N. (2017). Ontogeny and homeostasis of CNS myeloid cells. *Nature Immunology*. https://doi.org/10.1038/ni.3703

Probert, L. (2000). TNFR1 signalling is critical for the development of demyelination and the limitation of T-cell responses during immune-mediated CNS disease. *Brain*. https://doi.org/10.1093/brain/123.10.2005

Probert, L. (2015). TNF and its receptors in the CNS: The essential, the desirable and the deleterious effects. *Neuroscience*. https://doi.org/10.1016/j.neuroscience.2015.06.038

Puli, L., Pomeshchik, Y., Olas, K., Malm, T., Koistinaho, J., & Tanila, H. (2012). Effects of human intravenous immunoglobulin on amyloid pathology and neuroinflammation in a mouse model of Alzheimer's disease. *Journal of Neuroinflammation*. https://doi.org/10.1186/1742-2094-9-105

Pupim, L., Unizony, S., Cid, M., Pilipski, L., Gandhi, R., Pirrello, J., … Paolini, J. (2019). 336. A PHASE 2, RANDOMIZED, DOUBLE-BLIND PLACEBO-CONTROLLED STUDY TO TEST THE EFFICACY AND SAFETY OF MAVRILIMUMAB IN GIANT CELL ARTERITIS: STUDY DESIGN AND METHODOLOGY. *Rheumatology*. https://doi.org/10.1093/rheumatology/kez063.060

Quelle, F. W., Sato, N., Witthuhn, B. A., Inhorn, R. C., Eder, M., Miyajima, A., … Ihle, J. N. (1994). JAK2 associates with the beta c chain of the receptor for granulocyte-macrophage colony-stimulating factor, and its activation requires the membrane-proximal region. *Molecular and Cellular Biology*. https://doi.org/10.1128/mcb.14.7.4335

Ramaglia, V., Hughes, T. R., Donev, R. M., Ruseva, M. M., Wu, X., Huitinga, I., … Morgan, B. P. (2012). C3-dependent mechanism of microglial priming relevant to multiple sclerosis. *Proceedings of the National Academy of Sciences of the United States of America*. https://doi.org/10.1073/pnas.1111924109

Ransohoff, R. M. (2016). A polarizing question: Do M1 and M2 microglia exist. *Nature Neuroscience*. https://doi.org/10.1038/nn.4338

Rasouli, J., Ciric, B., Imitola, J., Gonnella, P., Hwang, D., Mahajan, K., … Rostami, A. (2015). Expression of GM-CSF in T Cells Is Increased in Multiple Sclerosis and Suppressed by IFN-β Therapy. *The Journal of Immunology*. https://doi.org/10.4049/jimmunol.1403243

Re, F., Belyanskaya, S. L., Riese, R. J., Cipriani, B., Fischer, F. R., Granucci, F., … Santambrogio, L. (2002). Granulocyte-Macrophage Colony-Stimulating Factor Induces an Expression Program in Neonatal Microglia That Primes Them for Antigen Presentation. *The Journal of Immunology*. https://doi.org/10.4049/jimmunol.169.5.2264

Renno, T., Krakowski, M., Piccirillo, C., Lin, J. Y., & Owens, T. (1995). TNF-alpha expression by resident microglia and infiltrating leukocytes in the central nervous system of mice with experimental allergic encephalomyelitis. Regulation by Th1 cytokines. *Journal of Immunology*.

Restorick, S. M., Durant, L., Kalra, S., Hassan-Smith, G., Rathbone, E., Douglas, M. R., & Curnow, S. J. (2017). CCR6+ Th cells in the cerebrospinal fluid of persons with multiple sclerosis are dominated by pathogenic non-classic Th1 cells and GM-CSF-only-secreting Th cells. *Brain, Behavior, and Immunity*. https://doi.org/10.1016/j.bbi.2017.03.008

Ridwan, S., Bauer, H., Frauenknecht, K., Von Pein, H., & Sommer, C. J. (2012). Distribution of granulocyte-monocyte colony-stimulating factor and its receptor a-subunit in the adult human brain with specific reference to Alzheimer's disease. *Journal of Neural Transmission*. https://doi.org/10.1007/s00702-012-0794-y

Ríos, N., Prolo, C., Álvarez, M. N., Piacenza, L., & Radi, R. (2017). Peroxynitrite Formation and Detection in Living Cells. In *Nitric Oxide: Biology and Pathobiology: Third Edition*. https://doi.org/10.1016/B978-0-12-804273-1.00021-1

Rivers, T. M., & Schwentke, F. F. (1935). Encephalomyelitis accompanied by myelin destruction experimentally produced in monkeys. *Journal of*

*Experimental Medicine*. https://doi.org/10.1084/jem.61.5.689

Robb, L., Drinkwater, C. C., Metcalf, D., Li, R., Kontgen, F., Nicola, N. A., & Begley, C. G. (1995). Hematopoietic and lung abnormalities in mice with a null mutation of the common ß subunit of the receptors for granulocyte-macrophage colony- stimulating factor and interleukins 3 and 5. *Proceedings of the National Academy of Sciences of the United States of America*. https://doi.org/10.1073/pnas.92.21.9565

Rojo, R., Raper, A., Ozdemir, D. D., Lefevre, L., Grabert, K., Wollscheid-Lengeling, E., … Pridans, C. (2019). Deletion of a Csf1r enhancer selectively impacts CSF1R expression and development of tissue macrophage populations. *Nature Communications*. https://doi.org/10.1038/s41467-019-11053-8

Romero, L. I., Tatro, J. B., Field, J. A., & Reichlin, S. (1996). Roles of IL-1 and TNF-α in endotoxin-induced activation of nitric oxide synthase in cultured rat brain cells. *American Journal of Physiology - Regulatory Integrative and Comparative Physiology*.

Rose, J. W., Burns, J. B., Bjorklund, J., Klein, J., Watt, H. E., & Carlson, N. G. (2007). Daclizumab phase II trial in relapsing and remitting multiple sclerosis: MRI and clinical results. *Neurology*. https://doi.org/10.1212/01.wnl.0000267662.41734.1f

Rothhammer, V., & Quintana, F. J. (2015). Control of autoimmune CNS inflammation by astrocytes. *Seminars in Immunopathology*. https://doi.org/10.1007/s00281-015-0515-3

Rumble, J. M., Huber, A. K., Krishnamoorthy, G., Srinivasan, A., Giles, D. A., Zhang, X., … Segal, B. M. (2015). Neutrophil-related factors as biomarkers in EAE and MS. *Journal of Experimental Medicine*. https://doi.org/10.1084/jem.20141015

Russell, H. I., York, I. A., Rock, K. L., & Monaco, J. J. (1999). Class II antigen processing defects in two H2(d) mouse cell lines are caused by point mutations in the H2-DMa gene. *European Journal of Immunology*. https://doi.org/10.1002/(SICI)1521-4141(199903)29:03<905::AID-IMMU905>3.0.CO;2-8

Sabin, A. B., & Wright, A. M. (1934). Acute ascending myelitis following a monkey bite, with the isolation of a virus capable of reproducing the disease. *Journal of Experimental Medicine*. https://doi.org/10.1084/jem.59.2.115

Sadeghian, M., Mastrolia, V., Rezaei Haddad, A., Mosley, A., Mullali, G., Schiza, D., … Smith, K. J. (2016). Mitochondrial dysfunction is an important cause of neurological deficits in an inflammatory model of multiple sclerosis. *Scientific Reports*. https://doi.org/10.1038/srep33249

Sáenz-Cuesta, M., Osorio-Querejeta, I., & Otaegui, D. (2014). Extracellular vesicles in multiple sclerosis: What are they telling us? *Frontiers in Cellular Neuroscience*. https://doi.org/10.3389/fncel.2014.00100

Saijo, K., Crotti, A., & Glass, C. K. (2013). Regulation of microglia activation and deactivation by nuclear receptors. *GLIA*. https://doi.org/10.1002/glia.22423

Sancéau, J., Kaisho, T., Hirano, T., & Wietzerbin, J. (1995). Triggering of the human interleukin-6 gene by interferon-γ and tumor necrosis factor-α in monocytic cells involves cooperation between interferon regulatory factor-1, NFεκB, and Sp1 transcription factors. *Journal of Biological Chemistry*. https://doi.org/10.1074/jbc.270.46.27920

Schafer, D. P., Lehrman, E. K., Kautzman, A. G., Koyama, R., Mardinly, A. R., Yamasaki, R., … Stevens, B. (2012). Microglia Sculpt Postnatal Neural Circuits in an Activity and Complement-Dependent Manner. *Neuron*. https://doi.org/10.1016/j.neuron.2012.03.026

Schneemann, M., & Schoeden, G. (2007). Macrophage biology and immunology: man is not a mouse. *Journal of Leukocyte Biology*. https://doi.org/10.1189/jlb.1106702

Schuh, C., Wimmer, I., Hametner, S., Haider, L., Van Dam, A. M., Liblau, R. S., … Lassmann, H. (2014). Oxidative tissue injury in multiple sclerosis is only partly reflected in experimental disease models. *Acta Neuropathologica*. https://doi.org/10.1007/s00401-014-1263-5

Serafini, B., Rosicarelli, B., Magliozzi, R., Stigliano, E., & Aloisi, F. (2004). Detection of ectopic B-cell follicles with germinal centers in the meninges of patients with secondary progressive multiple sclerosis. *Brain Pathology*. https://doi.org/10.1111/j.1750-3639.2004.tb00049.x

Setiadi, A. F., Abbas, A. R., Jeet, S., Wong, K., Bischof, A., Peng, I., … Townsend, M. J. (2019). IL-17A is associated with the breakdown of the blood-brain barrier in relapsing-remitting multiple sclerosis. *Journal of Neuroimmunology*. https://doi.org/10.1016/j.jneuroim.2019.04.011

Sheng, W., Yang, F., Zhou, Y., Yang, H., Low, P. Y., Kemeny, D. M., … Fu, X. Y. (2014). STAT5 programs a distinct subset of GM-CSF-producing T helper cells that is essential for autoimmune neuroinflammation. *Cell Research*. https://doi.org/10.1038/cr.2014.154

Sheridan, J. W., & Metcalf, D. (1972). Studies on the bone marrow colony stimulating factor (CSF): Relation of tissue CSF to serum CSF. *Journal of Cellular Physiology*. https://doi.org/10.1002/jcp.1040800114

Shibata, Y., Berclaz, P. Y., Chroneos, Z. C., Yoshida, M., Whitsett, J. A., & Trapnell, B. C. (2001). GM-CSF regulates alveolar macrophage differentiation and innate immunity in the lung through PU.1. *Immunity*. https://doi.org/10.1016/S1074-7613(01)00218-7

Shinozaki, S., Chang, K., Sakai, M., Shimizu, N., Yamada, M., Tanaka, T., … Kaneki, M. (2014). Inflammatory stimuli induce inhibitory S-nitrosylation of the deacetylase SIRT1 to increase acetylation and activation of p53 and p65. *Science Signaling*. https://doi.org/10.1126/scisignal.2005375

Shiomi, A., Usui, T., & Mimori, T. (2016). GM-CSF as a therapeutic target in autoimmune diseases. *Inflammation and Regeneration*. https://doi.org/10.1186/s41232-016-0014-5

Shivtiel, S., Kollet, O., Lapid, K., Schajnovitz, A., Goichberg, P., Kalinkovich, A., … Lapidot, T. (2008). CD45 regulates retention, motility, and numbers of hematopoietic progenitors, and affects osteoclast remodeling of metaphyseal trabecules. *The Journal of Experimental Medicine*. https://doi.org/10.1084/jem.20080072

Sierra, A., Encinas, J. M., Deudero, J. J. P., Chancey, J. H., Enikolopov, G., Overstreet-Wadiche, L. S., … Maletic-Savatic, M. (2010). Microglia shape adult hippocampal neurogenesis through apoptosis-coupled phagocytosis. *Cell Stem Cell*. https://doi.org/10.1016/j.stem.2010.08.014

Simpson, J. E., Newcombe, J., Cuzner, M. L., & Woodroofe, M. N. (1998). Expression of monocyte chemoattractant protein-1 and other ß- chemokines by resident glia and inflammatory cells in multiple sclerosis lesions. *Journal of Neuroimmunology*. https://doi.org/10.1016/S0165-5728(97)00208-7

Singh, S. K., Streng-Ouwehand, I., Litjens, M., Kalay, H., Saeland, E., & Van Kooyk, Y. (2011). Tumour-associated glycan modifications of antigen enhance MGL2 dependent uptake and MHC class i restricted CD8 T cell responses. *International Journal of Cancer*. https://doi.org/10.1002/ijc.25458

Singh, S., Metz, I., Amor, S., Van Der Valk, P., Stadelmann, C., & Brück, W. (2013). Microglial nodules in early multiple sclerosis white matter are associated with degenerating axons. *Acta Neuropathologica*. https://doi.org/10.1007/s00401-013-1082-0

Snapper, C. M., Moorman, M. A., Rosas, F. R., Kehry, M. R., Maliszewski, C. R., & Mond, J. J. (1995). IL-3 and granulocyte-macrophage colony-stimulating factor strongly induce Ig secretion by sort-purified murine B cell activated through the membrane Ig, but not the CD40, signaling pathway. *Journal of Immunology (Baltimore, Md. : 1950)*.

Sohet, F., Lin, C., Munji, R. N., Lee, S. Y., Ruderisch, N., Soung, A., … Daneman, R. (2015). LSR/angulin-1 is a tricellular tight junction protein involved in blood-brain barrier formation. *Journal of Cell Biology*. https://doi.org/10.1083/jcb.201410131

Sorensen, A., Moffat, K., Thomson, C., & Barnett, S. C. (2008). Astrocytes, but not olfactory ensheathing cells or Schwann cells, promote myelination of CNS axons in vitro. *GLIA*. https://doi.org/10.1002/glia.20650

Sosa, R. A., Murphey, C., Ji, N., Cardona, A. E., & Forsthuber, T. G. (2013). The Kinetics of Myelin Antigen Uptake by Myeloid Cells in the Central Nervous System during Experimental Autoimmune Encephalomyelitis. *The Journal of Immunology*. https://doi.org/10.4049/jimmunol.1300771

Spath, S., Komuczki, J., Hermann, M., Pelczar, P., Mair, F., Schreiner, B., & Becher, B. (2017). Dysregulation of the Cytokine GM-CSF Induces Spontaneous Phagocyte Invasion and Immunopathology in the Central Nervous System. *Immunity*. https://doi.org/10.1016/j.immuni.2017.01.007

Stanley, E., Lieschke, G. J., Grail, D., Metcalf, D., Hodgson, G., Gall, J. A., … Dunn, A. R. (2006). Granulocyte/macrophage colony-stimulating factor-deficient mice show no major perturbation of hematopoiesis but develop a characteristic pulmonary pathology. *Proceedings of the National Academy of Sciences*. https://doi.org/10.1073/pnas.91.12.5592

Steele, C., Marrero, L., Swain, S., Harmsen, A. G., Zheng, M., Brown, G. D., … Kolls, J. K. (2003). Alveolar Macrophage–mediated Killing of Pneumocystis carinii f. sp. muris Involves Molecular Recognition by the Dectin-1 ß-Glucan Receptor . *The Journal of Experimental Medicine*. https://doi.org/10.1084/jem.20030932

Steidl, S., Ratsch, O., Brocks, B., Dürr, M., & Thomassen-Wolf, E. (2008). In vitro affinity maturation of human GM-CSF antibodies by targeted CDR-diversification. *Molecular Immunology*. https://doi.org/10.1016/j.molimm.2008.07.013

Stein, B. M., Keshav, S., Harris, N., & Gordon, S. (1992). Interleukin 4 Potently Enhances Murine Macrophage Mannose Receptor Activity: A Marker of Alternative Immunologic Macrophage Activation By Michael Stein, Satish Keshav, Neil Harris,* and Siamon Gordon. *J Exp Med*.

Stevens, B., Allen, N. J., Vazquez, L. E., Howell, G. R., Christopherson, K. S., Nouri, N., … Barres, B. A. (2007). The Classical Complement Cascade Mediates CNS Synapse Elimination. *Cell*. https://doi.org/10.1016/j.cell.2007.10.036

Stone, S., Jamison, S., Yue, Y., Durose, W., Schmidt-Ullrich, R., & Lin, W. (2017). NF-γB activation protects oligodendrocytes against inflammation. *Journal of Neuroscience*. https://doi.org/10.1523/JNEUROSCI.1608-17.2017

Stromnes, I. M., & Goverman, J. M. (2006). Passive induction of experimental allergic encephalomyelitis. *Nature Protocols*. https://doi.org/10.1038/nprot.2006.284

Sutterwala, F. S., Ogura, Y., Szczepanik, M., Lara-Tejero, M., Lichtenberger, G. S., Grant, E. P., … Flavell, R. A. (2006). Critical role for NALP3/CIAS1/cryopyrin in innate and adaptive immunity through its regulation of caspase-1. *Immunity*. https://doi.org/10.1016/j.immuni.2006.02.004

Ta, T. T., Dikmen, H. O., Schilling, S., Chausse, B., Lewen, A., Hollnagel, J. O., & Kann, O. (2019). Priming of microglia with IFN-γ slows neuronal gamma oscillations in situ. *Proceedings of the National Academy of Sciences of the United States of America*. https://doi.org/10.1073/pnas.1813562116

Taylor, B. S., De Vera, M. E., Ganster, R. W., Wang, Q., Shapiro, R. A., Morris, S. M., … Geller, D. A. (1998). Multiple NF-κB enhancer elements regulate cytokine induction of the human inducible nitric oxide synthase gene. *Journal of Biological Chemistry*. https://doi.org/10.1074/jbc.273.24.15148

Thomson, C. E., McCulloch, M., Sorenson, A., Barnett, S. C., Seed, B. V., Griffiths, I. R., & McLaughlin, M. (2008). Myelinated, synapsing cultures of murine spinal cord - Validation as an in vitro model of the central nervous system. *European Journal of Neuroscience*. https://doi.org/10.1111/j.1460-9568.2008.06415.x

Thomson, Christine E., Hunter, A. M., Griffiths, I. R., Edgar, J. M., & McCulloch, M. C. (2006). Murine spinal cord explants: A model for evaluating axonal growth and myelination in vitro. *Journal of Neuroscience Research*. https://doi.org/10.1002/jnr.21084

Thored, P., Heldmann, U., Gomes-Leal, W., Gisler, R., Darsalia, V., Taneera, J., … Lindvall, O. (2009). Long-term accumulation of microglia with proneurogenic phenotype concomitant with persistent neurogenesis in adult subventricular zone after stroke. *GLIA*. https://doi.org/10.1002/glia.20810

Tran, E. H., Prince, E. N., & Owens, T. (2000). IFN-γ Shapes Immune Invasion of the Central Nervous System Via Regulation of Chemokines. *The Journal of Immunology*. https://doi.org/10.4049/jimmunol.164.5.2759

Trapnell, B. C., Carey, B. C., Uchida, K., & Suzuki, T. (2009). Pulmonary alveolar proteinosis, a primary immunodeficiency of impaired GM-CSF stimulation of macrophages. *Current Opinion in Immunology*. https://doi.org/10.1016/j.coi.2009.09.004

Trapp, B. D., Peterson, J., Ransohoff, R. M., Rudick, R., Mörk, S., & Bö, L. (1998). Axonal transection in the lesions of multiple sclerosis. *New England Journal of Medicine*. https://doi.org/10.1056/NEJM199801293380502

Trettel, F., Di Castro, M. A., & Limatola, C. (2019). Chemokines: Key Molecules that Orchestrate Communication among Neurons, Microglia and Astrocytes to Preserve Brain Function. *Neuroscience*. https://doi.org/10.1016/j.neuroscience.2019.07.035

Trivedi, A., Noble-Haeusslein, L. J., Levine, J. M., Santucci, A. D., Reeves, T. M., & Phillips, L. L. (2019). Matrix metalloproteinase signals following neurotrauma are right on cue. *Cellular and Molecular Life Sciences*. https://doi.org/10.1007/s00018-019-03176-4

Tsutsui, M., Hirase, R., Miyamura, S., Nagayasu, K., Nakagawa, T., Mori, Y., …

Kaneko, S. (2018). TRPM2 exacerbates central nervous system inflammation in experimental autoimmune encephalomyelitis by increasing production of CXCL2 chemokines. *Journal of Neuroscience*. https://doi.org/10.1523/JNEUROSCI.2203-17.2018

Tutuncu, M., Tang, J., Zeid, N. A., Kale, N., Crusan, D. J., Atkinson, E. J., … Kantarci, O. H. (2013). Onset of progressive phase is an age-dependent clinical milestone in multiple sclerosis. *Multiple Sclerosis Journal*. https://doi.org/10.1177/1352458512451510

Uchida, K., Nakata, K., Suzuki, T., Luisetti, M., Watanabe, M., Koch, D. E., … Trapnell, B. C. (2009). Granulocyte/macrophage-colony-stimulating factor autoantibodies and myeloid cell immune functions in healthy subjects. *Blood*. https://doi.org/10.1182/blood-2008-05-155689

Van Leeuwen, B. H., Martinson, M. E., Webb, G. C., & Young, I. G. (1989). Molecular organization of the cytokine gene cluster, involving the human IL-3, IL-4, IL-5, and GM-CSF genes, on human chromosome 5. *Blood*.

Visser, E. M., Wilde, K., Wilson, J. F., Yong, K. K., & Counsell, C. E. (2012). A new prevalence study of multiple sclerosis in Orkney, Shetland and Aberdeen city. *Journal of Neurology, Neurosurgery and Psychiatry*. https://doi.org/10.1136/jnnp-2011-301546

Voet, S., Mc Guire, C., Hagemeyer, N., Martens, A., Schroeder, A., Wieghofer, P., … Van Loo, G. (2018). A20 critically controls microglia activation and inhibits inflammasome-dependent neuroinflammation. *Nature Communications*. https://doi.org/10.1038/s41467-018-04376-5

Voet, S., Prinz, M., & van Loo, G. (2019). Microglia in Central Nervous System Inflammation and Multiple Sclerosis Pathology. *Trends in Molecular Medicine*. https://doi.org/10.1016/j.molmed.2018.11.005

Vogel, D. Y. S., Kooij, G., Heijnen, P. D. A. M., Breur, M., Peferoen, L. A. N., van der Valk, P., … Dijkstra, C. D. (2015). GM-CSF promotes migration of human monocytes across the blood brain barrier. *European Journal of Immunology*. https://doi.org/10.1002/eji.201444960

Vogel, D. Y. S., Vereyken, E. J. F., Glim, J. E., Heijnen, P. D. A. M., Moeton, M., van der Valk, P., … Dijkstra, C. D. (2013). Macrophages in inflammatory multiple sclerosis lesions have an intermediate activation status. *Journal of Neuroinflammation*. https://doi.org/10.1186/1742-2094-10-35

Voß, E. V., Škuljec, J., Gudi, V., Skripuletz, T., Pul, R., Trebst, C., & Stangel, M. (2012). Characterisation of microglia during de- and remyelination: Can they create a repair promoting environment? *Neurobiology of Disease*. https://doi.org/10.1016/j.nbd.2011.09.008

Waisman, A., & Johann, L. (2018). Antigen-presenting cell diversity for T cell reactivation in central nervous system autoimmunity. *Journal of Molecular*

*Medicine*. https://doi.org/10.1007/s00109-018-1709-7

Wajant, H., & Siegmund, D. (2019). TNFR1 and TNFR2 in the control of the life and death balance of macrophages. *Frontiers in Cell and Developmental Biology*. https://doi.org/10.3389/fcell.2019.00091

Wake, H., Moorhouse, A. J., Jinno, S., Kohsaka, S., & Nabekura, J. (2009). Resting microglia directly monitor the functional state of synapses in vivo and determine the fate of ischemic terminals. *Journal of Neuroscience*. https://doi.org/10.1523/JNEUROSCI.4363-08.2009

Waldner, H., Whitters, M. J., Sobel, R. A., Collins, M., & Kuchroo, V. K. (2000). Fulminant spontaneous autoimmunity of the central nervous system in mice transgenic for the myelin proteolipid protein-specific T cell receptor. *Proceedings of the National Academy of Sciences of the United States of America*. https://doi.org/10.1073/pnas.97.7.3412

Wang, K., Song, F., Fernandez-Escobar, A., Luo, G., Wang, J. H., & Sun, Y. (2018). The Properties of Cytokines in Multiple Sclerosis: Pros and Cons. *American Journal of the Medical Sciences*. https://doi.org/10.1016/j.amjms.2018.08.018

Weiner, H. L., Dau, P., Birnbaum, G., Feldstein, M., Khatri, B., Petajan, J., & Mcquillen, M. P. (1983). Plasma Exchange in Acute Multiple Sclerosis: Design of a Cooperative Study. *Archives of Neurology*. https://doi.org/10.1001/archneur.1983.04050100031010

Wekerle, H., Linington, C., Lassmann, H., & Meyermann, R. (1986). Cellular immune reactivity within the CNS. *Trends in Neurosciences*. https://doi.org/10.1016/0166-2236(86)90077-9

Willenborg, D. O., Staykova, M. A., & Cowden, W. B. (1999). Our shifting understanding of the role of nitric oxide in autoimmune encephalomyelitis: A review. *Journal of Neuroimmunology*. https://doi.org/10.1016/S0165-5728(99)00212-X

Williamson, D. J., Begley, C. G., Vadas, M. A., & Metcalf, D. (1988). The detection and initial characterization of colony-stimulating factors in synovial fluid. *Clinical and Experimental Immunology*.

Wlodarczyk, A., Benmamar-Badel, A., Cédile, O., Jensen, K. N., Kramer, I., Elsborg, N. B., & Owens, T. (2019). CSF1R stimulation promotes increased neuroprotection by CD11c+ microglia in EAE. *Frontiers in Cellular Neuroscience*. https://doi.org/10.3389/fncel.2018.00523

Wolf, Y., Shemer, A., Levy-Efrati, L., Gross, M., Kim, J. S., Engel, A., … Jung, S. (2018). Microglial MHC class II is dispensable for experimental autoimmune encephalomyelitis and cuprizone-induced demyelination. *European Journal of Immunology*. https://doi.org/10.1002/eji.201847540

Wolf, Y., Shemer, A., Polonsky, M., Gross, M., Mildner, A., Yona, S., … Jung, S. (2017). Autonomous TNF is critical for in vivo monocyte survival in steady state and inflammation. *Journal of Experimental Medicine*. https://doi.org/10.1084/jem.20160499

Wong, G. G., Witek, J. S., Temple, P. A., Wilkens, K. M., Leary, A. C., Luxenberg, D. P., … Clark, S. C. (1985). Human GM-CSF: Molecular cloning of the complementary DNA and purification of the natural and recombinant proteins. *Science*. https://doi.org/10.1126/science.3923623

Yamasaki, R., Lu, H., Butovsky, O., Ohno, N., Rietsch, A. M., Cialic, R., … Ransohoff, R. M. (2014). Differential roles of microglia and monocytes in the inflamed central nervous system. *Journal of Experimental Medicine*. https://doi.org/10.1084/jem.20132477

ZEHNTNER, S. P., BRISEBOIS, M., TRAN, E., OWENS, T., & FOURNIER, S. (2003). Constitutive expression of a costimulatory ligand on antigen-presenting cells in the nervous system drives demyelinating disease. *The FASEB Journal*. https://doi.org/10.1096/fj.03-0199fje

Zhan, Yang, Paolicelli, R. C., Sforazzini, F., Weinhard, L., Bolasco, G., Pagani, F., … Gross, C. T. (2014). Deficient neuron-microglia signaling results in impaired functional brain connectivity and social behavior. *Nature Neuroscience*. https://doi.org/10.1038/nn.3641

Zhan, Yifan, Lieschke, G. J., Grail, D., Dunn, A. R., & Cheers, C. (1998). Essential roles for granulocyle-macrophage colony-stimulating factor (GM-CSF) and G-CSF in the sustained hematopoietic response of Listeria monocytogenes-infected mice. *Blood*.

Zhang, X., Laubach, V. E., Alley, E. W., Edwards, K. A., Sherman, P. A., Russell, S. W., & Murphy, W. J. (1996). Transcriptional basis for hyporesponsiveness of the human inducible nitric oxide synthase gene to lipopolysaccharide/interferon-γ. *Journal of Leukocyte Biology*. https://doi.org/10.1002/jlb.59.4.575

Zhang, Y., Sloan, S. A., Bennett, M. L., Scholze, A. R., Caneda, C., Liddelow, S. A., … Guarnieri, P. (2014). An RNA-sequencing transcriptome and splicing database of glia, neurons, and vascular cells of the cerebral cortex. *Journal of Neuroscience*. https://doi.org/10.1523/JNEUROSCI.1860-14.2014

Zrzavy, T., Hametner, S., Wimmer, I., Butovsky, O., Weiner, H. L., & Lassmann, H. (2017a). Loss of “homeostatic” microglia and patterns of their activation in active multiple sclerosis. *Brain*. https://doi.org/10.1093/brain/awx113

Zrzavy, T., Hametner, S., Wimmer, I., Butovsky, O., Weiner, H. L., & Lassmann, H. (2017b). Loss of “homeostatic” microglia and patterns of their activation in active multiple sclerosis. *Brain*. https://doi.org/10.1093/brain/awx113